Molecular Characterization of the CGL1 (HeLa x Normal Fibroblast) Human Hybrid Cell System and Ionizing Radiation Induced Segregants

by

Jake S. Pirkkanen

A thesis submitted in partial fulfillment
of the requirements for the degree of
Doctor of Philosophy (PhD) in Biomolecular Sciences

The Faculty of Graduate Studies
Laurentian University
Sudbury, Ontario, Canada

THESIS DEFENCE COMMITTEE/COMITÉ DE SOUTENANCE DE THÈSE
Laurentian Université/Université Laurentienne
Faculty of Graduate Studies/Faculté des études supérieures

Title of Thesis Titre de la thèse	Molecular Characterization of the CGL1 (HeLa x Normal Fibroblast) Human Hybrid Cell System and Ionizing Radiation Induced Segregants
Name of Candidate Nom du candidat	Pirkkanen, Jake
Degree Diplôme	Doctor or Philosophy
Department/Program Département/Programme	Biomolecular Sciences
Date of Defence Date de la soutenance	July 03, 2019

APPROVED/APPROUVÉ

Thesis Examiners/Examinateurs de thèse:

Dr. Douglas Boreham
(Supervisor/Directeur de thèse)

Dr. Gregory Ross
(Committee member/Membre du comité)

Dr. TC Tai
(Committee member/Membre du comité)

Dr. John Gunn
(Committee member/Membre du comité)

Dr. Marianne Sowa
(External Examiner/Examinateur externe)

Dr. Frank Mallory
(Internal Examiner/Examinateur interne)

Approved for the Faculty of Graduate Studies
Approuvé pour la Faculté des études supérieures
Dr. David Lesbarrères
Monsieur David Lesbarrères
Dean, Faculty of Graduate Studies
Doyen, Faculté des études supérieures

ACCESSIBILITY CLAUSE AND PERMISSION TO USE

Abstract

Cellular neoplastic transformation assays have been utilized for many years as an *in vitro* method for assessing the effect of various stimuli on transformation frequency, and a variety of mouse and human cell systems have been generated for experimental use. The CGL1 cell system is a non-tumorigenic pre-neoplastic human hybrid tissue cell model that was derived from the fusion of tumorigenic HeLa cervical cancer cells with non-tumorigenic normal human skin fibroblasts. It has been used for many decades to explore the effects of a variety of ionizing radiation types, doses and dose rates on neoplastic transformation rate. Additionally, irradiated segregants of CGL1 with contrasting tumorigenic phenotypes have been isolated and studied. The non-tumorigenic and tumorigenic segregants of the CGL1 system have been an excellent model for studying these effects in the context of neoplastic transformation. However, there have been few attempts in the last several decades to employ global gene expression technologies to further investigate these model cell segregants. The central goal of this thesis was to utilize modern transcriptomic array capabilities and molecular functional assay techniques to characterize the cell system at an unprecedented level in the context of genetic and molecular mechanisms. To this end, global human transcriptomic microarray technology was implemented to characterize the CGL1 cell system, including radiation induced segregants CON and GIM, as well as GIM cells re-expressing candidate tumor suppressor gene FRA1. This research elucidated significant differentially expressed genes, pathway level differences, putative upstream regulators and proposed mechanistic causal factors influencing differences between tumorigenic and non-tumorigenic segregants of the CGL1 model. Additionally, novel findings regarding the role of candidate tumor suppressor gene FRA1 have been discovered with respect to the mechanisms influencing an altered

tumorigenic phenotype. The experimental work contained within this thesis brings this well-established model system of neoplastic transformation into a contemporary molecular light. These findings significantly update and contribute to our understanding of the mechanisms driving phenotypic differences between these cells in the context of tumorigenicity, and provide new information for future proposed research endeavors.

Keywords: CGL1, hybrid cells, neoplastic transformation, ionizing radiation, transcriptomics, gene expression, carcinogenesis, microarray profiling, tumor suppressor gene

Acknowledgments

Foremost, I must express an immeasurable amount of gratitude and heartfelt appreciation towards my PhD supervisor, Dr. Douglas Boreham. Over these years he has unwaveringly supported this academic pursuit by proving invaluable and seemingly inexhaustible guidance, opportunities and resources. My academic, professional and personal life have been vastly enhanced by the experience that Dr. Boreham has provided, and for that I am truly grateful.

This work would additionally not have been possible without vital support from my PhD thesis committee, Drs. T.C. Tai, Greg Ross and John Gunn. Their insight and feedback undoubtedly influenced the direction of my work, and without their collective interest and encouragement I would not have reached this point.

There is an enormous amount of appreciation and credit due to Dr. Marc Mendonca as well as the members of Dr. Boreham's research laboratory for their ceaseless support and guidance. These peers and mentors were the foundation on which this work was built, and those who helped keep it all together when things felt as if they would fall apart. Their friendship and mentorship were unprecedented both within the research laboratory as well as outside of it, and truly this thesis would not have been possible without them.

Finally, no amount of written thanks can truly reflect the acknowledgement due to my family for their support over the years. As in all other facets of my life, I have been gifted with their unrelenting support during this academic pursuit even with inherent sacrifices. Their love and confidence in me has never wavered, and this has been the light that guided the path along this journey.

Table of Contents

List of Tables

List of Figures

List of Appendices

List of Abbreviations

ACTN1 - actinin, α1
ADCY7 - adenylate cyclase 7
ALDH1A3 - aldehyde dehydrogenase 1 family, member A3
AP-1 - activator protein 1 transcription factor
ALPI - intestinal alkaline phosphatase
ALPP - placental alkaline phosphatase
ALPPL2 - alkaline phosphatase, placental-like 2
ALPL - alkaline phosphatase, liver/bone/kidney
ARHGAP - Rho GTPase activating protein
ARHGEF28 - Rho guanine nucleotide exchange factor 28
ATF7IP2 - activating transcription factor 7 interacting protein 2
BAMBI - BMP and activin membrane-bound inhibitor
Ca^{2+} - calcium ion
cAMP - cyclic adenosine monophosphate
CAM - cell adhesion molecule
CAMK4 - calcium/calmodulin-dependent protein kinase IV
CDH - cadherins
CDKN2B - cyclin-dependent kinase inhibitor 2B
CES3 - carboxylesterase 3
CGL1 - human hybrid cell line (HeLa x normal fibroblast)
COL - collagens
CON - gamma irradiated control cell line
CRE - cAMP response element
CREB - cAMP response element-binding protein
CREB3L1 - CRE binding protein 3-like 1
CREB5 - CRE binding protein 5
CREBBP - CREB binding protein
CREM - CRE modulator
CRTC3 - CREB regulated transcription coactivator 3
DAPK1 - death-associated protein kinase 1
DEGs - differentially expressed genes
DGKD - diacylglycerol kinase, delta
DPYD - dihydropyrimidine dehydrogenase
DUSP1 - dual specificity phosphatase 1
ECM - extracellular matrix
EFEMP2 - EGF-containing fibulin-like ECM protein 2

EGA - exploratory grouping analysis
EGF - epidermal growth factor
FDR - False Discovery Rate
FGF2 - fibroblast growth factor 2
FMN - formins
FN1 - fibronectin 1
FOS - fos proto-oncogene, AP-1 transcription factor subunit
FRA1 - FOS-related antigen 1
FST - follistatin
GADD45 - growth arrest and DNA-damage-inducible
GAL3ST2 - galactose-3-O-sulfotransferase 2
GAPDH - glyceraldehyde 3-phosphate dehydrogenase
GCLM - glutamate-cysteine ligase, modifier subunit
GCR - galactic cosmic radiation
GDA - guanine deaminase
GFPT1 - glutamine-fructose-6-phosphate transaminase 1
GIM - gamma induced mutant cell line
GIM-FRA1 - GIM overexpressing the FRA1 gene
GIM-pcDNA3 - GIM pcDNA3 vector control
GLS - glutaminase
GO - Gene Ontology
GOIs - genes of interest
GOT1 - glutamic-oxaloacetic transaminase 1
Gy - gray (unit of absorbed ionizing radiation dose in joules kilogram^{-1})
HeLa - immortal Henrietta Lacks cervical cancer cell
HMGA2 - high mobility group AT-hook 2
HPD - 4-hydroxyphenylpyruvate dioxygenase
HSPC3 - heat shock protein HSP90-β
HTA - Human Transcriptome Array
IDH1 - isocitrate dehydrogenase 1
IL7R - interleukin-7 receptor
IPA - Ingenuity Pathway Analysis
iPG - iPathwayGuide
IR - ionizing radiation
ITG - integrins
JUN - jun proto-oncogene, AP-1 transcription factor subunit
KYNU - kynureninase
LAMA1 - laminin α1
MEM - minimal essential cell growth medium
MYLK3 - myosin light chain kinase 3

MYO - myosin
NBR - natural background radiation
NDST1 - N-deacetylase/N-sulfotransferase 1
NEXN - nexilin
PACS1 - phosphofurin acidic cluster sorting protein 1
PC - pyruvate carboxylase
PCA - principal component analysis
PDE - phosphodiesterase
PDK4 - pyruvate dehydrogenase kinase, isozyme 4
PDP1 - pyruvate dehydrogenase phosphatase catalytic subunit 1
PI15 - peptidase inhibitor 15
PKA - protein kinase A
PKIB - protein kinase inhibitor β
PKIG - protein kinase inhibitor γ
PRKG1 - protein kinase, cGMP-dependent, type I
PXN - paxillin
RAB1B - ras-related protein Rab1B
RHO - ras homolog family member
ROS - reactive oxygen species
RPS6KA5 - ribosomal protein S6 kinase polypeptide 5
RPS18 - ribosomal protein S18
RT-qPCR - reverse transcribed quantitative polymerase chain reaction
SEM - standard error of the mean
siRNA - small interfering ribonucleic acid
SF3B2 - splicing factor 2B subunit 2
SLC - solute carrier family
SMAD - mothers against decapentaplegic homolog family
SMURF2 - SMAD specific E3 ubiquitin protein ligase 2
Sv - Sievert (unit of absorbed ionizing radiation dose in joules kilogram^{-1})
TAC - Transcriptome Analysis Console
TGFβ - transforming growth factor beta
TGFβI - TGFβ-induced
THBS - thrombospondin
TRIO - trio Rho guanine nucleotide exchange factor
VCL - vinculin
WB - Western Blue®
ZEB2 - zinc finger E-box binding homeobox 2

Chapter 1: Introduction

Since the advent of cancer biology as a scientific and medically established field of research, investigations into the mechanisms of carcinogenesis have been a major focal point. Its origins can be traced as far back as 1775, when English surgeon Percivall Pott recognized the causal link between cancer incidence and the occupation of chimney sweeps. In the early 20th century, German biologist Theodor Boveri published an undeniably seminal monograph; *Concerning the Origin of Malignant Tumors.* In this work he postulated revolutionary concepts regarding the mechanisms of oncogenesis, and undoubtedly impacted the field of cancer research forever. Hanahan and Weinberg's papers *The Hallmarks of Cancer* and *Hallmarks of Cancer: The Next Generation* (Hanahan et al. 2000, Hanahan et al. 2011) elegantly highlight the history of these efforts, where we are now, and where future research may lead.

Efforts into empirically understanding mechanisms that influence development of a normal cell into one that is tumorigenic have continued to be a fundamental component of the research field. To this end, *in vitro* neoplastic transformation assays have been established and utilized for many decades. In the 1960's focus on mammalian cell applications led to research employing a variety of immortalized rat, mouse, hamster and human hybrids (Barski et al. 1962, Harris et al. 1965, Harris et al. 1966, Matsuya et al. 1968, Scaletta et al. 1965, Weiss et al. 1967). During this era of studies however, challenges were met using rodent intraspecies or human rodent interspecies hybrid cell models, notably spontaneous chromosomal loss and genomic instability. The CGL1 human hybrid cell system was established in the laboratory of Eric Stanbridge in the early 1980's,

representing a major turning point in the utilization of an *in vitro* human hybrid tissue culture based model to study the molecular mechanisms of neoplastic transformation.

The CGL1 cell line is a pre-neoplastic non-tumorigenic segregant from the hybridization of HeLa, a tumorigenic human cervical cancer cell, and a non-tumorigenic human skin fibroblast (Stanbridge et al. 1981, Stanbridge et al. 1980). The cell line was non-tumorigenic when subcutaneously injected into mice and genetically stable *in vitro*¸ providing an opportunity to examine mechanisms of neoplastic transformation in a tissue culture based assay. For several decades the CGL1 system has been utilized in both *in vitro* and *in vivo* studies as a unique model to study these mechanisms, with key pioneering work from the laboratories of Drs. Eric Stanbridge, Leslie Redpath and Marc Mendonca (Mendonca et al. 1991, Redpath 1988, Redpath et al. 2001, Redpath et al. 2003, Redpath et al. 1985, Stanbridge 1987). The relatively simplistic quantitative CGL1 neoplastic transformation assay was utilized over many years to investigate *in vitro*, the effect of a variety of biological insults on transformation frequency, particularly ionizing radiation exposure. These studies would lead to the isolation of phenotypically unique segregants of irradiated CGL1 that would allow for novel future investigations. Gamma irradiated mutant (GIM) and control (CON) segregants were isolated from CGL1 cells that had been irradiated with 7Gy of ionizing gamma radiation (Mendonca et al. 1991). GIMs were found to re-express a previously established antigenic marker of neoplastic transformation, intestinal alkaline phosphatase (ALPI), and also formed tumors *in vivo.* CON cell segregants, although also isolated from irradiated CGL1 cells, were found to be non-tumorigenic. A summarizing hierarchy of the origins of the cell lines is shown in Figure 1.

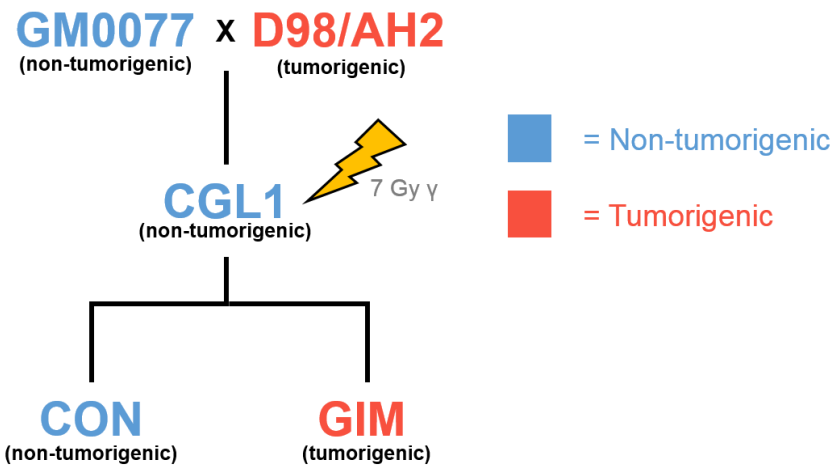

Figure 1: A simplistic hierarchy of the origins of the CGL1, CON and GIM cell lines.

Together, the CGL1, GIM and CON cell lines were studied extensively, resulting in new findings regarding the mechanisms of neoplastic transformation in this model system as well as novel putative tumor suppressor genes (Mendonca et al. 1993, Mendonca et al. 2000, Mendonca et al. 1995, Mendonca et al. 1998). Work continued for several years specifically exploring mechanisms of tumor suppression in the CGL1 cell system and its radiation induced GIM and CON segregants (Mendonca et al. 2004, Mendonca et al. 1999). As technologies advanced that allowed for larger scale detection of differential gene expression, a small number of studies were undertaken to explore variations between tumorigenic and non-tumorigenic members of the CGL1 system (Nishizuka et al. 2001, Nishizuka et al. 2001, Tsujimoto et al. 1999). These studies helped to validate the invariable association of ALPI re-expression as the invariable marker of neoplastic transformation in the CGL1 system. Additionally these studies were able to elucidate, albeit in a limited manner by today's technological standards, a variety of differentially expressed genes (DEGs) between tumorigenic and non-tumorigenic human hybrid cells. These studies from almost two decades ago represent the last published efforts to investigate the molecular gene expression profile of the CGL1 cell system, while attempting to link these findings to potential mechanisms

driving their phenotypic differences. Recent advances in global gene expression profiling technology and data analysis algorithms present an opportunity to characterize the CGL1 human hybrid cell system at an unprecedented level. In addition, modern methods are available to validate findings and together, these data can be utilized to empirically investigate the molecular mechanisms responsible for the differential tumorigenic phenotypes between cell lines.

In this thesis, the overall objective was to re-characterize CGL1 related cell segregants utilizing up-to-date experimental technologies. To this end, first, a systematic and comprehensive review of the CGL1 system was performed (Chapter 2). This is intended to provide the first inclusive historical review of the CGL1 human hybrid cell system. This includes its origins, historical empirical findings, utilization in the neoplastic transformation assay and contributions to the field of cancer biology research. Next, modern global transcriptomic profiling was utilized to characterize CGL1, specifically the phenotypically different GIM and CON segregants (Chapter 3). This, along with validation by several functional assays, revealed a previously unprecedented number of differentially expressed genes, as well as mechanistic pathway and gene network level variances. This study brought into a modern light for the first time in almost two decades, an understanding of the CGL1 model cellular system and its related segregants. Finally, the effects of re-expression of a candidate tumor suppressor gene in GIM cells was explored by global gene expression profiling (Chapter 4). The findings linked DEGs and impacted pathways to the alteration of a tumorigenic phenotype in cells overexpressing the candidate tumor suppressor. A published commentary (Thome, Tharmalingam, Pirkkanen, et al., 2017) on future research directions utilizing this model system in a novel research environment can be found in thesis Appendix A.

Hypothesis:

The global gene expression profile will be significantly altered between tumorigenic GIM and non-tumorigenic CON segregants of the CGL1 system. Re-expression of candidate tumor suppressor gene FRA1 in tumorigenic GIMs will significantly alter their tumorigenic phenotype. This will occur via gene level re-organization of the AP-1 transcription factor complex and modification of extracellular matrix, cellular adhesion and migration profiles.

H_0: There will be no difference between gene expression profiles of GIM and CON. The re-expression of FRA1 in GIM cells has no effect on their tumorigenic phenotype and will not affect gene level organization of the AP-1 transcription factor complex or extracellular matrix, cellular adhesion and migration profiles.

The following experimental objectives will be utilized to evaluate the proposed hypothesis:

Objectives:

Determine the differentially expressed gene profile between GIM and CON segregants of the CGL1 using global transcriptomic profiling technologies

Perform pathway level and gene ontological investigations utilizing differential gene expression profiling to establish mechanisms of tumorigenic phenotypic deviation

Validate findings by functional assays to corroborate proposed mechanisms and evaluate putative factors that influence neoplastic transformation within the system

Utilize the aforementioned technologies to perform novel investigation on transfected GIM cell segregants that overexpresses candidate tumor suppressor gene FRA1

Causally and mechanistically link re-expression of FRA1 in GIM cells to significantly impacted gene expression profiles and alteration of the tumorigenic phenotype

Chapter 2: The CGL1 (HeLa x Normal Skin Fibroblast) Human Hybrid Cell Line: A History of Ionizing Radiation Induced Effects on Neoplastic Transformation and Novel Future Directions in SNOLAB

RADIATION RESEARCH **188**, 512–524 (2017)
0033-7587/17 $15.00

DOI: 10.1667/RR14911.1

REVIEW

The CGL1 (HeLa × Normal Skin Fibroblast) Human Hybrid Cell Line: A History of Ionizing Radiation Induced Effects on Neoplastic Transformation and Novel Future Directions in SNOLAB

Jake S. Pirkkanen,[a,1] Douglas R. Boreham[a,b,c] and Marc S. Mendonca[d,2]

[a] *Department of Biology, Laurentian University, Sudbury, Ontario, Canada, P3E 2C6;* [b] *Northern Ontario School of Medicine, Sudbury, Ontario, Canada, P3E 2C6;* [c] *Bruce Power, Tiverton, Ontario, Canada, N0G 2T0; and* [d] *Department of Radiation Oncology, Radiation and Cancer Biology Laboratories, and Department of Medical & Molecular Genetics, Indiana University School of Medicine, Indianapolis, Indiana 46202*

[*Published*: Radiation Research]

2.1. Abstract

Cellular transformation assays have been utilized for many years as powerful *in vitro* methods for examining neoplastic transformation potential/frequency and mechanisms of carcinogenesis for both chemical and radiological carcinogens. These mouse and human cell based assays are labor intensive but do provide quantitative information on the numbers of neoplastically transformed foci produced after carcinogenic exposure and potential molecular mechanisms involved. Several mouse and human cell systems have been generated to undertake these studies, and they vary in experimental length and endpoint assessment. The CGL1 human cell hybrid neoplastic model is a non-tumorigenic pre-neoplastic cell that was derived from the fusion of HeLa cervical cancer cells and a normal human skin fibroblast. It has been utilized for several decades to study the carcinogenic/neoplastic transformation potential of a variety of ionizing radiation doses, dose rates and radiation types, including UV, X-ray, gamma-ray, neutrons, protons and alpha particles. It is unique in that the CGL1 assay has a relatively short assay time of 18-21 days, and rather than relying on morphological endpoints to detect neoplastic transformation utilizes a simple staining method that detects the tumorigenic marker alkaline phosphatase on the neoplastically transformed cells cell surface. In addition to being of human origin, the CGL1 assay is able to detect and quantify the carcinogenic potential of very low doses of ionizing radiation (in the mGy range), and utilizes a neoplastic endpoint (re-expression of ALPI) that can be detected on both viable and paraformaldehyde fixed cells. In this article, we review the history of the CGL1 neoplastic transformation model system from its initial development through the wide variety of studies examining the effects of all types of ionizing radiation on neoplastic transformation. In addition, we discuss the potential of the CGL1 model system to investigate the effects of near zero background radiation levels available within the radiation biology lab established in SNOLAB.

2.2. Introduction

The creation of somatic whole cell hybrids involves the *in vitro* fusion of two different parental eukaryotic cell types to form a karyotypically unique hybrid cell line which can have significantly different genetic and phenotypic properties from the initial two parental cell types. At the chromosomal and gene levels, the fusion and selection of stable hybrid cell lines frequently involves loss and occasionally gain of chromosomes from one or the other original parental cell genomes. For mammalian cell applications, immortalized rat, mouse, hamster and human hybrids have been developed and utilized since the 1960s (Harris et al. 1965, Harris et al. 1966, Matsuya et al. 1968, Weiss et al. 1967). These hybrid eukaryotic cell lines have been useful scientific tools for chromosomal and genomic mapping of many genes including tumor suppressor genes and also important for monoclonal antibody production (Yagami et al. 2013, Zhang 2012). In some of these hybrids, the presence of a selection marker (i.e., antibiotic resistance genes) on a specific human chromosome allowed for preferential loss of a majority of the other human chromosomes in the hybrid and the retention of marked human chromosome. In addition, these various hybrids have allowed investigation of genomic instability after exposure to chemical mutagens or ionizing radiation but were also useful for studying neoplastic transformation or carcinogenicity induced by either chemicals or ionizing radiation (Kim et al. 2006, Limoli et al. 2003, Limoli et al. 2000, Marder et al. 1993, Morgan et al. 1996, Morgan et al. 1995, Smith et al. 2003). However, over time investigators observed that the rodent intraspecies or interspecies human rodent cellular hybrids, presented numerous challenges including constitutive genomic instability and high spontaneous rates of chromosomal loss after exposure to chemical carcinogens or x-rays. Interestingly, several of these original reports suggested that the malignant properties of a neoplastic and normal mouse cellular hybrid were oncogene driven and dominant (Barski et al.

1962, Scaletta et al. 1965), as these cells would produce tumors if introduced into a host. However, other investigators showed evidence of suppression or partial suppression of malignancy in some cell hybrids (Bregula et al. 1971, Harris 1969, Klein et al. 1973, Wiener et al. 1971, Wiener et al. 1973, Wiener et al. 1974), suggesting a recessive phenotype indicative of tumor suppressor gene activity (Ephrussi et al. 1969, Harris et al. 1969, Sabin 1981). In these experiments some of these hybrid cells would only form tumors when the hybrid cells were injected into mice at very high cell numbers versus their original cancer cell parent. In retrospect, this was probably not clear evidence of complete tumor suppression, because tumors eventually did appear, however data strongly suggest that chromosomal loss was likely the causative factor. Indeed, later studies of tumor growth done with cross species hybrid cells indicated that complete versus partial suppression was due to either the absence or presence of chromosomal instability that over time lead to loss of putative tumor suppressor genes (Sabin 1981).

The above studies were critical for setting the standards for the development of human cell based systems to investigate the chromosomal and molecular basis of chemical of radiation induced neoplastic transformation / carcinogenesis. However, the development of these human cell based neoplastic transformation assays turned out to be technically very difficult because human cells in general are very resistant to chemical and ionizing radiation induced transformation; and even when transformation did occur the frequency of transformation in human cells as compared to those of rodent origin is reduced by orders of magnitude to 1 in 1 million or 1 in 10 million cells analyzed (Borek 1980, Borek 1985). Despite these difficulties, human bronchial and breast epithelial cell based transformation systems were developed to investigate mechanisms of neoplastic transformation after high LET alpha particles. These cell systems identified

chromosomal changes, allelic imbalances, and candidate tumor suppressor genes such Betaig-H3, integrin α5β1, p16 and p21(cip1), but *in vitro* quantitative assays for neoplastic transformation with these systems after radiation exposure were simply not technically possible (Hei et al. 2001, Li et al. 2007, Piao et al. 2001, Roy et al. 2001, Roy et al. 2003, Suzuki et al. 2001, Willey et al. 1993, Zhao et al. 2001, Zhao et al. 2002). It was only after the development of the stable human hybrid cell line called CGL1, a fusion of malignant and nonmalignant human cells, were both highly quantitative measurements of ionizing radiation induced neoplastic transformation frequency and investigation of the cellular and molecular mechanisms involved in radiation induced neoplastic transformation possible. A summary of some of the major developments in hybrid cells and in the CGL1 human hybrid neoplastic transformation assay are shown in Table 1.

Table 1: A summary of various major developments in hybrid cells and CGL1 human hybrid neoplastic transformation assays

Manuscript	**Study**
(Barski et al. 1962)	Hybridization of somatic mouse cell lines
(Harris et al. 1965)	Established human × mouse hybrid cell lines
(Silagi et al. 1969)	Hybridization of two human cell lines
(Harris et al. 1969)	Fusion of mouse cells to study suppression of malignancy
(Chen et al. 1969)	First to report mouse cells for studies of malignant transformation
(Reznikoff et al. 1973)	Establishment of the C3H/10T1/2 assay
(Stanbridge 1976)	Used two HeLa cells variants (D98/AH-2 and HBU) to study suppression of malignancy
(Stanbridge et al. 1980)	Obtained CGL1, CGL2, CGL3 and CGL4 from ESH5 (D98/AH-2 × GM0077 hybrid)
(Stanbridge et al. 1981)	Studied chromosome stability of human cells hybrids. Identified two chromosomes (11 and 14) that are linked to control of tumorigenic expression
(Der et al. 1981)	Identified p75-150 as membrane phosphoprotein marker in human hybrid cells
(Stanbridge et al. 1982)	Analyzed tumorigenicity and transformation of different hybrid human cell lines
(Redpath 1988)	Developed a quantitative assay for neoplastic transformation with the nontumorigenic human hybrid CGL1 cell line using gamma radiation and established first a dose-response relationship with CGL1.
(Colman et al. 1988)	Compared the radiation sensitives of non-tumorigenic and tumorigenic human hybrid cells lines
(Sun et al. 1988)	Further characterized the radiation induced immunoperoxidase based neoplastic transformation assay in CGL1 hybrid cells. Investigated influence of cell density

(Mendonca et al. 1989)	Defined persistently lower plating efficiency post irradiation and delayed expression of lethal mutations in irradiated CGL1 hybrid cells
(Mendonca et al. 1989)	Isolated HeLa × normal fibroblasts cells that expressed radiation induced tumor-associated antigen from irradiated CGL1 hybrid cells
(Mendonca et al. 1990)	Demonstrated long-term incubation at low extracellular pH lowers radiation induced neoplastic transformation
(Latham et al. 1990)	Cloned p75/150 cDNA identifying it as IAP
(Mendonca et al. 1991)	Isolated CONs and GIMs. Characterization of cells lines, including IAP
(Mendonca et al. 1992)	Developed Western blue as a staining method for HeLa × normal fibroblast cells
(Mendonca et al. 1993)	Demonstrated that the induction of the neoplastically transformed foci by radiation was delayed and correlated with the onset of genomic instability and delayed death in the CGL1 hybrid cells
(Redpath et al. 1994)	Studied the effects of temperature (22°C) on the repair of potentially lethal and potentially transforming damage
(Mendonca et al. 1995)	Loss of tumor suppressor loci on fibroblast chromosomes 11 is associated with radiation induced neoplastic transformation of CGL1 hybrid human cells
(Bettega et al. 1997)	Alpha-particle-induced neoplastic transformation of synchronized CGL1 hybrid human cells
(Mendonca et al. 1998)	Loss of putative tumor suppressor loci on fibroblast chromosomes 11 and 14 may be required for radiation induced neoplastic transformation of CGL1 hybrid human cells
(Mendonca et al. 1999)	Previous loss of fibroblast chromosomes 11 increases radiosensitivity and radiation induced neoplastic transformation frequency of CGL1 hybrid human cells
(de Feijter-Rupp et al. 1998)	Studied the changes in gap junctional intercellular communication in Human hybrid cell lines. Absence of gap junctions and gap messages was noted and might be related to loss of specific chromosomes
(Suzuki et al. 1999)	Showed an enhanced expression of glucose transporter GLUT3 in human hybrid cells
(Tsujimoto et al. 1999)	Studied different gene expression in human hybrid cells
(Mendonca et al. 1999)	Delayed apoptosis associated with radiation induced neoplastic transformation of human hybrid cells
(Mendonca et al. 2000)	Previous loss of fibroblast chromosomes 14 increases radiosensitivity but lowers CGL1 susceptibility to radiation induced neoplastic transformation frequency
(Lewis et al. 2001)	Bystander killing induced by medium transfer is cytotoxic and neoplastically transforming to CGL1 human hybrid cells
(Frankenberg et al. 2002)	Studied neoplastic transformation of CGL1 hybrid cells after irradiation with mammography X-rays
(Srivatsan et al. 2002)	Identified a deletion location of 300Kb interval in chromosome 11q13 in HeLa cells
(Mendonca et al. 2004)	Detection of homozygous deletions within the 11q13 cervical cancer tumor suppressor locus in radiation induced, neoplastic transformed CGL1 human hybrid cells
(Mendonca et al. 2005)	A radiation induced acute apoptosis precedes the delayed apoptosis and neoplastic transformation of CGL1 hybrid cells
(Elmore et al. 2005)	Studied neoplastic transformation by low doses of protons in human CGL1 hybrid cells
(Mendonca et al. 2007)	Inhibition of NF-kB increases radiation sensitivity of CGL1 human hybrid cells
(Veena et al. 2008)	Inactivation of the Cystatin E/M tumor suppressor gene in cervical cancer
(Bettega et al. 2009)	Studied neoplastic transformation by carbon ions in human CGL1 hybrid cells

2.3. CGL1

The CGL1 cell line is a pre-neoplastic non-tumorigenic hybrid cell. Stanbridge and colleagues first created the original hybrid cell line called ESH5 from a fusion of the cervical cancer cell line HeLa D98/AH.2 (a HGPRT− variant) and a normal proliferating diploid male skin fibroblast (GM0077) of human origin in HAT selective medium (Der et al. 1981, Stanbridge 1976, Stanbridge et al. 1981). After the third subclone, CGL1 was isolated from the ESH5 cells after growth in methylcellulose. Genetic and chromosomal analyses revealed that CGL1 was very chromosomally stable with a mode of 96 to 100 chromosomes on average, and essentially has four copies of each chromosome i.e. two copies of each chromosome from both the HeLa and the fibroblast parent cells, plus HeLa marker chromosomes (Stanbridge et al. 1981). When injected subcutaneously into nude mice CGL1 is non-tumorigenic and remains genetically stable (Mendonca et al. 1995, Mendonca et al. 1998, Stanbridge et al. 1981). As opposed to rodent or a non-mammalian source, CGL1 was shown to be stable in tissue culture for that could therefore potentially be used to quantitatively assess neoplastic transformation *in vitro* (Redpath 1988, Redpath et al. 1985, Redpath et al. 1987, Sun et al. 1986). Stanbridge *et al*. initial reports of the creation of stable human hybrid cells was subsequently confirmed by others (Klinger 1980, Klinger et al. 1978, Stanbridge 1976). The CGL1 hybrid cell failed to grow tumors in nude mice even when injected at cell densities as high as 1×10^7 and provided clear evidence of complete tumor growth suppression, as opposed to partial growth suppression that had been observed by others (Klinger 1980, Stanbridge 1976, Stanbridge et al. 1982). It was initially unclear whether this suppression was due to specific chromosomal or gene loss, but these mechanisms were proposed to likely be contributing factors. The subsequent fusion of a senescent fibroblast cell with an immortal cancer cell resulting in a hybrid with indefinite proliferative capacity was also of great interest because it suggested that the

limited ability of normal cells to proliferate indefinitely was a recessive trait (Norwood et al. 1974, Schneider 1973). The characteristics of chromosomal stability, suppression of tumorigenicity, and yet retention of phenotypic properties of transformed cells in culture, made CGL1 potentially advantageous for studying what factors influenced the spontaneous or experimentally induced rates of neoplastic transformation in CGL1 cells.

2.4. Characterization of non-tumorigenic CGL1 and spontaneous tumorigenic segregants CGL3 and CGL4

In addition to CGL1, two spontaneously transformed hybrid cell lines were isolated from the original ESH5 hybrid fusion (Stanbridge et al. 1981, Stanbridge et al. 1980). Two of these spontaneous tumorigenic hybrid lines named CGL3 and CGL4 displayed unique characteristics including altered cellular morphology that more resembled the epithelial HeLa tumorigenic parental cell than the more fibroblast like CGL1 hybrid. These tumorigenic CGL3 and CGL4 segregants were determined to consistently express a p75/150 antigen associated with epithelial morphology, which was determined after subsequent studies to be intestinal alkaline phosphatase (ALPI) (Der et al. 1981, Latham et al. 1990, Srivatsan et al. 1986, Stanbridge et al. 1981). Abnormal regulation of alkaline phosphatases had been previously observed in tumorigenic cell lines and is commonly observed in human tumors (Harris 1990, Millan 1988) but ALPI was found to be the exclusive isozyme expressed in CGL1 (Mendonca et al. 1992). The expression of ALPI which was only detected in the HeLa parent cells and the tumorigenic CGL3 and CGL4 hybrids suggested that ALPI was a potentially more reliable tumorigenic marker that could potentially be utilized to detect radiation induced neoplastic transformation of nontumorigenic CGL1 cells since morphological endpoints in this system eventually were determined to be inadequate indicators of

neoplastic transformation (Mendonca et al. 1991, Redpath 1988).

2.5. ALPI detection

A major step forward in the utilization of CGL1 in the quantitative assessment of neoplastic transformation frequency was the development of neoplastic transformation assay that used a primary p75 antibody and a secondary immunoperoxidase antibody to detect neoplastically transformed foci among the non-transformed CGL1 cells in T-75 cell culture flasks (Mendonca et al. 1990, Redpath 1987, Redpath 1988, Redpath et al. 1989, Sun et al. 1988, Sun et al. 1988). However, it was the eventual use of the "Western Blue" (WB) method that repurposed the WB dye that contains 5-bromo-4-chloro-3-indolyl-phosphate (BCIP) and nitro blue tetrazolium (NBT) (normally used for Western blots) to directly detect the p75/ALPI cellular foci in the transformation flasks, which both greatly simplified and reduced cost of the neoplastically transformed foci detection procedure (Mendonca et al. 1992). The WB staining method was possible because intestinal alkaline phosphatase, which is expressed in the neoplastically transformed cells enzymatically cleaves the phosphate group of BCIP and the subsequent contact with NBT results in a colored precipitant which can be detected stereo-microscopically. Viable as well as fixed neoplastic transformation cultures of CGL1 cells can be stained and rapidly assessed for neoplastically transformed colonies (Mendonca et al. 1992). The p75 immunoperoxidase antibody and WB staining procedures have been successfully utilized to quantitatively assess transformation frequency induced by a variety of radiation types, including UV, X-ray, gamma ray, neutrons, protons and alpha particles (Mendonca et al. 1991, Pant et al. 2003, Redpath 1988, Redpath et al. 1990, Redpath et al. 1989, Redpath et al. 1987, Sun et al. 1988). As stated above, over time it has been demonstrated that the WB method is not only faster and considerably less

expensive compared to immunohistochemical and flow cytometry based methods because the WB method does not require large amounts of expensive primary and secondary antibodies. Furthermore, data also strongly suggests that the higher rates of transformation observed utilizing the WB staining method is due to an increase in the sensitivity of the method to detect low levels of ALPI expression (Mendonca et al. 1992).

2.6. The CGL1 neoplastic transformation assay

The quantitative assay for studying radiation induced neoplastic transformation with CGL1 cells was developed by Redpath, Sun, Stanbridge, Colman and Mendonca at the University of California, Irvine, from the mid to late 1980s through early 1990s (Colman et al. 1988, Mendonca et al. 1991, Mendonca et al. 1992, Mendonca et al. 1989, Mendonca et al. 1990, Redpath 1987, Redpath 1988, Redpath et al. 1990, Redpath et al. 1991, Redpath et al. 1985, Redpath et al. 1987, Redpath et al. 1989, Sun et al. 1988, Sun et al. 1988, Sun et al. 1986). From the outset, the CGL1 assay was meticulously characterized for variables such as: initial CGL1 cell plating densities, serum types and serum concentration, transformation flask refeeding schedules, ionizing radiation dose ranges, time of replating after irradiation into the T-75 transformation flasks, total overall length of incubation to allow foci development, as well as the influence of pH and temperature on foci formation (Colman et al. 1988, Mendonca et al. 1991, Mendonca et al. 1992, Mendonca et al. 1989, Mendonca et al. 1990, Redpath 1987, Redpath 1988, Redpath et al. 1990, Redpath et al. 1991, Redpath et al. 1985, Redpath et al. 1987, Redpath et al. 1989, Sun et al. 1988, Sun et al. 1988, Sun et al. 1986).

The influence of each of these variables on the frequency of neoplastic transformation observed after various types of irradiation is of critical importance and will be summarized here. CGL1

stocks are grown in a standard MEM supplemented with 5% calf serum supplemented with glutamine and antibiotics and an antifungal. It is critical that the cell culture growth media is maintained at pH 7.2, since it was shown that lower acidic pH in the range 6.6–6.8 during the 21-day incubation period to allow foci formation, greatly suppressed the observed radiation induced neoplastic transformation frequency (Mendonca et al. 1990, Redpath et al. 1987, Sun et al. 1988). For a standard X-ray or gamma ray neoplastic transformation assay, sub-confluent monolayers of CGL1 cells are irradiated with source and dose of radiation being determined by the investigator. For many of the initial ionizing radiation experiments a range of doses between 0 and 7 Gy of gamma or X-ray were utilized to determine dose response. However, many later studies frequently utilized 0 and 7 Gy because higher radiation doses did not result in higher neoplastic transformation frequencies i.e. a plateau was observed (Mendonca et al. 1990, Redpath 1987, Redpath 1988, Redpath et al. 1989, Sun et al. 1988, Sun et al. 1988). The irradiated CGL1 cells are incubated for 6 hours post irradiation to allow for PLD repair as this was shown to also maximize the observed number of neoplastically foci/transformation frequency per Gy (Mendonca et al. 1990, Redpath 1987, Redpath 1988, Redpath et al. 1989, Sun et al. 1988, Sun et al. 1988). After 6 hours, the cells are harvested by standard cell culture methods, counted and then seeded into T-25 flasks for survival assays and into T-75 tissue culture flasks for the neoplastic transformation assays containing their regular cell culture media. The T-25 flasks are plated separately to determine the plating efficiencies (PEs) of irradiated and un-irradiated cells (Mendonca et al. 1991, Redpath et al. 1987, Sun et al. 1988) by plating 100–1,000 cells in T-25 flasks depending on survival levels after irradiation. Cell numbers seeded will vary depending on dose received and expected cell survival, but in general are plated at 50 cells per square centimeter for the transformation assay and 5 cells per square centimeter for the plating efficiencies

(Mendonca et al. 1993, Mendonca et al. 1989). After seven days, the flasks are fed (growth media is replaced) twice a week leading up to 21 days (Redpath et al. 1987, Sun et al. 1988). The cells are then fixed in paraformaldehyde, rinsed with PBS and then stained with Western Blue to detect the neoplastically transformed ALPI positive colonies (stained foci) via stereomicroscopy. A general timeline of the CGL1 neoplastic transformation assay is shown in Figure. 2.

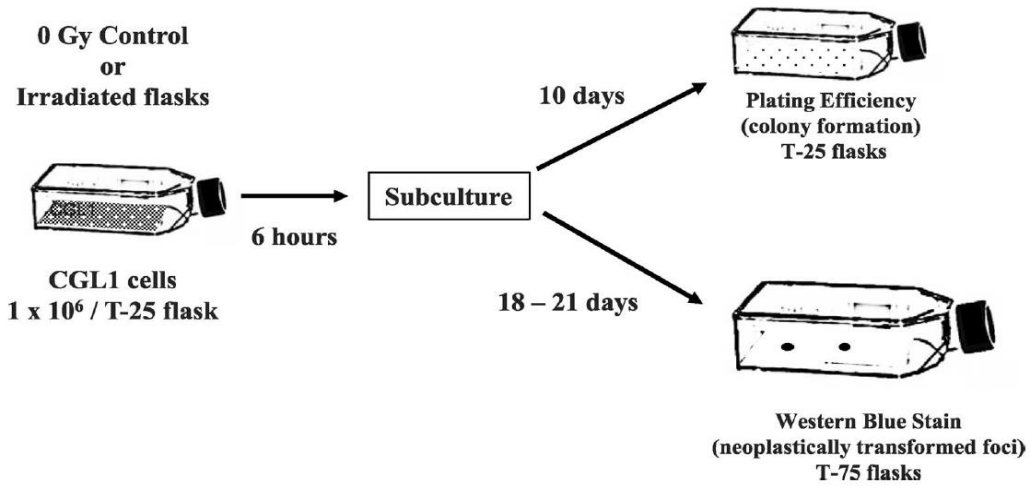

Figure 2: A general timeline of the *in vitro* CGL1 neoplastic transformation tissue culture assay

Neoplastic transformation frequency is calculated by counting the number of stained ALPI positive foci within each flask and the number of surviving cells in the T-75 transformation flasks calculated from the plating efficiencies. The neoplastic transformation efficiency is calculated by two methods. In the first method, the neoplastic transformation frequency (TF) is calculated by dividing the total number of neoplastically ALPI positive foci observed in all the transformation flasks at each radiation dose by the number of total surviving CGL1 cells at that radiation dose (Mendonca et al. 1990, Redpath 1987). In the second method, the fraction of transformation flasks containing foci at each radiation dose are calculated by simply diving the number of flasks with foci by the total number of flasks plated at each radiation dose (Kennedy et al. 1984, Mendonca et

al. 1990, Redpath 1987).

2.7. Summaries of CGL1 radiation induced transformation (TF) assays gamma-ray data

The initial studies of radiation induced neoplastic transformation of CGL1 were performed with Cs-137 gamma rays. Redpath and colleagues demonstrated that the spontaneous background neoplastic transformation frequencies for the 21-day neoplastic transformation assay with CGL1 cells *in vitro* was variable, but in the range of 0.1 to 1×10^{-5} (Mendonca et al. 1992, Redpath et al. 1987, Sun et al. 1988). Gamma-ray dose response studies at 2, 4, 7 and 10 Gy showed increasing radiation induced neoplastic transformation frequencies from 1×10^{-4} at 2 Gy, up to 6 to 8×10^{-4} at 7 and 10 Gy. Both the spontaneous and radiation induced neoplastic transformation frequencies were found to be strongly dependent on initial cell density plated into the transformation flasks, pH of the growth medium, length of incubation period after irradiation before re-plating for the transformation assay and the total length of the neoplastic transformation assay (Mendonca et al. 1990, Redpath 1987, Redpath 1988, Redpath et al. 1989, Sun et al. 1988, Sun et al. 1988). In general, the optimal conditions that produced the most consistent results in terms of induction of radiation induced neoplastic transformation frequency per Gy of ionizing radiation are: 1. wait 6 h post irradiation sub-confluent monolayers of CGL1 cells before plating the cells in T-25 flasks for cell survival and into T75 flasks for the neoplastic transformation assay; 2. adjust the plating density of the CGL1 cells in the neoplastic transformation T-75 flasks to 50 cells per cm^2 for the controls at 0 Gy and for each ionizing radiation dose level being investigated; 3. beginning on day 7 or 8 post-plating feed all the transformation flasks two times per week to maintain the pH between 7.2 and 7.4 in the transformation flasks; 4. on day 9 or 10 post-plating fix and stain the

T-25 survival flasks with 70% ethanol and crystal violet and count colonies and determine survival at 0 Gy and the various X-ray doses to be investigated; 4. on days 19 to 21 post-plating fix the cell monolayers in the T-75 transformation flasks with paraformaldehyde in PBS and stain with Western Blue to detect the neoplastically transformed ALPI positive foci; 5. gently rinse the transformation flasks several times with PBS at pH 7.2 and leave the last PBS rinse in the flasks; 6. visually score each transformation flask for blue neoplastically transformed foci by eye and with a stereo-microscope; 7. calculate transformation frequency by dividing the number of foci detected at the 0 Gy and the various X-ray doses being investigated by the number of total viable cells at risk for the 0 Gy and X-rays doses tested.

2.8. Kinetics of foci development, delayed death and apoptosis

For several decades, research has been done to investigate the delayed expression/appearance of ionizing radiation induced neoplastically transformed foci in CGL1 cell cultures (Lewis et al. 2001, Mendonca et al. 1993, Mendonca et al. 1999, Mendonca et al. 1999, Mendonca et al. 1989, Mendonca et al. 1998). It was initially proposed that the observed delay in foci formation was due to insensitivity of the detection method, however as previously mentioned, with the advent of the WB staining method this was no longer a plausible explanation. However, during the initial characterization it was shown that plating efficiency in irradiated cells never reaches the same levels as un-irradiated cells during the 21-day assay, but reaches a plateau at a lower plating efficiency level at day 9 or 10 and then surprisingly the PE began to significantly decrease for the next 10 days (Mendonca et al. 1993, Mendonca et al. 1989, Mendonca et al. 1998). A decrease in plating efficiency of un-irradiated CGL1 cells in the transformation flasks does not occur during the 21-day assay period. It was eventually shown that this reduction of PE was due to the onset of

delayed death or lethal mutations in the progeny of the irradiated CGL1 cells due to the onset of genomic instability (Mendonca et al. 1993, Mendonca et al. 1989, Mendonca et al. 1998). Further studies demonstrated that this expression of delayed death and reduction in PE was due to the induction of a novel form of delayed apoptosis involving p53 transcriptional upregulation and induction of the pro-apoptotic BAX mRNA and protein (Mendonca et al. 1998). It was subsequently shown that that this delayed apoptosis was not due to an aberrant acute apoptosis as this was clearly detected in later studies with the CGL1 assay (Mendonca et al. 2005).

2.9. Adaptive response and bystander effect studies with CGL1

The above data with the CGL1 system was focused on relatively high doses of X-rays and gamma rays, however there was also strong interest in understanding the radiation biology of very low doses of ionizing radiation and any potential role for bystander or adaptive and protective responses that may be important at lower radiation doses. Adaptive responses are defined to be altered responses that are observed when cells are first exposed to a low dose of radiation and subsequently challenged with a higher dose versus the response observed with the higher radiation dose alone. The first studies into adaptive response in the context of neoplastic transformation showed that a priming low dose radiation exposure changed the efficacy of a challenge dose to induce damage and led to suppression of neoplastic transformation in mouse cell line C3H10T1/2 (Azzam et al. 1996, Azzam et al. 1994). Interestingly, these data also indicated that very low doses of radiation reduced the levels of neoplastic transformation frequency below that of the un-irradiated spontaneous controls. Several studies have explored these very low dose adaptive responses in CGL1 cells (Elmore et al. 2008, Ko et al. 2006, Lewis et al. 2001, Redpath 2004, Redpath et al. 2007, Redpath et al. 2001, Redpath et al. 2003). In one of the initial studies, CGL1

cells were irradiated with 1 cGy of gamma radiation and incubated for 24 h (Redpath et al. 1998). The transformation frequency was found to be significantly reduced in cultures that had been held for 24 h after receiving a priming dose of 1 cGy as compared to un-irradiated controls or cells that had received 1 cGy but had been plated immediately. A later experiment looked at the use of 0.1, 0.5, 5 and 10 cGy of gamma radiation on the effect of neoplastic transformation in CGL1 cells that had similarly been held prior to plating (Redpath et al. 2001). It was observed in pooled data that transformation frequency was reduced for the low dose irradiated CGL1 cells when compared to sham-irradiated CGL1 cells (Redpath et al. 2001). The transfer of cell culture medium from irradiated cell cultures has been shown to reduce survival in to un-irradiated cell cultures (Mothersill et al. 1998, Seymour et al. 2000, Seymour et al. 1997). This bystander effect has been proposed to occur via cellular gap junction interactions, or excreted cell signal/cytokine based mechanisms (Azzam et al. 1998, Grosovsky 1999, Prise et al. 1998, Zhou et al. 2000). It has been shown in studies that media transfer from irradiated CGL1 cell cultures was able to effect plating efficiencies significantly when transferred to un-irradiated CGL1 cells and significantly increased the neoplastic transformation frequency above the CGL1 spontaneous neoplastic transformation frequency (Lewis et al. 2001). In addition, the CGL1 bystander study demonstrated that bystander effects were not only cytotoxic but also carcinogenic (Lewis et al. 2001).

2.10. Low-dose and dose-rate radiation studies

Dose and dose rate as well as radiation type and quality play a crucial role in the biological effects of ionizing radiation. There has long been a scientific interest in the biological effects of ionizing radiation at very low-dose (i.e., <100cGy) and dose-rate exposures for a variety of radiation types. Furthermore, elucidating the effects this has on neoplastic transformation and any potential

hormetic response is of significant importance. Some of the first initial low dose studies utilized the C3H10T1/2 neoplastic transformation model. Investigation of these subtle low dose effects, that were undetectable in normal cell cultures, were now possible with C3H10T1/2 cells (Azzam et al. 1996, Raaphorst et al. 1985, Reznikoff et al. 1973). These initial low-dose C3H10T1/2 studies (Azzam et al. 1996, Azzam et al. 1994) explored low dose and adaptive responses with an assortment of doses and dose rates as well as types of radiation, often with nonlinear results.

It was shown that a single ionizing radiation (γ ray) dose of 1–100 mGy at a dose rate of 2.4 mGy min^{-1} lowered the frequency of neoplastic transformation below the spontaneous level (Azzam et al. 1996). It was also shown that chronic doses (0.1, 0.65 or 1.5 Gy at a dose rate of 0.0024 Gy min^{-1} of γ rays) protected against an acute challenge dose of 4 Gy (X-rays). In these studies it was noted that protective level from acute challenge was not dependent on the size of the initial adaptive dose, potentially indicative of a no threshold switch based mechanism (Azzam et al. 1994). Analogous studies into these low dose effects were continued in the CGL1 human hybrid cell system after its development. Similar to C3H10T1/2 model, the CGL1 neoplastic transformation model was found to be an appropriately sensitive system for the detection of very low radiation dose effects (Redpath et al. 1998, Redpath et al. 2001, Redpath et al. 2003), that have not been observed in other tissue culture models (Mendonca et al. 1992, Redpath et al. 1987).

A range of radiation types, dose rates and doses have been investigated with CGL1, and as has been reported with the C3H10T1/2 assays, these data demonstrate interesting non-linear results at low dose and dose rates. For example, in one study, CGL1 cells were exposed to fission spectrum neutrons at two dose rates, 0.22 cGy min^{-1} and 10.7 cGy min^{-1} to achieve a total dose of 45 cGy (Redpath et al. 1995). The low-dose-rate was determined to be more effective at inducing re-expression of ALPI and neoplastic transformation of CGL1 cells without any evidence of

increasing cell death. Using the Western Blue detection method, this study showed an inverse dose rate effect on rates of neoplastic transformation as had been shown previously with fission spectrum neutrons using the older immunohistochemical detection method (Redpath et al. 1990, Redpath et al. 1991). This effect had been originally shown in C3H10T1/2 cells also using fission spectrum neutrons (Hill et al. 1982, Hill et al. 1984). In another study, 60kVp X-rays at doses of 0, 0.04, 0.1, 0.4, 4.0, 9.0, 18.0 and 36.0 cGy were used to assess neoplastic transformation frequency in CGL1 cells. A significant decrease in transformation frequency was observed at 0.04, 0.1 and 0.4 cGy, as well as at 4.0 and 9.0 cGy (though not significantly) as compared to 0 cGy controls. In an analogous study using the CGL1 model system, gamma radiation (667 KeV photons) from a Cs-137 source showed a similar trend (Redpath et al. 1998, Redpath et al. 2001). Taken together the data indicate that at these very low radiation doses there is a "U" or "J" shaped dose-response curve for radiation induced neoplastic transformation. This suggests that at very low doses of ionizing radiation, the initial decrease in neoplastic transformation frequency investigators have observed may be due to induction of an adaptive/protective hermetic response to very low-dose radiation exposure, which disappears as the dose of radiation increases.

A study of diagnostically and medically relevant levels of X-rays (28 kVp) showed suppression of transformation frequency in a dose range of 0.05–10 cGy to levels below that of no dose control exposures (Ko et al. 2004). A study utilizing doses of 0–600 mGy protons (232 MeV) in CGL1 (Elmore et al. 2005) further showed evidence of neoplastic transformation suppression at doses up to 50mGy. Interestingly these low-dose and dose-rate U-shaped dose-response curves for neoplastic transformation do not support a linear no threshold model. Rather, these data suggest that there appears to be a threshold for which low-dose and dose-rate ionizing radiation in a variety of qualities can suppress transformation.

2.11. Mechanisms of IR induced neoplastic transformation of CGL1 cells

Gamma-radiation induced mutants (GIMs) and control (CON) cell lines were isolated from CGL1 neoplastic transformation assays (Mendonca et al. 1991, Mendonca et al. 1989). These GIMS were selected for radiation induced re-expression of the tumorigenic marker intestinal alkaline phosphatase to further investigation the correlation between ALPI expression, tumorigenicity and the molecular mechanisms involved in the radiation induced expression of CGL1 cells. The GIMS were found to be quite morphologically distinct from CGL1, and while the isolated cell lines all had variable levels of ALPI expression, all were found to be tumorigenic when subcutaneously injected into nude nu/nu mice (Mendonca et al. 1991). The CON cell lines are morphologically quite similar to CGL1 as well as ALPI negative and non-tumorigenic, but were isolated from 7 Gy gamma-irradiated CGL1 cells. These data indicated that exposure to radiation and any random subsequent chromosomal or genomic changes alone were not sufficient for malignancy, but that re-expression of ALPI and the specific underlying chromosomal, genomic, and molecular changes associated with ALPI re-expression appeared to be involved.

The initial experimental analysis of CGL1 and the subsequent isolated GIM variants suggested that the loss of a single copy of chromosomes 11 and 14 correlated with both ALPI re-expression as well as malignancy determined by subcutaneous injection in nu/nu mice (Kaelbling et al. 1986, Saxon et al. 1986, Srivatsan et al. 1986, Stanbridge et al. 1981). Previous investigators had shown the microcell mediated transfer of fibroblast chromosome 11 back into the spontaneously arising tumorigenic CGL3 hybrid cells caused a suppression of ALPI expression as well as tumorigenicity (Saxon et al. 1986). Later work by Mendonca *et al.* found that late passage subclones of CON1 (Mendonca et al. 1995, Mendonca et al. 1998) lost one copy of the fibroblast chromosome 11, but

were still negative for ALPI expression. Analysis of GIM and CON cell lines by RFLP and chromosome painting suggested that both copies of fibroblast chromosome 11 contained a putative tumor suppressor locus, and that the loss or inactivation of both tumor suppressor loci would result in radiation induced neoplastic transformation *in vitro* (Mendonca et al. 1995). Fine mapping with PCR based markers confirmed loss of one copy of the fibroblast chromosome 11 in the radiation induced tumorigenic GIMs and evidence of a small 5–20 kB deletion in the remaining copy of the fibroblast chromosome 11 (Mendonca et al. 2004). These deletion mapping studies identified PACS-1, FRA-1, GAL3ST2 and SF3B2 and RAB1B as candidate tumor suppressor genes (Mendonca et al. 2004).

2.12. Future directions: SNOLAB - an ultra-low dose research environment

Life has evolved in the ubiquitous presence of ionizing radiation, from natural sources both terrestrial and cosmic. Terrestrial sources of radiation are radioactive elements found in rocks, soil, water and air. This includes isotopes of uranium, thorium and potassium, as well as their daughter products, predominantly radon gas. Galactic cosmic radiation (GCR) in space largely consists of high-energy particles, positively charged ions and larger nuclei. These cosmic particles produce secondary radiation in the Earth′s atmosphere, which can reach the surface of the planet and interact with organisms. This natural background radiation (NBR) pervades the Earth's surface and, as such, is a normal component of biological life. However, NBR levels are dependent on several factors, including altitude, terrestrial geology and geomagnetic field. Annual doses from NBR can range from 2–260 mSv depending on location, with some evidence suggesting that even within this range of NBR levels biological effects are observable (Attar et al. 2007, Ghiassi-nejad et al. 2002, Ghiassi-Nejad et al. 2004, Masoomi et al. 2006, Yazdani et al. 2009, Zakeri et al.

2011).

Many current radiobiological studies investigate responses to low doses and dose rates of ionizing radiation and these data yield important models for the associated health risks of these exposures. The hypersensitivity model suggests that there is a greater biological risk at lower doses of radiation (Joiner et al. 2001)**.** The linear no threshold model proposes that cancer risk increases with radiation dose in a linear relationship while the threshold model infers that below a certain dose there is no increased risk (Martin 2005)**.** The hormetic model suggests that below a given dose, instead of increased risk, the health effects may be prophylactic (Scott 2014)**.** However, all of these models inherently include NBR exposure and consequently there is a deficit in our understanding of the biological effects of ionizing radiation exposure at levels sub-NBR.

Over the last four decades, little has been elucidated about the biological effects of ultra-low NBR environments, although some interesting observations have been published. Work with *Paramecium caudatum* involved cultures grown within lead shielded chambers designed to minimize GCR (Planel et al. 1976). An inhibition of cellular division and subsequent decrease in growth rate in the cultures was observed as compared to those grown in a basal NBR environment. Furthermore, the attenuated growth rates returned to normal levels when exposed to externally generated radiation at levels and rates analogous to NBR. This work was recently replicated (Kawanishi et al. 2012) and comparable results have also been observed in *Synechococcus lividus* (Conter et al. 1983). These experiments presented an important initial case for the significant stimulatory effect of terrestrial and cosmic NBR on cellular proliferation, with a potential role of ROS considered (Croute et al. 1982, Planel et al. 1987). There has been limited use of subterranean laboratory facilities to shield cultures from GCR including work with the extremely radiation resistant bacteria *Deinococcus radiodurans* (Castillo et al. 2015) and diploid yeast *Saccharomyces*

cerevisiae (Satta et al. 2002). These cultures were grown underground in the Waste Isolation Pilot Plant (WIPP) in New Mexico, United States and the Gran Sasso National Laboratory (LNGS) in Abruzzo, Italy, respectively. The trend amongst these different model systems grown in sub-NBR environments is of negative biological effects in terms of growth rate and susceptibility to challenge with chemical and radiological stressors (Gajendiran et al. 2002). One of the most significant gaps in these limited data is the insufficient amount of experimentation with mammalian cells, though a few preliminary experiments have been performed. Chinese hamster V79 and Human lymphoblastoid TK6 cells grown underground in LNGS and WIPP were shown to have decreased cell density, lowered ROS scavenging, increased background and induced mutation rate, increased apoptotic sensitivity, greater micronuclei formation and increased expression of certain heat shock proteins (Carbone et al. 2009, Carbone et al. 2010, Satta et al. 2002, Smith et al. 2011).

Although these findings are important to begin to understand the biological effects of sub-NBR exposure, there is significant variation between research groups in terms of the model organism used, type of shielding and level below NBR achieved experimentally. One of the most significant factors behind the dearth of empirical data is simply the scarcity of facilities that can accommodate this type of research. However, it is unquestionable that the ideal location to perform this type of research is underground, rather than at the surface of the planet where GCR contamination is intrinsic. Located approximately 30km from Laurentian University and The Northern Ontario School of Medicine (NOSM) in Sudbury, ON, Canada, there exists a world-class Canadian research facility that has been specifically engineered and constructed to effectively eradicate GCR. The Sudbury Neutrino Observatory (SNOLAB) is a Nobel Prize winning astroparticle physics laboratory located in Vale's active Creighton Nickel Mine and has the deepest and lowest

NBR biological research laboratory environment in the world. Situated 2km (6,800 ft.) underground, it is incomparable to any other facility in terms of depth and proximity to Laurentian University and NOSM. The facility is comprised of 5,000 m^2 of Class 2000 clean room (maximum 2×10^3 particles ≥ 0.5 μm/ft^3) located within norite rock, which consists of 1% stable K^{39} (~0.001% radioactive K^{40}), 0.13 ppm uranium and 5.56 ppm thorium (Smith 2012). The 2,070 m of rock overburden above SNOLAB provides within the facility an attenuated muon flux of 3×10^{-6} m^{-2} s^{-1}, a thermal neutron flux of 4.7×10^{-2} m^{-2} s^{-1} and a fast neutron flux of 4.6×10^{-2} m^{-2} s^{-1} (Smith 2012). This translates to approximately 50 million times less GCR than would be measured at the surface. Radon gas (Rn^{222}) is the most profuse and challenging radiological issue facing sub-NBR experiments underground and is present within SNOLAB at an average level of approximately 130 Bq m^{-3}. Attempts to keep radiological contamination of terrestrial origin are a major priority within the facility, as the ore dust in the active mine located outside of the facility contains approximately 60 mg g^{-1} Fe, 1.1 μg g^{-1} U and about 5.6 μg g^{-1} Th (Boger et al. 2000). This is achieved, in part, by 10 full HEPA filtered air exchanges h^{-1} within SNOLAB. This air is scrubbed and recirculated to help reduce increased radon emanation (Smith 2012). Additionally, there is an 8.0-mm thick polymer coating over the rock walls within SNOLAB to further address this issue (Smith 2012). Low levels of neutrons and gamma rays still infiltrate via this polymer coating through spontaneous fission of elements radioactive decay, but remain at levels still far below surface NBR.

2.13. Future directions: CGL1 ultra low dose studies

We propose to utilize the exceptional ultra-low ionizing sub-NBR environment that SNOLAB offers to quantitatively assess biological effects in an established human tissue culture model. The working hypothesis is that ionizing NBR promotes and maintains genomic stability through highly conserved adaptive response mechanisms and that the absence of which will lead to reduced cell growth, increased neoplastic transformation rates, sensitivity to oxidative stress and higher baseline levels of DNA damage. The CGL1 cell line is an ideal tissue culture system for quantitatively investigating the biological effects of an ultra-low dose radiation environment. We propose to use CGL1 cells to whether growth in the ultra-low background radiation available in SNOLAB influences CGL1 population doubling time, plating efficiency, spontaneous levels of DNA damage repair by micronucleus formation and γH2AX formation assays and spontaneous levels of neoplastic transformation in CGL1 cells grown underground in SNOLAB compared to CGL1 cells kept at the surface control laboratory space. If we observe differences in the CGL1 cells grown at ultra-low dose radiation levels down in SNOLAB versus CGL1 cells grown natural background radiation (NBR) levels at the surface lab, we will evaluate gene expression differences by cDNA microarray and quantitative RT-qPCR assays to observe regulatory changes that may occur as culture time in the sub-NBR increases analyses and determine the genetic and epigenetic mechanisms driving these changes and will provide important mechanistic information in the evaluation of how ultra-low doses of radiation alter CGL1 cells.

The Western Blue based CGL1 cell neoplastic transformation assay is highly sensitive and has been used to detect very small changes spontaneous transformation frequency when the cells are irradiated with a few mGy of ionizing radiation (Elmore et al. 2008, Elmore et al. 2005, Ko et al.

2006, Redpath et al. 1998, Redpath et al. 2001, Redpath et al. 2003). Therefore, we propose that in the ultra-low radiation environment that SNOLAB provides, the CGL1 based transformation assay is ideal to detect small changes in spontaneous background neoplastic transformation frequency.

SNOLAB's ultra-low dose sub-NBR environment and close proximity to both Laurentian University and the Northern Ontario School of Medicine provide the ideal environment for the recently established "Researching the Effects of the Presence and Absence of Ionizing Radiation" (REPAIR) project. These facilities will allow us to test whether CGL1 cells, adapted to the ultra-low dose NBR environment underground, will alter either the spontaneous, X-ray and/or radon-induced levels of neoplastic transformation and the cellular and molecular mechanisms involved. CGL1 cell growth rate, micronucleus and γH2AX, changes in gene expression, rates of neoplastic transformation and capacity to react to changes in oxidative stress levels will be assessed in sub-NBR adapted CGL1 cells grown underground in SNOLAB versus the CGL1 cells kept at surface NBR doses. We strongly believe that the resulting SNOLAB data will be of high scientific value and will contribute to a better understanding of ultra-low dose radiation biology.

2.14. Acknowledgements

The REPAIR project is financially supported through an industrial research grant from Bruce Power, the Mitacs Accelerate program and the Natural Sciences and Research Council of Canada.

Chapter 3: Transcriptomic Profiling of Gamma Ray Induced Mutants from the CGL1 Human Hybrid Cell System Reveals Novel Insights into the Mechanisms of Radiation Induced Carcinogenesis

Jake Pirkkanen[a,], Sujeenthar Tharmalingam[b], Igor H. Morais[a], Daniel Lam-Sidun[b], Christopher Thome[b], Andrew M. Zarnke[a], Laura V. Benjamin[c], Adam C. Losch[c], Anthony J. Borgmann[c], Helen Chin Sinex[c], Marc S. Mendonca[c] and Douglas R. Boreham[b,d]

[a,]Laurentian University, 935 Ramsey Lake Rd, Sudbury, Ontario, P3E 2C6, Canada
[b] Northern Ontario School of Medicine, 935 Ramsey Lake Rd, Sudbury, Ontario, P3E 2C6, Canada
[c]Department of Radiation Oncology, Radiation and Cancer Biology Laboratories, and Department of Medical & Molecular Genetics, Indiana University School of Medicine, Indianapolis, Indiana 46202, USA
[d] Bruce Power, PO Box 1540, 177 Tie Rd, R.R. 2, Tiverton, Ontario, N0G 2T0, Canada

[*In review*: Free Radical Biology and Medicine]
Submitted March 16th 2019

3.1. Introduction

Recent technological advances have rapidly changed the ability to investigate the mechanisms of neoplastic transformation in human cells. Modern tools such as omics-based techniques can probe differences in gene expression at an unprecedented global level. Combined with pathway level analyses that reference annotated data, these techniques can aid in the discovery of novel molecular signatures that drive carcinogenesis, many of which are currently unknown or not well established.

Somatic cell hybrid systems generated by combining cancerous with non-cancerous cells provide useful model systems to study neoplastic transformation (Kaelbling et al. 1986, Klinger 1980, Stanbridge 1987, Stanbridge et al. 1982). The resulting segregant cells demonstrate a range of genetic and phenotypic properties that can be utilized to identify pathway level mechanisms which regulate carcinogenesis at a molecular level. The non-tumorigenic CGL1 human hybrid cell line is derived from the hybridization of a tumorigenic HeLa cell and a normal human fibroblast. The CGL1 system and related cell lines have been studied extensively for many decades to investigate radiation induced neoplastic transformation (Pirkkanen et al. 2017). It is an excellent system used for both quantitative and mechanistic studies of radiation induced transformation. Tumorigenic gamma-induced mutant (GIM) and non-tumorigenic gamma irradiated control (CON) segregants were both isolated independently from irradiated CGL1 cells (Mendonca et al. 1991, Mendonca et al. 1989). These cell lines represent a unique opportunity to better understand the underlying molecular mechanisms which contribute to ionizing radiation mediated tumorigenic transformation in a human hybrid cell line.

Here, we present a whole-transcriptome gene expression profiling and pathway level enrichment analysis of radiation induced tumorigenic GIM and non-tumorigenic CON cells. Using the

GeneChip Human Transcriptome 2.0 Array, we have identified 1,067 differentially expressed genes (DEGs) between tumorigenic GIMs and non-tumorigenic CONs using conservative cutoff thresholds for fold change and p-value. Additionally, 72 pathways were found to be significantly impacted as well as 930 Gene Ontology (GO) terms significantly enriched. Enriched GO terms suggest shifts in ECM and cellular adhesion profiles, dysregulation of cyclic AMP (cAMP) signaling, and alterations in nutrient transport and cellular energetics as pathway level differences that may contribute to radiation induced carcinogenesis. Furthermore, putative upstream master regulator analysis in addition to functional assays revealed that reduced in SMAD3 expression resulted in down-regulation of TGFβ1 signaling in tumorigenic GIMs. This study provides novel insights into gene expression and pathway level differences that are involved in radiation induced carcinogenesis in the CGL1 human hybrid cellular system.

3.2. Materials and Methods

3.2.1. Cell culture

CGL1, GIM and CON cell lines were originally established and isolated as previously described (Mendonca et al. 1991). Briefly, CGL1 was isolated from the original tumorigenic ESH5 HeLa x normal fibroblast hybrid. Tumorigenic GIM cell lines (GIM4B, GIM12D, GIM18A, GIM19E, GIM30DE, GIM31DA) and non-tumorigenic CON cells lines (CON1, CON2, CON3 and CON5) were independently isolated from CGL1 cells exposed to 7 Gy of γ radiation (Figure 3A). All cell lines were incubated in humidity at 37°C with 5% CO_2, in 1X Minimum Essential Medium (Corning, 10-010CV) supplemented with 5% calf serum (Sigma, C8056) and 1% Penicillin-Streptomycin (Corning, 30001CI). Representative photomicrographs of sub-confluent cell cultures in T-75 flasks were imaged on an EVOS XL Core microscope (Thermo Fisher Scientific) at 10X

magnification (Figure 3B).

3.2.2. Alkaline phosphatase assay

Alkaline phosphatase activity was quantified using an Alkaline Phosphatase Assay Kit (abcam, ab83369). Using $1x10^6$ cells, the assay was performed in 96-well plates and quantified on a PowerWave XS microplate reader (BioTek) at 405nm.

3.2.3. RNA extraction

Total RNA isolation was performed utilizing either a kit-based or phenol/chloroform extraction method adapted from Rio et al. 2010 (Rio et al. 2010). For kit-based extractions, RNA was isolated using a RNeasy Mini Kit (Qiagen, 74104) with inclusion of QIAshredder columns (Qiagen, 79654) followed by on-column DNAse digestion (Qiagen, 79254). Extracted RNA was subjected to DNAse I (Sigma, AMPD1) treatment. Quantity and quality of RNA extractions was analyzed by gel electrophoresis and NanoDrop spectrophotometry (Thermo Fisher, ND-1000).

3.2.4. cDNA Synthesis

cDNA was synthesized in 50 µL reaction volumes consisting of 2µg DNase treated RNA, 1 µg random hexamers (Sigma, 11034731001), 2.5µL of 10mM mixed dNTPs (VWR, CA71003-178, CA71003-180, CA71003-182, CA71003-184), 10uL of 5X M-MLV reaction buffer (Promega, M531A), and 2 µL of 200U μL^{-1} M-MLV reverse transcriptase (Promega, M1708).

3.2.5. Design and validation of RT-qPCR primers

Forward and reverse primer pairs for qPCR analysis were designed in-house and validated under stringent conditions: primers with a reaction efficiency between 90% to 110% and R^2 value >0.99

were considered validated and acceptable for qPCR analysis. Optimal annealing temperature for each primer pair was identified by performing temperature gradient analysis. Appendix B lists the primer sequences and relevant information for all genes analyzed via RT-qPCR.

3.2.6. RT-qPCR sample preparation, thermocycling conditions and data analysis

SYBR green based RT-qPCR experiments were performed in 15µL reaction volumes using the Quantstudio 5 qPCR instrument (ThermoFisher Scientific). Final reaction mix included 1X SensiFAST Sybr Lo-Rox qPCR mastermix (FroggaBio, CSA-01195), 600 nM forward and reverse primers and 7.5 ng of input cDNA. The following qPCR protocol was followed for 40 cycles: 95 ˚C for 30 seconds, 60 or 62˚C for 30 seconds, 72˚C for 30 seconds, then readout of the plate data. Following 40 cycles, primer melt curve analysis was run to validate single amplicon specificity. Cycle threshold (C_T) data was analyzed using the QuantStudio™ Design and Analysis Software v1.4.1 (Applied Biosystems). Samples were normalized to the geometric mean of three control housekeeping genes: HSPC3, RPS18 and GAPDH. Relative expression of genes was calculated utilizing the $\Delta\Delta C_T$ method using the following formula: $2^{\Delta\Delta}C_T = 2^{(\Delta C_T \text{ gene} - \Delta C_T \text{housekeeping genes})}$. Average $2^{\Delta\Delta}C_T$ and standard error of the means (SEMs) were calculated.

3.2.7. Human Transcriptome Array 2.0

The following cell lines were utilized in microarray experiments: non-tumorigenic CGL1, CON1, CON2, CON3 and CON5 cells, and tumorigenic GIM4B, GIM12D, GIM18A, GIM19E, GIM30DE, and GIM31DA cells. Isolated RNA was processed at The Centre for Applied Genomics (TCAG) Microarray Facility (The Hospital for Sick Children, ON, Canada). RNA integrity analysis was performed at TCAG (Agilent 2100 Bioanalyzer, Agilent Technologies), and only samples with an RNA integrity number (≥8.0) and A:260/280 >1.95 were considered for

downstream use. Experimental samples were assayed at TCAG utilizing the GeneChip Human Transcriptome Array (HTA) 2.0 (ThermoFisher Scientific). Data were analyzed utilizing the Transcriptome Analysis Console (TAC) Software 4.0.0.25 (Thermo Fisher) with the Genome Reference Consortium Human Build 37 (hg19) as the reference genome. For data processing as well as sample number and statistical consideration, GIM and CON isolates were grouped for microarray analysis (n=6 and n=4 respectively). Differential gene selection criteria were as follows: <-2 or >2 for gene fold change and <0.1 for false discovery rate (FDR) corrected p-values.

3.2.8. GO enrichment analysis

Pathway level GO term enrichment analysis was evaluated using Advaita Bio's iPathwayGuide (iPG) (www.advaitabio.com/ipathwayguide). This analysis was performed utilizing the Kyoto Encyclopedia of Genes and Genomes (84.0+/10-26, Oct 17), and GO (2017-Nov6) online databases. For GO and significant pathway terms, iPG utilized the "Impact Analysis" approach as previously described (Draghici et al. 2007, Khatri et al. 2007, Tarca et al. 2009). In addition, Elim pruning (Alexa et al. 2006) or FDR correction was applied to GO and pathway analysis respectively with a p-value threshold of <0.05.

3.2.9. Upstream regulator analysis

Predicted upstream gene regulators and network analysis were generated through the use of the Ingenuity Pathway Analysis (IPA) software (QIAGEN Inc., www.qiagenbio-informatics.com/products/ingenuity-pathway-analysis). Upstream regulators were considered statistically significant when overlap p-value was <0.01 and with activation Z-score of <-2 or >2.

3.2.10. TGFβ assay

TGFβ1 (abcam, ab50036) was resuspended in a diluent of 10mM citric acid (Fisher, A104) pH 3.0, 1X PBS (Fisher, BP399-1) and 2mg/mL albumin (Sigma, A7906). 48 hours prior to the start of the assay, $1x10^5$ GIM19 or CON2 cells were seeded into T25 flasks. TGFβ1 was added to the cells in the experimental wells at a final concentration of 5ng/uL with equal volume of diluent added to control wells respectively. At 0, 4, 8, 16 and 24 hours post addition of 5ng/uL TGFβ1, media was aspirated, cells were washed with 1mL ice cold 1X PBS, followed by addition of 1mL of TRI Reagent (Sigma, T9424). Flasks were sealed with paraffin and placed into a -80°C freezer until sample processing.

3.2.11. Statistics

For the alkaline phosphatase activity assay and RT-qPCR experiments, data is presented as mean ± SEM. Comparisons between groups were performed using one-way ANOVA followed by Tukey's post-hoc analysis. A resulting p-value of <0.05 was considered statistically significant. Statistical methodology for transcriptome analysis is detailed in the TAC User Guide (assets.thermofisher.com/TFS-Assets/LSG/manuals/tac_user_manual.pdf). Briefly, one-way ANOVA (ebayes) was performed and False Discovery Rate (FDR) p-value correction was applied. For pathway level analysis, iPG utilized the Impact Analysis method (Draghici et al. 2007, Khatri et al. 2007, Tarca et al. 2009). GO term (Ashburner et al. 2000) p-values were calculated in iPG using the hypergeometric distribution (Draghici et al. 2007, Khatri et al. 2007, Tarca et al. 2009). Statistically significantly enriched GO terms were further pruned by the Elim method (Alexa et al. 2006). For IPA upstream regulators analysis, statistical methods for obtaining overlap p-value of enriched genes within a network and the activation z-score is previously described (Kramer et al.

2014).

3.3. Results

3.3.1. Verification of CON and GIM cell lines

Intestinal alkaline phosphatase (ALPI) expression and function have been previously established as the canonical marker of tumorigenicity in the CGL1 cell system (Der et al. 1981, Latham et al. 1990, Mendonca et al. 1991). To verify whether CGL1, CON and GIM cell lines demonstrated appropriate tumorigenic profiles, alkaline phosphatase expression and activity were determined. RT-qPCR analysis of ALPI mRNA expression demonstrated minimal ALPI mRNA levels in CGL1 and CONs, whereas GIMs expressed 500 to 2000-fold ALPI mRNA compared to CONs (Figure 3C).

Alkaline phosphatase activity was determined by colorimetric assay (Figure 3D). As expected, the non-tumorigenic cell line CGL1 and CON segregants demonstrated very little alkaline phosphatase activity (0.02 Units/mL on average). Conversely, the tumorigenic GIM segregants showed robust dephosphorylation activity ranging from 0.94 to 7.52 Units/mL. Taken together, these results demonstrate that expression and activity of a known marker in this cell system appropriately correlates with previously established phenotypes.

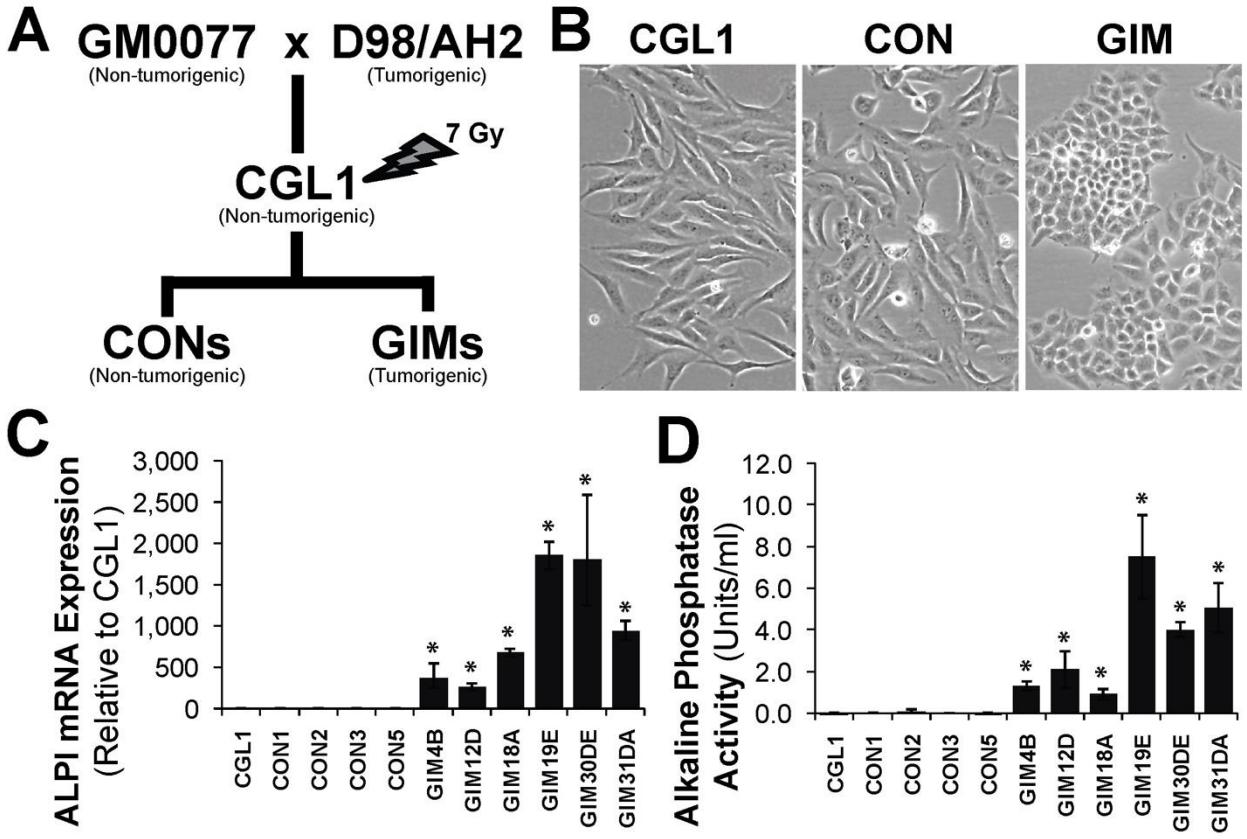

Figure 3: Hierarchy of experimental cell lines, representative photomicrographs and ALPI expression

(A) Hierarchical origins of experimental cell lines. CGL1 cells were derived from a normal human fibroblast (GM0077) and a tumorigenic HeLa cell (D98/AH2). Exposure of CGL1 cells to 7 Gy γ-radiation resulted in tumorigenic gamma-induced mutants (GIMs) and non-tumorigenic gamma irradiated controls (CONs). **(B)** Representative phase-contrast photomicrographs of CGL1, GIM (GIM19), and CON (CON2) cells (10X). **(C)** Intestinal alkaline phosphatase (ALPI) mRNA expression in the CGL1, CON and GIM cell lines. Average ALPI mRNA expression± SEM for non-tumorigenic (CGL1 and CONs) versus tumorigenic (GIMS) cells, represented as relative to CGL1 (N = 2). **(D)** Alkaline phosphatase (ALP) activity in the CGL1, CON and GIM cell lines. Average ALP activity in Units/ml ± SEM (N = 3). CGL1 and CON cells showed limited ALPI expression and activity (average = 0.02 Units/mL), whereas the GIMs demonstrated robust ALPI expression and activity (0.94 to 7.52 Units/m). Overall, ALPI mRNA expression correlates well with ALP activity. * denotes statistical significance between CGL1 ($p < 0.05$).

3.3.2. Transcriptomic Analysis

Microarray analysis revealed a total of 1,067 DEGs in GIM vs. CON, with 437 up-regulated and 630 down-regulated as represented in volcano plot form (Figure 4A). The full list of upregulated and down-regulated DEGs based on fold change are presented in Appendix C. Importantly, comparison of non-tumorigenic CGL1 and CON revealed no DEGs, demonstrating that CGL1 and CONs share similar transcriptomic landscape.

3.3.3. Unbiased Grouping Analysis

Exploratory grouping analysis of CGL1, CON and GIM transcriptome datasets resulted in a clear non-homogenous distribution of samples into two distinct clusters (Figure 4B). The cluster plot illustrates that the non-tumorigenic CON cells and the tumorigenic GIM cells aggregated in spatially disparate regions. Here, CGL1 clustered with CON cells, further demonstrating that CGL1 and CONs share similar gene expression profiles.

PCA mapping was performed on all transcriptome datasets after initial quality control data processing and the resulting scores for the first three principal components are presented in Figure 4C. The three principal components accounted for 76.0% of the variance in the datasets demonstrating that the 3-dimensional plot is an appropriate visual representation of the transcriptomic datasets. Given the statistical strength of the PCA plot, we conclude that the non-tumorigenic CGL1 and CON gene expression profiles are similar and tightly grouped while the tumorigenic GIM cells form a separate distinct grouping.

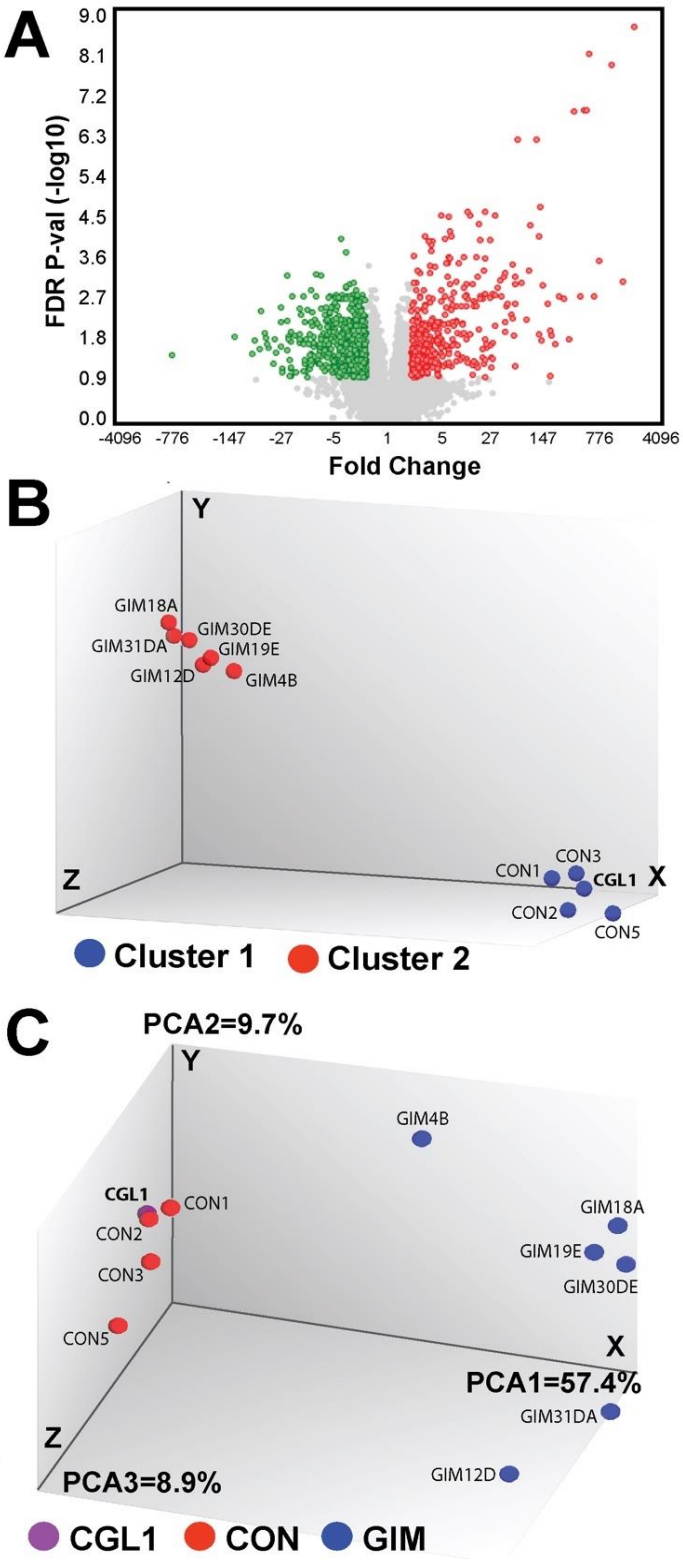

Figure 4: Volcano plot, exploratory grouping analysis and principal component analysis of GIM vs CON

(A) Volcano plot depicting the transcriptomic profile of the tumorigenic GIMs versus the non-tumorigenic CONs. The volcano plot was generated by plotting the negative log of the false discovery rate (FDR) p-value on the y-axis and the fold change on the x-axis. Highly dysregulated genes appear to the left and right sides of the plot, while genes higher on the graph indicate increased statistical significance. Differentially expressed genes in GIMs versus CONs with FDR p-value below 0.1 are marked in red (>2 fold change) and green (<-2 fold change). A total of 1,067 genes were dysregulated in GIMs relative to CONs, with 437 up-regulated and 630 down-regulated. **(B)** Exploratory grouping analysis (EGA) of whole-transcriptome datasets from non-tumorigenic CGL1 and CONs and tumorigenic GIMs. EGA analysis was performed without pre-defining known sample attributes. Data analysis indicates a clear non-homogeneous distribution of the cells into two distinct clusters: non-tumorigenic CGL1 and CONs (blue), and tumorigenic GIMS (red). **(C)** Principal component analysis (PCA) of microarray data. PCA was performed on all transcriptome datasets and the resulting scores for the first three principal components are presented. The three principal components accounted for 76.0% of the variance in the datasets. This analysis revealed that the non-tumorigenic CGL1 and CON gene expression are similar and tightly grouped while the tumorigenic GIM cells form a separate distinct grouping.

3.3.4. RT-qPCR Validation of Transcriptome Results

To corroborate the transcriptomic microarray results prior to further downstream analysis, selected genes from the array were cross-verified using RT-qPCR analysis. Genes were chosen to include top up and down-regulated DEGs as well as moderately expressed DEGs. A full list of the 54 genes analyzed via RT-qPCR analysis compared to microarray is presented in Appendix D. Comparison of fold changes between RT-qPCR and microarray data were generally similar and in the same order of magnitude taking into consideration probe and method differences between the two assays. Furthermore, directionality of gene expression was consistent between the two assays, providing validation for downstream microarray data analysis.

3.3.5. Transcriptome Pathway Analysis

In order to classify the biological profile of the 1,067 DEGs in GIMs relative to CONs, Gene ontology (GO) enrichment analysis was performed using iPG, which hierarchically ranks the co-occurrence of the DEGs with annotated genes from the GO classification system. Elim pruning was further applied to obtain GO terms with increased statistical significance. Table 2 presents the top GO terms for each of the three components, the number of DEGs in the experimental data compared to the total number of genes annotated to a given GO term and the statistical significance of the GO term.

Table 2: Gene ontology enrichment of differentially expressed genes in GIM vs CON

Top enriched GO terms categorized as biological processes, molecular functions and cellular components are presented. The number of DEGs identified in each GO term is provided along with the total number of genes annotated within the GO database (ALL). GO profiles suggest that the gene expression dataset for GIM demonstrates shifts in ECM and cellular adhesion profiles, as well as dysregulation of cAMP/PDE/PKA pathways when compared to CONs.

GO Term	Biological Process	# genes (DEG/ALL)	p-value
GO:0030198	extracellular matrix organization	46 / 329	3.50E-08
GO:0006198	cAMP catabolic process	8 / 17	9.20E-08
GO:0007155	cell adhesion	124 / 1305	3.40E-07
GO:0010718	positive regulation of epithelial to mesenchymal transition	11 / 47	1.40E-06
GO:0030501	positive regulation of bone mineralization	9 / 35	5.60E-06
GO:0030199	collagen fibril organization	10 / 44	5.70E-06
GO:0001938	positive regulation of endothelial cell proliferation	13 / 76	6.80E-06
GO:0043524	negative regulation of neuron apoptotic process	17 / 134	1.80E-05
GO:0001666	response to hypoxia	30 / 333	1.90E-05
GO:0051384	response to glucocorticoid	19 / 143	2.00E-05

GO Term	Molecular Functions	# genes (DEG/ALL)	p-value
GO:0004115	3',5'-cyclic-AMP phosphodiesterase activity	8 / 15	2.50E-08
GO:0045294	alpha-catenin binding	6 / 10	6.10E-07
GO:0051015	actin filament binding	18 / 153	2.70E-05
GO:0005201	extracellular matrix structural constituent	12 / 78	4.30E-05
GO:0038191	neuropilin binding	5 / 12	5.40E-05
GO:0043236	laminin binding	8 / 29	1.90E-04
GO:0046332	SMAD binding	16 / 73	2.30E-04
GO:0030215	semaphorin receptor binding	4 / 10	3.90E-04
GO:0042392	sphingosine-1-phosphate phosphatase activity	3 / 5	5.50E-04
GO:0043559	insulin binding	3 / 5	5.50E-04

GO Term	Cellular Components	# genes (DEG/ALL)	p-value
GO:0005925	focal adhesion	49 / 382	8.10E-14
GO:0009986	cell surface	66 / 751	8.60E-09
GO:0005916	fascia adherens	7 / 10	1.20E-08
GO:0005886	plasma membrane	285 / 5036	1.40E-08
GO:0001725	stress fiber	10 / 52	2.20E-05
GO:0005604	basement membrane	16 / 89	1.50E-04
GO:0030426	growth cone	16 / 148	1.70E-04
GO:0031225	anchored component of membrane	16 / 154	2.70E-04
GO:0030667	secretory granule membrane	24 / 290	3.20E-04
GO:0005829	cytosol	220 / 4743	3.50E-04

Overall analysis of GIMs relative to CONs suggests shifts in ECM and cellular adhesion profiles (Figure 5A, B), dysregulation of cyclic AMP (cAMP) signaling (Figure 5C, D), and alterations in nutrient transport and cellular energetics (Figure 5E, F). These systems will be further discussed below.

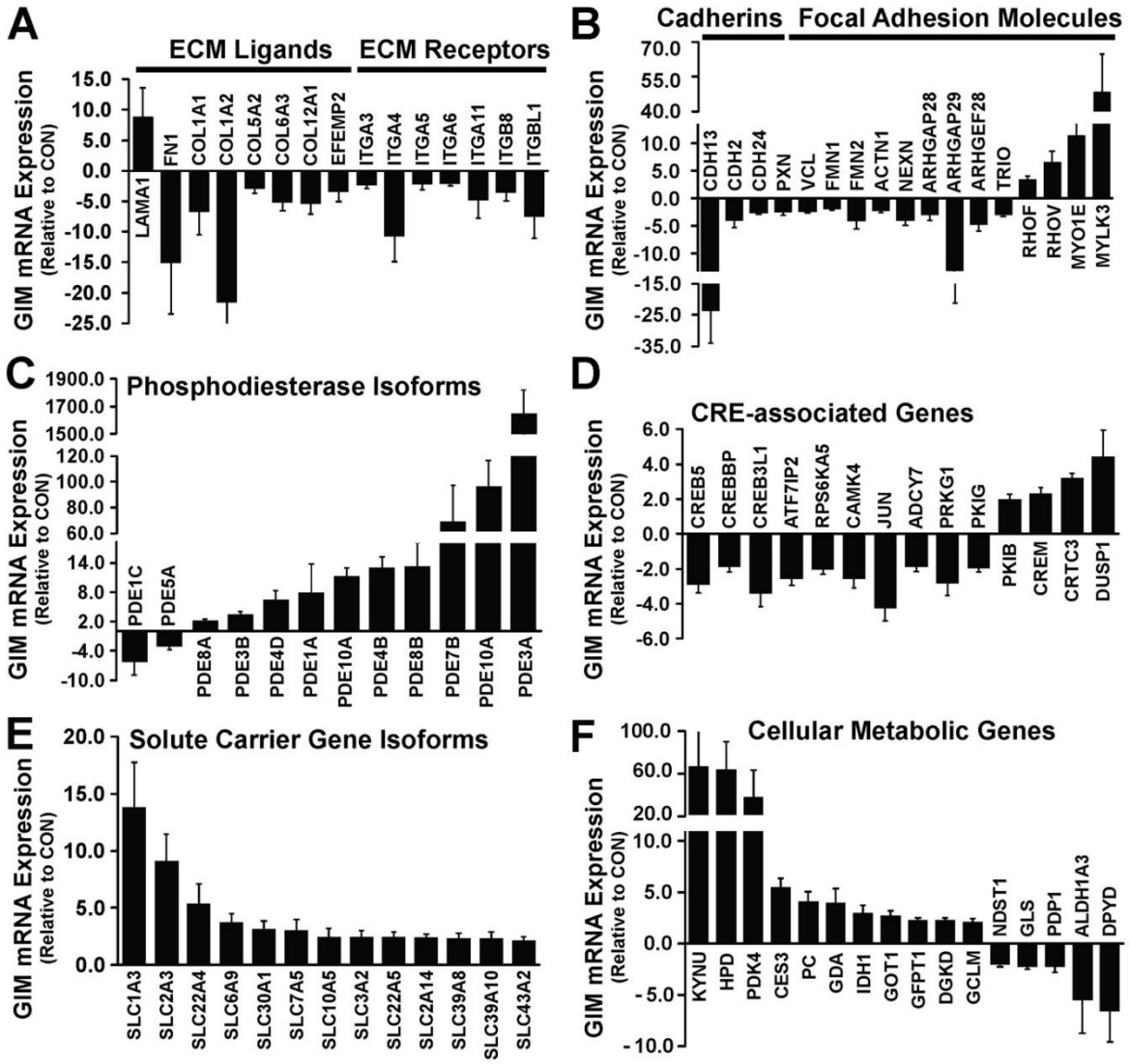

Figure 5: Microarray gene expression for genes of interest in GIM vs CON

(A) ECM ligands/receptors, **(B)** cadherins and focal adhesion molecules **(C)** re-expression of phosphodiesterase (PDE) isoforms **(D)** cAMP response element (CRE)-associated genes, **(E)** solute carrier family isoforms and **(F)** genes involved in cellular metabolism. Data represented as gene expression fold change ± SEM in GIMs relative to CONs. All results were statistically significant ($p < 0.05$)

3.3.6. ECM, Adhesion and Cell Morphology

GIMs demonstrated an overall reduction in genes for ECM ligands and integrin receptors compared to CONs. With the exception of increased laminin (LAMA1) expression, expression of fibronectin (FN1) and collagen (COL1A1, COL1A2, COL5A2, COL6A3 and COL12A1) were greatly down-regulated in GIM vs. CON (Figure 5A). In addition, parallel reduction in the expression of integrin receptors for fibronectin and collagen (ITGA3, ITGA4, ITGA5, ITGA6, ITGA11, ITGB8 and ITGBL1) suggests overall loss of ECM adhesion. Interestingly, epithelial cells bind to basement membranes using laminin, thus increased laminin expression suggests that GIMs have an epithelial-like ECM preference. This corresponding morphology can be visually observed in representative images of CGL1, GIM and CON (Figure 3B).

GIMs also showed significantly reduced expression of cadherins (CDH13, CDH2 and CDH24) which suggests reduced cell-to-cell adhesion and loss of contact-inhibition (Figure 5B). This is further demonstrated by cytoskeletal alterations which showed reduced expression of genes involved in maintaining focal adhesion complexes. Indeed, several of the most significantly impacted pathways determined by both experimental DEG data and Impact Analysis perturbation were regulation of the actin cytoskeleton (KEGG: 04810), focal adhesion (KEGG: 04510), and extracellular matrix receptor interaction (KEGG: 04512). In addition, focal adhesion (GO:0005925) was found to be the most significant cellular component GO term (Table 2). Here, genes for key focal adhesion proteins (paxillin, vinculin, formins, actinin α1, nexilin, Rho GTPases, and Rho guanine nucleotide exchange factors) were robustly downregulated in GIMs compared to CONs (Figure 5B). Furthermore, GIMs demonstrated increased expression of cell migration related genes (RHOV, RHOF, MYO1E, MYLK3). Taken together, the overall reduction in genes which regulate expression of ECM ligands, integrin receptors, cadherins and focal

adhesion molecules suggests that GIMs are able to proliferate independent of the signals provided by the surrounding ECM environment and cell-to-cell communication. Essentially, GIMs are not bound by the limitations in growth that result from ECM and cell-to-cell mediated inhibition of proliferation. This can be viewed in the representative photomicrographs of CGL1, GIM and CON in Figure 3B.

3.3.7. Dysregulation of cAMP Signaling

Robust re-expression of numerous phosphodiesterase (PDE) isoforms (PDEs 3A, 3B, 4B, 4D, 7B, 8A, 8B and 10A) demonstrated that cAMP-mediated signaling is disrupted in GIMs compared to CONs. In fact, PDEs represented many of the top up and down-regulated DEGs in GIM vs. CON in terms of fold change and significance (Figure 5C; Appendix C). The upregulated PDEs either hydrolyze cAMP specifically or can inactivate both cAMP and cGMP. Under normal conditions, production of cAMP leads to activation of CREB (cAMP response element-binding protein) which binds to cAMP response element (CRE) sequences in promoter regions to upregulate gene expression (Mayr et al. 2001). Indeed, evidence for increased inactivation of cAMP is further strengthened by downregulation of numerous genes which are regulated by CREB. These downregulated genes include CREB5, CREBBP, CREB3L1, ATF7IP2, RPS6KA5, CAMK4, JUN, ADCY7, PRKG1 and PKIG (Figure 5D). In addition, CREB transcription coactivators such as PKIB, CREM, CRTC3 and DUSP1 showed increased expression in GIMs, possibly to compensate for reduced cAMP signaling. Furthermore, GO enrichment analysis identified 3',5'-cyclic-nucleotide phosphodiesterase activity (GO: 0004114) as the most significant Elim pruned molecular function. Overall, the data presented above illustrates that GIMs demonstrate reduced cAMP mediated signaling compared to CONs. This phenotype has been recognized as an important role in the carcinogenic phenotype of other cell-types (Fajardo et al. 2014, Savai et al.

2010, Vitale et al. 2009).

3.3.8. Shifts in Nutrient Transport and Cellular Energetics

Re-expression of numerous solute carrier gene (SLC) isoforms (SLC 2A3, 22A4, 6A9, 30A1, 7A5, 10A5, 3A2, 22A5, 2A14, 39A8, 39A10 and 43A2) were identified in GIMs relative to CONs (Figure 5E). These SLC proteins are important for the transport of various types of nutrients ranging from glucose, amino acids (glutamate, glycine), fatty acids, organic cations and metal ions (He et al. 2009). Collectively, the upregulation of SLC isoforms demonstrates that enhanced nutrient transport is an important tumorigenic mechanism employed by GIMs.

Shifts in metabolic enzymes which regulate cellular energy production are important for the increased replicative potential associated with tumorigenic cells (Phan et al. 2014). Analysis of genes involved in the regulation of cellular metabolism in GIMs relative to CONs illustrates gene profile shifts which suggest enhanced cellular energy production (Figure 5F). For example, downregulation of pyruvate dehyrogenase phosphatase (PDP1) coupled with upregulation of pyruvate dehydrogenase kinase (PDK4), pyruvate carboxylase (PC) and isocitrate dehydrogenase (IDH1) shows that GIMs shunt pyruvate to oxaloacetate and eventually to α-ketoglutarate for enhanced production of ATP via the TCA cycle (Figure 5F). This system is further augmented by robust upregulation of kynureninase (KYNU) which is known to increase the biosynthesis of NAD cofactors required for the TCA cycle (Toma et al. 1997). Similarly, GIMs upregulated hydroxyphenylpyruvate dioxygenase (HPD), carboxylesterase (CES3) and diacylglycerol kinase (DGKD), genes which enhance energy production via fatty acid and ketone body metabolism (Kadochi et al. 2017). Another method of energy production employed by GIMs may involve the upregulation of glutamic-oxaloacetic transaminase 1 (GOT1) and glutamine-fructose-6-phosphate

transaminase (GFPT1) which alter oxidative metabolism (Abrego et al. 2017, Carvalho-Cruz et al. 2018). Taken together, the upregulation of numerous genes involved in cellular metabolism demonstrates that GIMs are able to employ numerous cellular energetic pathways for enhanced energy production.

3.3.9. Upstream Master Regulator Analysis

Utilizing the Ingenuity Knowledge Base database, the IPA software explores causal network and gene regulator cascades at multiple levels to identify master transcription regulators that can potentially explain the experimental DEGs (Kramer et al. 2014). The full list of upstream regulators ranked by z-score with predicted inhibitory or activating regulatory action is presented in Appendix E. Upstream regulators with negative z-score refer to master regulators that are predicted to be down-regulated in GIM relative to CON, and vice versa.

TGFβ1 was identified as the most significantly down-regulated upstream regulator in GIMs relative to CONs indicated by negative z-score of -5.2 (p-overlap = 1.35E-30). Figure 6 illustrates that TGFβ1 controls the expression of 160 genes present in the DEG list for GIM versus CON. The majority of genes activated by TGFβ1 were down-regulated in GIMs relative to CONs demonstrated by blue arrows predicting reduced activation by TGFβ1. Furthermore, SMAD3, a downstream signaling mediator of TGFβ1 was the second highest predicted upstream inhibitor. The analysis also suggested SMAD7, an inhibitor of TGFβ1 signaling, as the highest ranked upstream activator. Taken together, multiple lines of evidence suggest that TGFβ1 signaling is inhibited in GIMs relative to CONs.

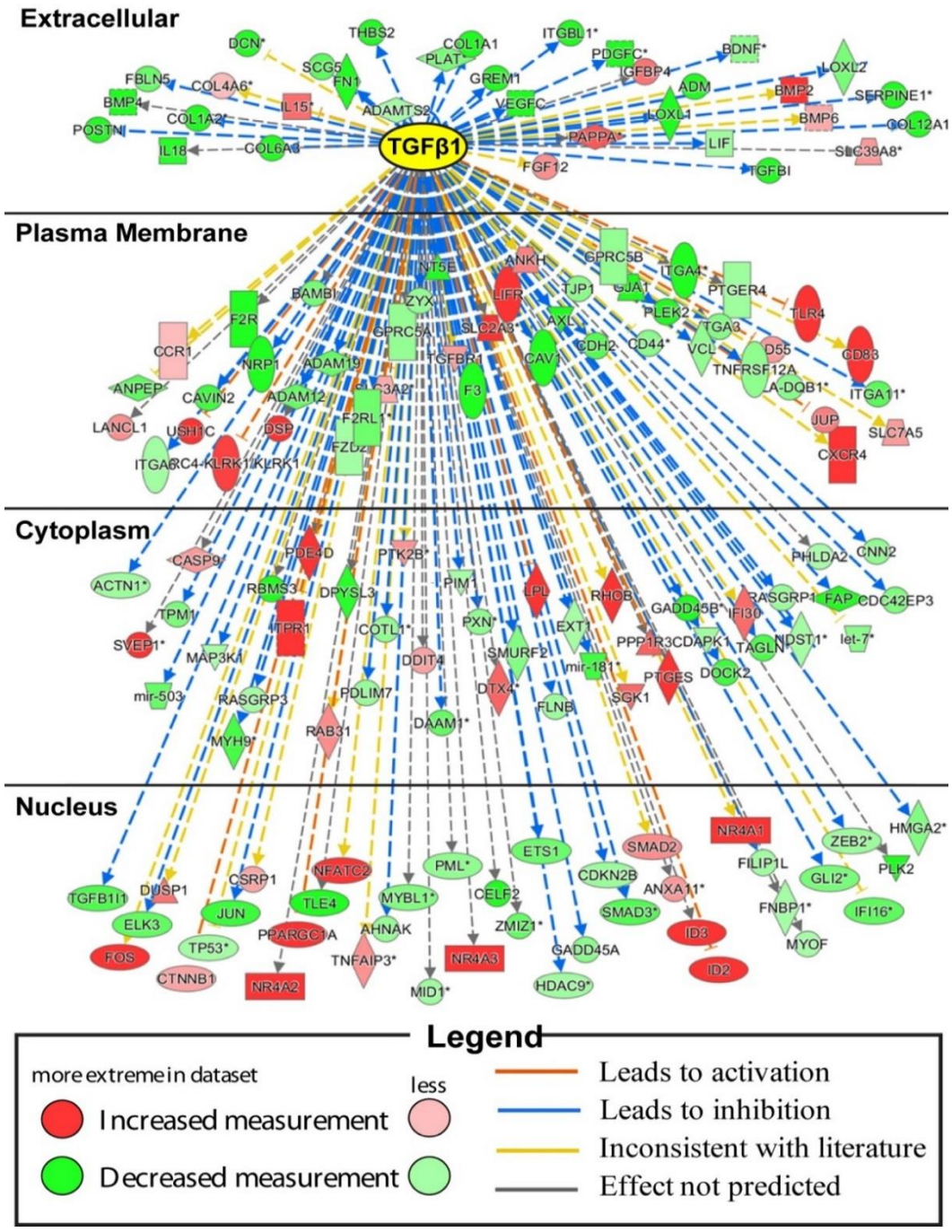

Figure 6: Genes downstream of TGFβ. a predicted upstream regulator in GIM vs CON

TGFβ1 is predicted to be down-regulated (z-score = -5.2; p-overlap = 1.35E-30) in GIMs relative to CONs. The IPA upstream regulator analysis revealed that TGFβ1 controls the expression of 160 genes present in the DEG list for GIM versus CON. The majority of genes activated by TGFβ1 are down-regulated (green) in GIMs relative to CONs demonstrated by blue arrows predicting reduced activation by TGFβ1. The schematic was generated using IPA (QIAGEN Inc., https://www.qiagenbioinformatics.com/products/ingenuity-pathway-analysis).

3.3.10. Expression of Genes Involved in TGFβ1 Signaling

To further explore the dysregulation of the TGFβ1 signaling in GIMs, the mRNA expression of genes implicated in TGFβ1 signaling was obtained from the DEG list and depicted in Figure 7. Figure 7A illustrates the canonical TGFβ1 signaling pathway and the TGFβ1 associated signaling molecules. Figure 7B reveals that mRNA levels for TGFβ1 and TGFβ-receptor type II and type III is similar in GIMs and CONs, while TGFβ-receptor type I is upregulated in GIMs. Likewise, TGFβ1 inhibitors BAMBI and SMURF2 were significantly down-regulated in GIMs relative to CONs. These results demonstrate that expression of TGFβ1, its receptors, and its inhibitors do not contribute to dysregulation of TGFβ1 signaling in GIMs. In fact, these results suggest that absence of TGFβ1 signaling enhanced the expression of TGFβ-receptor type I while inhibiting the expression of BAMBI and SMURF2 in an attempt to upregulate downstream TGFβ1 signaling cascade. Next, the mRNA expression of all SMAD isomers is shown in Figure 7C. SMADs are the intracellular transducers of the TGFβ1 signaling (Hata et al. 2016). Here, SMAD3 was significantly downregulated in GIM compared to GON, while SMAD2 was upregulated. All other SMADs were expressed at equal levels in GIM and CON. This important finding demonstrates that reduced SMAD3 expression is a plausible explanation why TGFβ1 signaling is down-regulated in GIMs relative to CONs. Finally, Figure 7D displays significantly reduced expression of several TGFβ1 target genes which further confirms that TGFβ1 signaling is inhibited in GIMs. Comprehensive analysis of all genes involved in TGFβ1 signaling suggests that decreased SMAD3 expression in GIMs is responsible for the lack of TGFβ1 signaling in GIMs.

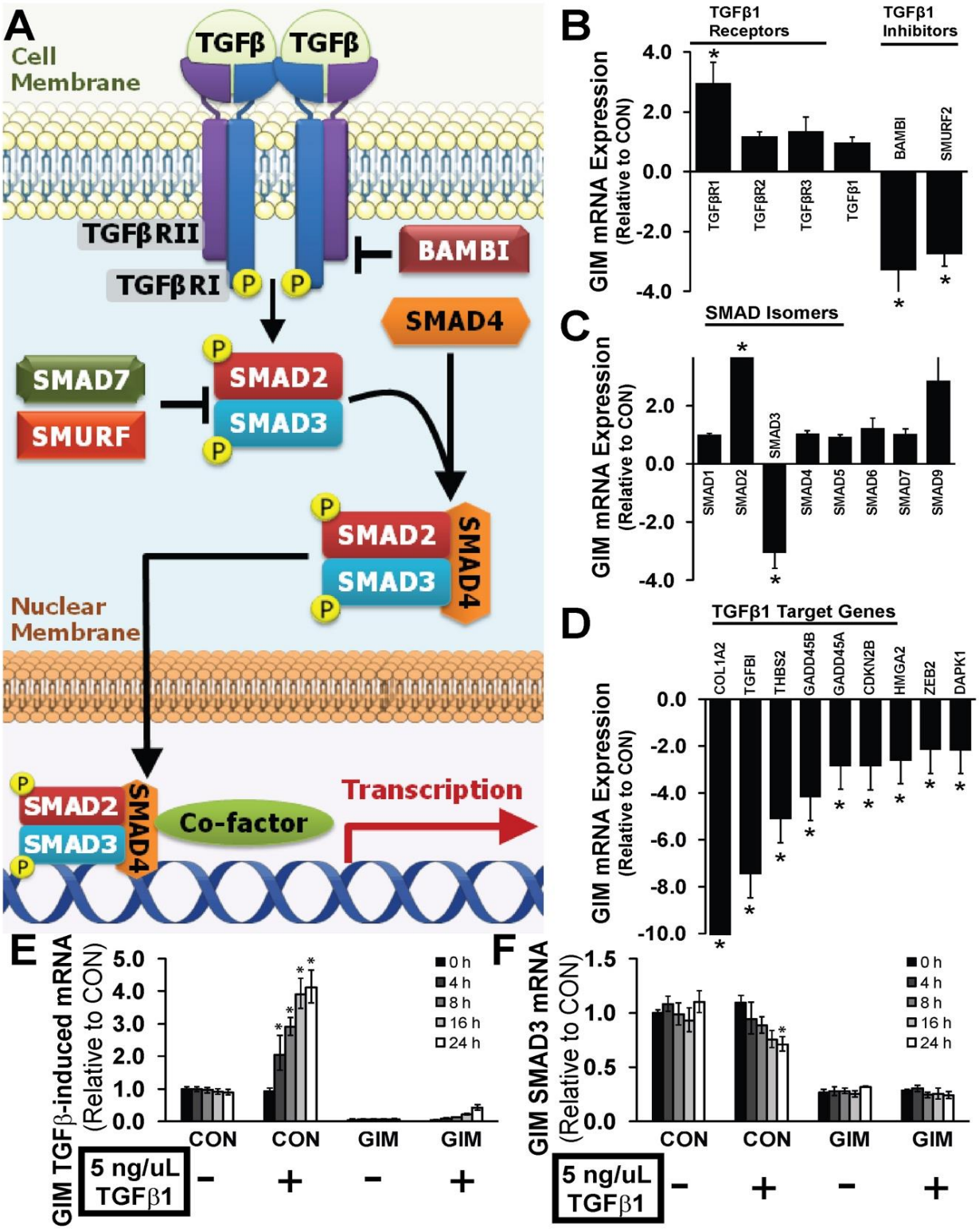

Figure 7: Canonical TGFβ signaling pathway, gene expression of TGFβ target genes and dysfunctional TGFβ signaling in GIM vs CON

(A) Canonical TGFβ1 signaling pathway. TGFβ1 binds to TGFβ-receptor type II, which activates TGFβ-receptor type I through phosphorylation. The activated receptor complex then phosphorylates receptor-regulated SMADs (SMAD2 and SMAD3), which then recruits SMAD4. The SMAD complex then translocates to the nucleus and serves as a transcription factor by upregulating the expression of various target genes. BAMBI, SMURF and SMAD7 are inhibitors of the TGFβ1 signaling pathway. **(B)** mRNA expression of TGFβ receptors, ligands and inhibitors, **(C)** SMAD isomers, and **(D)** TGFβ1 downstream target genes in GIMs relative to CONs. Data represented as gene expression fold change ± SEM in GIMs relative to CONs (* denotes p-value <0.05 and FDR p-value <0.10). Comprehensive analysis of genes involved in TGFβ1 signaling demonstrates that reduced SMAD3 expression is a plausible explanation why TGFβ1 signaling is down-regulated in GIMs relative to CONs. **(E)** Functional validation of TGFβ1 signaling in representative GIM (GIM19) and CON (CON2) cells. Administration of 5 ng/μL TGFβ1 protein resulted in robust upregulation of TGFβ-induced mRNA expression (a TGFβ1 target gene) in CON2 cells. 5 ng/μL. **(F)** TGFβ1 also resulted in a time-dependent decrease in SMAD3 mRNA expression in CON2 cells. Conversely, 5 ng/μL TGFβ1 administration to GIM19 cells had no response in terms of TGFβ-induced and SMAD3 mRNA expression. Data represented as gene expression fold change ± SEM (relative to CON2 at time 0h in the absence of 5 ng/μL TGFβ1 ligand). * denotes statistical significance compared to time 0h ($p < 0.05$). These functional results corroborate the IPA upstream regulator analysis in demonstrating that TGFβ1 signaling is inhibited in GIMs. We predict that decreased SMAD3 expression in GIMs is responsible for the lack of TGFβ1 signaling.

3.3.11. Functional Validation of Altered TGFβ1 Signaling in GIMs

Down-regulation of TGFβ1 signaling in GIMs was functionally investigated by administering 5 ng/μL TGFβ1 protein to representative GIM (GIM19) and CON (CON2) cells and determining the mRNA expression levels of TGFβ-induced (a TGFβ1 target gene) and SMAD3 (Figure 7 E, F). 5 ng/μL TGFβ1 protein resulted in robust time-dependent upregulation of TGFβ-induced mRNA expression in CON2 cells and a decrease in SMAD3 mRNA expression at 24 h. This verified that CON2 cells have a functionally active TGFβ1 signaling system. Conversely, 5 ng/μL TGFβ1 administration to GIM19 cells had no response in terms of TGFβ-induced and SMAD3 mRNA expression. These functional results corroborate the IPA upstream regulator analysis in demonstrating that TGFβ1 signaling is inhibited in GIMs.

3.4. Discussion

The overall goal of this study was to analyze gene expression and pathway level differences between tumorigenic and non-tumorigenic segregants of irradiated CGL1 cells. GIM and CON cells were isolated from CGL1 irradiated with 7 Gy of γ radiation, but are phenotypically tumorigenic or non-tumorigenic respectively. This system has been extensively utilized as a model system for mechanistically exploring neoplastic transformation. However, this study represents the most comprehensive global gene expression and pathway level analysis performed in this model system to date. This study identified major pathway level regulatory differences and associated differential gene expression in comparison of tumorigenic (GIM) and non-tumorigenic (CON) segregants. Gene expression and pathway level analysis of GIM vs. CON was in consensus with significant discoveries previously observed in this system in other gene expression studies (Nishizuka et al. 2001).

3.4.1. ECM / morphologically relevant changes

Changes in the ECM have been previously studied in HeLa x normal fibroblast hybrids and these alterations have been associated with re-expression of a tumorigenic phenotype (Der et al. 1980). Collagen plays a critical role in cancer cell migration, metastasis, invasion and tumorigenicity (Desgrosellier et al. 2010). Type I collagens (COL1A1 and COL1A2) are ECM components found to be significantly down-regulated in GIM vs. CON. COL1A2 has been reported as a tumorigenic inhibitor in transformed fibroblasts (Travers et al. 1996). The observed shift in ECM profile based on expression of fibronectin and laminin is interesting, as laminins are known to promote the invasive tumorigenic phenotype (Givant-Horwitz et al. 2005). Although many ECM receptors including those that interact with laminins are downregulated in GIM, laminin 1 is significantly upregulated. This is concurrent with robust downregulation of fibronectin and other ECM ligands.

Based on DEGs experimentally observed in microarray data, many of the most significantly enriched biological process and molecular function GO terms defined in GIM vs. CON included those related to ECM components and action. This included ECM organization, cell adhesion, positive regulation of epithelial to mesenchymal transition, collagen fibril organization, ECM structural constituent, and laminin binding. Though tumorigenic GIM and non-tumorigenic CON are irradiated segregants of CGL1, both cell-types have significantly distinct ECM properties that may be utilized to characterize and identify tumorigenic phenotype.

3.4.2. cAMP, PDE, PKA

PKA modulates a number of cellular substrates, including gene transcription factors and intracellular calcium (Ca^{2+}) regulating proteins (Bugrim 1999). Pathway analysis predicts that GIMs demonstrate increased intracellular Ca^{2+} activity based on elevated expression of IP3

receptors (ITPR1) and interacting protein ITPRIP as well as cAMP and cGMP which are regulators of cell growth (Fajardo et al. 2014). Adenylyl or guanyly cyclases, which are regulated by intracellular Ca^{2+}, have been suggested to target cancer cell inhibition (Vitale et al. 2009). Up-regulation of ITPRIP and ITPR1 was observed in GIM vs. CON. Increased expression of ITRP1, which mediates Ca^{2+} release, has been shown to have a role in protecting cancer cells from autophagy (Messai et al. 2014).

The dysregulation of essential secondary messengers (e.g. cAMP, Ca^{2+}) disrupts intracellular signaling and can have a profound effect on a number of significant molecular events associated with cancer (Yan et al. 2016). It appears that ionizing radiation induced dysregulation of cAMP, PDE and PKA genes in GIMs plays a role in the shift from non-tumorigenic to tumorigenic phenotype.

3.4.3. Shifts in Nutrient Transport and Cellular Energetics

The utilization of alternate metabolic and energy producing pathways are a common hallmark of cancerous cells, including differential expression of solute transport carriers (El-Gebali et al. 2013), which support the enhanced energy and nutritional needs of the tumor cell. In GIMs there is significant up-regulation of many solute transport carrier members as well cellular metabolic genes. Notably these include KYNU, HPD and PDK4 (Figure 5F) which we correlate with enhanced ATP production and energy production via alternative fatty acid and ketone body metabolism. It appears GIMs have shifted these energetic profiles in a reversion more towards its tumorigenic HeLa parental component. The importance of solute carriers in HeLa x normal fibroblast human hybrid cells, specifically SLC2A3 (GLUT3), the increased expression of which has been associated with tumor suppressor dysfunction (Suzuki et al. 1999). Of particular note,

SLC2A3 is highly up-regulated in GIMs as compared to CONs in our microarray study (Figure 5E).

3.4.4. TGF-β signaling pathway

TGF-β is known to affect a great number of molecular level events including cellular differentiation, proliferation, migration, as well as have both tumor suppressive and promoting capabilities (Lebrun 2012). The signaling cascade involving TGF-β, its receptors, receptor activated SMADs and other genes of significance are altered in GIM vs. CON analysis. Altered TGF-β1 signaling was found based on increased expression of genes including receptor regulated SMADs (SMAD2, SMAD 3) and TGF-β suppressible ID2 and ID3, as well as down-regulation of major TGF-β mediator thrombospondin (THBS1, THBS2). TGF-β1 was found by IPA to be the most statistically significant upstream regulator, and SMAD binding (GO:0046332) to be one of the most significant molecular function GO terms defined by iPG. R-SMAD (GO:0070412) and I-SMAD were also found to be highly statistically significant molecular function GO terms. Interestingly, SMAD2 was found to be up-regulated and SMAD3 to be down-regulated though SMAD2 and SMAD3 can have different regulatory effects in the TGF-β signaling pathway. It is possible that the increase in SMAD2 may be a compensatory mechanism due to reduced SMAD3 expression. It has been shown that down-regulation of SMAD3 expression (as seen in GIM vs. CON) can alter TGF-β induced arrest of the cell cycle (Kretschmer et al. 2003). SMAD7 has been shown to be commonly overexpressed in cancer cells and a promoter of transformation (Nagaraj et al. 2010), as well as an inhibitor of TGF-β and SMAD2 (Taylor-Weiner et al. 2015). SMAD7 expression was not found to be differentially expressed. Interestingly, SMAD7 inhibition of SMAD2 can be inhibited by integrin α3β1 facilitated laminin sensing. Additionally, TGF-β1 was determined to be one of the most significant putative upstream activating regulators. As such, its

activation may promote a tumor suppressive, or shift back towards a more normal non-tumorigenic phenotype. In the fibrotic process, a known effect of radiation exposure, TGF-β1 is involved in the production of many ECM proteins and modulation of integrins, as well as ECM remodeling (Kitahara et al. 2002). Furthermore, fibroblasts treated with TGF-β1 have been shown to increase levels of ECM associated collagens. It has been noted that repression of TGF-β receptors as well as loss of SMAD expression has been implicated in cervical cancer (Karunagaran et al. 2008).

3.4.5. Potential tumor suppressor genes expressed on chromosome 11

Significant work with CGL1 has previously explored the molecular mechanisms driving altered tumorigenic phenotype between the human hybrid cell segregants (Pirkkanen et al. 2017). Evidence from these studies revealed the role of chromosome 11 as a location of a putative functional tumor suppressor gene(s) (Kaelbling et al. 1986, Mendonca et al. 1995, Mendonca et al. 1999, Saxon et al. 1986, Srivatsan et al. 1986). Significant loss of one or multiple copies of chromosome 11 has been previously observed in GIMs (Mendonca et al. 1995, Mendonca et al. 1998, Suzuki et al. 1998). This loss correlates with increased expression of ALPI, which as aforementioned is the canonical marker of neoplastic transformation in the CGL1 system. Previous research showed that the transfer of chromosome 11 via microcell mediation into a tumorigenic segregant of the HeLa x fibroblast hybrid reduced ALPI expression and tumorigenic capability (Saxon et al. 1986). Researchers also showed that non-tumorigenic CON cell segregants which had lost a copy of chromosome 11 became more sensitive to x-irradiation and radiation induced neoplastic transformation (Mendonca et al. 1999). This correlation between a neoplastically transformed phenotype and the loss of chromosome 11 were the impetus for further examinations in the search for putative loci with tumor suppressive capacity. The list of all downregulated DEGs found on chromosome 11 in GIMs as compared to CONs are found in Table 3. Though correlative,

we propose that members of this list have potential implication in the tumorigenic phenotype and includes genes that have previously been suggested as potentially possessing tumor suppressive functionality (Mendonca et al. 2004). It is important however to note that putative tumor suppression genes may operate in a trans-regulatory capacity, as has been previously emphasized (Suzuki et al. 1998). We feel however, that the genes listed in Table 3 represent interesting targets worthy of future investigation and may play a significant role in the suppression of radiation induced neoplastic transformation in the CGL1 cellular system.

Table 3: Potential tumor suppressor genes expressed on chromosome 11

Loss of chromosome 11 has been attributed to the development of the tumorigenic phenotype. Numerous reports indicate that chromosome 11 contains a putative tumor suppressor loci and that loss or inactivation of this loci is a plausible mechanism for the development of radiation induced carcinogenesis (Mendonca et al., 1995, Mendonca et al., 1998, Pirkkanen et al., 2017). The table lists genes expressed on chromosome 11 that are down-regulated in tumorigenic GIMs relative to non-tumorigenic CONs. Therefore, we predict that genes listed in this table can be implicated as potential tumor suppressor genes since absence of these genes may drive radiation induced tumorigenesis.

Gene Symbol	Gene Description	Fold Change	Chromosome Location
SBF2-AS1	SBF2 antisense RNA 1	-8.58	11p15.4
LUZP2	leucine zipper protein 2	-7.87	11p14.3
FADS3	fatty acid desaturase 3	-6.07	11q12.2
ADM	Adrenomedullin	-5.30	11p15.4
FOSL1	FOS-like antigen 1	-5.11	11q13.1
IL18	interleukin 18	-5.04	11q23.1
CREB3L1	cAMP responsive element binding protein 3-like 1	-4.37	11p11.2
EFEMP2	EGF containing fibulin-like extracellular matrix protein 2	-4.31	11q13.1
FJX1	four jointed box 1	-3.88	11q23.3
UBASH3B	ubiquitin associated and SH3 domain containing B	-3.61	11q24.1
ETS1	v-ets avian erythroblastosis virus E26 oncogene homolog 1	-3.47	11q24.3
CD44	CD44 molecule (Indian blood group)	-2.80	11p13.0
LPXN	Leupaxin	-2.71	11q12.1
MAML2	mastermind-like transcriptional coactivator 2	-2.61	11q21.0
AHNAK	AHNAK nucleoprotein	-2.50	11q12.3
GAB2	GRB2-associated binding protein 2	-2.44	11q14.1
TRIM6	tripartite motif containing 6	-2.41	11p15.4
LDLRAD3	Low density lipoprotein receptor class A domain	-2.37	11p13.0
FIBIN	fin bud initiation factor homolog (zebrafish)	-2.15	11p14.2
PHLDA2	pleckstrin homology-like domain, family A, member 2	-2.06	11p15.4
E2F8	E2F transcription factor 8	-2.02	11p15.1
BDNF	brain-derived neurotrophic factor	-2.01	11q14.1

3.5. Conclusions

This study represents a modern global gene expression approach to elucidate differential gene expression and pathway level differences in an established human hybrid model system of ionizing radiation induced transformation. The similarity in transcriptomic landscape between GIM and CON independent segregants respectively suggests that radiation induced carcinogenesis is not a random event. The intention of this study was to use a modern transcriptome wide approach to characterize irradiated segregants of the CGL1 human hybrid cell system. This study has now brought irradiated isolates GIM and CON into a contemporary perspective in terms of transcriptomic gene expression landscape, and identified specific pathway level differences and the putative factors that may be driving radiation induced neoplastic transformation.

Chapter 4: Re-expression of Tumor Suppressor Candidate FRA1 in Gamma Induced Mutants of the CGL1 Hybrid Cell System Significantly Impacts Gene Expression and Alters the Tumorigenic Phenotype

4.1. Introduction

The CGL1 human hybrid cell system has been utilized for many decades as an excellent cellular tool for investigating neoplastic transformation in a variety of experimental conditions as previously reviewed (Pirkkanen et al. 2017). In addition to CGL1, a non-tumorigenic HeLa x normal fibroblast human hybrid, several other related cell lines have been established (Figure 3A, Appendix H) (Mendonca et al. 1991). The CON and GIM cell segregants were isolated from irradiated CGL1 cells, but displayed opposite tumorigenic phenotypes *in vitro* and *in vivo*. The CON cells were found to be morphologically akin to CGL1 (Figure 3B) and did not form tumors when injected subcutaneously into mice. The GIM segregants, also isolated from irradiated CGL1, were morphologically distinct (Figure 3B) and tumorigenic when injected into mice. A major focus for many years was the investigation of causal mechanisms influencing the phenotypic differences between CGL1, CON and GIM cell lines.

Substantial work has been done previously implicating genetic factors related to chromosome 11 to the alteration of tumorigenic phenotype in human hybrid cells (Mendonca et al. 2004, Mendonca et al. 1999, Mendonca et al. 1998, Saxon et al. 1986, Srivatsan et al. 1986, Srivatsan et al. 2002). This work led to the proposal of several candidate tumor suppressor genes whose deletion or silencing was responsible for the tumorigenic phenotype observed in GIMs isolated from irradiated CGL1 cells. These genes included PACS1, GAL3ST2, SF3B2, RAB1B and AP-1 transcription factor complex family member FRA1 (Mendonca et al. 2004, Pirkkanen et al. 2017). Further experimental work and analysis excluded SF3B2 and RAB1B as candidates (Zainabadi et al. 2005). Experimental work continued in the laboratories of Drs. Marc Mendonca and Eri Srivatsan focusing on the PACS1 and FRA1 genes as potential tumor suppressor gene candidates. Eventually

PACS1 was additionally removed as a candidate.

The research laboratory of Dr. Mendonca continued robust experimental work focusing on FRA1 as a proposed tumor suppressor gene (*in preparation*). Screening by Western Blot analysis revealed complete loss of FRA1 protein expression in the tumorigenic GIMs. Analysis by Southern and Northern blot confirmed that the observed loss of FRA1 protein expression was not due to gene rearrangement or deletion. To further investigate FRA1 as a putative tumor suppressor gene, the gene was transfected and re-expressed in multiple tumorigenic GIM cell lines. Re-expression of FRA1 in GIMs was confirmed and validated at the protein level. These GIM-FRA1 cell lines were subsequently grown and expanded for *in vivo* tumorigenicity studies. When injected into nude mice, GIM-FRA1 cells were found to induce no tumor formation. Whereas GIMs containing only the pcDNA3 transfection vector induced significant tumor development when injected into nude mice. This work demonstrated that FRA1 re-expression in a normally tumorigenic cell line suppresses tumor formation *in vivo*. Subsequent work utilizing siRNA showed that reduction of FRA1 protein expression was possible *in vitro* utilizing this method. Furthermore, it was found that siRNA silencing of FRA1 in a normally non-tumorigenic cell indeed induced tumor growth *in vivo* when CGL1-siFRA clones were injected subcutaneously into nude mice. Together these findings represented pioneering novel evidence implicating the loss of FRA1 expression as involved in the neoplastic transformation of tumorigenic segregants of the CGL1 human hybrid cell system.

The objective of the following research was to characterize GIM-FRA1 cells for the first time utilizing modern global gene expression technology and data analysis tools. The overall goal being to understand on a global transcriptomic scale the effects of FRA1 re-expression in GIMs, and to propose causal mechanisms for the association of FRA1 expression and suppression of

tumorigenicity.

4.2. Materials and Methods

4.2.1. Cell culture

All cell lines were obtained from Dr. Marc Mendonca (Indiana University School of Medicine, Indianapolis, Indiana, USA). The human hybrid cell lines were originally established and isolated as previously described (Mendonca et al. 1991, Stanbridge et al. 1981, Stanbridge et al. 1980). Briefly, CGL1 was isolated from the original ESH5 D98/AH2 x GM0077 hybrid. Independently isolated GIM (GIM12D, GIM19E, and GIM31DA) and CON (CON1, CON2, CON3 and CON5) cells lines were isolated from CGL1 cells exposed to 7 Gy of γ radiation. The GIM cell lines over-expressing FRA1 (GIM12D-FRA1, GIM19E-FRA1 and GIM31DA-FRA1) and vector controls (GIM12D-pcDNA3, GIM19E-pcDNA3 and GIM31DA-pcDNA3) were experimentally generated by Dr. Mendonca (*in preparation*). Briefly, selected GIMs were transfected via electroporation with a commercially available FRA1/Neo plasmid or with a control/empty pcDNA3/Neo vector plasmid. After 24 to 48 hours, selective antibiotic G418 was added to the growth media and resistant clones allowed to develop. Individual resistant clones from FRA1 and vector control transfected cells were isolated and FRA expression verified by western blot analysis.

All cell lines were incubated in humidity at 37°C with 5% CO_2. CON cell lines were grown in 1X Minimum Essential Medium (Corning, 10-010CV) supplemented with 5% calf serum (Sigma, C8056) and 1% Penicillin-Streptomycin (Corning, 30-001-CI). The FRA over-expressing GIMs and pcDNA3 vector control cells lines were grown in the same media but additionally supplemented with Geneticin G418 sulfate (Gibco, 11811-023) resuspended in UltraPure nuclease free distilled water (Invitrogen, 10977). The G418 solution was 0.22 μm filter sterilized (Millipore,

SLGP033RS) and added to tissue culture media to a final concentration of 300 μg mL^{-1}. Routine cell splitting was performed with 0.05% trypsin-EDTA (Gibco, 25300) and cell counts achieved by trypan blue staining (MP, 1691049) on a Vi-CELL XR cell viability analyzer (Beckman Coulter). Tissue culture was tested for mycoplasma contamination using the Mycoplasma Detection Kit-QuickTest (Biotool, B39032) according to manufacturer's instructions.

4.2.2. RNA extraction

Total RNA isolation was performed utilizing a kit based extraction method. RNA was isolated using an RNeasy Mini Kit (Qiagen, 74104) with inclusion of QIAshredder columns (Qiagen, 79654) followed by on column DNAse digestion (Qiagen, 79254) according to the manufacturer's instructions. Purified RNA samples were eluted using nuclease free H_2O. Quantity and quality of RNA was analyzed by NanoDrop spectrophotometry (Thermo Fisher, ND-1000). To prevent unwanted degradation of RNA during isolation, laboratory surfaces and instruments were decontaminated with RNase-OFF (Takara Bio, 9037).

4.2.3. cDNA synthesis

cDNA was synthesized in a reaction mixture as follows. To a sterile tube, 2μg RNA and 1 μg random hexamers (Sigma, 11034731001) were added, then total volume brought to 23μL with sterile nuclease free H_20 (Invitrogen, 10977). This was mixed, centrifuged briefly, and incubated at 70ºC for 5 min, immediately chilled on ice, and tubes briefly centrifuged again. To each tube, 2.5μL of 10mM per base mixed dNTPs (VWR, CA71003-178, CA71003-180, CA71003-182, CA71003-184), 10uL of 5X M-MLV reaction buffer (Promega, M531A), 2 μL of 200U μL^{-1} M-MLV reverse transcriptase (Promega, M1708) and 12.5μL nuclease free H_20 were added to bring the reaction to a final volume of 50μL. Reaction tubes were mixed, briefly centrifuged and

incubated at 37ºC for 60 min. Synthesized cDNA was stored at -20ºC until downstream use.

4.2.4. Primer design and validation

Forward and reverse primer pairs for RT-qPCR analysis were independently designed and validated in house. Briefly, forward and reverse primer pairs for housekeeping genes and genes of interest were designed considering a base pair length of 16-25, melting temperature of 55 - 65 C and GC content of 50-60% to be optimal for downstream use. The reaction efficiency of each primer pair was calculated according to the formula $E = [10^{(-1/slope)}-1]$. Primers with reaction efficiency between 90% to 110%, and R^2 value greater than 0.99 were considered validated and acceptable for RT-qPCR analysis. In addition, optimal annealing temperature for each primer pair was identified by performing temperature gradient analysis and identifying annealing temperature which resulted in smallest Ct value. Relevant information for primers used in this experiment can be found in Appendix F

4.2.5. RT-qPCR sample preparation, thermocycling conditions and data analysis

For RT-qPCR experiments, SYBR green based 15µL volume reactions were performed utilizing the Quantstudio 5 RT-qPCR instrument (ThermoFisher Scientific). The final reaction mixture was prepared with 1X SensiFAST Sybr Lo-Rox qRTPCR mastermix (FroggaBio, CSA-01195), 600 nM forward and reverse primers and 7.5 ng of cDNA input sample. Reactions took place in MicroAmp optical 96-well reaction plates (Applied Biosystems, N8010560) sealed with optical adhesive film (Applied Biosystems, 4360954). The thermocycling conditions were as follows for 40 cycles: 95°C for 30 seconds, 57, 60 or 62°C for 30 seconds, 72°C for 30 seconds, then data readout by the instrument. Following the 40 cycles, single amplicon specificity was validated by primer melt curve analysis. Cycle threshold (C_T) data analysis was performed utilizing the

QuantStudio™ Design and Analysis Software v1.4.1 (Applied Biosystems) with samples normalized to the geometric mean of housekeeping genes HSPC3, RPS18 and GAPDH. Relative expression of genes was calculated utilizing the $\Delta\Delta C_T$ method using the following formula: $2^{\Delta\Delta}C_T = 2(^{\Delta}C_T{}^{\text{gene}} - {}^{\Delta}C_T{}^{\text{housekeeping genes}})$. Average $2^{\Delta\Delta}$ C_T and standard error of the means (SEMs) were calculated. For RT-qPCR experiments with genes of interest, representative GIM-FRA1, GIM-pcDNA3 and CON cell lines were used and the assay performed in triplicate.

4.2.6. Human Transcriptome Array 2.0

CON1, CON2, CON3, CON5, FRA over expressing clones GIM12D-FRA, GIM19E-FRA, GIM31DA-FRA, as well as plasmid vector controls GIM12D-pcDNA3, GIM19E-pcDNA3 and GIM31DA-pcDNA3 were subjected to full transcriptome analysis. Isolated RNA from selected cell lines was re-quantified by NanoDrop spectrophotometry (Thermo Fisher, ND-1000), and diluted using nuclease free H_2O to approximately 100 ng μL^{-1}. Samples were shipped on dry ice to The Centre for Applied Genomics (TCAG) Microarray Facility at The Hospital for Sick Children, ON, Canada. Upon arrival at TCAG samples were subjected to RNA integrity analysis using either an Agilent 2100 Bioanalyzer (Agilent Technologies) or the Agilent 2200 RNA ScreenTape System (Agilent Technologies). Only samples with an acceptable RNA integrity number (>8.0) and A:260/280 as well as A:260/230 >1.95 were considered for downstream use. Experimental samples were assayed at TCAG utilizing the GeneChip Human Transcriptome Array (HTA) 2.0 (Affymetrix). Arrays were prepared with 400ng RNA, utilizing the GeneChip WT Plus Reagent Kit (Thermo Fisher, 902280) according to manufacturer's instructions. Biotin allonamide triphosphate was used as a labeling reagent and hybridization occurred for 16-18 hours at 45˚C with 5.5 µg input cDNA. Samples were washed utilizing the FS450_0001 fluidics protocol and scanned using a GeneChip Scanner 3000 (Thermo Fisher). Quality control was performed in

Expression Console 1.4.1.46 (Affymetrix) to identify possible outlier samples, divergent probe intensities and signal concordance. Internal labeling and hybridization controls as well as Positive vs Negative area under the curve thresholds were all required to pass quality control to be considered for analysis. Data obtained via HTA 2.0 array at TCAG were analyzed utilizing the Transcriptome Analysis Console (TAC) Software 4.0.0.25 (Thermo Fisher) and the Genome Reference Consortium Human Build 37 (hg19), as a reference genome. For data processing, sample number and statistical consideration samples were grouped for comparison: GIM-FRA1 (n=3) vs GIM-pcDNA3 (n=3) and GIM-FRA1 (n=3) vs CON (n=4). DEG criteria were as follows, <-2 or >2 for gene fold change and <0.05 for p-values.

4.2.7. iPG analysis

The Data (significantly impacted pathways, biological processes, molecular interactions, miRNAs, SNPs, etc.) were analyzed using Advaita Bio's iPathwayGuide (www.advaitabio.com/ipathwayguide). This software analysis tool implements the Impact Analysis approach that takes into consideration the direction and type of all signals on a pathway, the position, role and type of every gene, etc. as described in (Draghici, 2007, Donato, 2013). Enrichment of GO terms and significant pathways was performed in the context of the latest Kyoto Encyclopedia of Genes and Genomes (84.0+/10-26, Oct 17) and GO (2017-Nov6) databases. Upstream regulators and network level analysis were performed in the context of the latest STRING (v.10.5 May 14th, 2017) and BioGRID (v.3.4.154. October 25th 2018) databases.

4.2.8. Statistical analysis

For RT-qPCR validation of DEGs data are presented as mean ± SEM. Statistical comparisons between groups were performed in either SPSS (IBM) or Prism 6 (GraphPad Software Inc.)

utilizing a one-way ANOVA followed by Tukey's post-hoc analysis. A subsequent p-value of <0.05 was considered statistically significant. For comparisons between microarrays (GIM vs CON compared to GIM-FRA1 vs CON) a Students t-test with two-tailed distribution and two-sample unequal variance was performed, with a p-value <0.05 considered significant. The statistical approach utilized by TAC in microarray analysis while determining DEGs is outlined in the TAC User Guide (assets.thermofisher.com/TFS-Assets/LGS/manuals/tac_user_manual.pdf). In brief, one-way ANOVA (ebayes) was performed and a p-value <0.05 was considered statistically significant for comparison between sample groups. For iPG analysis, the proprietary Impact Analysis method was utilized. Statistical methods for GO term enrichment (Elim pruning, Min DE genes/term:3), pathway, networks and upstream regulator analysis as previously described, a FDR p-value <0.05 was considered significant for these analyses.

4.3. Results

4.3.1. Transcriptome Analysis Console (TAC)

Initial TAC analysis of GIM-FRA1 compared to GIM-pcDNA3 revealed 365 DEGs meeting threshold filter criteria (Figure 8). Of this 225 were up-regulated and 140 down-regulated with greater than 75% coding transcripts. The full list of DEGs ranked in order of increasing p-value are found in Appendix G. FRA1 was found to be the most statistically significant DEG in the comparison of GIM-FRA1 to GIM-pcDNA3. The two most down-regulated genes were ALPI and PI15. Downstream comparison GIM vs CON and GIM-FRA1 vs CON microarray analysis revealed numerous changes which are attributed to the re-expression of FRA1.

Figure 8: Volcano plot of differentially expressed genes in GIM-FRA1 vs GIM-pcDNA3

Up-regulated (red) and down-regulated (green) DEGs in comparison of GIM-FRA1 vs GIM-pcDNA3.The volcano plot was generated by plotting the negative log of the p-value on the y-axis and the fold change on the x-axis. A total of 365 DEGs met threshold filter criteria, 225 up-regulated and 140 down-regulated.

4.3.2. Exploratory grouping and principal component analysis

Exploratory grouping analysis of GIM-FRA1, GIM-pcDNA3 and CON cell lines utilized in this experiment showed that they group closely within their cell type (Figure 9).

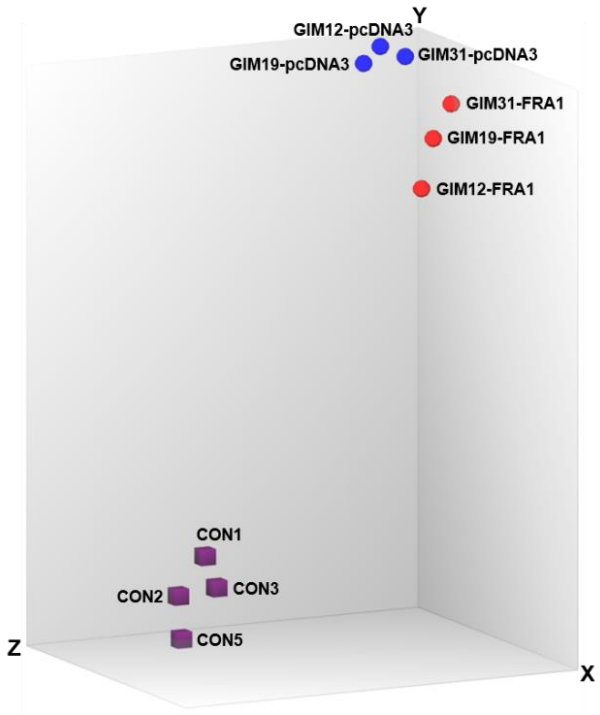

Figure 9: Exploratory grouping analysis of GIM-FRA1, GIM-pcDNA3 and CON cell lines Analysis was performed without pre-defining sample information, e.g. phenotype.

Although GIM-FRA1 and GIM-pcDNA3 cell lines were determined to be within the same cluster, all three cell line types display a spatially distinct grouping. PCA analysis shows that although there is some variance between cell lines within a group, there is discrete grouping with the three principal components accounting for 71.1% of dataset variance (Figure 10).

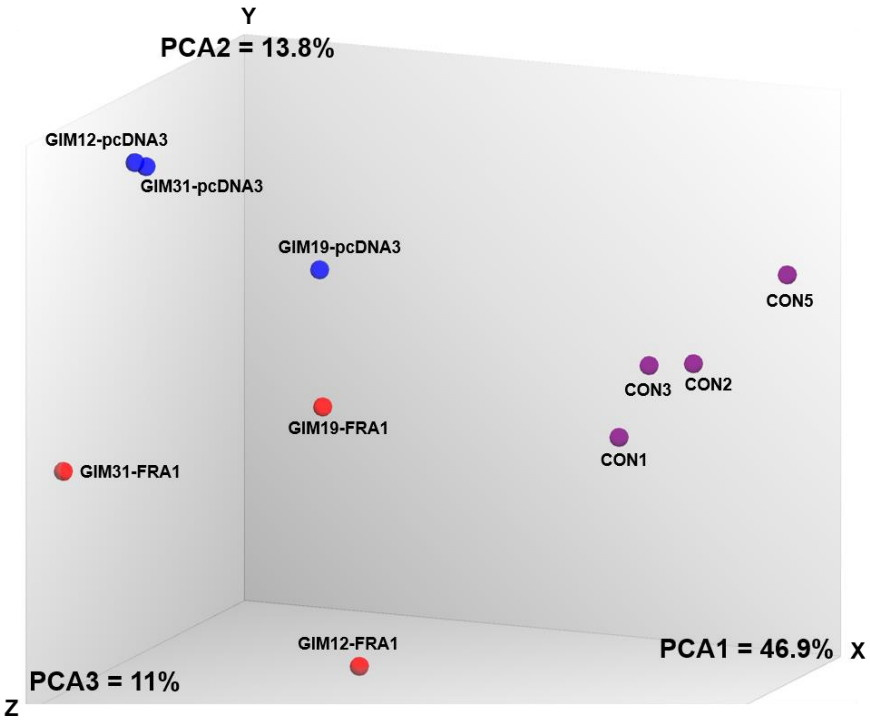

Figure 10: Principal component analysis of GIM-FRA1, GIM-pcDNA3 and CON cell lines

The three principal components accounted for 71.1% of the variance. Although some variability exists within cell lines, discrete grouping is observed.

4.3.3. Alkaline phosphatase expression

The re-expression of ALPI has been previously established and validated as the invariable indicator of the tumorigenic phenotype in the CGL1 model system and its related cell line segregants (Latham et al. 1990, Mendonca et al. 1991). RT-qPCR showed that GIM-pcDNA3 vector controls express substantially higher levels of ALPI as normalized to CON (Figure 11A). The GIM-FRA1 cell line has a highly significant reduction (p-value <0.005) in ALPI expression compared to the GIM-pcDNA3 control. Transcriptome microarray analysis shows that GIM-FRA1 expressing cells compared to CON is significantly downregulated compared to GIM vs CON analysis (Figure 11B). This experiment also revealed the slight reduction of three other alkaline

phosphatases in this same comparison. Additionally, iPG revealed alkaline phosphatase activity as the most statistically significant enriched Molecular Function GO term (Table 4)

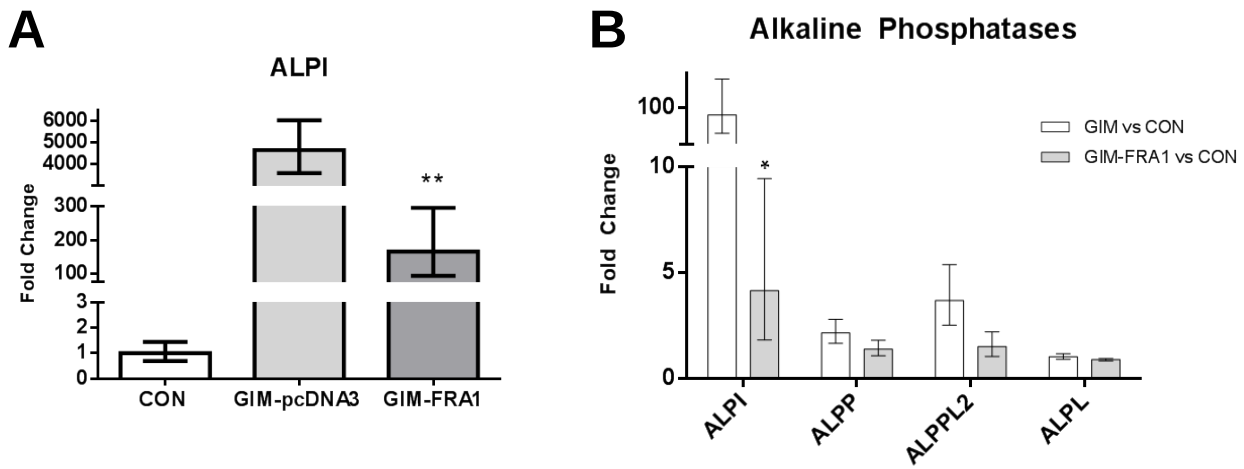

Figure 11: RT-qPCR and microarray analysis of alkaline phosphatase expression in GIM-FRA1, GIM-pcDNA3 and CON cell lines

(A) RT-qPCR analyis of ALPI levels are significantly reduced in GIMs overexpressing FRA1 compared to GIM-pcDNA3, ** denotes p-value <0.005. **(B)** Comparison GIM vs CON and GIM-FRA1 vs CON microarrays shows reduction of several alkaline phosphatases, including ALPI. * denotes p-value <0.05.

4.3.4. AP-1 Complex

Members of the AP-1 transcription factor complex were shown to be differentially regulated in GIM-FRA1 vs CONs as compared to GIM vs CON. These findings were observed with RT-qPCR with the significant up-regulation of FRA1 (Figure 12A) and cJUN (Figure 12B) in GIM-FRA1 vs GIM-pcDNA3. cFOS was found to be down-regulated (Figure 12C) in GIM-FRA1 cells compared to GIM-pcDNA3 however it was marginally outside of established statistical significance (p-value = 0.071). Up-regulation of cJUN and FRA1 were observed in microarray comparison as well as down-regulation of cFOS (Figure 12D).

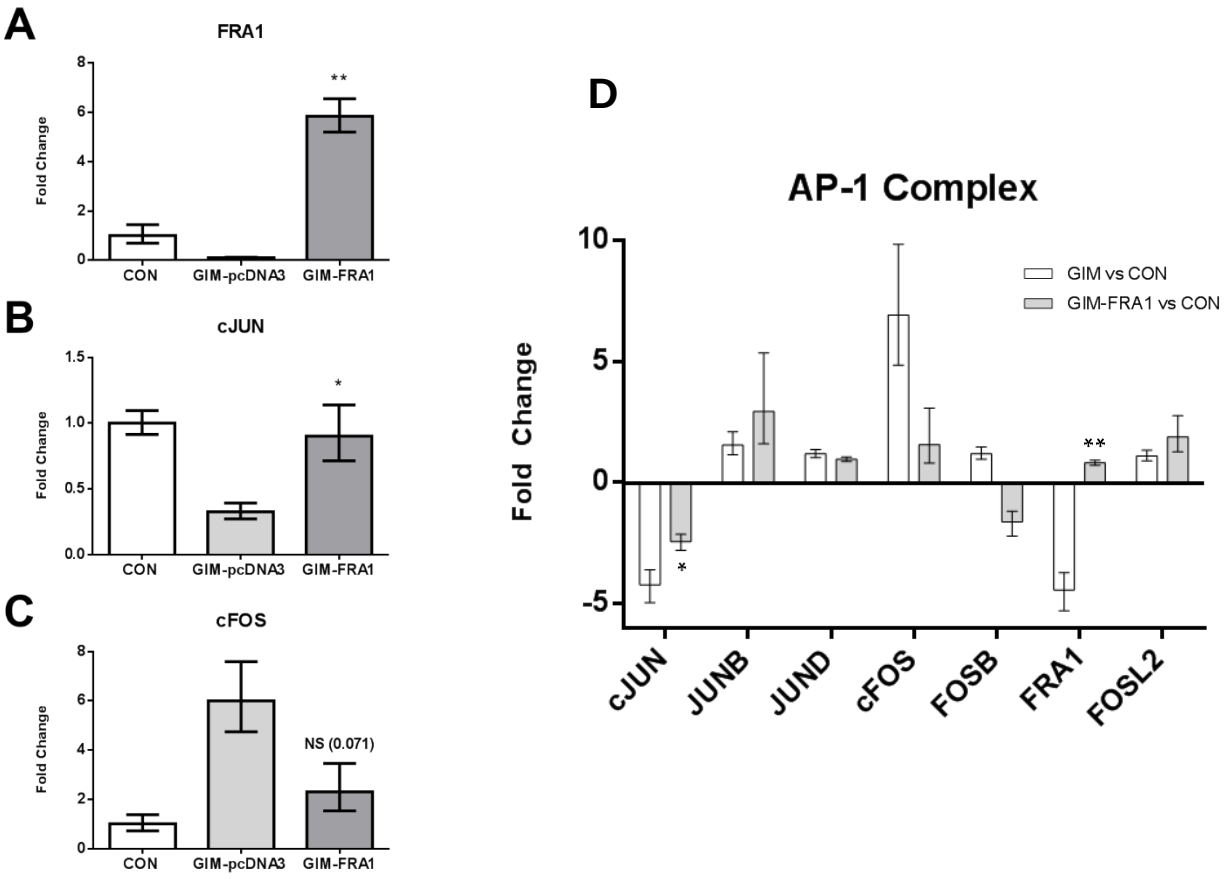

Figure 12: RT-qPCR and microarray analysis of AP-1 transcription factor complex gene members in GIM-FRA1, GIM-pcDNA3 and CON cell lines

(A) FRA1, **(B)** cJUN and **(C)** cFOS. FRA1 and cJUN are significantly upregulated in GIM-FRA1 compared to GIM-pcDNA3, * denotes p-value <0.05 and ** denotes p-value <0.005. **(D)** microarray comparison of JUN and FOS family members. GIM-FRA1 vs CON compared to GIM vs CON follows RT-qPCR data with the up-regulation of FRA1 and cJUN and the down-regulation of cFOS suggests a molecular rearrangement of the AP-1 transcription factor complex in GIM cells that over express FRA1. * denotes p-value <0.05 and ** denotes p-value <0.005.

4.3.5.. Phosphodiesterases

The downregulation of PDEs 10A and 3B in GIM-FRA1 cells compared to GIM-pcDNA3 was observed in RT-qPCR analysis (Figure 13A, B). In microarray analysis, GIM-FRA1 vs CON showed substantial downregulation of PDEs 4B, 7B and 10A compared to GIM vs CON (Figure 13C). Downregulation of PDEs 3B and 4D were also observed but to a lesser degree.

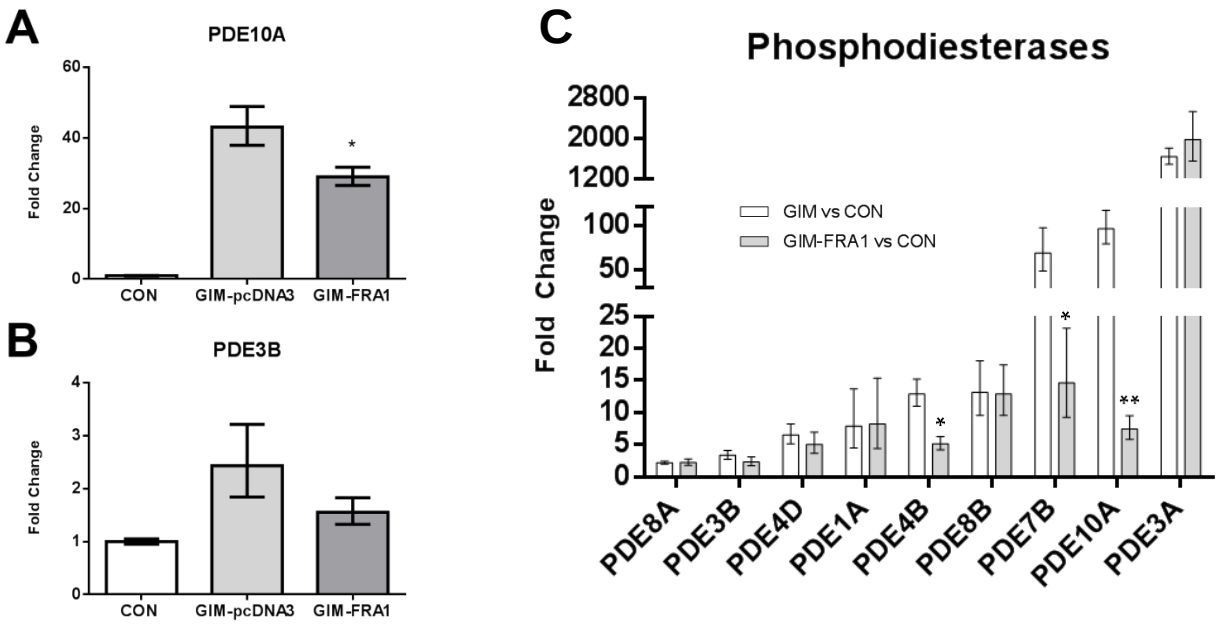

Figure 13: RT-qPCR and microarray analysis of phosphodiesterases in GIM-FRA1, GIM-pcDNA3 and CON cell lines

RT-qPCR analysis of **(A)** PDE10A and **(B)** PDE3B. * denotes p-value <0.05. **(C)** Microarray comparison of PDE family members. * denotes p-value <0.05 and ** denotes p-value <0.005. Substantial downregulation of PDEs 4B, 7B and 10A was observed as well as PDEs 3B and 4D to a lesser degree.

4.3.6. Extracellular Matrix Ligands and Receptors, cellular adhesion and migration

Analysis of GIM-FRA1 cells compared to GIM-pcDNA3 revealed significant changes in genes related to the ECM, cellular adhesion, migration and proliferation. Many of the top 10 significantly enriched biological process, molecular function and cellular component GO terms were related to these changes (Table 4).

Table 4: Enriched gene ontology terms based on differentially expressed genes in GIM-FRA1 vs GIM-pcDNA3

GO terms are organized into 3 categories: Biological Process, Molecular Functions and Cellular Components.

GO Term	Biological Process	# genes (DEG/ALL)	p-value
GO:0007565	female pregnancy	11 / 185	1.20E-05
GO:0001889	liver development	9 /20	2.20E-05
GO:0008285	negative regulation of cell proliferation	20 / 666	1.20E-04
GO:0009612	response to mechanical stimulus	10 / 206	1.70E-04
GO:0070673	response to interleukin-18	3 / 10	1.80E-04
GO:0051592	response to calcium ion	7 / 115	4.20E-04
GO:0030512	negative regulation of TGFβ receptor signaling pathway	5 / 67	1.15E-03
GO:0001936	regulation of endothelial cell proliferation	6 / 103	1.36E-03
GO:0048646	anatomical structure formation involved in morphogenesis	27 / 990	1.59E-03
GO:0032496	response to lipopolysaccharide	12 / 307	1.69E-03

GO Term	Molecular Functions	# genes (DEG/ALL)	p-value
GO:0004035	alkaline phosphatase activity	3 / 4	6.40E-06
GO:0047144	2-acylglycerol-3-phosphate O-acyltransferase activity	3 / 9	1.30E-04
GO:0043236	laminin binding	4 / 29	3.50E-04
GO:0003841	1-acylglycerol-3-phosphate O-acyltransferase activity	3 / 19	1.36E-03
GO:0008083	growth factor activity	7 / 158	2.69E-03
GO:0005178	integrin binding	5 / 110	9.72E-03
GO:0043394	proteoglycan binding	4 / 38	1.83E-02
GO:0005160	TGFβ receptor binding	3 / 48	1.89E-02
GO:0019899	enzyme binding	36 / 2,079	3.16E-02
GO:0042826	histone deacetylase binding	4 / 103	3.35E-02

GO Term	Cellular Components	# genes (DEG/ALL)	p-value
GO:0009897	external side of plasma membrane	10 / 248	6.60E-04
GO:0031093	platelet alpha granule lumen	5 / 66	1.01E-03
GO:0005911	cell-cell junction	13 / 409	1.01E-03
GO:0000786	nucleosome	5 / 86	3.27E-03
GO:0005925	focal adhesion	11 / 382	5.15E-03
GO:0070062	extracellular exosome	44 / 2,665	8.79E-03
GO:0031225	anchored component of membrane	6 / 154	9.24E-03
GO:0045178	basal part of cell	4 / 46	1.42E-02
GO:0016324	apical plasma membrane	8 / 286	1.88E-02
GO:0005903	brush border	4/ 95	2.48E-02

Comparison of GIM vs CON with GIM-FRA1 vs GIM-pcDNA3 microarray analysis revealed significant dysregulation of genes related to the ECM including LAMA1, FN1, COL1A1, COL1A2, COL12A1 (Figure 14A), as well as related integrins, notably ITGA3, ITGA4, ITGA5, ITGA6 and ITGB8 (Figure 14B)

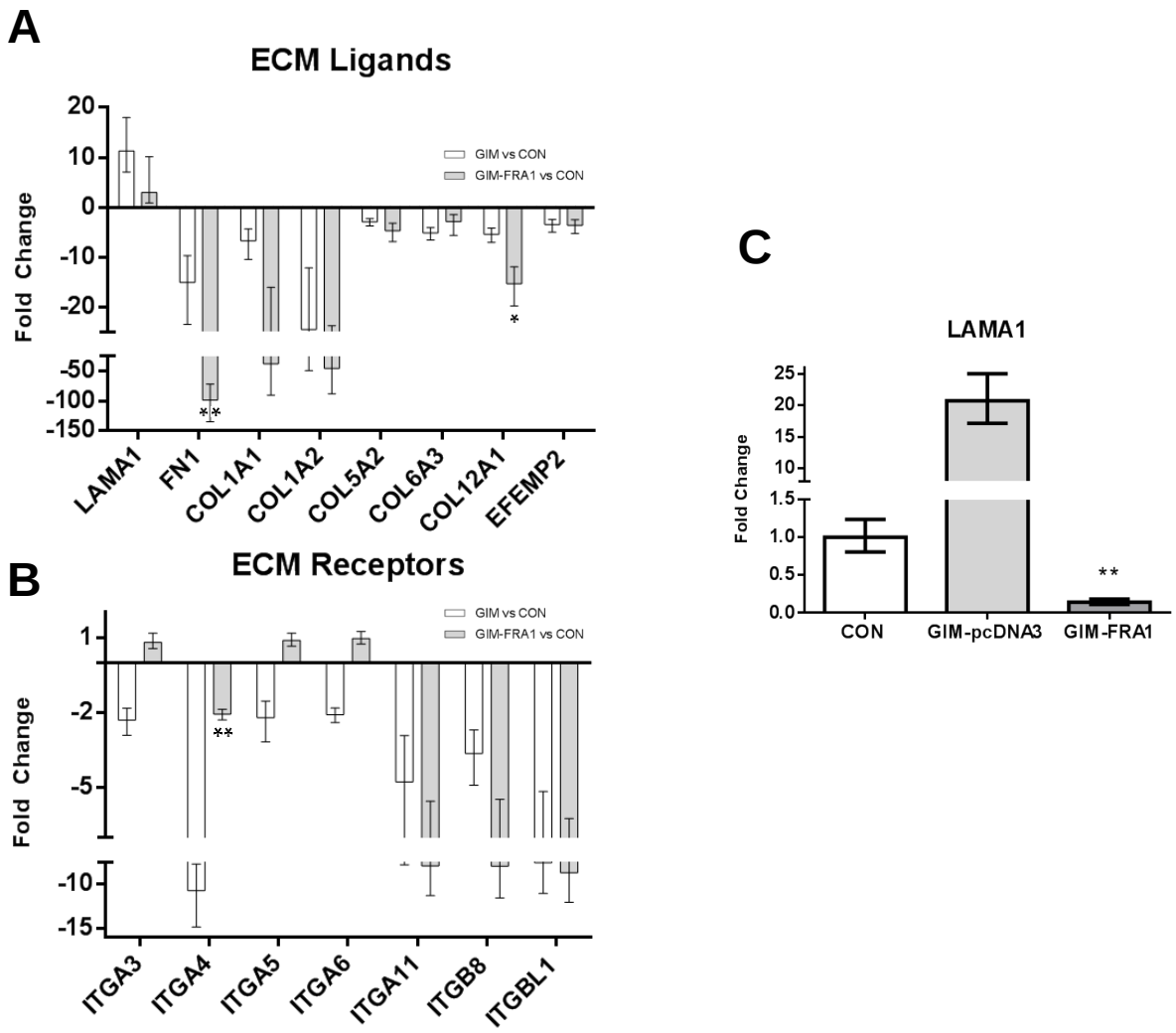

Figure 14: RT-qPCR and microarray analysis of extracellular matrix ligands and receptors in GIM-FRA1, GIM-pcDNA3 and CON cell lines

Microarray analysis of **(A)** ECM ligands and **(B)** receptors. * denotes p-value <0.05 and ** denotes p-value <0.005. **(C)** RT-qPCR analysis shows significant downregulation of LAMA1 in GIM-FRA1 compared to GIM-pcDNA3. * denotes p-value <0.05.

Highly significant downregulation of LAMA1 in GIM-FRA1 compared to GIM-pcDNA3 was confirmed by RT-qPCR analysis (Figure 14C). Additionally, the top 2 predicted upstream regulators in GIM-FRA1 compared to GIM-pcDNA3 are growth factors FGF2 and EGF (Table 5).

Table 5: Predicted upstream regulators determined by iPG analysis in GIM-FRA1 vs GIM-pcDNA3

Upstream Regulator	p-value	Entrez ID
FGF2	0.006	2247
EGF	0.009	1950
PTHLH	0.009	5744
ATF2	0.009	1386
SMAD4	0.013	4089
TNF	0.034	7124
KAT2B	0.038	8850
RELA	0.038	5970

It is of importance to note that all upstream regulators were predicted as activators, no upstream regulators were determined to be statistically significant inhibitors.

The up-regulation of RHOB and significant down-regulation of RHOV were observed by RT-qPCR in comparison of GIM-FRA1 to GIM-pcDNA3 (Figure 15A, B). GIM vs CON microarray analysis compared to GIM-FRA1 vs CON additionally indicated reduction in multiple genes related to cellular migration and adhesion including RHOB, RHOF, RHOV, MYO1E and substantial downregulation of MYLK3 (Figure 15C). In addition, cell adhesion molecules were predicted to be one of the most significantly impacted pathways in iPG analysis (Table 6)

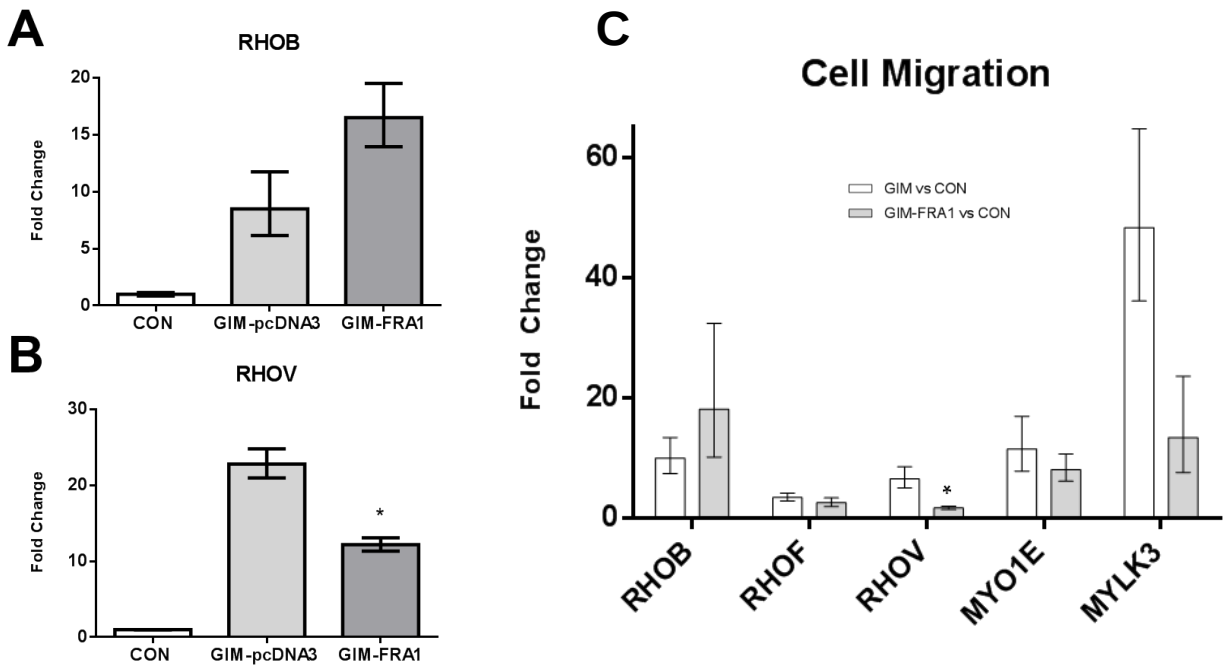

Figure 15: RT-qPCR and microarray analysis of cell migration related genes in GIM-FRA1, GIM-pcDNA3 and CON cell lines

(A) RHOB and **(B)** RHOV. Significant down-regulation of RHOV in comparison of GIM-FRA1 to GIM-pcDNA3 was observed,* denotes p-value <0.05. **(C)** Microarray comparison of cell migration related genes. Up-regulation of RHOB and down-regulation of RHOV was observed as seen in RT-qPCR analysis, as well as down-regulation of RHOF, MYO1E and MYLK3. * denotes p-value <0.05.

Table 6: Significantly impacted pathways in GIM-FRA1 vs GIM-pcDNA3

Impacted Pathway	**p-value**
Proteoglycans in cancer	2.36E-03
AGE-RAGE signaling pathway in diabetic complications	8.35E-03
Inflammatory bowel disease (IBD)	8.35E-03
Regulation of actin cytoskeleton	8.35E-03
TGF-beta signaling pathway	8.35E-03
Thiamine metabolism	8.35E-03
Cell adhesion molecules (CAMs)	8.35E-03
FoxO signaling pathway	8.35E-03
TNF signaling pathway	1.57E-02
Transcriptional misregulation in cancer	1.77E-02

4.3.7. FRA1 as a regulator

GIMs that overexpress the FRA1 gene have differential expression of many genes compared to their controls. The influence of FRA1 to this end has been explored. In GIM vs CON analysis PI15 was the fourth highest and IL7R the third most down-regulated out of 1,067 DEGs. It appears that FRA1 re-expression has a dramatic influence on the expression of these genes (Figure 16). The influence of FRA1 expression in this cell system are discussed in further detail in the following section.

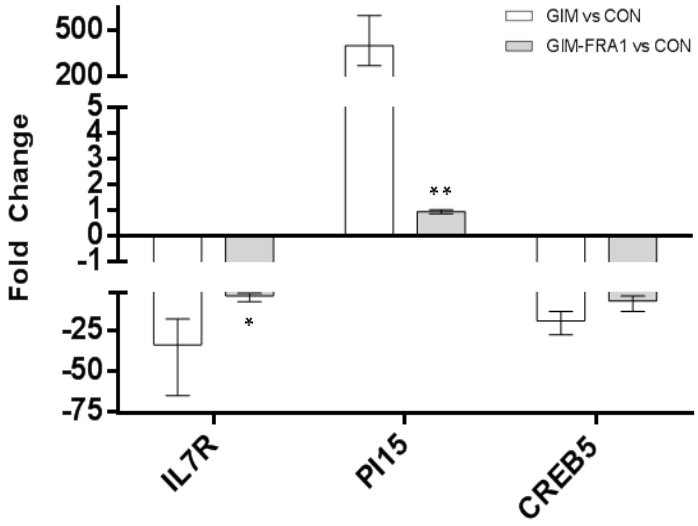

Figure 16: Microarray comparison of proposed genes regulated by FRA1 re-expression in GIM-FRA1 compared to GIM-pcDNA3

Comparison of microarray suggest that FRA1 re-expression in GIMs influences the expression of many genes, including IL7R, PI15. * denotes p-value <0.05 and ** denotes p-value <0.005.

4.4. Discussion

4.4.1. Exploratory Grouping Analysis and Principal Component Analysis

Exploratory grouping analysis (EGA) and principal component analysis (PCA) were performed on the CON, GIM-FRA1 and GIM-pcDNA3 cell lines utilized in this study. Transcriptome Analysis Console's EGA module enables analysis of relationships between samples based on un-defined raw data input. In other words, it does not group samples based on user defined information, but instead is unbiased in its grouping of samples based on their expression patterns. PCA is another visual statistical method that transforms observed variables that are potentially interrelated. The PCA results in linearly unrelated variables referred to as principal components which when mapped can be investigated for patterns within large sets of data. Graphical representations of large complex biological data sets are advantageous during initial examination and analysis of, for example, transcriptomics microarray data. EGA analysis of the GIM-FRA1, GIM-pcDNA3 and CON cell lines utilized in this experiment revealed that they group closely within cell types, all three exhibiting spatially distinct grouping (Figure 9). PCA analysis revealed discrete grouping with the three principal components accounting for 71.1% of dataset variance (Figure 10).

4.4.2. Alkaline Phosphatases

The re-expression of ALPI is well established and utilized as the invariable marker of the transformed tumorigenic phenotype in the CGL1 human hybrid system and its segregants (Latham et al. 1990, Mendonca et al. 1991). It has been previously shown that non-tumorigenic CGL1 and CONs express essentially no ALPI at the gene level with RT-qPCR, and protein level with alkaline phosphatase activity assays (Figure 3C, D). Conversely, GIMs express significantly higher levels

as validated with both assays. In this study GIM-FRA1 cells overexpressing FRA1 were shown to have highly significant (p-value <0.005) reductions of ALPI as compared to GIM-pcDNA3 vector controls as determined by RT-qPCR (Figure 11A). This significant reduction in ALPI was also observed with microarray experiments in terms of GIM vs CON compared to GIM-FRA1 vs CON. Interestingly, this study also revealed the reduction of several other alkaline phosphatase family members, ALPP, ALPP2 and ALPL (Figure 11B), although these were not as considerable as ALPI. The reduction of these additional alkaline phosphatase family members has not been shown previously in these cell lines. The highly significant reduction of ALPI in normally tumorigenic GIMs, which re-express FRA1, suggests that there has been a major shift in their phenotype based on the established marker of ALPI re-expression. This initial finding by microarray and RT-qPCR analysis suggests that GIMs that overexpress FRA1 are shifted phenotypically to a non-cancerous state.

4.4.3. AP-1 complex

FRA-1 is a member of the FOS family of transcription factors and a component of the AP-1 transcription factor complex. This complex also involves other members of the FOS and JUN family. The AP-1 complex is known to influence a variety of important molecular events relevant to carcinogenesis such as cellular proliferation, invasion, metastasis and apoptosis (Ibrahim et al. 2018, Milde-Langosch 2005, Soto et al. 2000). RT-qPCR showed that GIM-FRA1 cells significantly upregulate AP-1 complex family members cJUN and FRA1 when compared to vector controls (Figure 12A, B). cFOS was observed to be down-regulated in this comparison but not significantly with a p-value = 0.071 (Figure 12C). This suggests a reorganization of the AP-1 transcription factor complex, which consists of JUN and FOS family member heterodimers. Significant dysregulation of JUN and FOS family members JUNB, JUND, FOSB or FOSL2 was

not observed.

4.4.4. Phosphodiesterases

Previous microarray analysis of GIM vs CON revealed robust re-expression of many PDE isoforms (Figure 5C). It is observed in this study that GIM-FRA1 cells compared to CON downregulate several of these members including to an extensive degree PDEs 7B and 10A as well as to a lesser amount PDEs 3B, 4D and 4B (Figure 13C). This suggests partial recovery of the previously disrupted cAMP signaling. Normal cAMP production leads to activation of CREB which together are involved in downstream gene regulation. Previously CREB5 was found to be significantly downregulated in GIM vs CON analysis. Microarray and RT-qPCR analysis reveals that there is significant upregulation of CREB5 expression in GIM-FRA1 compared to GIM-pcDNA3, however this expression does not recover to CON levels. Moreover, it appears that re-expression of FRA1 in GIMs may lead to some recovery of dysregulated cAMP mediated signaling in GIMs.

4.4.5. TGFβ related signaling

In analysis of GIMs compared to CON (Chapter 3) one of the most significant findings was an apparent alteration in canonical TGFβ signaling. In this study, TGFβ was again found to be one of the most significantly enriched Molecular Function GO terms and TGFβ signaling one the most impacted pathways in iPG analysis (Table 4, Table 6). Further analysis of DEGs revealed that there is up-regulation of TGFβ signaling pathway genes THBS1 and follistatin (FST) in GIM-FRA1 vs CON as compared to GIM vs CON analysis in which both genes were significantly downregulated. THBS1 has been shown to be a key activator of TGF-β *in vivo* and expressed significantly lower in cervical cancer tumors (Crawford et al. 1998, Kodama et al. 2001, Murphy-

Ullrich et al. 2000). Based on iPG perturbation analysis of the TGFβ signaling pathway, it is proposed that the significant upregulation of THBS1 results in a regulatory interaction with latent TGFβ binding proteins resulting in up regulation of TGFβ signaling. A significant increase in canonical TGFβ signaling pathway cofactor SMAD2 was observed in GIM-FRA1 compared to GIM-pcDNA3. iPG pathway perturbation analysis suggests that the increase in FST in GIM-FRA1 compared to GIM-pcDNA3 further supports up-regulation of TGFβ signaling. Additionally, the upregulation of FST in iPG pathway perturbation analysis was proposed to as well upregulate TGFβ signaling. FST has also been shown to be an inhibitor of metastasis and invasiveness of cancer (Seachrist et al. 2017, Talmadge 2008, Zabkiewicz et al. 2017). Although further functional assay validation is warranted, it is proposed that FRA1 re-expression may recover previously observed dysregulation of the canonical TGFβ signaling in tumorigenic GIM vs non-tumorigenic CON analysis.

4.4.6. Extracellular Matrix Ligands and Receptors, cellular adhesion and migration

Epithelial cells, for example HeLa, use laminin to bind to basement membranes and laminins have been shown to promote an invasive tumorigenic phenotype (Fullar et al. 2015). It is observed that re-expression of FRA1 in GIMs vs CONs has downregulated genes related to ECM ligands and receptors, cellular adhesion and migration (Figure 14, Figure 15). Downregulation of LAMA1 expression as compared to GIM vs CON was observed, and although there is a recovery of expression for fibronectin related integrins ITGA4 and ITGA5, there is robust downregulation of related integrin ITGB8 and an observed further downregulation of FN1. The downregulation of genes related to cell migration was also observed in GIMs that overexpress FRA1 vs CON compared to GIM vs CON. Numerous collagens which have been shown to influence cancer formation, were observed including COL1A1, COL1A2 and COL12A1. In addition, multiple

genes related to cellular adhesion and migration were observed in comparison of the microarrays including RHOB, RHOF, RHOV, MYO1E and substantial downregulation of MYLK3. Many of the top 10 significantly enriched biological process, molecular function and cellular component GO terms were related to these changes (Table 4). This included negative regulation of cell proliferation, laminin binding, integrin binding, external side of the plasma membrane, focal adhesion, anchored component of the membrane and basal part of the cell. One of the top impacted pathways was Cell adhesion molecules (CAMs). Remodeling of the ECM has previously been shown to have a significant effect on tumorigenic phenotype (Fullar et al. 2015, Liu et al. 2017).

4.4.7. FRA1 as a master regulator of differential gene expression and altered tumorigenic phenotype in GIM-FRA1 cells

As previously discussed, there is novel evidence implicating that suppression or loss of FRA1 expression drives the neoplastic transformation of tumorigenic segregants of the CGL1 human hybrid cell system (*in preparation*). The re-expression of FRA1 in GIMs is proposed to have a significant regulatory effect on several key phenotypically relevant elements.

Altered expression of the AP-1 complex including downregulation of FRA1 has been shown previously in cancer cells, including cervical cancer (Prusty et al. 2005, Tyagi et al. 2017, Xiao et al. 2015). The re-expression of FRA1 in GIMs appears to indeed influence the rearrangement of this transcription factor complex. Specifically in terms of the up-regulation of cJUN and the down-regulation of cFOS compared to GIM vs CON analysis. It has previously been shown that molecular restructuring of the AP-1 complex can significantly influence the tumorigenic phenotype (Milde-Langosch 2005, Soto et al. 1999, Soto et al. 2000, Verde et al. 2007, Zhang et al. 2005). Transformation of non-tumorigenic to tumorigenic hybrid cells has been correlated with

the up-regulation of cJUN and FRA1, and the down-regulation of cFOS. Indeed, in microarray comparisons, GIM-FRA1 cells vs CON compared with GIM vs CON analysis show up-regulation of cJUN and FRA1 expression levels, as well as down-regulation of cFOS (Figure 12).

Significantly impacted GO terms in GIMs re-expressing FRA1 included negative regulation of cell proliferation, integrin binding, focal adhesion, anchored component of the membrane, basal part of cell and proteoglycan binding based on DEGs. Further analysis reveals that many ECM related genes are differentially expressed in GIM-FRA1 cells compared to GIM-pcDNA3. Additionally, numerous enriched GO terms and impacted pathways were related to ECM ligands and receptors as well as cellular adhesion and migration. It is proposed that FRA1 acts in a regulatory capacity for these known critical hallmarks of cancer, and in part influences the lack of tumorigenicity of GIM-FRA1 cells observed *in vivo*.

GIM-FRA1 cell lines exhibit differential expression of many genes compared to GIM-pcDNA3 vector only controls. In GIM vs CON analysis, PI15 was found to be the fourth highest and IL7R the third most down-regulated out of over 1,000 DEGs. This study reveals that FRA1 re-expression has a significant influence on the expression of these genes (Figure 16). Although further functional investigation into the altered expression of genes, e.g. PI15, is warranted as previously suggested, it appears that FRA1 plays a significant role in the modulation of differential tumorigenic phenotypes observed.

4.5. Conclusions

The overall goal of the research in this thesis chapter was to elucidate the role FRA1 plays in gene regulation and mechanistic links to the suppression of tumorigenicity in neoplastically transformed segregants of CGL1. Initial TAC analysis of GIM-FRA1 vs GIM-pcDNA3 revealed 365 DEGs based on threshold criteria. The most statistically significant DEG was determined to be FRA1. Among others were ALPI, AP-1 family member cJUN, PI15 and IL7R. A cursory analysis of CGL1 family members in this study reveals robust down-regulation of ALPI in GIM-FRA1 compared to GIM-pcDNA3, inductive of its tumorigenic phenotype. Downstream iPG software analysis reveals a variety of genes and pathways altered in GIMs re-expressing FRA1 including certain phosphodiesterases, ECM ligands and receptors, cellular migration and adhesion profiles as well as shifts in alkaline phosphatase expression as compared to those seen in GIM vs CON. As expected, FRA1 re-expression does not reverse all gene and pathway expression profiles observed in GIM vs CON analysis (Chapter 3). However, with the evidence that GIM-FRA1 cells are non-tumorigenic *in vivo* (*in preparation*), postulates as to the mechanism of observed tumor suppressive capacity are made. For example, recovery of gene expression profiles of molecular mechanisms related to their adherence, migratory and invasive capacity is believed to resulting in the failure of GIM-FRA1 cells to form tumors *in vivo*. The role of restructuring of AP-1 transcription factor complex family members is considered in regard to their differential expression with FRA1 re-expression. As previously discussed, the shift in expression profiles of cFOS, cJUN and FRA1 have been implicated as having an important role in influencing processes such as cellular proliferation, invasion and transformation in cancer (Hess et al. 2004, Ibrahim et al. 2018, Soto et al. 2000, Tyagi et al. 2017, Verde et al. 2007, Zhang et al. 2005).

When comparing GIMs to GIM-pcDNA3 only 8 genes meet threshold criteria (FC >2, <-2, FDR p-value <0.1), 5 of which are non-coding and have no affiliated gene symbol or description. The remaining are 2 miRNAs and a snoRNA. The DEGs elucidated in GIM-FRA1 vs GIM-pcDNA3 analysis we therefore considered to be directly or indirectly regulated by re-expression of FRA1. Known or predicted gene targets of FRA1 were explored utilizing the online databases GeneTrail Atlas v.1.0 (Backes et al. 2007), HumanNet v.1 (Lee et al. 2011), TRRUST v.2 (Han et al. 2018) and STRING v.10 (Szklarczyk et al. 2015). These databases contain thousands of target regulatory relationships and functional gene networks based on data and text mining of greater than 20 million scientific articles, experimentally validated protein-encoding genes and predictive modeling based on omics databases. By searching for targets of FRA1 and compiling the data from GeneTrail, HumanNet, TRRUST and STRING, 92 genes were revealed as known or predicted targets of FRA1. Of this, 8 were found to be differentially expressed in GIM-FRA1 vs GIM-pcDNA3 comparison, CCND1, CREB5, FOSL1, IL6, ITGA6, JUN, NFE2L3 and PLAUR. All of these genes were up-regulated in comparison of GIM-FRA1 to GIM-pcDNA3 and are found within the statistically significant DEGs determined by TAC analysis (Appendix G). Though not all gene interaction databases were exhaustively queried, it is proposed as potentially novel findings that the remainder of DEGs in this experiment may be directly or indirectly regulated by the FRA1 gene. It is significant to note that this potential new evidence of genes regulated by FRA1 will supplement microarray analysis software that search and reference annotated data.

Chapter 5: Conclusions and future directions

The overarching goal of the work outlined in this thesis was to re-characterize the CGL1 (HeLa x normal fibroblast) human hybrid cell system and related segregants. To this end, modern gene expression profiling technology, software analysis and functional validations were utilized to reveal novel differentially expressed genes and pathway level alterations between tumorigenic and non-tumorigenic segregants. In addition, a comprehensive review of the model, its origins and historical research milestones was prepared as a context in which to base new research findings.

Very limited research has been published with attempts to characterize the gene expression profiles of cell lines within this model system, or to link these findings to causal mechanisms driving their tumorigenic phenotypes. As a result of systematically reviewing the history of prior research with CGL1, only a few published papers were discovered in this regard (Nishizuka et al. 2001, Nishizuka et al. 2001, Tsujimoto et al. 1999). These studies investigated a variety of the cell line segregants related to CGL1 to perform gene expression profiling using a several techniques (Appendix H). In the late 1990's, Tsujimoto et al. utilized differential display RT-qPCR to explore DEGs in non-tumorigenic CGL1 and CON2, and tumorigenic CGL3 and GIM31 cell lines. This study revealed only 7 known genes differentially expressed in the tumorigenic cells, though at the time differential display RT-qPCR was being replaced with newer and superior microarray technologies. The limitations of this technique were clear as this study failed to determine ALPI to be differentially expressed, which was already known to be invariably associated with tumorigenicity in the CGL1 system. However, 5 of these genes were found also to be upregulated in GIM vs CON analysis (Chapter 3). In the early 2000's, Nishizuka et al. published the first and

only microarray technology based study to explore gene expression correlations to the tumorigenic phenotype in cells of the CGL1 system. This study found 14 genes upregulated and 15 downregulated in comparison of non-tumorigenic CGL1 and CGL2 to tumorigenic CGL3 and CGL4. In profiling of GIM vs CON (Chapter 3) many of these genes were found to be differentially expressed, and all matched the directionality of expression found in CGL1 and CGL2 compared to CGL3 and CGL4. It is important to note that this comparison was not between radiation induced neoplastically transformed segregants as in Chapter 3. Nonetheless, many of the genes correlate with the tumorigenic phenotype and directionality of gene expression as found by Niskizuka et al. in 2001.

It has now been nearly two decades since any published attempts to perform gene expression profiling on any CGL1 family members has been conducted. Although CON3 and GIM31 were investigated (Tsujimoto et al. 1999), no additional work looking at gene expression profiles of other radiation induced segregants has been published. Additionally, the penultimate chapter of this thesis represents the first attempts on gene expression profiling of the non-tumorigenic GIM-FRA1 cells and tumorigenic GIM-pcDNA3 vector controls. This thesis sought to re-characterize these model cells with modern up-to-date technologies available in order to supplement and bring into new understanding their differentially expressed gene expression profiles. In doing so, new molecular level understandings can be linked to mechanistic and pathway level events that occur in neoplastically transformed CGL1 cells.

Global transcriptomic profiling was utilized with the phenotypically different GIM and CON radiation induced segregants of CGL1 (Chapter 3). This, along with validation by several functional assays, revealed a previously unprecedented number of DEGs, as well as pathway and gene network level alterations as hypothesized. Further analysis of the 1,067 DEGs revealed

enriched GO terms, affected pathways and networks, as well as putative upstream master regulators. These analyses revealed that tumorigenic GIMs demonstrate shifts in cellular adhesion and ECM profiles, altered cAMP signaling, as well as cellular energetics and nutrient transport. A projected upstream regulator TGFβ was investigated with functional gene expression assays revealing altered canonical signaling in neoplastically transformed GIMs as compared to CONs. Taken together, this study presented novel insight into the possible mechanistic contributions that lead to the tumorigenic phenotype of GIM cells as compared to irradiated segregant non-tumorigenic CONs.

As previously described (Chapter 4), significant research with the CGL1 system over many years has implicated chromosome 11 in the shift to tumorigenic phenotypes in human hybrid cells (Mendonca et al. 2004, Mendonca et al. 1999, Mendonca et al. 1998, Saxon et al. 1986, Srivatsan et al. 1986, Srivatsan et al. 2002). These efforts led to the proposal of several candidate tumor suppressor genes which were further studied in greater experimental depth. Research efforts in the laboratory of Dr. Marc Mendonca eventually revealed important novel evidence implicating the loss of FRA1 expression as involved in the neoplastic transformation of tumorigenic segregants of the CGL1 human hybrid cell system (Chapter 4). Tumorigenic GIM cells were transfected to re-express the candidate tumor suppressor gene FRA1, which resulted in the significant discovery that these GIM-FRA1 cells produce no tumors *in vivo* (*in preparation*). Though some validation of gene and protein makers for genes of interest, for example ALPI, were performed, there existed an opportunity to characterize these unique segregants utilizing modern global gene expression profiling technology. To this end, non-tumorigenic GIM-FRA1 and tumorigenic GIM-pcDNA3 vector control cell lines were investigated in order to understand the gene level influence of FRA1 re-expression and causally link it to the suppression of tumorigenicity.

With human transcriptome microarray and RT-qPCR technology, the gene expression profiles of GIM-FRA1 and GIM-pcDNA3 were investigated resulting in the discovery of 365 DEGs. These were analyzed downstream in the context of what genes FRA1 re-expression in GIM cells are altered in terms of differential expression, and in the context of how GIM-FRA1 cells compared to CON related to GIM vs CON analysis for GOIs. The re-expression of FRA1 in GIMs is shown to effect a variety of genes and therefore subsequent pathways related to ECM ligands and receptors, cellular adhesion and migration, as well as shifts in phosphodiesterase and alkaline phosphatase profiles compared to those seen in GIM vs CON. Although the human hybrid cells do retain some known markers of tumorigenic cells in the genetic balance between parental HeLa and normal fibroblast, the *in vivo* phenotypes have been established. Therefore it is proposed that FRA1 acts in a tumor suppressive capacity in GIM-FRA1 cells at least in part by significantly altering components related to their adherence, migratory and invasive capacity, resulting in the cessation of tumor formation *in vivo*.

In all of the cell lines mentioned within this thesis including non-tumorigenic CGL1, CGL2, CON and GIM-FRA1 as well as tumorigenic CGL3, CGL4, GIM and GIM-pcDNA3, the re-expression of ALPI is the well-established antigenic marker of neoplastic transformation. The marker has been validated in numerous *in vitro* and *in vivo* studies with CGL1 and related cell lines (Latham et al. 1990, Mendonca et al. 1991). There have long been reported associations in the literature as to elevated alkaline phosphatase levels in cancer cells, as well as investigation into the biological relevance of this observation (Harris 1990, Millan 1988, Millan 1990). Although the mechanisms regulating re-expression of ALPI in CGL1 cell members is not yet fully know, it is clear there is a direct correlation between its expression and the tumorigenic phenotype. It has been formerly proposed and evidence provided that trans-regulatory control of ALPI is correlated to chromosome

11 (Latham et al. 1992, Saxon et al. 1986). It is therefore suggested, especially in light of GIM-FRA1 studies in this thesis, that FRA1 acts in a regulatory capacity on this established and validated antigenic marker of neoplastic transformation. The results of this thesis also lead to the proposal that FRA1 acts in this capacity on a variety of other genes as well, for example PI15, IL7R, several PDE family members and others, the biological relevance of which remains a practical line of future scientific exploration. Studies in this thesis further support as previously discussed the influence of AP-1 transcription factor complex reorganization, which has been linked to observed altered phenotypes in these studies such as cellular proliferation and invasion (Ibrahim et al. 2018, Prusty et al. 2005, Soto et al. 2000, Xiao et al. 2015). As FRA1 is a family member of the AP-1 complex, it would indeed be a prudent future line of study to investigate the role of FRA1 re-expression in tumorigenic cells utilizing functional assays such invasion, adhesion and migration experiments.

The CGL1 cell system has been used for many decades as an excellent research model *in vitro* and *in vivo to* study neoplastic transformation in a variety of contexts. As a continuation of this foundational work, this thesis intended to bring this model into a modern perspective utilizing contemporary technology and tools to re-characterize their established phenotypes. To this end, global gene expression microarray technology and functional validation of this cell system was pursued, the results of which have been detailed within this thesis. However, there is still much to be explored, and it is a belief that the results contained herein will supplement in the pursuit of these future research endeavors. A major proposition is to utilize the capacity of the CGL1 system as a sensitive neoplastic transformation assay (as detailed in Chapter 2) in a truly novel research environment (Appendix A). Another goal currently in progress is to utilize CRISPR gene editing technology to selectively knock out FRA1 expression in the CGL1 system. As previously

discussed, siRNA silencing of FRA1 in CGL1 cells was shown to induce tumor growth *in vivo*. If successful CRISPR knockout of the FRA1 gene in non-tumorigenic CGL1 or CON cells demonstrates this same result it with further strengthen FRA1 as a true tumor suppressor gene. Another goal currently in progress is ionizing radiation based studies with the cell system. Survival curves and flow cytometry based γH2AX DNA DSB experimental assays have been performed utilizing CON, GIM, GIM-FRA1 and GIM-pcDNA3 cell lines (*in preparation*). These findings will contribute to our understanding of the effects and mechanisms involved in the radiation induced neoplastic transformation of CGL1 cells.

Ultimately, continued research utilizing the CGL1 human hybrid cell system and its unique related segregants warrants future original exploration, and that the results contained within this thesis will supplement and support such investigations.

References:

Abrego, J., V. Gunda, E. Vernucci, S. K. Shukla, R. J. King, A. Dasgupta, G. Goode, D. Murthy, F. Yu and P. K. Singh (2017). "GOT1-mediated anaplerotic glutamine metabolism regulates chronic acidosis stress in pancreatic cancer cells." Cancer Lett **400**: 37-46.

Ahmad, Q. R., R. C. Allen, T. C. Andersen, D. A. J, J. C. Barton, E. W. Beier, M. Bercovitch, J. Bigu, S. D. Biller, R. A. Black, I. Blevis, R. J. Boardman, J. Boger, E. Bonvin, M. G. Boulay, et al. (2002). "Direct evidence for neutrino flavor transformation from neutral-current interactions in the Sudbury Neutrino Observatory." Phys Rev Lett **89**(1): 011301.

Alexa, A., J. Rahnenfuhrer and T. Lengauer (2006). "Improved scoring of functional groups from gene expression data by decorrelating GO graph structure." Bioinformatics **22**(13): 1600-1607.

Antonelli, F., N. Bell, O. Sapora, G. Simone, E. Sorrentino, M. A. Tabocchini, L. Conti Devirgiliis, C. Carbone, M. Balata, L. Ioannucci and S. Nisi (2008). PULEX. LNGS Annual Report 2007**:** 229-235.

Antonelli, F., M. Belli, M. Pinto, O. Sapora, E. Sorrentino, G. Simone, M. A. Tabocchini, F. Amicarelli, L. Conti Devirgiliis, M. C. Carbone, M. Balata, L. Ioannucci, S. Nisi and L. Satta (2008). "PULEX: Influence of environment radiation background on biochemistry and biology of cultured cells and on their response to genotoxic agents." Il Nuovo Cimento C **31**(1): 49-56.

Ashburner, M., C. A. Ball, J. A. Blake, D. Botstein, H. Butler, J. M. Cherry, A. P. Davis, K. Dolinski, S. S. Dwight, J. T. Eppig, M. A. Harris, D. P. Hill, L. Issel-Tarver, A. Kasarskis, S. Lewis, et al. (2000). "Gene ontology: tool for the unification of biology. The Gene Ontology Consortium." Nat Genet **25**(1): 25-29.

Attar, M., Y. Molaie Kondolousy and N. Khansari (2007). "Effect of high dose natural ionizing radiation on the immune system of the exposed residents of Ramsar Town, Iran." Iran J Allergy Asthma Immunol **6**(2): 73-78.

Azzam, E. I., S. M. de Toledo, T. Gooding and J. B. Little (1998). "Intercellular communication is involved in the bystander regulation of gene expression in human cells exposed to very low fluences of alpha particles." Radiat Res **150**(5): 497-504.

Azzam, E. I., S. M. de Toledo, G. P. Raaphorst and R. E. Mitchel (1996). "Low-dose ionizing radiation decreases the frequency of neoplastic transformation to a level below the spontaneous rate in C3H 10T1/2 cells." Radiat Res **146**(4): 369-373.

Azzam, E. I., G. P. Raaphorst and R. E. Mitchel (1994). "Radiation-induced adaptive response for protection against micronucleus formation and neoplastic transformation in C3H 10T1/2 mouse embryo cells." Radiat Res **138**(1 Suppl): S28-31.

Backes, C., A. Keller, J. Kuentzer, B. Kneissl, N. Comtesse, Y. A. Elnakady, R. Muller, E. Meese and H. P. Lenhof (2007). "GeneTrail--advanced gene set enrichment analysis." Nucleic Acids Res **35**(Web Server issue): W186-192.

Barski, G. and F. Cornefert (1962). "Characteristics of "hybrid"-type clonal cell lines obtained from mixed cultures in vitro." J Natl Cancer Inst **28**: 801-821.

Bettega, D., P. Calzolari, P. Hessel, C. G. Stucchi and W. K. Weyrather (2009). "Neoplastic transformation induced by carbon ions." Int J Radiat Oncol Biol Phys **73**(3): 861-868.

Bettega, D., P. Calzolari, A. Piazzolla, L. Tallone and J. L. Redpath (1997). "Alpha-particle-induced neoplastic transformation in synchronized hybrid cells of HeLa and human skin fibroblasts." Int J Radiat Biol **72**(5): 523-529.

Boger, J., R. L. Hahn, J. K. Rowley, A. L. Carter, B. Hollebone, D. Kessler, I. Blevis and T. S. Collaboration (2000). "The Sudbury Neutrino Observatory." Nucl Instr Meth Phys Res A **449**(1-2): 172-207.

Borek, C. (1980). "X-ray induced in vitro neoplastic transformation of human diploid cells." Nature **283**(5749): 776-778.

Borek, C. (1985). "Cellular and molecular mechanisms in malignant transformation of diploid rodent and human cells by radiation." Carcinog Compr Surv **9**: 365-378.

Boveri, T. (2008). "Concerning the origin of malignant tumours by Theodor Boveri. Translated and annotated by Henry Harris." J Cell Sci **121 Suppl 1**: 1-84.

Bregula, U., G. Klein and H. Harris (1971). J. Cell Sci. **8**: 673-680.

Brooke, L. T. (1975). "Effect of Different Constant Incubation Temperatures on Egg Survival and Embryonic Development in Lake Whitefish (Coregonus clupeaformis)." Trans Am Fish Soc **104**(3): 555-559.

Brooks, A. L. and L. T. Dauer (2014). "Advances in radiation biology: effect on nuclear medicine." Semin Nucl Med **44**(3): 179-186.

Bugrim, A. E. (1999). "Regulation of Ca2+ release by cAMP-dependent protein kinase. A mechanism for agonist-specific calcium signaling?" Cell Calcium **25**(3): 219-226.

Calabrese, E. J. and L. A. Baldwin (2001). "U-shaped dose-responses in biology, toxicology, and public health." Annu Rev Public Health **22**: 15-33.

Carbone, M. C., M. Pinto, F. Antonelli, F. Amicarelli, M. Balata, M. Belli, L. Conti Devirgiliis, L. Ioannucci, S. Nisi, O. Sapora, L. Satta, G. Simone, E. Sorrentino and M. A. Tabocchini (2009). "The Cosmic Silence experiment: on the putative adaptive role of environmental ionizing

radiation." Radiat Environ Biophys **48**(2): 189-196.

Carbone, M. C., M. Pinto, F. Antonelli and M. Balata (2010). "Effects of deprivation of background environmental radiation on cultured human cells." Il Nuovo Cimento B **125**(4): 469-477.

Carvalho-Cruz, P., F. Alisson-Silva, A. R. Todeschini and W. B. Dias (2018). "Cellular glycosylation senses metabolic changes and modulates cell plasticity during epithelial to mesenchymal transition." Dev Dyn **247**(3): 481-491.

Castillo, H., D. Schoderbek, S. Dulal, G. Escobar, J. Wood, R. Nelson and G. Smith (2015). "Stress induction in the bacteria Shewanella oneidensis and Deinococcus radiodurans in response to below-background ionizing radiation." Int J Radiat Biol **91**(9): 749-756.

Chen, T. T. and C. Heidelberger (1969). "Quantitative studies on the malignant transformation of mouse prostate cells by carcinogenic hydrocarbons in vitro." Int J Cancer **4**(2): 166-178.

Colman, M., S. Bahtt, M. Candelaria, C. Sun and J. L. Redpath (1988). "A comparison of the radiation sensitivities of non-tumorigenic and tumorigenic human hybrid cell lines." Int J Radiat Biol **53**(4): 609-616.

Conter, A. (1987). "Preirradiation of medium induces a subsequent stimulation or inhibition of growth according to the physiological state in Synechococcus lividus in culture." Radiat Res **109**(2): 342-346.

Conter, A., D. Dupouy and H. Planel (1983). "Demonstration of a biological effect of natural ionizing radiations." Int J Radiat Biol Relat Stud Phys Chem Med **43**(4): 421-432.

Crawford, S. E., V. Stellmach, J. E. Murphy-Ullrich, S. M. Ribeiro, J. Lawler, R. O. Hynes, G. P. Boivin and N. Bouck (1998). "Thrombospondin-1 is a major activator of TGF-beta1 in vivo." Cell **93**(7): 1159-1170.

Croute, F., D. Dupouy, J. P. Charley, J. P. Soleilhavoup and H. Planel (1980). "Effects of autogamy in Paramecium tetraurelia on catalase activity and on radiosensitivity to natural ionizing radiations." J Protozool **27**(1): 132-135.

Croute, F., J. P. Soleilhavoup, S. Vidal, D. Dupouy and H. Planel (1982). "Paramecium tetraurelia Growth Stimulation under Low-Level Chronic Irradiation: Investigations on a Possible Mechanism." Radiation Research **92**(3): 8.

de Feijter-Rupp, H. L., T. Hayashi, G. H. Kalimi, P. Edwards, J. L. Redpath, C. C. Chang, E. J. Stanbridge and J. E. Trosko (1998). "Restored gap junctional communication in non-tumorigenic HeLa-normal human fibroblast hybrids." Carcinogenesis **19**(5): 747-754.

Der, C. J. and E. J. Stanbridge (1980). "Alterations in the extracellular matrix organization associated with the reexpression of tumorigenicity in human cell hybrids." Int J Cancer **26**(4):

451-459.

Der, C. J. and E. J. Stanbridge (1981). "A tumor-specific membrane phosphoprotein marker in human cell hybrids." Cell **26**: 429-438.

Desgrosellier, J. S. and D. A. Cheresh (2010). "Integrins in cancer: biological implications and therapeutic opportunities." Nat Rev Cancer **10**(1): 9-22.

Draghici, S., P. Khatri, A. L. Tarca, K. Amin, A. Done, C. Voichita, C. Georgescu and R. Romero (2007). "A systems biology approach for pathway level analysis." Genome Res **17**(10): 1537-1545.

Duncan, F., A. J. Noble and D. Sinclair (2010). "The Construction and Anticipated Science of SNOLAB." Annu Rev Nucl Part Sci **60**: 163-180.

El-Gebali, S., S. Bentz, M. A. Hediger and P. Anderle (2013). "Solute carriers (SLCs) in cancer." Mol Aspects Med **34**(2-3): 719-734.

Elmore, E., X. Y. Lao, R. Kapadia, E. Giedzinski, C. Limoli and J. L. Redpath (2008). "Low doses of very low-dose-rate low-LET radiation suppress radiation-induced neoplastic transformation in vitro and induce an adaptive response." Radiat Res **169**(3): 311-318.

Elmore, E., X. Y. Lao, M. Ko, S. Rightnar, G. Nelson and J. Redpath (2005). "Neoplastic transformation in vitro induced by low doses of 232 MeV protons." Int J Radiat Biol **81**(4): 291-297.

Ephrussi, B., R. L. Davidson, M. C. Weiss, H. Harris and G. Klein (1969). "Malignancy of somatic cell hybrids." Nature **224**(5226): 1314-1316.

Fajardo, A. M., G. A. Piazza and H. N. Tinsley (2014). "The role of cyclic nucleotide signaling pathways in cancer: targets for prevention and treatment." Cancers (Basel) **6**(1): 436-458.

Frankenberg, D., K. Kelnhofer, I. Garg, K. Bar and M. Frankenberg-Schwager (2002). "Enhanced mutation and neoplastic transformation in human cells by 29 kVp relative to 200 kVp X rays indicating a strong dependence of RBE on photon energy." Radiat Prot Dosimetry **99**(1-4): 261-264.

Fratini, E., C. Carbone, D. Capece, G. Esposito, G. Simone, M. A. Tabocchini, M. Tomasi, M. Belli and L. Satta (2015). "Low-radiation environment affects the development of protection mechanisms in V79 cells." Radiat Environ Biophys **54**(2): 183-194.

Fullar, A., J. Dudas, L. Olah, P. Hollosi, Z. Papp, G. Sobel, K. Karaszi, S. Paku, K. Baghy and I. Kovalszky (2015). "Remodeling of extracellular matrix by normal and tumor-associated fibroblasts promotes cervical cancer progression." BMC Cancer **15**: 256.

Gajendiran, N. and R. K. Jeevanram (2002). "Environmental radiation as the conditioning factor

for the survival of yeast Saccharomyces cerevisiae." Indian Journal of Experimental Biology **40**(1): 6.

Ghiassi-nejad, M., S. M. Mortazavi, J. R. Cameron, A. Niroomand-rad and P. A. Karam (2002). "Very high background radiation areas of Ramsar, Iran: preliminary biological studies." Health Phys **82**(1): 87-93.

Ghiassi-Nejad, M., F. Zakeri, R. G. Assaei and A. Kariminia (2004). "Long-term immune and cytogenetic effects of high level natural radiation on Ramsar inhabitants in Iran." J Environ Radioact **74**(1-3): 107-116.

Givant-Horwitz, V., B. Davidson and R. Reich (2005). "Laminin-induced signaling in tumor cells." Cancer Lett **223**(1): 1-10.

Grosovsky, A. J. (1999). "Radiation-induced mutations in unirradiated DNA." Proc. Natl. Acad. Sci. USA **96**: 5346-5347.

Han, H., J. W. Cho, S. Lee, A. Yun, H. Kim, D. Bae, S. Yang, C. Y. Kim, M. Lee, E. Kim, S. Lee, B. Kang, D. Jeong, Y. Kim, H. N. Jeon, et al. (2018). "TRRUST v2: an expanded reference database of human and mouse transcriptional regulatory interactions." Nucleic Acids Res **46**(D1): D380-D386.

Hanahan, D. and R. A. Weinberg (2000). "The hallmarks of cancer." Cell **100**(1): 57-70.

Hanahan, D. and R. A. Weinberg (2011). "Hallmarks of cancer: the next generation." Cell **144**(5): 646-674.

Harris, H. (1969). Nature **223**: 363-368.

Harris, H. (1990). "The human alkaline phosphatases: what we know and what we don't know." Clin Chim Acta **186**(2): 133-150.

Harris, H., O. J. Miller, G. Klein, P. Worst and T. Tachibana (1969). "Suppression of malignancy by cell fusion." Nature **223**(5204): 363-368.

Harris, H. and J. F. Watkins (1965). "Hybrid Cells Derived from Mouse and Man: Artificial Heterokaryons of Mammalian Cells from Different Species." Nature **205**: 640-646.

Harris, H., J. F. Watkins, C. E. Ford and G. I. Schoefl (1966). "Artificial heterokaryons of animal cells from different species." J Cell Sci **1**(1): 1-30.

Hata, A. and Y. G. Chen (2016). "TGF-beta Signaling from Receptors to Smads." Cold Spring Harb Perspect Biol **8**(9).

He, L., K. Vasiliou and D. W. Nebert (2009). "Analysis and update of the human solute carrier (SLC) gene superfamily." Hum Genomics **3**(2): 195-206.

Hei, T. K., Y. L. Zhao, D. Roy, C. Q. Piao, G. Calaf and E. J. Hall (2001). "Molecular alterations in tumorigenic human bronchial and breast epithelial cells induced by high LET radiation." Adv Space Res **27**(2): 411-419.

Hess, J., P. Angel and M. Schorpp-Kistner (2004). "AP-1 subunits: quarrel and harmony among siblings." J Cell Sci **117**(Pt 25): 5965-5973.

Hill, C. K., F. M. Buonaguro, C. P. Myers, A. Han and M. M. Elkind (1982). "Fission-spectrum neutrons at reduced dose rates enhance neoplastic transformation." Nature **298**(5869): 67-69.

Hill, C. K., A. Han and M. M. Elkind (1984). "Fission-spectrum neutrons at a low dose rate enhance neoplastic transformation in the linear, low dose region (0-10 cGy)." Int J Radiat Biol Relat Stud Phys Chem Med **46**(1): 11-15.

Ibrahim, S. A. E., A. Abudu, E. Jonhson, N. Aftab, S. Conrad and M. Fluck (2018). "The role of AP-1 in self-sufficient proliferation and migration of cancer cells and its potential impact on an autocrine/paracrine loop." Oncotarget **9**(76): 34259-34278.

Joiner, M. C., B. Marples, P. Lambin, S. C. Short and I. Turesson (2001). "Low-dose hypersensitivity: current status and possible mechanisms." Int J Radiat Oncol Biol Phys **49**(2): 379-389.

Kadochi, Y., S. Mori, R. Fujiwara-Tani, Y. Luo, Y. Nishiguchi, S. Kishi, K. Fujii, H. Ohmori and H. Kuniyasu (2017). "Remodeling of energy metabolism by a ketone body and medium-chain fatty acid suppressed the proliferation of CT26 mouse colon cancer cells." Oncol Lett **14**(1): 673-680.

Kaelbling, M. and H. P. Klinger (1986). "Suppression of tumorigenicity in somatic cell hybrids. III. Cosegregation of human chromosome 11 of a normal cell and suppression of tumorigenicity in intraspecies hybrids of normal diploid x malignant cells." Cytogenet Cell Genet **41**(2): 65-70.

Karunagaran, D. and G. Jinesh (2008). TGF-β, Smads and Cervical Cancer. Transforming Growth Factor-β in Cancer Therapy, Volume II: Cancer Treatment and Therapy. S. B. Jakowlew. Totowa, NJ, Humana Press**:** 33-49.

Kawanishi, M., K. Okuyama, K. Shiraishi, Y. Matsuda, R. Taniguchi, N. Shiomi, M. Yonezawa and T. Yagi (2012). "Growth retardation of Paramecium and mouse cells by shielding them from background radiation." J Radiat Res **53**(3): 404-410.

Kennedy, A. R., J. Cairns and J. B. Little (1984). "Timing of steps in transformation of C3H10 T1/2 cells by X-irradiation." Nature **307**: 85-86.

Khatri, P., S. Draghici, A. L. Tarca, S. S. Hassan and R. Romero (2007). "A system biology approach for the steady-state analysis of gene signaling networks." Progress in Pattern Recognition, Image Analysis and Applications, Proceedings **4756**: 32-+.

Kim, G. J., K. Chandrasekaran and W. F. Morgan (2006). "Mitochondrial dysfunction, persistently elevated levels of reactive oxygen species and radiation-induced genomic instability: a review." Mutagenesis **21**(6): 361-367.

Kitahara, O., T. Katagiri, T. Tsunoda, Y. Harima and Y. Nakamura (2002). "Classification of sensitivity or resistance of cervical cancers to ionizing radiation according to expression profiles of 62 genes selected by cDNA microarray analysis." Neoplasia **4**(4): 295-303.

Klein, G., S. Friberg, F. Wiener and H. Harris (1973). J. natn. Cancer Inst. **50**: 1259-1268.

Klinger, H. P. (1980). "Suppression of tumorigenicity in somatic cell hybrids. I. Suppression and reexpression of tumorigenicity in diploid human X D98AH2 hybrids and independent segregation of tumorigenicity from other cell phenotypes." Cytogenet Cell Genet **27**(4): 254-266.

Klinger, H. P., A. S. Baim, C. K. Eun, T. B. Shows and F. H. Ruddle (1978). "Human chromosomes which affect tumorigenicity in hybrids of diploid human with heteroploid human or rodent cells." Cytogenet Cell Genet **22**(1-6): 245-249.

Ko, M., X. Y. Lao, R. Kapadia, E. Elmore and J. L. Redpath (2006). "Neoplastic transformation in vitro by low doses of ionizing radiation: role of adaptive response and bystander effects." Mutat Res **597**(1-2): 11-17.

Ko, S. J., X. Y. Liao, S. Molloi, E. Elmore and J. L. Redpath (2004). "Neoplastic transformation in vitro after exposure to low doses of mammographic-energy X rays: quantitative and mechanistic aspects." Radiat Res **162**(6): 646-654.

Kodama, J., I. Hashimoto, N. Seki, A. Hongo, M. Yoshinouchi, H. Okuda and T. Kudo (2001). "Thrombospondin-1 and -2 messenger RNA expression in invasive cervical cancer: correlation with angiogenesis and prognosis." Clin Cancer Res **7**(9): 2826-2831.

Kramer, A., J. Green, J. Pollard, Jr. and S. Tugendreich (2014). "Causal analysis approaches in Ingenuity Pathway Analysis." Bioinformatics **30**(4): 523-530.

Kretschmer, A., K. Moepert, S. Dames, M. Sternberger, J. Kaufmann and A. Klippel (2003). "Differential regulation of TGF-beta signaling through Smad2, Smad3 and Smad4." Oncogene **22**(43): 6748-6763.

Latham, K. M. and E. J. Stanbridge (1990). "Identification of the HeLa tumor-associated antigen, p75/150, as intestinal alkaline phosphatase and evidence for its transcriptional regulation." Proceedings of the National Academy of the Sciences of the United States of America **87**: 1263-1267.

Latham, K. M. and E. J. Stanbridge (1992). "Examination of the oncogenic potential of a tumor-associated antigen, intestinal alkaline phosphatase, in HeLa x fibroblast cell hybrids." Cancer Res **52**(3): 616-622.

Lebrun, J. J. (2012). "The Dual Role of TGFbeta in Human Cancer: From Tumor Suppression to Cancer Metastasis." ISRN Mol Biol **2012**: 381428.

Lee, I., U. M. Blom, P. I. Wang, J. E. Shim and E. M. Marcotte (2011). "Prioritizing candidate disease genes by network-based boosting of genome-wide association data." Genome Res **21**(7): 1109-1121.

Lemon, J. A., N. Phan and D. R. Boreham (2017). "Multiple CT Scans Extend Lifespan by Delaying Cancer Progression in Cancer-Prone Mice." Radiat Res **188**(4.2): 495-504.

Lemon, J. A., N. Phan and D. R. Boreham (2017). "Single CT Scan Prolongs Survival by Extending Cancer Latency in Trp53 Heterozygous Mice." Radiat Res **188**(4.2): 505-511.

Lewis, D. A., B. M. Mayhugh, Y. Qin, K. Trott and M. S. Mendonca (2001). "Production of delayed death and neoplastic transformation in CGL1 cells by radiation-induced bystander effects." Radiat Res **156**(3): 251-258.

Li, H., Y. Gu, J. Miki, B. Hukku, D. G. McLeod, T. K. Hei and J. S. Rhim (2007). "Malignant transformation of human benign prostate epithelial cells by high linear energy transfer alpha-particles." Int J Oncol **31**(3): 537-544.

Limoli, C. L., E. Giedzinski, W. F. Morgan, S. G. Swarts, G. D. Jones and W. Hyun (2003). "Persistent oxidative stress in chromosomally unstable cells." Cancer Res **63**(12): 3107-3111.

Limoli, C. L., B. Ponnaiya, J. J. Corcoran, E. Giedzinski, M. I. Kaplan, A. Hartmann and W. F. Morgan (2000). "Genomic instability induced by high and low LET ionizing radiation." Adv Space Res **25**(10): 2107-2117.

Liu, S., G. Liao and G. Li (2017). "Regulatory effects of COL1A1 on apoptosis induced by radiation in cervical cancer cells." Cancer Cell Int **17**: 73.

Luckey, T. D. (1986). "Ionizing radiation promotes protozoan reproduction." Radiat Res **108**(2): 215-221.

Marder, B. A. and W. F. Morgan (1993). "Delayed chromosomal instabiltiy induced by DNA damage." Molecular and Cellular Biology **13**(11): 6667-6677.

Martin, C. J. (2005). "The LNT model provides the best approach for practical implementation of radiation protection." Br J Radiol **78**(925): 14-16.

Masoomi, J. R., S. Mohammadi, M. Amini and M. Ghiassi-Nejad (2006). "High background radiation areas of Ramsar in Iran: evaluation of DNA damage by alkaline single cell gel electrophoresis (SCGE)." J Environ Radioact **86**(2): 176-186.

Matsuya, Y., H. Green and C. Basilico (1968). "Properties and uses of human-mouse hybrid cell

lines." Nature **220**(5173): 1199-1202.

Mayr, B. and M. Montminy (2001). "Transcriptional regulation by the phosphorylation-dependent factor CREB." Nat Rev Mol Cell Biol **2**(8): 599-609.

Mendonca, M. S., R. J. Antoniono, K. M. Latham, E. J. Stanbridge and J. L. Redpath (1991). "Characterization of intestinal alkaline phosphatase expression and the tumorigenic potential of gamma-irradiated HeLa x fibroblast cell hybrids." Cancer Res **51**(16): 4455-4462.

Mendonca, M. S., R. J. Antoniono and J. L. Redpath (1993). "Delayed heritable damage and epigenetics in radiation-induced neoplastic transformation of human hybrid cells." Radiat Res **134**(2): 209-216.

Mendonca, M. S., R. J. Antoniono, C. Sun and J. L. Redpath (1992). "A simplified and rapid staining method for the HeLa x skin fibroblast human hybrid cell neoplastic transformation assay." Radiat Res **131**(3): 345-350.

Mendonca, M. S., H. Chin-Sinex, J. Gomez-Millan, N. Datzman, M. Hardacre, K. Comerford, H. Nakshatri, M. Nye, L. Benjamin, S. Mehta, F. Patino and C. Sweeney (2007). "Parthenolide sensitizes cells to X-ray-induced cell killing through inhibition of NF-kappaB and split-dose repair." Radiat Res **168**(6): 689-697.

Mendonca, M. S., L. A. Desmond, T. M. Temples, D. L. Farrington and B. M. Mayhugh (2000). "Loss of chromosome 14 increases the radiosensitivity of CGL1 human hybrid cells but lowers their susceptibility to radiation-induced neoplastic transformation." Mutagenesis **15**(3): 187-193.

Mendonca, M. S., D. L. Farrington, B. M. Mayhugh, Y. Qin, T. Temples, K. Comerford, R. Chakrabarti, K. Zainabadi, J. L. Redpath, E. J. Stanbridge and E. S. Srivatsan (2004). "Homozygous deletions within the 11q13 cervical cancer tumor-suppressor locus in radiation-induced, neoplastically transformed human hybrid cells." Genes Chromosomes Cancer **39**(4): 277-287.

Mendonca, M. S., C. L. Fasching, E. S. Srivatsan, E. J. Stanbridge and J. L. Redpath (1995). "Loss of a putative chromosome 11 tumor suppresor locus after gamma ray-induced neoplastic transformation of HeLa X fibroblast human cell hybrids." Radiation Research **143**: 34-44.

Mendonca, M. S., K. Howard, L. A. Desmond and C. W. Derrow (1999). "Previous loss of chromosome 11 containing a suppressor locus increases radiosensitivity, neoplastic transformation frequency and delayed death in HeLa x fibroblast human hybrid cells." Mutagenesis **14**(5): 483-490.

Mendonca, M. S., K. Howard, C. L. Fasching, D. L. Farrington, L. A. Desmond, E. J. Stanbridge and J. L. Redpath (1998). "Loss of suppressor loci on chromosomes 11 and 14 may be required for radiation-induced neoplastic transformation of HeLa x skin fibroblast human cell hybrids." Radiat Res **149**(3): 246-255.

Mendonca, M. S., K. L. Howard, D. L. Farrington, L. A. Desmond, T. M. Temples, B. M. Mayhugh, J. J. Pink and D. A. Boothman (1999). "Delayed apoptotic responses associated with radiation-induced neoplastic transformation of human hybrid cells." Cancer Res **59**(16): 3972-3979.

Mendonca, M. S., W. Kurohara, R. Antoniono and J. L. Redpath (1989). "Plating efficiency as a function of time post-irradiation: Evidence for the delayed expression of lethal mutations." Radiation Research **119**: 389-393.

Mendonca, M. S., B. M. Mayhugh, B. McDowell, H. Chin-Sinex, M. L. Smith, J. R. Dynlacht, D. F. Spandau and D. A. Lewis (2005). "A radiation-induced acute apoptosis involving TP53 and BAX precedes the delayed apoptosis and neoplastic transformation of CGL1 human hybrid cells." Radiat Res **163**(6): 614-622.

Mendonca, M. S. and J. L. Redpath (1989). "Isolation of human cell hybrids (HeLa x skin fibroblast) expressing a radiation-induced tumour-associated antigen." Br J Cancer **60**(3): 324-326.

Mendonca, M. S., C. Sun and J. L. Redpath (1990). "Suppression of radiation-induced neoplastic transformation of human cell hybrids by long term incubation at low extracellular pH." Cancer Res **50**(7): 2123-2127.

Mendonca, M. S., T. M. Temples, D. L. Farrington and C. Bloch (1998). "Evidence for a role of delayed death and genomic instability in radiation-induced neoplastic transformation of human hybrid cells." Int J Radiat Biol **74**(6): 755-764.

Messai, Y., M. Z. Noman, M. Hasmim, B. Janji, A. Tittarelli, M. Boutet, V. Baud, E. Viry, K. Billot, A. Nanbakhsh, T. Ben Safta, C. Richon, S. Ferlicot, E. Donnadieu, S. Couve, et al. (2014). "ITPR1 protects renal cancer cells against natural killer cells by inducing autophagy." Cancer Res **74**(23): 6820-6832.

Milde-Langosch, K. (2005). "The Fos family of transcription factors and their role in tumourigenesis." Eur J Cancer **41**(16): 2449-2461.

Millan, J. L. (1988). "Oncodevelopmental expression and structure of alkaline phosphatase genes." Anticancer Res **8**(5A): 995-1004.

Millan, J. L. (1990). "Oncodevelopmental alkaline phosphatases: in search for a function." Prog Clin Biol Res **344**: 453-475.

Mitz, C., C. Thome, M. E. Cybulski, L. Laframboise, C. M. Somers, R. G. Manzon, J. Y. Wilson and D. R. Boreham (2014). "A self-contained, controlled hatchery system for rearing lake whitefish embryos for experimental aquaculture." N Am J Aquacult **76**(3): 179-184.

Mitz, C., C. Thome, M. E. Cybulski, C. M. Somers, R. G. Manzon, J. Y. Wilson and D. R. Boreham (2017). "Is There a Trade-Off between Radiation-Stimulated Growth and Metabolic

Efficiency?" Radiat Res **188**(4.2): 486-494.

Morgan, W. F., J. P. Day, M. I. Kaplan, E. M. McGhee and C. L. Limoli (1996). "Genomic instability induced by ionizing radiation." Radiation Research **146**(3): 247-258.

Morgan, W. F. and J. P. Murname (1995). "A role for genomic instabiltiy in cellular radioresistance?" Cancer and Metastasis Reviews **14**(1): 49-58.

Mothersill, C. and C. B. Seymour (1998). "Cell-cell contact during gamma irradiation is not required to induce a bystander effect in normal human keratinocytes: evidence for release during irradiation of a signal controlling survival into the medium." Radiat Res **149**(3): 256-262.

Mueller, C. A., J. Eme, R. G. Manzon, C. M. Somers, D. R. Boreham and J. Y. Wilson (2015). "Embryonic critical windows: changes in incubation temperature alter survival, hatchling phenotype, and cost of development in lake whitefish (Coregonus clupeaformis)." J Comp Physiol B **185**(3): 315-331.

Murphy-Ullrich, J. E. and M. Poczatek (2000). "Activation of latent TGF-beta by thrombospondin-1: mechanisms and physiology." Cytokine Growth Factor Rev **11**(1-2): 59-69.

Nagaraj, N. S. and P. K. Datta (2010). "Targeting the transforming growth factor-beta signaling pathway in human cancer." Expert Opin Investig Drugs **19**(1): 77-91.

Nishizuka, S., H. Tsujimoto and E. J. Stanbridge (2001). "Detection of differentially expressed genes in HeLa x fibroblast hybrids using subtractive suppression hybridization." Cancer Res **61**(11): 4536-4540.

Nishizuka, S., S. T. Winokur, M. Simon, J. Martin, H. Tsujimoto and E. J. Stanbridge (2001). "Oligonucleotide microarray expression analysis of genes whose expression is correlated with tumorigenic and non-tumorigenic phenotype of HeLa x human fibroblast hybrid cells." Cancer Lett **165**(2): 201-209.

Norwood, T. H., W. R. Pendergrass, C. A. Sprague and G. M. Martin (1974). Proc. natn. Acad. Sci. U.S.A. **71**: 2231-2235.

Pant, M. C., X. Y. Liao, Q. Lu, S. Molloi, E. Elmore and J. L. Redpath (2003). "Mechanisms of suppression of neoplastic transformation in vitro by low doses of low LET radiation." Carcinogenesis **24**(12): 1961-1965.

Phan, L. M., S. C. Yeung and M. H. Lee (2014). "Cancer metabolic reprogramming: importance, main features, and potentials for precise targeted anti-cancer therapies." Cancer Biol Med **11**(1): 1-19.

Phan, N., M. De Lisio, G. Parise and D. R. Boreham (2012). "Biological effects and adaptive response from single and repeated computed tomography scans in reticulocytes and bone marrow of C57BL/6 mice." Radiat Res **177**(2): 164-175.

Piao, C. Q., Y. L. Zhao and T. K. Hei (2001). "Analysis of p16 and p21(Cip1) expression in tumorigenic human bronchial epithelial cells induced by asbestos." Oncogene **20**(50): 7301-7306.

Pirkkanen, J. S., D. R. Boreham and M. S. Mendonca (2017). "The CGL1 (HeLa x Normal Skin Fibroblast) Human Hybrid Cell Line: A History of Ionizing Radiation Induced Effects on Neoplastic Transformation and Novel Future Directions in SNOLAB." Radiat Res **188**(4.2): 512-524.

Planel, G., J. P. Soleilhavoup, R. Tixador, F. Croute and G. Richoilley (1976). Demonstration of a stimulating effect of natural ionizing radiation and of very low radiation doses on cell multiplication. Biological and environmental effects of low-level radiation: proceedings of a symposium.**:** 127-140.

Planel, H., J. P. Soleilhavoup, R. Tixador, F. Croute and G. Richoilley (1976). Biological and Environmental Effects of Low-level Radiation: v. 1 (IAEA Proceedings Series). Vienna, Austria, International Atomic Energy Agency.

Planel, H., J. P. Soleilhavoup, R. Tixador, G. Richoilley, A. Conter, F. Croute, C. Caratero and Y. Gaubin (1987). "Influence on cell proliferation of background radiation or exposure to very low, chronic gamma radiation." Health Phys **52**(5): 571-578.

Pott, P. (1993). "[The first description of an occupational cancer in 1777 (scrotal cancer, cancer of chimney sweeps)]." Bull Soc Liban Hist Med(4): 98-101.

Prise, K. M., O. V. Belyakov, M. Folkard and B. D. Michael (1998). "Studies of bystander effects in human fibroblasts using a charged particle microbeam." Int J Radiat Biol **74**(6): 793-798.

Prusty, B. K. and B. C. Das (2005). "Constitutive activation of transcription factor AP-1 in cervical cancer and suppression of human papillomavirus (HPV) transcription and AP-1 activity in HeLa cells by curcumin." Int J Cancer **113**(6): 951-960.

Puukila, S., J. A. Lemon, S. J. Lees, T. C. Tai, D. R. Boreham and N. Khaper (2017). "Impact of Ionizing Radiation on the Cardiovascular System: A Review." Radiat Res **188**(4.2): 539-546.

Raaphorst, G. P., E. I. Azzam, J. Borsa and M. D. Sargent (1985). "In vitro transformation by bromodeoxyuridine and X irradiation in C3H 10T1/2 cells." Radiat Res **101**(2): 279-291.

Redpath, J. L. (1987). Radiation-induced neoplastic transformation of human cell hybrids. Anticarcinogenesis and Radiation Protection. P. A. Cerutti, O. F. Nygaard and M. G. Simic. New York, Plenum Press**:** 335-340.

Redpath, J. L. (1988). Radiation-Induced Neoplastic Transformation of Human Cell Hybrids. Anticarcinogenesis and Radiation Protection. P. A. Cerutti, O. F. Nygaard and M. G. Simic.

Boston, MA, Springer US**:** 335-340.

Redpath, J. L. (2004). "Radiation-induced neoplastic transformation in vitro: evidence for a protective effect at low doses of low LET radiation." Cancer Metastasis Rev **23**(3-4): 333-339.

Redpath, J. L. and R. J. Antoniono (1998). "Induction of an adaptive response against spontaneous neoplastic transformation in vitro by low-dose gamma radiation." Radiat Res **149**(5): 517-520.

Redpath, J. L., R. J. Antoniono, M. S. Mendonca and C. Sun (1994). "The effect of postirradiation holding at 22 degrees C on the repair of sublethal, potentially lethal and potentially neoplastic transforming damage in gamma-irradiated HeLa x skin fibroblast human hybrid cells." Radiat Res **137**(3): 323-329.

Redpath, J. L., R. J. Antoniono, C. Sun, H. M. Gerstenberg and W. F. Blakely (1995). "Late mitosis/early G1 phase and mid-G1 phase are not hypersensitive cell cycle phases for neoplastic transformation of HeLa x skin fibroblast human hybrid cells induced by fission-spectrum neutrons." Radiat Res **141**(1): 37-43.

Redpath, J. L. and E. Elmore (2007). "Radiation-induced neoplastic transformation in vitro, hormesis and risk assessment." Dose Response **5**(2): 123-130.

Redpath, J. L., C. K. Hill, C. A. Jones and C. Sun (1990). "Fission-neutron-induced expression of a tumour-associated antigen in human cell hybrids (HeLa x skin fibroblasts): evidence for increased expression at low dose rate." Int J Radiat Biol **58**(4): 673-680.

Redpath, J. L., D. Liang, T. H. Taylor, C. Christie and E. Elmore (2001). "The shape of the dose-response curve for radiation-induced neoplastic transformation in vitro: evidence for an adaptive response against neoplastic transformation at low doses of low-LET radiation." Radiat Res **156**(6): 700-707.

Redpath, J. L., Q. Lu, X. Lao, S. Molloi and E. Elmore (2003). "Low doses of diagnostic energy X-rays protect against neoplastic transformation in vitro." Int J Radiat Biol **79**(4): 235-240.

Redpath, J. L. and C. Sun (1989). "UVC-induced expression of a tumor-associated antigen in human cell hybrids (HeLa X skin fibroblasts): repair of potentially lethal and potentially transforming damage." Carcinogenesis **10**(4): 723-726.

Redpath, J. L., C. Sun and W. F. Blakely (1991). "Effect of fission-neutron dose rate on th induction of a tumor associated antigen in human cell hybrids (HeLa X skin fibroblasts)." Radiation Research **128**: S71.

Redpath, J. L., C. Sun, M. Colman and E. J. Stanbridge (1985). "Radiobiological studies of human hybrid cells (skin fibroblasts x HeLa) and their tumorigenic segregants." Int J Radiat Biol **48**(4): 479-483.

Redpath, J. L., C. Sun, M. Colman and E. J. Stanbridge (1987). "Neoplastic transformation of human hybrid cells by gamma radiation: a quantitative assay." Radiat Res **110**(3): 468-472.

Redpath, J. L., C. Sun, M. S. Mendonca, M. Colman and E. J. Stanbridge (1989). The application of a human hybrid cell system to studies of radiation induced neoplastic cell transformation: quantitative, cellular, and molecular aspects. Proceedings of Workshop on cell transformation systems relevant to radiation induced cancer in man, Dublin.

Reznikoff, C. A., J. S. Bertram, D. W. Brankow and C. Heidelberger (1973). "Quantitative and qualitative studies of chemical transformation of cloned C3H mouse embryo cells sensitive to postconfluence inhibition of cell division." Cancer Res **33**(12): 3239-3249.

Reznikoff, C. A., D. W. Brankow and C. Heidelberger (1973). "Establishment and characterization of a cloned line of C3H mouse embryo cells sensitive to postconfluence inhibition of division." Cancer Res **33**(12): 3231-3238.

Rindi, A., F. Celani, M. Lindozzi and S. Miozzi (1988). "Underground neutron flux measurement." Nucl Instr Meth Phys Res A **272**(3): 871-874.

Rio, D. C., M. Ares, Jr., G. J. Hannon and T. W. Nilsen (2010). "Purification of RNA using TRIzol (TRI reagent)." Cold Spring Harb Protoc **2010**(6): pdb prot5439.

Roy, D., G. Calaf and T. K. Hei (2001). "Frequent allelic imbalance on chromosome 6 and 17 correlate with radiation-induced neoplastic transformation of human breast epithelial cells." Carcinogenesis **22**(10): 1685-1692.

Roy, D., G. Calaf and T. K. Hei (2003). "Role of Vitamin D receptor gene in radiation-induced neoplastic transformation of human breast epithelial cell." Steroids **68**(7-8): 621-627.

Sabin, A. B. (1981). "Suppression of malignancy in human cancer cells: issues and challenges." Proc Natl Acad Sci U S A **78**(11): 7129-7133.

Satta, L., F. Antonelli, M. Belli, O. Sapora, G. Simone, E. Sorrentino, M. A. Tabocchini, F. Amicarelli, C. Ara, M. P. Ceru, S. Colafarina, L. Conti Devirgiliis, A. De Marco, M. Balata, A. Falgiani, et al. (2002). "Influence of a low background radiation environment on biochemical and biological responses in V79 cells." Radiat Environ Biophys **41**(3): 217-224.

Satta, L., G. Augusti-Tocco, R. Ceccarelli, A. Esposito, M. Fiore, P. Paggi, I. Poggesi, R. Ricordy, G. Scarsella and E. Cundari (1995). "Low environmental radiation background impairs biological defence of the yeast Saccharomyces cerevisiae to chemical radiomimetic agents." Mutat Res **347**(3-4): 129-133.

Savai, R., S. S. Pullamsetti, G. A. Banat, N. Weissmann, H. A. Ghofrani, F. Grimminger and R. T. Schermuly (2010). "Targeting cancer with phosphodiesterase inhibitors." Expert Opin Investig Drugs **19**(1): 117-131.

Saxon, P. J., E. S. Srivatsan and E. J. Stanbridge (1986). "Introduction of human chromosome 11 via microcell transfer controls tumorigenic expression of HeLa cells." EMBO Journal **5**(13): 3461-3466.

Scaletta, L. J. and B. Ephrussi (1965). "Hybridization of Normal and Neoplastic Cells in vitro." Nature **205**(4977): 1169-1169.

Schneider, J. A. (1973). Birth Defects **9**: 160-168.

Scott, B. R. (2014). "Radiation-hormesis phenotypes, the related mechanisms and implications for disease prevention and therapy." J Cell Commun Signal **8**(4): 341-352.

Seachrist, D. D., S. T. Sizemore, E. Johnson, F. W. Abdul-Karim, K. L. Weber Bonk and R. A. Keri (2017). "Follistatin is a metastasis suppressor in a mouse model of HER2-positive breast cancer." Breast Cancer Res **19**(1): 66.

Seymour, C. B. and C. Mothersill (2000). "Relative contribution of bystander and targeted cell killing to the low-dose region of the radiation dose-response curve." Radiat Res **153**(5 Pt 1): 508-511.

Seymour, C. M. and C (1997). "Medium from irradiated human epithelial cells but not human fibroblasts reduces the clonogenic survival of unirradiated cells." Int J Radiat Biol **71**(4): 421-427.

Silagi, S., G. Darlington and S. A. Bruce (1969). "Hybridization of two biochemically marked human cell lines." Proc Natl Acad Sci U S A **62**(4): 1085-1092.

Smith, G. B., Y. Grof, A. Navarrette and R. A. Guilmette (2011). "Exploring biological effects of low level radiation from the other side of background." Health Phys **100**(3): 263-265.

Smith, L. E., S. Nagar, G. J. Kim and W. F. Morgan (2003). "Radiation-induced genomic instability: radiation quality and dose response." Health Phys **85**(1): 23-29.

Smith, N. J. T. (2012). "The SNOLAB deep underground facility." Eur Phys J Plus **127**(108).

Soto, U., B. C. Das, M. Lengert, P. Finzer, H. zur Hausen and F. Rosl (1999). "Conversion of HPV 18 positive non-tumorigenic HeLa-fibroblast hybrids to invasive growth involves loss of TNF-alpha mediated repression of viral transcription and modification of the AP-1 transcription complex." Oncogene **18**(21): 3187-3198.

Soto, U., C. Denk, P. Finzer, K. J. Hutter, H. zur Hausen and F. Rosl (2000). "Genetic complementation to non-tumorigenicity in cervical-carcinoma cells correlates with alterations in AP-1 composition." Int J Cancer **86**(6): 811-817.

Sreetharan, S., C. Thome, C. Mitz, J. Eme, C. A. Mueller, E. N. Hulley, R. G. Manzon, C. M. Somers, D. R. Boreham and J. Y. Wilson (2015). "Embryonic development of lake whitefish

Coregonus clupeaformis: a staging series, analysis of growth and effects of fixation." J Fish Biol **87**(3): 539-558.

Srivatsan, E. S., W. F. Benedict and E. J. Stanbridge (1986). "Implication of chromosome 11 in the suppression of neoplastic expression in human cell hybrids." Cancer Research **46**: 6174-6179.

Srivatsan, E. S., R. Chakrabarti, K. Zainabadi, S. D. Pack, P. Benyamini, M. S. Mendonca, P. K. Yang, K. Kang, D. Motamedi, M. P. Sawicki, Z. Zhuang, R. A. Jesudasan, U. Bengtsson, C. Sun, B. A. Roe, et al. (2002). "Localization of deletion to a 300 Kb interval of chromosome 11q13 in cervical cancer." Oncogene **21**(36): 5631-5642.

Stanbridge, E. J. (1976). "Suppression of malignancy in human cells." Nature **260**: 17-20.

Stanbridge, E. J. (1987). Genetic regulation of tumorigenic expression in somatic cell hybrids. Advances in Viral Oncology. G. Klein. New York, Raven Press. **6:** 83-101.

Stanbridge, E. J., C. J. Der, C. J. Doersen, R. Y. Nishimi, D. M. Peehl, B. E. Weissman and J. E. Wilkinson (1982). "Human cell hybrids: analysis of transformation and tumorigenicity." Science **215**(4530): 252-259.

Stanbridge, E. J., R. R. Flandermeyer, D. W. Daniels and W. A. Nelson-Rees (1981). "Specific chromosome loss associated with the expression of tumorigenicity in human cell hybrids." Somatic Cell Genet **7**(6): 699-712.

Stanbridge, E. J. and J. Wilkinson (1980). "Dissociation of anchorage independence form tumorigenicity in human cell hybrids." Int J Cancer **26**(1): 1-8.

Sun, C., M. Colman and J. L. Redpath (1988). "Suppression of the radiation-induced expression of a tumor-associated antigen in human cell hybrids by the protease inhibitor antipain." Carcinogenesis **9**(12): 2333-2335.

Sun, C. and J. L. Redpath (1988). "Application of a freeze-thaw technique to studies of radiation-induced cell transformation." Int J Radiat Biol **54**: 825-827.

Sun, C., J. L. Redpath, M. Colman and E. J. Stanbridge (1986). "Repair of potentially lethal radiation damage in confluent and non-confluent cultures of human hybrid cells." Int J Radiat Biol **49**(3): 395-402.

Sun, C., J. L. Redpath, M. Colman and E. J. Stanbridge (1988). "Further studies on the radiation-induced expression of a tumor-specific antigen in human cell hybrids." Radiat Res **114**(1): 84-93.

Suzuki, M., C. Q. Piao, Y. L. Zhao and T. K. Hei (2001). "Karyotype analysis of tumorigenic human bronchial epithelial cells transformed by chrysolite asbestos using chemically induced premature chromosome condensation technique." Int J Mol Med **8**(1): 43-47.

Suzuki, T., A. Iwazaki, H. Katagiri, Y. Oka, J. L. Redpath, E. J. Stanbridge and T. Kitagawa (1999). "Enhanced expression of glucose transporter GLUT3 in tumorigenic HeLa cell hybrids associated with tumor suppressor dysfunction." Eur J Biochem **262**(2): 534-540.

Suzuki, T., Y. Suzuki, K. Hanada, A. Hashimoto, J. L. Redpath, E. J. Stanbridge, M. Nishijima and T. Kitagawa (1998). "Reduction of caveolin-1 expression in tumorigenic human cell hybrids." J Biochem **124**(2): 383-388.

Szklarczyk, D., A. Franceschini, S. Wyder, K. Forslund, D. Heller, J. Huerta-Cepas, M. Simonovic, A. Roth, A. Santos, K. P. Tsafou, M. Kuhn, P. Bork, L. J. Jensen and C. von Mering (2015). "STRING v10: protein-protein interaction networks, integrated over the tree of life." Nucleic Acids Res **43**(Database issue): D447-452.

Takizawa, Y., J. Yamashita, A. Wakizaka and H. Tanooka (1992). Background radiation can stimulate the proliferation of mouse-L-5178Y cells. international conference on radiation effects and protection. J. A. E. R. Institution. Mito, Japan, Japan Atomic Energy Research Institution. **24:** 234-236.

Talmadge, J. E. (2008). "Follistatin as an inhibitor of experimental metastasis." Clin Cancer Res **14**(3): 624-626.

Tang, F. R. and W. K. Loke (2015). "Molecular mechanisms of low dose ionizing radiation-induced hormesis, adaptive responses, radioresistance, bystander effects, and genomic instability." Int J Radiat Biol **91**(1): 13-27.

Tarca, A. L., S. Draghici, P. Khatri, S. S. Hassan, P. Mittal, J. S. Kim, C. J. Kim, J. P. Kusanovic and R. Romero (2009). "A novel signaling pathway impact analysis." Bioinformatics **25**(1): 75-82.

Taylor-Weiner, H., N. Ravi and A. J. Engler (2015). "Traction forces mediated by integrin signaling are necessary for definitive endoderm specification." J Cell Sci **128**(10): 1961-1968.

Tharmalingam, S., S. Sreetharan, A. V. Kulesza, D. R. Boreham and T. C. Tai (2017). "Low-Dose Ionizing Radiation Exposure, Oxidative Stress and Epigenetic Programing of Health and Disease." Radiat Res **188**(4.2): 525-538.

Thome, C., C. Mitz, E. N. Hulley, C. M. Somers, R. G. Manzon, J. Y. Wilson and D. R. Boreham (2017). "Initial Characterization of the Growth Stimulation and Heat-Shock-Induced Adaptive Response in Developing Lake Whitefish Embryos after Ionizing Radiation Exposure." Radiat Res **188**(4.2): 475-485.

Tixador, R., G. Richoilley, E. Monrozies, H. Planel and G. Tap (1981). "Effects of very low doses of ionizing radiation on the clonal life-span in Paramecium tetraurelia." Int J Radiat Biol Relat Stud Phys Chem Med **39**(1): 47-54.

Toma, S., M. Nakamura, S. Tone, E. Okuno, R. Kido, J. Breton, N. Avanzi, L. Cozzi, C.

Speciale, M. Mostardini, S. Gatti and L. Benatti (1997). "Cloning and recombinant expression of rat and human kynureninase." FEBS Lett **408**(1): 5-10.

Travers, H., N. S. French and J. D. Norton (1996). "Suppression of tumorigenicity in Ras-transformed fibroblasts by alpha 2(I) collagen." Cell Growth Differ **7**(10): 1353-1360.

Tsujimoto, H., S. Nishizuka, J. L. Redpath and E. J. Stanbridge (1999). "Differential gene expression in tumorigenic and nontumorigenic HeLa x normal human fibroblast hybrid cells." Mol Carcinog **26**(4): 298-304.

Tyagi, A., K. Vishnoi, H. Kaur, Y. Srivastava, B. G. Roy, B. C. Das and A. C. Bharti (2017). "Cervical cancer stem cells manifest radioresistance: Association with upregulated AP-1 activity." Sci Rep **7**(1): 4781.

Veena, M. S., G. Lee, D. Keppler, M. S. Mendonca, J. L. Redpath, E. J. Stanbridge, S. P. Wilczynski and E. S. Srivatsan (2008). "Inactivation of the cystatin E/M tumor suppressor gene in cervical cancer." Genes Chromosomes Cancer **47**(9): 740-754.

Verde, P., L. Casalino, F. Talotta, M. Yaniv and J. B. Weitzman (2007). "Deciphering AP-1 function in tumorigenesis: fra-ternizing on target promoters." Cell Cycle **6**(21): 2633-2639.

Vitale, G., A. Dicitore, D. Mari and F. Cavagnini (2009). "A new therapeutic strategy against cancer: cAMP elevating drugs and leptin." Cancer Biol Ther **8**(12): 1191-1193.

Weiss, M. C. and H. Green (1967). "Human-mouse hybrid cell lines containing partial complements of human chromosomes and functioning human genes." Proc Natl Acad Sci U S A **58**(3): 1104-1111.

Wiener, F., G. Klein and H. Harris (1971). J. Cell Sci. **8**: 681-692.

Wiener, F., G. Klein and H. Harris (1973). J. Cell Sci. **12**: 253-261.

Wiener, F., G. Klein and H. Harris (1974). J. Cell Sci. **15**: 177-183.

Willey, J. C., T. K. Hei, C. Q. Piao, L. Madrid, J. J. Willey, M. J. Apostolakos and B. Hukku (1993). "Radiation-induced deletion of chromosomal regions containing tumor suppressor genes in human bronchial epithelial cells." Carcinogenesis **14**(6): 1181-1188.

Xiao, S., Y. Zhou, W. Yi, G. Luo, B. Jiang, Q. Tian, Y. Li and M. Xue (2015). "Fra-1 is downregulated in cervical cancer tissues and promotes cervical cancer cell apoptosis by p53 signaling pathway in vitro." Int J Oncol **46**(4): 1677-1684.

Yagami, H., H. Kato, K. Tsumoto and M. Tomita (2013). "Monoclonal antibodies based on hybridoma technology." Pharm Pat Anal **2**(2): 249-263.

Yan, K., L. N. Gao, Y. L. Cui, Y. Zhang and X. Zhou (2016). "The cyclic AMP signaling

pathway: Exploring targets for successful drug discovery (Review)." Mol Med Rep **13**(5): 3715-3723.

Yazdani, M., H. Naderi-Manesh, K. Khajeh, M. R. Soudi, S. M. Asghari and M. Sharifzadeh (2009). "Isolation and characterization of a novel gamma-radiation-resistant bacterium from hot spring in Iran." J Basic Microbiol **49**(1): 119-127.

Zabkiewicz, C., J. Resaul, R. Hargest, W. G. Jiang and L. Ye (2017). "Increased Expression of Follistatin in Breast Cancer Reduces Invasiveness and Clinically Correlates with Better Survival." Cancer Genomics Proteomics **14**(4): 241-251.

Zainabadi, K., P. Benyamini, R. Chakrabarti, M. S. Veena, S. C. Chandrasekharappa, R. A. Gatti and E. S. Srivatsan (2005). "A 700-kb physical and transcription map of the cervical cancer tumor suppressor gene locus on chromosome 11q13." Genomics **85**(6): 704-714.

Zakeri, F., M. R. Rajabpour, S. A. Haeri, R. Kanda, I. Hayata, S. Nakamura, T. Sugahara and M. J. Ahmadpour (2011). "Chromosome aberrations in peripheral blood lymphocytes of individuals living in high background radiation areas of Ramsar, Iran." Radiat Environ Biophys **50**(4): 571-578.

Zhang, C. (2012). "Hybridoma technology for the generation of monoclonal antibodies." Methods Mol Biol **901**: 117-135.

Zhang, W., J. Hart, H. L. McLeod and H. L. Wang (2005). "Differential expression of the AP-1 transcription factor family members in human colorectal epithelial and neuroendocrine neoplasms." Am J Clin Pathol **124**(1): 11-19.

Zhao, Y. L., C. Q. Piao, E. J. Hall and T. K. Hei (2001). "Mechanisms of radiation-induced neoplastic transformation of human bronchial epithelial cells." Radiat Res **155**(1 Pt 2): 230-234.

Zhao, Y. L., C. Q. Piao and T. K. Hei (2002). "Overexpression of Betaig-h3 gene downregulates integrin alpha5beta1 and suppresses tumorigenicity in radiation-induced tumorigenic human bronchial epithelial cells." Br J Cancer **86**(12): 1923-1928.

Zhou, H., G. Randers-Pehrson, C. A. Waldren, D. Vannais, E. J. Hall and T. K. Hei (2000). "Induction of a bystander mutagenic effect of alpha particles in mammalian cells." Proc Natl Acad Sci U S A **97**(5): 2099-2104.

Appendices:

Appendix A: The REPAIR Project: Examining the Biological Impacts of Sub-Background Radiation Exposure within SNOLAB, a Deep Underground Laboratory

RADIATION RESEARCH **188**, 000–000 (2017)
0033-7587/17 $15.00

DOI: 10.1667/RR14654.1

COMMENTARY

The REPAIR Project: Examining the Biological Impacts of Sub-Background Radiation Exposure within SNOLAB, a Deep Underground Laboratory

Christopher Thome,[a,b,1] Sujeenthar Tharmalingam,[a,b,1] Jake Pirkkanen,[b,1] Andrew Zarnke,[b,1] Taylor Laframboise[a] and Douglas R. Boreham[a,b,c,2]

[a] *Division of Medical Sciences, Northern Ontario School of Medicine and* [b] *Department of Biology, Laurentian University, Sudbury, Canada, P3E 2C6; and* [c] *Bruce Power, Tiverton, Canada, N0G 2T0*

[*Published*: Radiation Research]

Abstract

Considerable attention has been given to understanding the biological impacts of low-dose ionizing radiation exposure at levels slightly above background. However, relatively few studies have examined the inverse, where natural background radiation is removed. The limited available data suggest that organisms exposed to sub-background radiation environments experience reduced growth and an impaired capacity to repair genetic damage. Shielding from background radiation is inherently difficult due to high-energy cosmic radiation. SNOLAB, located in Sudbury, Ontario, Canada is a unique facility for examining the impacts of sub-background radiation exposure. Originally constructed for astroparticle physics research, the laboratory is located within an active nickel mine at a depth of over 2000 m. The rock overburden provides shielding equivalent to 6000 m of water, thereby almost completely eliminating cosmic radiation. Additional features of the facility help to reduce radiological contamination from the surrounding rock. We are currently establishing a biological research program within SNOLAB; the REPAIR project (Researching the Effects of the Presence and Absence of Ionizing Radiation). We hypothesize that natural background radiation is essential for life and maintains genomic stability, and that prolonged exposure to sub-background radiation environments will be detrimental to biological systems. Using a combination of whole organism and cell culture model systems, the impacts of exposure to a sub-background environment will be examined on growth and development, as well as markers of genomic damage, DNA repair capacity and oxidative stress. The results of this research will provide further insight into the biological effects of low-dose radiation exposure as well as elucidate some of the processes that may drive evolution and selection in living systems. In this Radiation Research focus issue, seven manuscripts (3 review articles and 4 original articles) relate to the presence or absence of low-dose ionizing radiation exposure.

Introduction

Biological systems on earth are continually exposed to natural background ionizing radiation, originating from a combination of cosmic and terrestrial sources. Cosmic radiation includes high-energy charged particles and atomic nuclei, which produce secondary radiation through atmospheric interaction, such as protons, neutrons and cosmogenic nuclides like carbon-14 and tritium. Terrestrial sources consist of long-lived primordial radioisotopes of uranium, thorium and potassium and their associated decay progeny, particularly radon gas. With the increase in man-made medical radiation exposures, considerable attention has been given to understanding the impacts of low-dose radiation at levels slightly above natural background. There is growing evidence supporting the sub-linear, threshold or hormetic models, where the biological risk at low-doses is significantly less than (or negative) compared to high-dose estimates (Brooks et al. 2014, Calabrese et al. 2001, Tang et al. 2015). However, relatively few studies have examined the inverse, where natural background radiation is removed.

Early experiments in the 1970's and 1980's examined the biological impacts of sub-background radiation exposure on the protozoa *Paramecium tetraurelia* (Croute et al. 1980, Planel et al. 1976, Planel et al. 1987). Growth rates were significantly reduced when cultures were incubated within a shielded lead box. When a low-dose source was introduced into the shielded container, to artificially reintroduce background radiation, growth rates were restored to baseline levels. This growth inhibition following the removal of background radiation was later verified in other experiments using prokaryotes (Conter 1987, Conter et al. 1983, Smith et al. 2011), single celled eukaryotes (Kawanishi et al. 2012, Luckey 1986) and mammalian cell culture models (Kawanishi et al. 2012, Takizawa et al. 1992).

In addition to alterations in growth rate, removal of background radiation promotes genotoxic damage. When grown in a sub-background environment, cultured cells showed an increase in basal levels of DNA damage and mutation rate (Carbone et al. 2010, Fratini et al. 2015, Satta et al. 2002). Low background adapted cells were also found to be more sensitive to induced genetic damage following exposure to a high dose radiation challenge (Antonelli et al. 2008, Carbone et al. 2009, Carbone et al. 2010, Gajendiran et al. 2002) or chemical agent (Antonelli et al. 2008, Satta et al. 2002, Satta et al. 1995). This increased sensitivity was correlated to a reduction in free radical scavenging ability (Antonelli et al. 2008, Carbone et al. 2009, Carbone et al. 2010, Satta et al. 2002). In many cases, changes in repair capacity or growth rate were only observed after prolonged incubation in a sub-background environment on the order of weeks to months (Antonelli et al. 2008, Fratini et al. 2015, Gajendiran et al. 2002, Kawanishi et al. 2012, Satta et al. 2002, Satta et al. 1995, Tixador et al. 1981).

What makes sub-background experiments so challenging to conduct is the inherent difficulty in shielding from high-energy cosmic radiation. Historically, most experiments have relied on lead or other heavy metals for shielding and have only achieved a modest reduction in background dose rates (Conter 1987, Conter et al. 1983, Croute et al. 1982, Gajendiran et al. 2002, Kawanishi et al. 2012, Planel et al. 1976, Planel et al. 1987, Takizawa et al. 1992, Tixador et al. 1981). Designing artificial shielding to obtain a significant reduction in cosmic radiation is impractical. The best way eliminate cosmic radiation is to conduct experiments within facilities built deep underground. Only a handful of subterranean laboratories exist in the world. One such facility, SNOLAB, is located in Sudbury, Ontario, Canada.

SNOLAB

The laboratory first opened in 1999 as the Sudbury Neutrino Observatory (SNO) after nearly a decade of construction. The facility was built within Creighton Mine, an active nickel mine, at a depth of 2070 m. To access the laboratory researchers must first travel down the mine shaft to the 6800 level (6800 feet underground), followed by a 1.5 km walk along one of the mine drifts (the laboratory was purposefully built to be isolated from the active mining sites). The original SNO experiment consisted of a single detector designed to measure neutrinos. The detector was the largest of its kind at that depth, measuring 12 m in diameter and filled with 1000 tonnes of heavy water (Boger et al. 2000). Using heavy water enabled SNO to measure all three flavors of neutrino (electron, muon and tau). The 2070 m overburden of rock effectively shielded out other sources of cosmic radiation, allowing SNO to detect the much lighter and very weakly interacting neutrinos. The SNO experiment provided the first direct evidence for neutrino oscillation, confirming that neutrinos possess mass (Ahmad et al. 2002). Electron neutrinos produced from solar nuclear fusion can change flavor into muon or tau neutrinos when travelling to earth. The discovery solved the solar neutrino problem; the deficit in early measurements of solar neutrinos compared to what was predicted based on the standard solar model. This breakthrough was recognized with the 2015 Nobel Prize in physics awarded to Dr. Arthur McDonald. The laboratory expanded beginning in 2004 and was renamed SNOLAB. Currently, SNOLAB has 3060 m^2 of laboratory space (Smith 2012). The original SNO detector is being repurposed to examine lower energy neutrinos and neutrinoless double beta decay using a liquid scintillator. Additional experiments are underway or are planned which will examine supernovae and dark matter. These experiments all rely on the cosmic ray shielding provided by the 2 km of overhead rock.

In addition to the overburden of rock, which almost completely eliminates cosmic radiation, further

measures have been established to help reduce radiation levels within SNOLAB. The experiment area of the laboratory is operated as a class 2000 clean room (fewer than 2000 particles, 0.5 μm or larger, per cubic foot). All personnel entering the facility must shower and change into clean clothes to reduce contamination from radioactive dust in the mine drift. All equipment and supplies must also be hand washed before entering SNOLAB. Radon levels are reduced through continuous air filtration at a rate of 50 $m^3 s^{-1}$, resulting in 10 full air changes per hour throughout the laboratory (Smith 2012).

Low levels of radiation are still present in SNOLAB, mainly from radioactive decay in the surrounding norite rock. The largest component is radon gas with levels in the laboratory at approximately 130 Bq m^{-3} (Smith 2012). Additionally, gamma radiation results from the decay of uranium and thorium progeny, and a small amount of neutron radiation is present from alpha particle interactions and spontaneous fission. Experiment specific shielding can be utilized to further control these sources of radiation. Neutrons and gamma rays can be reduced with the addition of water and lead shielding respectively. Radon gas can be reduced using air-controlled chambers, such as glove boxes, which are filled with air from aged gas cylinders. With a half-life of 3.8 days, radon levels will decay several orders of magnitude within a few weeks.

Several other underground astroparticle physics laboratories exist around the world, however, very few of them have biological research programs. The largest facility for underground biology is the Laboratori Nazionali del Gran Sasso (LNGS) in Italy. Unlike SNOLAB, which was built within a mine, LNGS was tunneled into the side of the Gran Sasso Mountain to achieve cosmic ray shielding. The laboratory at LNGS has a rock overburden of 1400 m and can achieve background dose rates down to approximately 30 μGy per year, a reduction of over 80 fold (Carbone et al. 2009). Due to differences in geological composition, the depth of underground laboratories is

generally stated in meters of water equivalent (MWE). LNGS has a MWE of 3950 m (Rindi et al. 1988), significantly less than SNOLAB, which has a MWE of 6000 m (Duncan et al. 2010). Biological experiments have also been conducted within the Waste Isolation Pilot Plant (WIPP), a nuclear waste repository in New Mexico. However, at a depth of 650 m, WIPP has considerably less shielding compared to SNOLAB or LNGS and only reduces background dose rates by a factor of 15 (Smith et al. 2011).

REPAIR Project

We are currently establishing a biological research program within SNOLAB; the REPAIR project (Researching the Effects of the Presence and Absence of Ionizing Radiation), focused on understanding the impacts of sub-background radiation exposure. The research space within SNOLAB will be the deepest underground biological laboratory in the world. Through utilizing the existing infrastructure, as well as some additional shielding, the REPAIR project will be able to monitor the response of biological system exposed to one of the lowest background dose rates ever achieved. We hypothesize that because living organisms have evolved in the continual presence of natural background radiation, it is essential for life and helps to maintain genomic stability. Prolonged exposure to sub-background environments will therefore be detrimental to biological systems. This will be tested using a combination of cell culture and whole organism models. We will examine a variety of endpoints, ranging from simple quantification of growth and development, to more complex metrics measuring oxidative stress, neoplastic transformation and genomic instability. This Radiation Research focus issue (FI) includes seven manuscripts (3 review articles and 4 original articles), relating to the presence or absence of low-dose radiation exposure, that describe relevant findings, methodologies and/or model systems pertaining to the research aims of the REPAIR project.

Cellular transformation assays have been utilized to assess the influence of ionizing radiation and other carcinogenic agents on neoplastic transformation. Evaluating the frequency of events in which normal cells alter phenotypically and become neoplastic, as well as the genetic and epigenetic mechanisms driving this change, provide important information in the evaluation of carcinogenesis. Investigating changes in gene regulation, DNA damage/repair and morphology can be linked to these phenotypic changes in order to better understand what may drive the neoplastic transformation of normal cells. The CGL1 cell line is a pre-neoplastic derivative of a HeLa x normal human fibroblast hybrid (Redpath et al. 1987) and is ideal due to its human origin, compared to other similar systems derived from rodent or non-mammalian sources. It is a stable and non-tumorigenic tissue culture system in which cell transformation can be induced by a radiological or chemical stress, and is therefore a good model for quantitatively investigating the effects of ionizing radiation on neoplastic transformation *in-vitro* (Pirkkanen et al. 2017).

Transformed CGL1 cells differentially express intestinal alkaline phosphatase (ALPI) as a surface antigen (Latham et al. 1990, Mendonca et al. 1991). This novel characteristic allows for a simplistic and expedited endpoint. When in the presence of the alkaline phosphatase chromogen Western Blue (WB), transformed cells yield a colored precipitant (Mendonca et al. 1992) which makes neoplastically transformed colonies easily distinguishable from non-transformed ALPI negative foci. This feature makes the CGL1 based transformation assay unique among others, as transformation events can be detected earlier and do not rely on scoring methods such as morphological assessment, which can be imprecise and tedious. Furthermore the WB substrate is inexpensive as compared to antibody immunohistochemical based detection and scoring methods. In the sub-background radiation environment that SNOLAB provides, the CGL1 based transformation assay is ideal for several reasons; it is sensitive to low-dose and low dose rate

radiation exposure (Lewis et al. 2001, Pant et al. 2003, Redpath et al. 1995), has a relatively short assay period of only 21 days, and the scoring endpoint works on viable as well as paraformaldehyde fixed cells. Therefore minimal infrastructure and reagent are necessary to complete this assay, making it attractive for utilization underground in SNOLAB.

A topic that is consistently absent from previous experiments is the impact of sub-background radiation exposure on complex multicellular whole organism models. All research to date has utilized either single celled organisms (Conter 1987, Conter et al. 1983, Croute et al. 1980, Gajendiran et al. 2002, Kawanishi et al. 2012, Luckey 1986, Planel et al. 1976, Planel et al. 1987, Satta et al. 1995, Smith et al. 2011, Tixador et al. 1981) or in-vitro cell culture models (Antonelli et al. 2008, Carbone et al. 2009, Carbone et al. 2010, Fratini et al. 2015, Kawanishi et al. 2012, Satta et al. 2002, Smith et al. 2011, Takizawa et al. 1992) and the observed results may not translate to the whole organism level. Animal work in underground facilities such as SNOLAB is hampered by space limitations and restrictions in laboratory access, which makes many species, such as murine models, extremely difficult to work with. Animal models must be low maintenance, have minimal space and resource requirements, and be able to survive for several days without researcher access.

Embryonic development in lake whitefish (*Coregonus clupeaformis*) is an ideal model species for studying sub-background exposure. We have previously examined the impacts of low-dose ionizing radiation (above background) on lake whitefish embryogenesis. Embryos responded to small changes in radiation environments, where a chronic exposure as low as 0.06 mGy per day resulted in significant growth stimulation (Thome et al. 2017). Growth stimulation was also observed with four fractionated low-doses of 15 mGy, in contrast to growth suppression observed at higher fractions of 2, 6 or 8 Gy (Mitz et al. 2017). This sensitivity to low-dose radiation suggests

that lake whitefish may be impacted by development in a sub-background environment. In addition, embryos can be easily raised in large numbers using only petri dishes, dechlorinated water and standard refrigeration units (Mitz et al. 2014). Lake whitefish develop slowly, close to 200 days depending on temperature (Brooke 1975, Mueller et al. 2015), which is important since many of the previous sub-background experiments observed impacts only after prolonged incubation (Antonelli et al. 2008, Fratini et al. 2015, Gajendiran et al. 2002, Kawanishi et al. 2012, Satta et al. 2002, Satta et al. 1995, Tixador et al. 1981). Lastly, embryos can be easily staged and quantified for growth rate (Sreetharan et al. 2015), one of the main endpoints examined in past studies. We plan to raise lake whitefish embryos within SNOLAB, representing the first sub-background experiment utilizing a complex whole organism model.

One of the themes that the REPAIR project will investigate is the response of low-background adapted cells and organisms to induced damage from a high-dose challenge exposure. Previous sub-background studies found reduced repair capacity when background radiation was removed (Antonelli et al. 2008, Carbone et al. 2009, Carbone et al. 2010, Fratini et al. 2015, Satta et al. 2002, Satta et al. 1995), which challenges the linear no-threshold hypothesis. This coincides with data demonstrating a radiation induced adaptive response at doses slightly above natural background. At the cellular levels, low-dose exposures below 100 mGy produce an adaptive response towards radiation induced DNA damage and genomic instability (Phan et al. 2012). At the whole organism level, a low-dose exposure can modify cancer progression. When cancer prone *Trp53*+/- mice were exposed to multiple CT scans (1 weekly scan for 10 weeks, 10 mGy per scan) after the induction of cancer by a previous high dose exposure, both cancer latency and overall lifespan were increased (Lemon et al. 2017). Similarly, cancer latency and lifespan were increased following a single 10 mGy CT scan (Lemon et al. 2017). Low-dose radiation can also reduce the

incidence of non-cancerous disease such as cardiac impairment and diabetes (Puukila et al. 2017). We predict that organisms and cells grown within the sub-background environment in SNOLAB will be more sensitive to induced damage.

Low linear energy transfer radiation acts mainly through the production of reactive oxygen intermediates. When cellular antioxidant defense mechanisms are unable to counteract the formation of oxidative stress, the excess free radicals damage biological macromolecules including nucleic acids. Previous results from sub-background experiments have been linked to changes in oxidative stress levels (Antonelli et al. 2008, Carbone et al. 2009, Carbone et al. 2010, Satta et al. 2002). Low-dose radiation induced phenotypical alterations can demonstrate non-Mendelian modes of inheritance. There is emerging evidence that low levels of oxidative stress can cause heritable gene expression modifications by altering the genomic structure, while the underlying DNA nucleotide sequence remains unchanged. These structural genome changes are referred to as epigenetic modifications (Tharmalingam et al. 2017). Oxidative stress generated from low doses of ionizing radiation provides a mechanistic link between radiation and epigenetic gene regulation. Cells can adapt to radiation exposure by modifying epigenetic gene regulation. These heritable cellular effects can either provide a positively adaptive phenotype or result in enhanced disease progression. The REPAIR project will aim to elucidate the effects of sub-background radiation exposure on oxidative stress and epigenetic programming.

Overall, the REPAIR project will provide an in-depth evaluation of the biological impacts of sub-background radiation exposure, an area of research that still remains poorly understood. SNOLAB is a unique facility and one of few in the world where this type of research can be conducted. We will examine sub-background effects using complex animal systems, such as embryonic development in lake whitefish. Numerous different cellular endpoints will be used, including

transformation frequency, which will provide insight into baseline levels of DNA damage and oxidative stress, as well as cellular repair capacity and genomic instability. The results of this project will extend our knowledge into the biological effects of low-dose ionizing radiation exposure and explore what happens in the absence of a physics stressor given that all living systems have evolved in the presence of low-level ionizing radiation.

Acknowledgements

We would like to thank SNOLAB and its staff for support through underground space, logistical and technical services. SNOLAB operations are supported by the Canada Foundation for Innovation and the Province of Ontario Ministry of Research and Innovation, with underground access provided by Vale at the Creighton mine site. The REPAIR project is supported through an industrial research grant from Bruce Power, as well as funding from the Natural Sciences and Research Council of Canada and Mitacs.

Appendix B: Technical primer information for genes analyzed by RT-qPCR in GIM vs CON analysis

Gene	Sequence (5'to 3')	T_A (°C)	Accession ID
ADD2	AAACGCTGCCCTGCAGATTA ATCCAGGTGGAAACTCCTGC	60	NM_001617.3
ALDH1A3	AGGGTGGGCAGACAAAATCC GGGGAAGTTCCATGGAGTGAT	60	NM_000693.3
ATP6AP1	AGCGACTTGCAGCTCTCTAC CCTCAATGCTCAGCTTGTCCTG	60	NM_001183.5
BMP2	GGAACGGACATTCGGTCCTT CACCATGGTCGACCTTTAGGA	60	NM_001200.3
BMP4	CGTCCAAGCTATCTCGAGCC CGGAATGGCTCCATAGGTCC	60	NM_001202.5
CACNB2	CACAGTGCAGCTTGGTGAAG GGAGTCTGCCGAACCATAGG	62	NM_000724.3
CAV1	TACGTAGACTCGGAGGGACAT CTTCTCGCTCAGCTCGTCTG	60	NM_001753.4
CDH13	CCTGGCTCCCACGGAAAATA CAGCAGCACCTGGGACAG	60	NM_001257.4
COL12A1	ACTCAGGTATCCGAGGACCC ATGTGTTAGCCGGAACCTGG	62	NM_004370.5
COL4A5	TGGAACCAAGGGAGAACGTG CCTTTGGTCCTGGCAGTGAT	60	NM_000495.4
EGFR	GAGCTCTTCGGGGAGCAG TCGTGCCTTGGCAAACTTTC	60	NM_005228.4
EPHA4	GCCCAGTGACCTGAAACTGT TGCTCCTGCCGCTTCTTC	60	NM_001304536.1
F2R	CCGCAGGCCAGAATCAAAAG TTCTCCTCATCCTCCCAAAATGG	60	NM_001992.4
F3	AGTTCAGGAAAGAAAACAGCCA TCCGGTTAACTGTTCGGGAG	60	NM_001993.4
FN1	AACAAACACTAATGTTAATTGCCCA TCTTGGCAGAGAGACATGCTT	60	NM_212482.2
FZD2	AACAAGTTCGGTTTTCAGTGGC GAGCTCCGTCCTCGGAGTG	60	NM_001466.3
FZD3	TCACGTGATGGCAGGTACAC TGCTGCTATGTCGTGACTGT	60	NM_017412.3
ALPI	TACACGTCCATCCTGTACGG TACACGTCCATCCTGTACGG	57	NM_001631.4
GAPDH	AATGAAGGGGTCATTGATGG AAGGTGAAGGTCGGAGTCAA	57	NM_002046.5
GFRA1	AGCGCAGATAAAGTGAGCCC ACCCAACCTGGACTCAACCG	60	NM_005264.5

HPD	GTCCCAGTAGGAGGTTTGACT GTTGCCAACCCAGAAGGTCA	60	NM_002150.2
HSPC3	TTAGGGAGGTCAGTGGGTTC CCCACACATTTGCTTGTGAT	57	NM_001271969.1
ID2	ATCCTGTCCTTGCAGGCTTC ACCGCTTATTCAGCCACACA	60	NM_002166.4
IL7R	TCCAACCGGCAGCAATGTAT AGGATCCATCTCCCCTGAGC	60	NM_002185.3
ITGA4	GCTGTGCCTGGGGGTC CACTAGGAGCCATCGGTTCG	60	NM_000885.5
ITGB8	GGCAGCTGTCTGTGAAAGTC CCGTCATTGGGCACCACTAT	60	NM_002214.2
ITPR1	GGAGTTTCAGCCCTCAGTGG CTTCAGGCACAGAGACCAGG	62	NM_001099952.2
KYNU	GGGATCCTAGCTGTTTTAGAGAA CGTTGGGTGGCATTTGAGTT	60	NM_003937.2
LAMA1	TCAGAAAGGCCTAAGCTGGC CACTGTTCTGGAAAAGCCCG	60	NM_005559.3
LINC00473	GCGTCAGCATACTTTGGCG GCCTCCCTGTGAATTCTCTCC	60	NR_026860.1
LOXL1	TCTGGCCAGCACAGCCTAT GTTGGGGAGGAAGTCTGCTG	60	NM_005576.3
LRRC7	TCCAGAGCAGTTTTGTGTGAGA TCAGGCTGAACCCTAGTAACA	60	NM_020794.2
MAP7	AGAAGACCAATGCAAGGCCA TGTAGCTGTCGGGTGCTTTT	60	NM_001198608.1
MAPK4	AGTGAACAGTGAAGCCATCG CTCAGCTGTTAGGCGATCCA	60	NM_002747.3
PC	GACGGCGAGGAGATAGTGTC GGACTGTTCGGAACTTCAGC	62	NM_000920.3
PDE1C	GAGTCGCCAACCAAGGAGAT GACCGTAATCTCTGGGACGTT	60	NM_001191056.3
PDE3A	TCCCGGTGTTTAAGAGGAGGA TGAATGCCCCATGAGCTGTT	60	NM_000921.4
PDE3B	GGCTATCGAGACATTCCTTATCACA GAACTGGCCGTGTTGTCAGA	60	NM_000922.3
PDE8B	CGTGAAGCAGGTGTCTTCTG ATAACCAGCTCTGTCGCAGG	60	NM_003719.3
PDK4	GCAGTGGTCCAAGATGCCTT ACACGATGTGAATTGGTTGGTC	60	NM_002612.3
PI15	TGCTACCACATAGCAAAGAACC AGAGTTAGGGTCTCTGCACAA	60	NM_001324403.1
POSTN	ACAAGAAGAGGTCACCAAGGTC CTTCCTCACGGGTGTGTCTC	60	NM_006475.2

PPP1R3C	TGCACCAGAATGATCCAGGTTT GTGGTGAATGTGCCAAGCAA	60	NM_005398.6
PRICKLE1	GCGCGAGCAGCCATTGTTT CTGACAGCCAAAGGCCAGTT	60	NM_153026.2
PTP4A1	ACATATTCCTCAATTCTGTGGTGT TGCATAGAGGTCGTGCTGTG	60	NM_003463.4
PTPRB	CCAGAGTATCACAGAGATCCAGTC GCACCTCTGTAGGGCATGAA	60	NM_001109754.3
RHOB	GTGTGTCTGTTCGACTCCCC AAGGGATATCAAGCTCCCGC	60	NM_004040.3
RHOV	TCAGCTACACCTGCAATGGG AAAATCCTCCTGTCCCGCTG	60	NM_133639.3
RPS18	ATTAAGGGTGTGGGCCGAAG GGTGATCACACGTTCCACCT	57	NM_022551.2
SEMA3D	AGGAAAGTGCAGACCATCGTT TTGGACATGTACCAGGCCGT	60	NM_152754.2
SEMA6D	AGTCAATTTTGCTGAGCCCCT GCCACTGAGCTACCTTCCTC	60	NM_020858.1
SERPINE1	ACGAGTCTTTCAGACCAAGAGC GCGGGCTGAGACTATGACAG	60	NM_000602.4

Appendix C: Differentially expressed genes in GIM vs CON analysis

D	Gene Symbol	Description	Fold Change	FDR P-val	Group
TC12000227.hg.1	PDE3A	phosphodiesterase 3A, cGMP-inhibited	1709.48	2.32E-09	Coding
TC05000808.hg.1			1206.61	0.0008	Coding
TC06002302.hg.1	LINC00473	long intergenic non-protein coding RNA 473	858.48	1.58E-08	Coding
TC08000497.hg.1	PI15	peptidase inhibitor 15	587.11	0.0003	Coding
TC06003872.hg.1	MAP7	microtubule-associated protein 7	515.49	0.0017	NonCoding
TC14000419.hg.1	SMOC1	SPARC related modular calcium binding 1	434.98	8.84E-09	Coding
TC12002281.hg.1	PDE3A	phosphodiesterase 3A, cGMP-inhibited	409.85	1.50E-07	NonCoding
TC06000097.hg.1	RNF182	ring finger protein 182	372.19	1.50E-07	Coding
TC05002683.hg.1			332.41	0.0017	NonCoding
TC06003993.hg.1	LINC00473	long intergenic non-protein coding RNA 473	276.56	1.65E-07	NonCoding
TC18000179.hg.1	MAPK4	mitogen-activated protein kinase 4	241.64	0.0145	Coding
TC05000809.hg.1	SPINK13	serine peptidase inhibitor, Kazal type 13 (putative)	201.81	0.002	Coding
TC05000805.hg.1	SPINK5	serine peptidase inhibitor, Kazal type 5	172.47	0.0017	Coding
TC02000902.hg.1	KYNU	kynureninase	158.11	0.0181	Coding
TC20000876.hg.1	SLPI	secretory leukocyte peptidase inhibitor	141.6	0.0118	Coding
TC06000060.hg.1	DSP	desmoplakin	134.93	0.0094	Coding
TC21000138.hg.1	CLIC6	chloride intracellular channel 6	132.3	0.0896	Coding
TC06003119.hg.1	SAMD5	sterile alpha motif domain containing 5	126.46	0.0024	NonCoding
TC11002594.hg.1	NAV2	neuron navigator 2	106.92	0.001	NonCoding
TC02001400.hg.1	ALPI	alkaline phosphatase, intestinal	102.22	0.0152	Coding
TC06002297.hg.1	PDE10A	phosphodiesterase 10A	99.1	1.91E-05	Coding
TC15000930.hg.1	MCTP2	multiple C2 domains, transmembrane 2	96.76	0.0117	Coding
TC08000310.hg.1	C8orf4	chromosome 8 open reading frame 4	95.22	8.49E-05	Coding
TC02001246.hg.1	CPS1	carbamoyl-phosphate synthase 1	89.18	6.52E-07	Coding
TC06003988.hg.1	PDE10A	phosphodiesterase 10A	71.92	4.95E-05	NonCoding
TC12002066.hg.1	HPD	4-hydroxyphenylpyruvate dioxygenase	70.93	0.0005	Coding
TC06002144.hg.1	MAP7	microtubule-associated protein 7	66.22	0.0056	Coding
TC06001015.hg.1	PDE7B	phosphodiesterase 7B	55.65	0.0008	Coding
TC08002245.hg.1	CSGALNACT1	chondroitin sulfate N-acetylgalactosaminyltransferase 1	49.55	6.52E-07	NonCoding
TC09000323.hg.1	MAMDC2	MAM domain containing 2	46.53	0.0009	Coding
TC16001085.hg.1	MYLK3	myosin light chain kinase 3	46.21	0.0006	Coding
TC11001124.hg.1	GRAMD1B	GRAM domain containing 1B	46.16	0.0025	Coding
TC06001155.hg.1			45.9	0.057	Coding
TC07001618.hg.1	PDK4	pyruvate dehydrogenase kinase, isozyme 4	43.81	0.0124	Coding
TC11002923.hg.1			43.61	0.005	NonCoding
TC05001289.hg.1	LIFR	leukemia inhibitory factor receptor alpha	42.94	0.0004	Coding
TC10001922.hg.1	CACNB2	calcium channel, voltage-dependent, beta 2 subunit	41.63	0.0043	NonCoding
TC05001676.hg.1	EPB41L4A	erythrocyte membrane protein band 4.1 like 4A	36.56	0.0025	Coding
TC05000866.hg.1	CYFIP2	cytoplasmic FMR1 interacting protein 2	36.05	0.0028	Coding
TC09000988.hg.1	MOB3B	MOB kinase activator 3B	34.25	0.0005	Coding
TC11001458.hg.1	USH1C	Usher syndrome 1C	34.23	0.01	Coding
TC02003860.hg.1	KCNE4	potassium channel, voltage gated subfamily E regulatory beta subunit 4	33.81	0.0061	NonCoding
TC04002356.hg.1	STOX2	storkhead box 2	32.98	0.0006	NonCoding
TC17002817.hg.1	NPTX1	neuronal pentraxin I	30.4	0.0017	NonCoding
TC02002445.hg.1	NR4A2	nuclear receptor subfamily 4, group A, member 2	29.53	0.0008	Coding
TC04000895.hg.1	STOX2	storkhead box 2	27.72	0.0011	Coding
TC04001940.hg.1			25.57	0.0072	NonCoding

TC21000506.hg.1	SIK1	salt-inducible kinase 1	25	2.94E-05	Coding
TC09000508.hg.1	NR4A3	nuclear receptor subfamily 4, group A, member 3	25	0.0016	Coding
TC04002671.hg.1	ETNPPL	ethanolamine-phosphate phospho-lyase	23.37	0.017	NonCoding
TC03000013.hg.1	ITPR1	inositol 1,4,5-trisphosphate receptor, type 1	23.17	0.0015	Coding
TC03002939.hg.1			23.09	0.0389	NonCoding
TC01002347.hg.1	ID3	inhibitor of DNA binding 3, dominant negative helix-loop-helix protein	22.5	0.0594	Coding
TC03001512.hg.1	ID2B	inhibitor of DNA binding 2B, dominant negative helix-loop-helix protein (pseudogene)	22.14	0.0354	Coding
TC06000099.hg.1	CD83	CD83 molecule	22.04	0.0001	Coding
TC11001123.hg.1	GRAMD1B	GRAM domain containing 1B	21.78	0.0197	Coding
TC02002847.hg.1	DNER	delta/notch like EGF repeat containing	21.31	0.0018	Coding
TC06001072.hg.1	SAMD5	sterile alpha motif domain containing 5	19.14	0.0217	Coding
TC11002922.hg.1	GRAMD1B	GRAM domain containing 1B	18.98	0.0184	NonCoding
TC18000815.hg.1	LAMA1	laminin, alpha 1	18.89	0.0408	NonCoding
TC06003871.hg.1			18.74	0.0144	NonCoding
TC09001475.hg.1	SVEP1	sushi, von Willebrand factor type A, EGF and pentraxin domain containing 1	18.49	0.0003	Coding
TC04000893.hg.1	STOX2	storkhead box 2	18.41	0.0015	Coding
TC01001820.hg.1	MARC1	mitochondrial amidoxime reducing component 1	18.32	2.46E-05	Coding
TC11003298.hg.1	SESN3	sestrin 3	18.29	0.0977	NonCoding
TC09000036.hg.1	INSL4	insulin-like 4 (placenta)	17.76	0.0489	Coding
TC12003271.hg.1	KLRC3	killer cell lectin-like receptor subfamily C, member 3	17.74	0.0005	Coding
TC07001828.hg.1	GPR37	G protein-coupled receptor 37 (endothelin receptor type B-like)	17.48	0.0242	Coding
TC02002102.hg.1	DUSP2	dual specificity phosphatase 2	17.37	0.0356	Coding
TC15000368.hg.1	SEMA6D	sema domain, transmembrane domain (TM), and cytoplasmic domain, (semaphorin) 6D	17.11	0.0019	Coding
TC04001084.hg.1	PPARGC1A	peroxisome proliferator-activated receptor gamma, coactivator 1 alpha	16.13	0.0001	Coding
TC05000165.hg.1	SLC1A3	solute carrier family 1 (glial high affinity glutamate transporter), member 3	16.11	0.0017	Coding
TC16001980.hg.1	CDYL2	chromodomain protein, Y-like 2	15.79	0.002	NonCoding
TC06001844.hg.1	LGSN	lengsin, lens protein with glutamine synthetase domain	15.67	0.009	Coding
TC06002301.hg.1	SDIM1	stress responsive DNAJB4 interacting membrane protein 1	15.64	4.53E-05	Coding
TC0X001427.hg.1	MCF2	MCF.2 cell line derived transforming sequence	15.05	0.0595	Coding
TC09002219.hg.1			14.59	0.0006	NonCoding
TC17001937.hg.1	NPTX1	neuronal pentraxin I	14.51	0.0028	Coding
TC08000150.hg.1			14.27	0.0508	Coding
TC01000733.hg.1	PDE4B	phosphodiesterase 4B, cAMP-specific	14.06	0.0002	Coding
TC05000381.hg.1	PDE8B	phosphodiesterase 8B	13.95	0.0025	Coding
TC04000413.hg.1	EPGN	epithelial mitogen	13.3	0.0022	Coding
TC05000967.hg.1	CPEB4	cytoplasmic polyadenylation element binding protein 4	13.26	0.0027	Coding
TC18000309.hg.1	LAMA1	laminin, alpha 1	13.21	0.0437	Coding
TC12002734.hg.1	SLC2A3	solute carrier family 2 (facilitated glucose transporter), member 3	12.93	0.0009	NonCoding
TC02002378.hg.1	CXCR4	chemokine (C-X-C motif) receptor 4	12.66	0.0838	Coding
TC02000041.hg.1	ID2	inhibitor of DNA binding 2, dominant negative helix-loop-helix protein	12.53	0.0522	Coding
TC06002300.hg.1	PDE10A	phosphodiesterase 10A	11.95	3.06E-05	Coding
TC15001492.hg.1	MYO1E	myosin IE	11.86	0.0111	Coding
TC05001601.hg.1	KIAA0825	KIAA0825	11.15	0.0019	Coding
TC17000147.hg.1	GLP2R	glucagon-like peptide 2 receptor	10.87	0.0466	Coding
TC06003991.hg.1			10.85	2.46E-05	NonCoding
TC06002049.hg.1	TRAPPC3L	trafficking protein particle complex 3-like	10.69	0.039	Coding
TC09000601.hg.1	TLR4	toll-like receptor 4	10.67	0.0009	Coding
TC11002346.hg.1	MPZL2	myelin protein zero-like 2	10.51	0.0145	Coding

TC02000116.hg.1	RHOB	ras homolog family member B	10.44	0.0028	Coding
TC12000414.hg.1	NR4A1	nuclear receptor subfamily 4, group A, member 1	10.41	0.0016	Coding
TC12001294.hg.1			10.2	0.0017	Coding
TC12001170.hg.1	SLC2A3	solute carrier family 2 (facilitated glucose transporter), member 3	9.86	0.0011	Coding
TC20000088.hg.1	BTBD3	BTB (POZ) domain containing 3	9.68	0.0002	Coding
TC15002559.hg.1	MYO1E	myosin IE	9.62	0.0106	NonCoding
TC20000416.hg.1	TSHZ2	teashirt zinc finger homeobox 2	9.5	0.0069	Coding
TC11002366.hg.1	MCAM	melanoma cell adhesion molecule	9.49	0.0064	Coding
TC09000085.hg.1	SH3GL2	SH3-domain GRB2-like 2	9.29	0.0357	Coding
TC12002823.hg.1	DENND5B	DENN/MADD domain containing 5B	9.12	0.0027	NonCoding
TC15001245.hg.1	RHOV	ras homolog family member V	9.08	0.0117	Coding
TC01006269.hg.1			9.01	0.0116	Coding
TC15000881.hg.1	SLCO3A1	solute carrier organic anion transporter family, member 3A1	8.86	0.0425	Coding
TC10001569.hg.1	AVPI1	arginine vasopressin-induced 1	8.28	0.0003	Coding
TC01004348.hg.1			8.13	0.0107	NonCoding
TC03000892.hg.1	SERPINI1	serpin peptidase inhibitor, clade I (neuroserpin), member 1	8.1	0.0296	Coding
TC04001461.hg.1	ETNPPL	ethanolamine-phosphate phospho-lyase	8	0.0195	Coding
TC19001139.hg.1	MUC16	mucin 16, cell surface associated	7.9	0.0429	Coding
TC08000149.hg.1	LPL	lipoprotein lipase	7.89	0.0008	Coding
TC12003272.hg.1	KLRC2	killer cell lectin-like receptor subfamily C, member 2	7.75	0.0061	Coding
TC09001012.hg.1	AQP3	aquaporin 3 (Gill blood group)	7.74	0.0059	Coding
TC02003799.hg.1			7.65	0.0028	NonCoding
TC02001247.hg.1	CPS1-IT1	CPS1 intronic transcript 1	7.63	0.0028	Coding
TC01001030.hg.1	FAM46C	family with sequence similarity 46, member C	7.61	0.0181	Coding
TC05001389.hg.1	PDE4D	phosphodiesterase 4D, cAMP-specific	7.28	0.0014	Coding
TC20000067.hg.1	BMP2	bone morphogenetic protein 2	7.26	0.0075	Coding
TC01000931.hg.1	FAM102B	family with sequence similarity 102, member B	7.24	0.006	Coding
TC20001393.hg.1			7.06	0.0027	NonCoding
TC0X002024.hg.1	DMD	dystrophin	6.96	0.0148	NonCoding
TC17000794.hg.1	PITPNC1	phosphatidylinositol transfer protein, cytoplasmic 1	6.93	0.0061	Coding
TC14000471.hg.1	FOS	FBJ murine osteosarcoma viral oncogene homolog	6.92	0.0197	Coding
TC20000048.hg.1	SMOX	spermine oxidase	6.74	0.0019	Coding
TC09001653.hg.1	PTGES	prostaglandin E synthase	6.7	0.0548	Coding
TC06002848.hg.1	PTP4A1	protein tyrosine phosphatase type IVA, member 1	6.65	8.19E-05	NonCoding
TC12001363.hg.1	DENND5B	DENN/MADD domain containing 5B	6.57	0.0033	Coding
TC06000697.hg.1	PTP4A1	protein tyrosine phosphatase type IVA, member 1	6.52	6.76E-05	Coding
TC12000228.hg.1	SLCO1C1	solute carrier organic anion transporter family, member 1C1	6.44	0.0003	Coding
TC16000525.hg.1	CES3	carboxylesterase 3	6.35	0.0009	Coding
TC05000633.hg.1	SLC22A4	solute carrier family 22 (organic cation/zwitterion transporter), member 4	6.28	0.0245	Coding
TC08001886.hg.1	PLEKHA2	pleckstrin homology domain containing, family A (phosphoinositide binding specific) member 2	6.25	3.11E-05	NonCoding
TC0Y000182.hg.1	CD24	CD24 molecule	6.21	0.0523	Coding
TC15001683.hg.1	NRG4	neuregulin 4	6.18	0.0064	Coding
TC06002145.hg.1	MAP7	microtubule-associated protein 7	6.15	0.0307	Coding
TC05000453.hg.1	SLF1	SMC5-SMC6 complex localization factor 1	6.15	0.0002	Coding
TC20000942.hg.1	NFATC2	nuclear factor of activated T-cells, cytoplasmic, calcineurin-dependent 2	6.07	0.0463	Coding
TC11001122.hg.1			6.06	0.0095	Coding
TC01003555.hg.1	PTP4A1P7	protein tyrosine phosphatase type IVA, member 1 pseudogene 7	5.99	0.0003	Coding
TC05002515.hg.1	SLF1	SMC5-SMC6 complex localization factor 1	5.9	0.0006	NonCoding
TC02000237.hg.1	QPCT	glutaminyl-peptide cyclotransferase	5.84	0.003	Coding
TC12001222.hg.1	KLRC4-KLRK1; KLRK1; KLRC4	KLRC4-KLRK1 readthrough; killer cell lectin-like receptor subfamily K, member 1; killer cell lectin-	5.71	0.02	Coding

		like receptor subfamily C, member 4			
TC04002887.hg.1	SORBS2	sorbin and SH3 domain containing 2	5.7	0.0504	NonCoding
TC04000894.hg.1			5.68	0.021	Coding
TC17000311.hg.1	KSR1	kinase suppressor of ras 1	5.67	0.0003	Coding
TC07001377.hg.1	COBL	cordon-bleu WH2 repeat protein	5.6	0.0017	Coding
TC09001326.hg.1	ROR2	receptor tyrosine kinase-like orphan receptor 2	5.58	9.82E-05	Coding
TC18000104.hg.1	TTC39C	tetratricopeptide repeat domain 39C	5.55	0.0042	Coding
TC10000138.hg.1	CACNB2	calcium channel, voltage-dependent, beta 2 subunit	5.52	0.0215	Coding
TC03002632.hg.1	PPM1L	protein phosphatase, Mg2+/Mn2+ dependent, 1L	5.39	0.0566	NonCoding
TC17001732.hg.1	RNF43	ring finger protein 43	5.23	0.007	Coding
TC17000807.hg.1	MAP2K6	mitogen-activated protein kinase kinase 6	5.11	0.0352	Coding
TC09000593.hg.1	PAPPA	pregnancy-associated plasma protein A, pappalysin 1	5.03	0.0176	Coding
TC03001207.hg.1	SH3BP5	SH3-domain binding protein 5 (BTK-associated)	5.01	0.0012	Coding
TC0X001303.hg.1	KLHL13	kelch-like family member 13	5.01	0.03	Coding
TC09000893.hg.1	ERMP1	endoplasmic reticulum metallopeptidase 1	4.93	0.0147	Coding
TC08001155.hg.1			4.91	0.0022	Coding
TC02002765.hg.1	TNS1	tensin 1	4.89	0.0176	Coding
TC08000296.hg.1	PLEKHA2	pleckstrin homology domain containing, family A (phosphoinositide binding specific) member 2	4.88	2.97E-05	Coding
TC17002394.hg.1			4.85	0.023	NonCoding
TC01005437.hg.1	SLC6A9	solute carrier family 6 (neurotransmitter transporter, glycine), member 9	4.8	0.0067	NonCoding
TC09000316.hg.1	PIP5K1B	phosphatidylinositol-4-phosphate 5-kinase, type I, beta	4.78	0.0184	Coding
TC02001774.hg.1	LOC101929723	uncharacterized LOC101929723	4.78	0.017	Coding
TC10001522.hg.1	PPP1R3C	protein phosphatase 1, regulatory subunit 3C	4.75	0.0138	Coding
TC11002686.hg.1	DTX4	deltex 4, E3 ubiquitin ligase	4.66	0.0062	NonCoding
TC19000981.hg.1	PLPP2	phospholipid phosphatase 2	4.65	0.0889	Coding
TC01005541.hg.1			4.64	0.0087	NonCoding
TC17002321.hg.1	PITPNC1	phosphatidylinositol transfer protein, cytoplasmic 1	4.62	0.0065	NonCoding
TC01000892.hg.1	PALMD; MIR548AA1	palmdelphin; microRNA 548aa-1	4.6	0.049	Coding
TC10000577.hg.1	LINC00857	long intergenic non-protein coding RNA 857	4.56	0.0187	Coding
TC02000259.hg.1	PKDCC	protein kinase domain containing, cytoplasmic	4.53	0.0117	Coding
TC06002126.hg.1	SGK1	serum/glucocorticoid regulated kinase 1	4.52	0.0188	Coding
TC10002169.hg.1	LINC00857	long intergenic non-protein coding RNA 857	4.48	0.018	NonCoding
TC07002501.hg.1	CUX1	cut-like homeobox 1	4.47	0.0072	NonCoding
TC16001294.hg.1	CDYL2	chromodomain protein, Y-like 2	4.46	0.0154	Coding
TC05001182.hg.1	FAM134B	family with sequence similarity 134, member B	4.45	0.0753	Coding
TC19002629.hg.1	IFI30	interferon, gamma-inducible protein 30	4.45	0.0837	Coding
TC07002464.hg.1	PPP1R9A	protein phosphatase 1, regulatory subunit 9A	4.43	0.0068	NonCoding
TC20000582.hg.1	RNF24	ring finger protein 24	4.42	0.0062	Coding
TC15002560.hg.1			4.41	0.0637	NonCoding
TC04002235.hg.1	IL15	interleukin 15	4.37	0.0493	NonCoding
TC11001976.hg.1	PC	pyruvate carboxylase	4.35	0.011	Coding
TC08000311.hg.1			4.31	0.0403	Coding
TC06002591.hg.1			4.28	0.0079	NonCoding
TC06000098.hg.1			4.27	0.015	Coding
TC05002066.hg.1	DUSP1	dual specificity phosphatase 1	4.22	0.0149	Coding
TC09000330.hg.1	GDA	guanine deaminase	4.17	0.0648	Coding
TC17000499.hg.1	IGFBP4	insulin like growth factor binding protein 4	4.15	0.0073	Coding
TC10001389.hg.1			4.13	0.0463	Coding
TC07003069.hg.1	PON2	paraoxonase 2	4.12	0.0083	NonCoding
TC08001022.hg.1	CSGALNACT1	chondroitin sulfate N-acetylgalactosaminyltransferase 1	4.11	0.0004	Coding
TC07001617.hg.1	PON2	paraoxonase 2	4.06	0.008	Coding
TC18000919.hg.1			4.02	0.0308	NonCoding

TC01003733.hg.1	PIK3C2B	phosphatidylinositol-4-phosphate 3-kinase, catalytic subunit type 2 beta	4	0.0283	Coding
TC17002907.hg.1	JUP	junction plakoglobin	3.88	0.0282	Coding
TC01002940.hg.1	VAV3	vav 3 guanine nucleotide exchange factor	3.87	0.0082	Coding
TC05002485.hg.1			3.85	0.0001	NonCoding
TC05002393.hg.1			3.84	0.0019	NonCoding
TC05001172.hg.1	ANKH	ANKH inorganic pyrophosphate transport regulator	3.83	0.0061	Coding
TC01002590.hg.1	SLC6A9	solute carrier family 6 (neurotransmitter transporter, glycine), member 9	3.81	0.0067	Coding
TC08000220.hg.1	FZD3	frizzled class receptor 3	3.81	0.0317	Coding
TC17002216.hg.1			3.79	0.0605	NonCoding
TC06001903.hg.1	FAM46A	family with sequence similarity 46, member A	3.78	0.0056	Coding
TC12003284.hg.1	RHOF	ras homolog family member F (in filopodia)	3.76	0.0052	Coding
TC18000608.hg.1			3.72	0.0255	NonCoding
TC0X002231.hg.1	MBNL3	muscleblind-like splicing regulator 3	3.66	0.0452	NonCoding
TC01000398.hg.1	PTPRU	protein tyrosine phosphatase, receptor type, U	3.66	0.0168	Coding
TC09000015.hg.1	VLDLR	very low density lipoprotein receptor	3.63	0.0254	Coding
TC09001190.hg.1	LOC101927069	uncharacterized LOC101927069	3.63	0.0331	Coding
TC09001008.hg.1	B4GALT1	UDP-Gal:betaGlcNAc beta 1,4-galactosyltransferase, polypeptide 1	3.61	0.0002	Coding
TC05002512.hg.1	NR2F1	nuclear receptor subfamily 2, group F, member 1	3.61	0.0404	NonCoding
TC11000345.hg.1	PRR5L	proline rich 5 like	3.6	0.024	Coding
TC18000059.hg.1	CHMP1B	charged multivesicular body protein 1B	3.59	0.0059	Coding
TC08001015.hg.1	ASAH1	N-acylsphingosine amidohydrolase (acid ceramidase) 1	3.58	0.0001	Coding
TC02002496.hg.1	SCN1A	sodium channel, voltage gated, type I alpha subunit	3.57	0.0153	Coding
TC02002541.hg.1	WIPF1	WAS/WASL interacting protein family, member 1	3.54	0.0005	Coding
TC07000565.hg.1	PPP1R9A	protein phosphatase 1, regulatory subunit 9A	3.54	0.0206	Coding
TC01003796.hg.1	SLC30A1	solute carrier family 30 (zinc transporter), member 1	3.51	0.0146	Coding
TC04001383.hg.1	SNCA	synuclein alpha	3.5	0.0326	Coding
TC02001351.hg.1	KCNE4	potassium channel, voltage gated subfamily E regulatory beta subunit 4	3.49	0.0129	Coding
TC17000582.hg.1	FMNL1	formin like 1	3.49	0.0023	Coding
TC18000496.hg.1	SMAD2	SMAD family member 2	3.47	0.0004	Coding
TC02000386.hg.1	MEIS1	Meis homeobox 1	3.47	0.0288	Coding
TC01000559.hg.1	DMAP1	DNA methyltransferase 1 associated protein 1	3.46	0.0125	Coding
TC01000385.hg.1	RAB42	RAB42, member RAS oncogene family	3.44	0.0019	Coding
TC07000476.hg.1	RHBDD2	rhomboid domain containing 2	3.43	0.0445	Coding
TC18000047.hg.1	RAB31	RAB31, member RAS oncogene family	3.43	0.0018	Coding
TC0X000084.hg.1	NHS	Nance-Horan syndrome (congenital cataracts and dental anomalies)	3.43	0.0149	Coding
TC02002733.hg.1	LANCL1	LanC lantibiotic synthetase component C-like 1 (bacterial)	3.37	0.0072	Coding
TC15000866.hg.1	CRTC3	CREB regulated transcription coactivator 3	3.36	0.0001	Coding
TC10001054.hg.1	FAM107B	family with sequence similarity 107, member B	3.36	0.0082	Coding
TC03002115.hg.1	FGF12	fibroblast growth factor 12	3.35	0.0174	Coding
TC18000020.hg.1	DLGAP1-AS1	DLGAP1 antisense RNA 1	3.31	0.0274	Coding
TC06003084.hg.1	TNFAIP3	tumor necrosis factor, alpha-induced protein 3	3.27	0.0571	NonCoding
TC06001312.hg.1	LOC100506885	uncharacterized LOC100506885	3.26	0.0138	Coding
TC09002580.hg.1			3.25	0.0812	NonCoding
TC08000207.hg.1	PTK2B	protein tyrosine kinase 2 beta	3.22	0.0594	Coding
TC09000394.hg.1	GAS1RR	GAS1 adjacent regulatory RNA	3.21	0.0373	Coding
TC21000289.hg.1			3.2	0.0744	Coding
TC06003713.hg.1			3.17	0.0119	NonCoding
TC21000785.hg.1	ADARB1	adenosine deaminase, RNA-specific, B1	3.17	0.0188	NonCoding
TC11003373.hg.1			3.16	0.0609	NonCoding
TC13001247.hg.1			3.16	0.0715	NonCoding
TC09002210.hg.1	PAPPA	pregnancy-associated plasma protein A, pappalysin 1	3.15	0.0696	NonCoding

TC04000254.hg.1	LIMCH1	LIM and calponin homology domains 1	3.13	0.01	Coding
TC03003359.hg.1	GXYLT2	glucoside xylosyltransferase 2	3.11	0.0535	Coding
TC11000214.hg.1	PDE3B	phosphodiesterase 3B, cGMP-inhibited	3.11	0.01	Coding
TC15002774.hg.1	CCPG1; MIR628	cell cycle progression 1; microRNA 628	3.09	0.0413	Coding
TC04001959.hg.1			3.09	0.0613	NonCoding
TC20001072.hg.1	LINC01433	long intergenic non-protein coding RNA 1433	3.09	0.0111	NonCoding
TC02000117.hg.1			3.09	0.027	Coding
TC01001288.hg.1	EFNA1	ephrin-A1	3.09	0.0151	Coding
TC13000347.hg.1			3.07	0.0718	Coding
TC03000104.hg.1	PLCL2; MIR3714	phospholipase C-like 2; microRNA 3714	3.07	0.0782	Coding
TC04002651.hg.1	SLC39A8	solute carrier family 39 (zinc transporter), member 8	3.06	0.0095	NonCoding
TC02002726.hg.1	IDH1	isocitrate dehydrogenase 1 (NADP+)	3.05	0.0576	Coding
TC10002734.hg.1	ANXA11	annexin A11	3.05	0.0036	NonCoding
TC01002245.hg.1	CASP9	caspase 9	3.03	0.0064	Coding
TC01001736.hg.1	CD55	CD55 molecule, decay accelerating factor for complement (Cromer blood group)	3.02	0.0027	Coding
TC01003888.hg.1			3.02	0.013	Coding
TC20000082.hg.1	SNAP25	synaptosome associated protein 25kDa	3	0.0072	Coding
TC16001335.hg.1	SLC7A5	solute carrier family 7 (amino acid transporter light chain, L system), member 5	3	0.0246	Coding
TC17000315.hg.1	NLK	nemo-like kinase	2.99	0.0135	Coding
TC17002323.hg.1	PITPNC1	phosphatidylinositol transfer protein, cytoplasmic 1	2.97	0.0195	NonCoding
TC10001585.hg.1	DNMBP	dynamin binding protein	2.97	0.0403	Coding
TC18000654.hg.1			2.97	0.0028	NonCoding
TC0X001937.hg.1	ATP6AP1	ATPase, H+ transporting, lysosomal accessory protein 1	2.97	8.49E-05	NonCoding
TC02002034.hg.1	TRABD2A	TraB domain containing 2A	2.96	0.0171	Coding
TC06002196.hg.1	FBXO30	F-box protein 30	2.95	0.0552	Coding
TC09000500.hg.1	TGFBR1	transforming growth factor, beta receptor 1	2.93	0.0334	Coding
TC06003507.hg.1	LOC100506885	uncharacterized LOC100506885	2.91	0.0163	NonCoding
TC05000084.hg.1	FAM105A	family with sequence similarity 105, member A	2.91	0.0719	Coding
TC18000918.hg.1			2.89	0.0253	NonCoding
TC04001014.hg.1	AFAP1	actin filament associated protein 1	2.85	0.0093	Coding
TC10001461.hg.1	ANXA11	annexin A11	2.85	0.0031	Coding
TC09001009.hg.1	BAG1	BCL2-associated athanogene	2.84	0.0012	Coding
TC18000058.hg.1	GNAL	guanine nucleotide binding protein (G protein), alpha activating activity polypeptide, olfactory type	2.84	0.0071	Coding
TC06003074.hg.1			2.83	0.023	NonCoding
TC09002209.hg.1	PAPPA	pregnancy-associated plasma protein A, pappalysin 1	2.83	0.0786	NonCoding
TC14001023.hg.1	SPTSSA	serine palmitoyltransferase, small subunit A	2.83	0.0371	Coding
TC05000635.hg.1	SLC22A5	solute carrier family 22 (organic cation/carnitine transporter), member 5	2.82	0.0129	Coding
TC11002345.hg.1	MPZL3	myelin protein zero-like 3	2.81	0.0345	Coding
TC10000449.hg.1	DDIT4	DNA damage inducible transcript 4	2.8	0.0389	Coding
TC0X001370.hg.1	MBNL3	muscleblind-like splicing regulator 3	2.77	0.0471	Coding
TC03000214.hg.1	CTNNB1	catenin (cadherin-associated protein), beta 1	2.76	0.0575	Coding
TC0X000025.hg.1	STS	steroid sulfatase (microsomal), isozyme S	2.74	0.0754	Coding
TC06002146.hg.1	MAP3K5	mitogen-activated protein kinase kinase kinase 5	2.73	0.0107	Coding
TC09001630.hg.1			2.73	0.0319	Coding
TC04000693.hg.1	IL15	interleukin 15	2.72	0.0646	Coding
TC13001054.hg.1			2.71	0.0149	NonCoding
TC10001580.hg.1	GOT1	glutamic-oxaloacetic transaminase 1, soluble	2.71	0.0064	Coding
TC19001586.hg.1	LYPD3	LY6/PLAUR domain containing 3	2.67	0.0399	Coding
TC06003479.hg.1			2.67	0.0088	NonCoding
TC01001201.hg.1	MLLT11	myeloid/lymphoid or mixed-lineage leukemia; translocated to, 11	2.66	0.0837	Coding
TC01003692.hg.1	CSRP1	cysteine and glycine-rich protein 1	2.66	0.009	Coding

TC08000178.hg.1	RHOBTB2	Rho-related BTB domain containing 2	2.65	0.0148	Coding
TC16000555.hg.1	PRMT7	protein arginine methyltransferase 7	2.64	0.0157	Coding
TC05001603.hg.1			2.61	0.0018	Coding
TC02000416.hg.1	PCYOX1	prenylcysteine oxidase 1	2.59	0.0017	Coding
TC08001369.hg.1	SLC10A5	solute carrier family 10, member 5	2.58	0.087	Coding
TC06001854.hg.1	LMBRD1	LMBR1 domain containing 1	2.58	0.0277	Coding
TC10000578.hg.1	LOC100130698	uncharacterized LOC100130698	2.57	0.0116	Coding
TC0X000721.hg.1	MAMLD1	mastermind-like domain containing 1	2.56	0.0125	Coding
TC17002395.hg.1			2.56	0.0137	NonCoding
TC02004706.hg.1	ATP5G3	ATP synthase, H+ transporting, mitochondrial Fo complex subunit C3 (subunit 9)	2.56	0.018	NonCoding
TC12002680.hg.1			2.56	0.0556	NonCoding
TC06003990.hg.1			2.56	0.0005	NonCoding
TC08001893.hg.1			2.54	0.0333	NonCoding
TC05002568.hg.1	DCP2	decapping mRNA 2	2.53	0.0078	NonCoding
TC10000968.hg.1			2.53	0.061	Coding
TC04000140.hg.1	CPEB2	cytoplasmic polyadenylation element binding protein 2	2.53	0.035	Coding
TC03001570.hg.1	ROBO1	roundabout guidance receptor 1	2.52	0.0622	Coding
TC11002708.hg.1	SLC3A2	solute carrier family 3 (amino acid transporter heavy chain), member 2	2.51	0.0283	NonCoding
TC14001370.hg.1	STON2	stonin 2	2.51	0.0319	Coding
TC20000629.hg.1			2.5	0.0112	Coding
TC06000062.hg.1	BMP6	bone morphogenetic protein 6	2.5	0.0696	Coding
TC12001168.hg.1	SLC2A14	solute carrier family 2 (facilitated glucose transporter), member 14	2.5	0.0051	Coding
TC01006089.hg.1	SLC30A1	solute carrier family 30 (zinc transporter), member 1	2.49	0.0353	NonCoding
TC18000761.hg.1	SOCS6	suppressor of cytokine signaling 6	2.49	0.0921	NonCoding
TC20000049.hg.1	LINC01433	long intergenic non-protein coding RNA 1433	2.49	0.0334	Coding
TC06000958.hg.1	TPD52L1	tumor protein D52-like 1	2.48	0.0519	Coding
TC06001282.hg.1	MCUR1	mitochondrial calcium uniporter regulator 1	2.48	0.0105	Coding
TC04002425.hg.1			2.46	0.0458	NonCoding
TC17000231.hg.1			2.45	0.0588	Coding
TC17001237.hg.1			2.45	0.0588	Coding
TC09001404.hg.1	CORO2A	coronin, actin binding protein, 2A	2.44	0.0669	Coding
TC12001041.hg.1			2.44	0.0242	Coding
TC21000241.hg.1	ADARB1	adenosine deaminase, RNA-specific, B1	2.44	0.0345	Coding
TC17001232.hg.1			2.44	0.0616	Coding
TC10001445.hg.1	DLG5	discs, large homolog 5 (Drosophila)	2.44	0.0336	Coding
TC17002650.hg.1			2.43	0.0915	NonCoding
TC10001562.hg.1	FRAT2	frequently rearranged in advanced T-cell lymphomas 2	2.43	0.0169	Coding
TC02001139.hg.1	SLC39A10	solute carrier family 39 (zinc transporter), member 10	2.43	0.0601	Coding
TC08000616.hg.1			2.43	0.0263	Coding
TC12001448.hg.1	ZNF641	zinc finger protein 641	2.42	0.0061	Coding
TC0X000532.hg.1	COL4A5	collagen, type IV, alpha 5	2.41	0.0005	Coding
TC01001079.hg.1			2.41	0.0162	Coding
TC15000824.hg.1	PDE8A	phosphodiesterase 8A	2.4	0.0033	Coding
TC19001275.hg.1	BST2	bone marrow stromal cell antigen 2	2.4	0.0851	Coding
TC08000493.hg.1	GDAP1	ganglioside induced differentiation associated protein 1	2.39	0.03	Coding
TC0X000528.hg.1	MID2	midline 2	2.39	0.0715	Coding
TC13001060.hg.1			2.37	0.0045	NonCoding
TC06002127.hg.1			2.37	0.0513	Coding
TC17001754.hg.1	RNFT1	ring finger protein, transmembrane 1	2.37	0.0309	Coding
TC17002849.hg.1	PER1	period circadian clock 1	2.36	0.0111	Coding
TC0Y000287.hg.1			2.36	0.0052	NonCoding

TC21000922.hg.1			2.35	0.042	NonCoding
TC04002924.hg.1	SLC39A8	solute carrier family 39 (zinc transporter), member 8	2.35	0.0226	Coding
TC02001948.hg.1	GFPT1	glutamine--fructose-6-phosphate transaminase 1	2.34	0.0061	Coding
TC0X000572.hg.1	WDR44	WD repeat domain 44	2.33	0.0832	Coding
TC11000567.hg.1	SLC3A2	solute carrier family 3 (amino acid transporter heavy chain), member 2	2.33	0.0219	Coding
TC08000714.hg.1	FAM83A	family with sequence similarity 83, member A	2.33	0.0171	Coding
TC0X001995.hg.1	PIR-FIGF	PIR-FIGF readthrough	2.31	0.0459	NonCoding
TC08000148.hg.1	INTS10	integrator complex subunit 10	2.3	0.0008	Coding
TC01003847.hg.1	DUSP10	dual specificity phosphatase 10	2.3	0.0967	Coding
TC06001073.hg.1			2.29	0.0403	Coding
TC17000883.hg.1	MGAT5B	mannosyl (alpha-1,6-)-glycoprotein beta-1,6-N-acetyl-glucosaminyltransferase, isozyme B	2.28	0.0146	Coding
TC05000284.hg.1	MAST4	microtubule associated serine/threonine kinase family member 4	2.28	0.0572	Coding
TC04000758.hg.1			2.28	0.0138	Coding
TC0X000771.hg.1	ATP6AP1	ATPase, H+ transporting, lysosomal accessory protein 1	2.27	0.0012	Coding
TC01006158.hg.1			2.27	0.0308	NonCoding
TC22001130.hg.1			2.26	0.0747	NonCoding
TC09001525.hg.1	PAPPA-AS1	PAPPA antisense RNA 1	2.26	0.0385	Coding
TC06002299.hg.1			2.26	0.0387	Coding
TC13000875.hg.1	RAB20	RAB20, member RAS oncogene family	2.25	0.0797	Coding
TC09002555.hg.1			2.24	0.0321	NonCoding
TC17001698.hg.1	TOB1	transducer of ERBB2, 1	2.24	0.0326	Coding
TC04000590.hg.1	UGT8	UDP glycosyltransferase 8	2.24	0.0229	Coding
TC04000754.hg.1	FAM160A1	family with sequence similarity 160, member A1	2.24	0.0147	Coding
TC20001429.hg.1			2.23	0.0272	NonCoding
TC11002283.hg.1			2.23	0.0564	Coding
TC10000238.hg.1	CREM	cAMP responsive element modulator	2.22	0.0144	Coding
TC06003992.hg.1			2.22	0.0337	NonCoding
TC12000232.hg.1	PYROXD1	pyridine nucleotide-disulphide oxidoreductase domain 1	2.22	0.0832	Coding
TC09002454.hg.1			2.22	0.0321	NonCoding
TC09001325.hg.1	NFIL3	nuclear factor, interleukin 3 regulated	2.21	0.0615	Coding
TC09000594.hg.1			2.21	0.0932	Coding
TC07001760.hg.1			2.2	0.0262	Coding
TC07001907.hg.1	KIAA1549	KIAA1549	2.19	0.021	Coding
TC02001576.hg.1	ROCK2	Rho-associated, coiled-coil containing protein kinase 2	2.18	0.043	Coding
TC10001641.hg.1	ITPRIP	inositol 1,4,5-trisphosphate receptor interacting protein	2.18	0.0316	Coding
TC0X000033.hg.1	TBL1X	transducin (beta)-like 1X-linked	2.17	0.011	Coding
TC14001209.hg.1	SGPP1	sphingosine-1-phosphate phosphatase 1	2.17	0.084	Coding
TC18000223.hg.1	ZCCHC2	zinc finger, CCHC domain containing 2	2.15	0.0002	Coding
TC17000904.hg.1	DNAH17-AS1	DNAH17 antisense RNA 1	2.15	0.039	Coding
TC12001904.hg.1	GLT8D2	glycosyltransferase 8 domain containing 2	2.15	0.0092	Coding
TC15000949.hg.1	IGF1R	insulin-like growth factor 1 receptor	2.14	0.0353	Coding
TC07001344.hg.1	TMED4	transmembrane p24 trafficking protein 4	2.14	0.0087	Coding
TC0X001584.hg.1	STS	steroid sulfatase (microsomal), isozyme S	2.14	0.0931	NonCoding
TC02001419.hg.1	DGKD	diacylglycerol kinase, delta 130kDa	2.14	0.0056	Coding
TC04000757.hg.1			2.14	0.0776	Coding
TC06000963.hg.1	HINT3	histidine triad nucleotide binding protein 3	2.13	0.0522	Coding
TC08002615.hg.1	FBXO16	F-box protein 16	2.13	0.0182	Coding
TC01005919.hg.1	MPC2	mitochondrial pyruvate carrier 2	2.13	0.0115	NonCoding
TC05000291.hg.1	PIK3R1	phosphoinositide-3-kinase, regulatory subunit 1 (alpha)	2.13	0.0465	Coding
TC08000613.hg.1	SPAG1	sperm associated antigen 1	2.13	0.0147	Coding

TC13000163.hg.1	SMIM2-AS1	SMIM2 antisense RNA 1	2.12	0.0154	Coding
TC0X001822.hg.1	COL4A5	collagen, type IV, alpha 5	2.12	0.0008	NonCoding
TC11002632.hg.1	PRR5L	proline rich 5 like	2.11	0.0332	NonCoding
TC13000193.hg.1	FNDC3A	fibronectin type III domain containing 3A	2.11	0.0995	Coding
TC01000373.hg.1	SMPDL3B	sphingomyelin phosphodiesterase, acid-like 3B	2.11	0.0024	Coding
TC11000484.hg.1	DTX4	deltex 4, E3 ubiquitin ligase	2.11	0.0141	Coding
TC04002268.hg.1			2.11	0.0309	NonCoding
TC17000977.hg.1	SLC43A2	solute carrier family 43 (amino acid system L transporter), member 2	2.11	0.0676	Coding
TC07001906.hg.1	ATP6V0A4	ATPase, H+ transporting, lysosomal V0 subunit a4	2.1	0.0172	Coding
TC13000855.hg.1	KDELC1	KDEL (Lys-Asp-Glu-Leu) containing 1	2.09	0.0229	Coding
TC09001602.hg.1	SNORA65	small nucleolar RNA, H/ACA box 65	2.09	0.0825	Coding
TC0X000873.hg.1	ASB9	ankyrin repeat and SOCS box containing 9	2.08	0.0721	Coding
TC04001430.hg.1	MANBA	mannosidase, beta A, lysosomal	2.08	0.0384	Coding
TC0X002327.hg.1	PIR	pirin	2.08	0.0735	Coding
TC0X000923.hg.1	APOO	apolipoprotein O	2.08	0.0403	Coding
TC10002216.hg.1	PCGF5	polycomb group ring finger 5	2.07	0.0591	NonCoding
TC02004133.hg.1	BRE-AS1	BRE antisense RNA 1	2.07	0.0059	NonCoding
TC15002546.hg.1	DYX1C1-CCPG1	DYX1C1-CCPG1 readthrough (NMD candidate)	2.07	0.0231	NonCoding
TC03001355.hg.1	CCR1	chemokine (C-C motif) receptor 1	2.07	0.0871	Coding
TC0X001358.hg.1	AIFM1	apoptosis-inducing factor, mitochondrion-associated, 1	2.07	0.0025	Coding
TC20001290.hg.1			2.07	0.0481	NonCoding
TC19000010.hg.1	HCN2	hyperpolarization activated cyclic nucleotide gated potassium channel 2	2.06	0.0539	Coding
TC01003664.hg.1			2.06	0.0699	Coding
TC15000324.hg.1	TMEM62	transmembrane protein 62	2.05	0.0249	Coding
TC05000535.hg.1	DCP2	decapping mRNA 2	2.05	0.0121	Coding
TC01002882.hg.1	GCLM	glutamate-cysteine ligase, modifier subunit	2.04	0.0558	Coding
TC03002827.hg.1			2.04	0.0302	NonCoding
TC06000923.hg.1	RWDD1	RWD domain containing 1	2.04	0.0871	Coding
TC09002181.hg.1	SVEP1	sushi, von Willebrand factor type A, EGF and pentraxin domain containing 1	2.03	0.0086	NonCoding
TC10001531.hg.1	IDE	insulin-degrading enzyme	2.03	0.0111	Coding
TC07002728.hg.1	LINC00689	long intergenic non-protein coding RNA 689	2.03	0.0269	NonCoding
TC06000948.hg.1	PKIB	protein kinase (cAMP-dependent, catalytic) inhibitor beta	2.02	0.0636	Coding
TC22000723.hg.1	C1QTNF6	C1q and tumor necrosis factor related protein 6	2.02	0.015	Coding
TC02002510.hg.1	FASTKD1	FAST kinase domains 1	2.02	0.0356	Coding
TC17002633.hg.1	P3H4	prolyl 3-hydroxylase family member 4 (non-enzymatic)	2.01	0.0862	NonCoding
TC0X001267.hg.1	COL4A6	collagen, type IV, alpha 6	2.01	0.0036	Coding
TC01000555.hg.1	ATP6V0B	ATPase, H+ transporting, lysosomal 21kDa, V0 subunit b	2.01	0.029	Coding
TC10001109.hg.1	ARHGAP21	Rho GTPase activating protein 21	2	0.0508	Coding
TC01002477.hg.1	TMEM54	transmembrane protein 54	-2	0.0446	Coding
TC0X001976.hg.1	MID1	midline 1	-2	0.0583	NonCoding
TC12000854.hg.1	ANKRD13A	ankyrin repeat domain 13A	-2	0.0106	Coding
TC02000929.hg.1	LYPD6	LY6/PLAUR domain containing 6	-2.01	0.0442	Coding
TC12001430.hg.1	AMIGO2	adhesion molecule with Ig-like domain 2	-2.01	0.0806	Coding
TC02000750.hg.1	STEAP3	STEAP family member 3, metalloreductase	-2.01	0.0452	Coding
TC11001513.hg.1	BDNF	brain-derived neurotrophic factor	-2.01	0.042	Coding
TC02000534.hg.1			-2.01	0.0309	Coding
TC11001478.hg.1	E2F8	E2F transcription factor 8	-2.02	0.094	Coding
TC09000038.hg.1	PDCD1LG2	programmed cell death 1 ligand 2	-2.02	0.0706	Coding
TC04001116.hg.1	RELL1	RELT-like 1	-2.02	0.0167	Coding
TC12000514.hg.1	RBMS2	RNA binding motif, single stranded interacting protein 2	-2.02	0.0443	Coding

TC02001481.hg.1	BOK	BCL2-related ovarian killer	-2.02	0.031	Coding
TC18000731.hg.1	NEDD4L	neural precursor cell expressed, developmentally down-regulated 4-like, E3 ubiquitin protein ligase	-2.02	0.0403	NonCoding
TC01003670.hg.1	MIR181A1HG	MIR181A1 host gene	-2.02	0.0119	Coding
TC15000581.hg.1	RAB8B	RAB8B, member RAS oncogene family	-2.02	0.0731	Coding
TC02002891.hg.1	ARL4C	ADP-ribosylation factor like GTPase 4C	-2.02	0.0802	Coding
TC15002009.hg.1	PCSK6	proprotein convertase subtilisin/kexin type 6	-2.02	0.002	Coding
TC02000199.hg.1	LBH	limb bud and heart development	-2.03	0.0045	Coding
TC01004783.hg.1	LINC01133	long intergenic non-protein coding RNA 1133	-2.03	0.0077	NonCoding
TC02001977.hg.1	EXOC6B	exocyst complex component 6B	-2.04	0.0558	Coding
TC07000450.hg.1	LIMK1	LIM domain kinase 1	-2.04	0.0219	Coding
TC18000692.hg.1	SETBP1	SET binding protein 1	-2.04	0.0948	NonCoding
TC01003566.hg.1	ABL2	ABL proto-oncogene 2, non-receptor tyrosine kinase	-2.04	0.0566	Coding
TC20000956.hg.1	ZNF217	zinc finger protein 217	-2.04	0.0319	Coding
TC02002063.hg.1			-2.05	0.0255	Coding
TC05000243.hg.1	MAP3K1	mitogen-activated protein kinase kinase kinase 1, E3 ubiquitin protein ligase	-2.05	0.087	Coding
TC01001422.hg.1	UAP1	UDP-N-acetylglucosamine pyrophosphorylase 1	-2.05	0.03	Coding
TC14001434.hg.1	RPS6KA5	ribosomal protein S6 kinase, 90kDa, polypeptide 5	-2.05	0.01	Coding
TC06000642.hg.1	C6orf141	chromosome 6 open reading frame 141	-2.05	0.067	Coding
TC01002632.hg.1	FOXD2-AS1	FOXD2 antisense RNA 1 (head to head)	-2.05	0.0854	Coding
TC06003138.hg.1			-2.05	0.0198	NonCoding
TC17001585.hg.1	GJC1	gap junction protein gamma 1	-2.05	0.0189	Coding
TC11001286.hg.1	PHLDA2	pleckstrin homology-like domain, family A, member 2	-2.06	0.0424	Coding
TC03002973.hg.1			-2.06	0.095	NonCoding
TC12001303.hg.1	C2CD5	C2 calcium-dependent domain containing 5	-2.06	0.0115	Coding
TC15001691.hg.1	PEAK1	pseudopodium-enriched atypical kinase 1	-2.06	0.0461	Coding
TC14002331.hg.1	FOXN3	forkhead box N3	-2.06	0.0504	Coding
TC02004536.hg.1			-2.07	0.0829	NonCoding
TC0X001392.hg.1	MIR503HG; MIR424	MIR503 host gene; microRNA 424	-2.07	0.0062	Coding
TC01002885.hg.1			-2.07	0.0556	Coding
TC08001548.hg.1	EXT1	exostosin glycosyltransferase 1	-2.07	0.0834	Coding
TC10001535.hg.1	MYOF	myoferlin	-2.08	0.0188	Coding
TC06000541.hg.1	PIM1	Pim-1 proto-oncogene, serine/threonine kinase	-2.08	0.0289	Coding
TC07003195.hg.1	HIPK2	homeodomain interacting protein kinase 2	-2.08	0.0714	NonCoding
TC02000764.hg.1	GLI2	GLI family zinc finger 2	-2.09	0.03	Coding
TC01003054.hg.1	NOTCH2	notch 2	-2.09	0.0496	Coding
TC03003338.hg.1	SATB1	SATB homeobox 1	-2.09	0.0769	Coding
TC16000439.hg.1	ADCY7	adenylate cyclase 7	-2.1	0.0285	Coding
TC15001161.hg.1	MTMR10	myotubularin related protein 10	-2.1	0.03	Coding
TC14000401.hg.1	GPHN	gephyrin	-2.11	0.0615	Coding
TC02003499.hg.1			-2.11	0.0416	NonCoding
TC09001656.hg.1	FNBP1	formin binding protein 1	-2.11	0.0252	Coding
TC16000096.hg.1	THOC6	THO complex 6	-2.12	0.0183	Coding
TC07001915.hg.1	HIPK2	homeodomain interacting protein kinase 2	-2.12	0.0633	Coding
TC03001233.hg.1	ZNF385D	zinc finger protein 385D	-2.12	0.0075	Coding
TC15001183.hg.1	FMN1	formin 1	-2.12	0.0365	Coding
TC01000891.hg.1	PLPPR4	phospholipid phosphatase related 4	-2.12	0.0797	Coding
TC05000831.hg.1	NDST1	N-deacetylase/N-sulfotransferase (heparan glucosaminyl) 1	-2.13	0.0093	Coding
TC15002674.hg.1			-2.13	0.0818	NonCoding
TC06003724.hg.1			-2.13	0.0399	NonCoding
TC0X000987.hg.1	FLJ25917; LOC401585	uncharacterized LOC401585	-2.13	0.0379	Coding
TC15000671.hg.1	PML	promyelocytic leukemia	-2.13	0.0425	Coding
TC17002468.hg.1	TP53	tumor protein p53	-2.14	0.0043	NonCoding

TC01001985.hg.1	ZBTB18	zinc finger and BTB domain containing 18	-2.14	0.023	Coding
TC15002635.hg.1	PEAK1	pseudopodium-enriched atypical kinase 1	-2.14	0.0484	NonCoding
TC02004967.hg.1	APLF; PROKR1	aprataxin and PNKP like factor; prokineticin receptor 1	-2.14	0.0057	Coding
TC11000332.hg.1	CD44	CD44 molecule (Indian blood group)	-2.15	0.0128	Coding
TC02004505.hg.1			-2.15	0.0264	NonCoding
TC11000277.hg.1	FIBIN	fin bud initiation factor homolog (zebrafish)	-2.15	0.064	Coding
TC03001262.hg.1			-2.15	0.0231	Coding
TC08001973.hg.1	MSC-AS1	MSC antisense RNA 1	-2.16	0.058	NonCoding
TC20000334.hg.1	PKIG	protein kinase (cAMP-dependent, catalytic) inhibitor gamma	-2.16	0.009	Coding
TC20000814.hg.1			-2.16	0.0961	Coding
TC02000221.hg.1	RASGRP3	RAS guanyl releasing protein 3 (calcium and DAG-regulated)	-2.16	0.0562	Coding
TC17000571.hg.1	FZD2	frizzled class receptor 2	-2.16	0.0077	Coding
TC02001122.hg.1	GLS	glutaminase	-2.17	0.0046	Coding
TC0X000133.hg.1	IL1RAPL1	interleukin 1 receptor accessory protein-like 1	-2.17	0.0077	Coding
TC08002532.hg.1			-2.17	0.0242	NonCoding
TC02001030.hg.1	ITGA6	integrin alpha 6	-2.17	0.0288	Coding
TC22001425.hg.1	APOBEC3B	apolipoprotein B mRNA editing enzyme, catalytic polypeptide-like 3B	-2.17	0.0465	Coding
TC05002130.hg.1	ADAMTS2	ADAM metallopeptidase with thrombospondin type 1 motif 2	-2.17	0.0042	Coding
TC20001589.hg.1	JPH2	junctophilin 2	-2.18	0.0095	NonCoding
TC04001130.hg.1	UGDH	UDP-glucose 6-dehydrogenase	-2.18	0.0316	Coding
TC08000279.hg.1	ADGRA2	adhesion G protein-coupled receptor A2	-2.19	0.0401	Coding
TC21000156.hg.1			-2.19	0.0059	Coding
TC08002487.hg.1			-2.19	0.0971	NonCoding
TC12000955.hg.1	P2RX7	purinergic receptor P2X, ligand gated ion channel, 7	-2.2	0.045	Coding
TC02003729.hg.1	ITGA4	integrin alpha 4	-2.2	0.0132	NonCoding
TC12001811.hg.1	EEA1	early endosome antigen 1	-2.2	0.0722	Coding
TC16000700.hg.1	CPNE7	copine VII	-2.21	0.0657	Coding
TC13000771.hg.1	MIR4500HG	MIR4500 host gene	-2.21	0.0159	Coding
TC09000335.hg.1	ANXA1	annexin A1	-2.21	0.0016	Coding
TC02002207.hg.1	MIR4435-2HG	MIR4435-2 host gene	-2.21	0.0194	Coding
TC17001532.hg.1	PTRF	polymerase I and transcript release factor	-2.21	0.0052	Coding
TC06002181.hg.1	HIVEP2	human immunodeficiency virus type I enhancer binding protein 2	-2.21	0.0171	Coding
TC09000480.hg.1	HABP4	hyaluronan binding protein 4	-2.22	0.0184	Coding
TC03001608.hg.1	FILIP1L	filamin A interacting protein 1-like	-2.22	0.0072	Coding
TC05000601.hg.1	GRAMD3	GRAM domain containing 3	-2.22	0.046	Coding
TC19001588.hg.1	ETHE1	ethylmalonic encephalopathy 1	-2.22	0.0796	Coding
TC01001638.hg.1	LHX9	LIM homeobox 9	-2.22	0.0496	Coding
TC06000931.hg.1	DCBLD1	discoidin, CUB and LCCL domain containing 1	-2.22	0.0634	Coding
TC10000801.hg.1	DUSP5	dual specificity phosphatase 5	-2.23	0.0496	Coding
TC12000329.hg.1	ANO6	anoctamin 6	-2.23	0.0019	Coding
TC02004620.hg.1	ZEB2	zinc finger E-box binding homeobox 2	-2.23	0.0889	NonCoding
TC15002637.hg.1			-2.23	0.0446	NonCoding
TC12003093.hg.1	LINC01234	long intergenic non-protein coding RNA 1234	-2.24	0.0614	NonCoding
TC14001255.hg.1	ACTN1	actinin, alpha 1	-2.24	0.0095	Coding
TC01006424.hg.1	MIR181A1HG	MIR181A1 host gene	-2.24	0.0058	NonCoding
TC19002544.hg.1			-2.24	0.0254	NonCoding
TC19001173.hg.1	MIR199A1	microRNA 199a-1	-2.24	0.0891	Coding
TC02001034.hg.1	ZAK	sterile alpha motif and leucine zipper containing kinase AZK	-2.24	0.0043	Coding
TC12002330.hg.1			-2.25	0.0078	NonCoding
TC05000135.hg.1	PDZD2	PDZ domain containing 2	-2.25	0.0874	Coding
TC02001071.hg.1	OSBPL6;	oxysterol binding protein-like 6; microRNA 548n	-2.25	0.093	Coding

	MIR548N				
TC10002415.hg.1			-2.25	0.0582	NonCoding
TC19001618.hg.1	ERCC2	excision repair cross-complementation group 2	-2.25	0.0308	Coding
TC22000647.hg.1	LIF	leukemia inhibitory factor	-2.25	0.03	Coding
TC07002171.hg.1	HDAC9	histone deacetylase 9	-2.26	0.0188	NonCoding
TC09002386.hg.1	GLIS3	GLIS family zinc finger 3	-2.26	0.0232	NonCoding
TC01005079.hg.1			-2.26	0.0319	NonCoding
TC19002518.hg.1	ERCC2	excision repair cross-complementation group 2	-2.26	0.0409	NonCoding
TC14001423.hg.1	PTPN21	protein tyrosine phosphatase, non-receptor type 21	-2.26	0.0267	Coding
TC09000398.hg.1	DAPK1	death-associated protein kinase 1	-2.26	0.0957	Coding
TC02002007.hg.1	EVA1A	eva-1 homolog A (C. elegans)	-2.27	0.0019	Coding
TC13000901.hg.1	RASA3	RAS p21 protein activator 3	-2.27	0.0723	Coding
TC0X001978.hg.1	MID1	midline 1	-2.27	0.0556	NonCoding
TC02001752.hg.1			-2.27	0.0549	Coding
TC11000334.hg.1			-2.27	0.0285	Coding
TC0Y000310.hg.1			-2.28	0.0838	NonCoding
TC18000145.hg.1	GALNT1	polypeptide N-acetylgalactosaminyltransferase 1	-2.28	0.0758	Coding
TC16000129.hg.1	VASN	vasorin	-2.28	0.0319	Coding
TC07002433.hg.1			-2.28	0.0032	NonCoding
TC01005462.hg.1			-2.29	0.0873	NonCoding
TC04002693.hg.1	PDE5A	phosphodiesterase 5A, cGMP-specific	-2.29	0.0101	NonCoding
TC20000985.hg.1	APCDD1L	adenomatosis polyposis coli down-regulated 1-like	-2.3	0.0307	Coding
TC09000634.hg.1	NEK6	NIMA-related kinase 6	-2.3	0.0253	Coding
TC05000184.hg.1	PTGER4	prostaglandin E receptor 4 (subtype EP4)	-2.3	0.0116	Coding
TC03003206.hg.1	TNIK	TRAF2 and NCK interacting kinase	-2.3	0.0057	NonCoding
TC19000765.hg.1	CLEC11A	C-type lectin domain family 11, member A	-2.3	0.0036	Coding
TC14002059.hg.1	ACTN1	actinin, alpha 1	-2.3	0.0074	NonCoding
TC13000825.hg.1	DOCK9	dedicator of cytokinesis 9	-2.31	0.0061	Coding
TC16000879.hg.1	CPPED1	calcineurin-like phosphoesterase domain containing 1	-2.31	0.0544	Coding
TC12000749.hg.1	NEDD1	neural precursor cell expressed, developmentally down-regulated 1	-2.31	0.0093	Coding
TC07002602.hg.1			-2.31	0.0563	NonCoding
TC15001922.hg.1	NR2F2-AS1	NR2F2 antisense RNA 1	-2.31	0.0125	Coding
TC02004623.hg.1	ZEB2	zinc finger E-box binding homeobox 2	-2.31	0.048	NonCoding
TC03000375.hg.1	FLNB	filamin B, beta	-2.32	0.0111	Coding
TC08001180.hg.1			-2.32	0.0463	Coding
TC07003166.hg.1			-2.32	0.048	NonCoding
TC04002929.hg.1	BST1	bone marrow stromal cell antigen 1	-2.32	0.0171	Coding
TC01002663.hg.1			-2.32	0.0111	Coding
TC03002599.hg.1			-2.32	0.0471	NonCoding
TC07000798.hg.1	STRIP2	striatin interacting protein 2	-2.32	0.0033	Coding
TC01002829.hg.1	DDAH1	dimethylarginine dimethylaminohydrolase 1	-2.33	0.0022	Coding
TC05002401.hg.1			-2.33	0.0066	NonCoding
TC01000493.hg.1	MACF1; KIAA0754	microtubule-actin crosslinking factor 1; KIAA0754	-2.33	0.0251	Coding
TC05002605.hg.1			-2.33	0.0428	NonCoding
TC08000571.hg.1	PDP1	pyruvate dehyrogenase phosphatase catalytic subunit 1	-2.34	0.0457	Coding
TC19001721.hg.1	RRAS	related RAS viral (r-ras) oncogene homolog	-2.34	0.0386	Coding
TC06003141.hg.1	TIAM2	T-cell lymphoma invasion and metastasis 2	-2.35	0.0034	NonCoding
TC09000965.hg.1	CDKN2B	cyclin-dependent kinase inhibitor 2B (p15, inhibits CDK4)	-2.36	0.0319	Coding
TC11000342.hg.1	LDLRAD3	low density lipoprotein receptor class A domain containing 3	-2.37	0.0088	Coding
TC12001901.hg.1	NT5DC3	5-nucleotidase domain containing 3	-2.37	0.0029	Coding
TC05000336.hg.1	MAP1B	microtubule associated protein 1B	-2.37	0.0926	Coding
TC01001539.hg.1	RASAL2	RAS protein activator like 2	-2.38	0.0237	Coding

TC09002707.hg.1	TMEM246	transmembrane protein 246	-2.38	0.039	NonCoding
TC12001992.hg.1	LINC01234	long intergenic non-protein coding RNA 1234	-2.39	0.055	Coding
TC17000111.hg.1			-2.39	0.0157	Coding
TC08000501.hg.1	ZFHX4	zinc finger homeobox 4	-2.39	0.0053	Coding
TC01002530.hg.1	FHL3	four and a half LIM domains 3	-2.4	0.0431	Coding
TC02001980.hg.1			-2.4	0.0308	Coding
TC15002273.hg.1			-2.4	0.0111	NonCoding
TC02000535.hg.1	LINC00152; MIR4435-2HG	long intergenic non-protein coding RNA 152; MIR4435-2 host gene	-2.4	0.0173	Coding
TC05000078.hg.1			-2.4	0.0564	Coding
TC11003441.hg.1	TRIM6	tripartite motif containing 6	-2.41	0.0985	Coding
TC16000154.hg.1	ATF7IP2	activating transcription factor 7 interacting protein 2	-2.41	0.0157	Coding
TC10002023.hg.1			-2.41	0.0061	NonCoding
TC07001127.hg.1	CYTH3	cytohesin 3	-2.41	0.0022	Coding
TC15001217.hg.1	RASGRP1	RAS guanyl releasing protein 1 (calcium and DAG-regulated)	-2.42	0.094	Coding
TC03001867.hg.1	PLSCR4	phospholipid scramblase 4	-2.42	0.0773	Coding
TC15002231.hg.1	TLN2	talin 2	-2.42	0.0616	NonCoding
TC02003382.hg.1	MIR4435-2HG; LINC00152	MIR4435-2 host gene; long intergenic non-protein coding RNA 152	-2.43	0.0141	NonCoding
TC12000407.hg.1	SCN8A	sodium channel, voltage gated, type VIII alpha subunit	-2.43	0.0575	Coding
TC05000497.hg.1	PAM	peptidylglycine alpha-amidating monooxygenase	-2.44	0.004	Coding
TC11002136.hg.1	GAB2	GRB2-associated binding protein 2	-2.44	0.0232	Coding
TC11002610.hg.1			-2.44	0.0602	NonCoding
TC05002110.hg.1	PDLIM7	PDZ and LIM domain 7 (enigma)	-2.44	0.0363	Coding
TC15002621.hg.1	LOXL1-AS1	LOXL1 antisense RNA 1	-2.45	0.0125	NonCoding
TC13001613.hg.1			-2.45	0.0208	NonCoding
TC18000033.hg.1	ARHGAP28	Rho GTPase activating protein 28	-2.47	0.0985	Coding
TC06001624.hg.1			-2.47	0.0634	Coding
TC01005639.hg.1			-2.47	0.0384	NonCoding
TC20001244.hg.1	SLC2A10	solute carrier family 2 (facilitated glucose transporter), member 10	-2.49	0.018	NonCoding
TC07000645.hg.1	MIR4653	microRNA 4653	-2.49	0.0832	Coding
TC01003624.hg.1	FAM129A	family with sequence similarity 129, member A	-2.49	0.0971	Coding
TC11001867.hg.1	AHNAK	AHNAK nucleoprotein	-2.5	0.0804	Coding
TC04001650.hg.1	TMEM154	transmembrane protein 154	-2.5	0.0307	Coding
TC19001930.hg.1	STK11	serine/threonine kinase 11	-2.5	0.0027	NonCoding
TC02002579.hg.1	ZNF385B	zinc finger protein 385B	-2.51	0.0029	Coding
TC07002955.hg.1			-2.51	0.0101	NonCoding
TC12000182.hg.1	GPRC5A; MIR614	G protein-coupled receptor, class C, group 5, member A; microRNA 614	-2.51	0.0609	Coding
TC13001345.hg.1			-2.51	0.03	NonCoding
TC07000125.hg.1	ITGB8	integrin beta 8	-2.52	0.0233	Coding
TC06002260.hg.1	SERAC1	serine active site containing 1	-2.53	0.0082	Coding
TC22000199.hg.1	NF2	neurofibromin 2 (merlin)	-2.53	0.0095	Coding
TC20000248.hg.1	PROCR	protein C receptor, endothelial	-2.53	0.096	Coding
TC12000868.hg.1	SH2B3	SH2B adaptor protein 3	-2.54	0.0365	Coding
TC07000935.hg.1	ZYX	zyxin	-2.54	0.0107	Coding
TC08001641.hg.1	ASAP1	ArfGAP with SH3 domain, ankyrin repeat and PH domain 1	-2.55	0.0123	Coding
TC05002980.hg.1			-2.55	0.0676	NonCoding
TC10001955.hg.1			-2.55	0.0565	NonCoding
TC10001324.hg.1	RTKN2	rhotekin 2	-2.55	0.0446	Coding
TC09000202.hg.1	GLIPR2	GLI pathogenesis-related 2	-2.55	0.0072	Coding
TC12002256.hg.1			-2.56	0.054	NonCoding
TC03001998.hg.1	TNIK	TRAF2 and NCK interacting kinase	-2.56	0.0042	Coding
TC16000921.hg.1	GPRC5B	G protein-coupled receptor, class C, group 5,	-2.56	0.0047	Coding

		member B			
TC08002307.hg.1			-2.56	0.0174	NonCoding
TC02000861.hg.1	LOC100507460	uncharacterized LOC100507460	-2.57	0.0307	Coding
TC0X002048.hg.1			-2.57	0.0069	NonCoding
TC05001265.hg.1	CAPSL	calcyphosine-like	-2.59	0.0069	Coding
TC10000476.hg.1	VCL	vinculin	-2.59	0.0108	Coding
TC14001432.hg.1	TTC7B	tetratricopeptide repeat domain 7B	-2.59	0.0386	Coding
TC05001311.hg.1	FLJ32255	uncharacterized LOC643977	-2.59	0.0889	Coding
TC16000274.hg.1			-2.59	0.0634	Coding
TC05002340.hg.1			-2.6	0.0395	NonCoding
TC16001314.hg.1	COTL1	coactosin-like F-actin binding protein 1	-2.6	0.0403	Coding
TC10001549.hg.1	PDLIM1	PDZ and LIM domain 1	-2.6	0.0096	Coding
TC15002275.hg.1	PML	promyelocytic leukemia	-2.6	0.0715	NonCoding
TC04002517.hg.1	UGDH	UDP-glucose 6-dehydrogenase	-2.6	0.0283	NonCoding
TC19002519.hg.1	ERCC2	excision repair cross-complementation group 2	-2.6	0.0307	NonCoding
TC12002617.hg.1	P2RX7	purinergic receptor P2X, ligand gated ion channel, 7	-2.61	0.0321	NonCoding
TC11002211.hg.1	MAML2	mastermind-like transcriptional coactivator 2	-2.61	0.0889	Coding
TC14001000.hg.1	PRKD1	protein kinase D1	-2.61	0.0158	Coding
TC16000095.hg.1	TNFRSF12A	tumor necrosis factor receptor superfamily, member 12A	-2.63	0.0016	Coding
TC10000347.hg.1	PRKG1	protein kinase, cGMP-dependent, type I	-2.64	0.0251	Coding
TC06001893.hg.1			-2.64	0.0264	Coding
TC12000818.hg.1	C12orf75	chromosome 12 open reading frame 75	-2.65	0.0615	Coding
TC12002037.hg.1	PXN	paxillin	-2.65	0.0259	Coding
TC10001334.hg.1			-2.65	0.0782	Coding
TC01003346.hg.1			-2.65	0.0294	Coding
TC13001666.hg.1			-2.66	0.0552	NonCoding
TC19000027.hg.1	CNN2	calponin 2	-2.66	0.0075	Coding
TC12000521.hg.1	LRP1	LDL receptor related protein 1	-2.67	0.0146	Coding
TC21000185.hg.1	BACE2	beta-site APP-cleaving enzyme 2	-2.67	0.0054	Coding
TC12000408.hg.1			-2.67	0.0576	Coding
TC08001075.hg.1	PNMA2	paraneoplastic Ma antigen 2	-2.68	0.0069	Coding
TC17002659.hg.1			-2.68	0.0013	NonCoding
TC12002392.hg.1			-2.68	0.0188	NonCoding
TC01001364.hg.1	PEA15	phosphoprotein enriched in astrocytes 15	-2.68	0.0094	Coding
TC02003588.hg.1			-2.7	0.0283	NonCoding
TC04000434.hg.1	FRAS1	Fraser extracellular matrix complex subunit 1	-2.7	0.0178	Coding
TC11001812.hg.1	LPXN	leupaxin	-2.71	0.006	Coding
TC07000328.hg.1	EGFR	epidermal growth factor receptor	-2.71	0.008	Coding
TC12000564.hg.1	SRGAP1	SLIT-ROBO Rho GTPase activating protein 1	-2.72	0.0182	Coding
TC12000558.hg.1	MIRLET7I	microRNA let-7i	-2.72	0.0092	Coding
TC06004140.hg.1	CNKSR3	CNKSR family member 3	-2.73	0.0022	Coding
TC0X000985.hg.1	MIR221	microRNA 221	-2.74	0.0564	Coding
TC08001286.hg.1	MYBL1	v-myb avian myeloblastosis viral oncogene homolog-like 1	-2.74	0.0776	Coding
TC15001225.hg.1	GPR176	G protein-coupled receptor 176	-2.74	0.0054	Coding
TC06001232.hg.1	PXDC1	PX domain containing 1	-2.74	0.0116	Coding
TC04001600.hg.1	INPP4B	inositol polyphosphate-4-phosphatase type II B	-2.74	0.0031	Coding
TC11003090.hg.1	BDNF	brain-derived neurotrophic factor	-2.75	0.0348	NonCoding
TC05000304.hg.1	OCLN	occludin	-2.75	0.0198	Coding
TC03003130.hg.1			-2.75	0.0443	NonCoding
TC08001823.hg.1			-2.77	0.0667	NonCoding
TC06000681.hg.1	BEND6	BEN domain containing 6	-2.78	0.0097	Coding
TC15001110.hg.1	TJP1	tight junction protein 1	-2.79	0.0111	Coding
TC01000745.hg.1	GADD45A	growth arrest and DNA-damage-inducible, alpha	-2.79	0.0556	Coding
TC07000955.hg.1	OR2A9P; OR2A20P	olfactory receptor, family 2, subfamily A, member 9 pseudogene; olfactory receptor, family 2, subfamily	-2.8	0.0378	Coding

		A, member 20 pseudogene			
TC04001947.hg.1			-2.8	0.0082	NonCoding
TC11000333.hg.1	CD44	CD44 molecule (Indian blood group)	-2.8	0.0316	Coding
TC04001487.hg.1	ARSJ	arylsulfatase family, member J	-2.81	0.0075	Coding
TC12002396.hg.1	LRP1	LDL receptor related protein 1	-2.81	0.0206	NonCoding
TC16001671.hg.1			-2.81	0.0205	NonCoding
TC06003411.hg.1	HLA-DQB1	major histocompatibility complex, class II, DQ beta 1	-2.82	0.084	NonCoding
TC15000622.hg.1	SMAD3	SMAD family member 3	-2.82	0.01	Coding
TC06000836.hg.1	GRIK2	glutamate receptor, ionotropic, kainate 2	-2.83	0.0553	Coding
TC05002544.hg.1	PAM	peptidylglycine alpha-amidating monooxygenase	-2.83	0.0043	NonCoding
TC01000783.hg.1	ST6GALNAC5	ST6 (alpha-N-acetyl-neuraminyl-2,3-beta-galactosyl-1,3)-N-acetylgalactosaminide alpha-2,6-sialyltransferase 5	-2.83	0.0116	Coding
TC18000202.hg.1	NEDD4L	neural precursor cell expressed, developmentally down-regulated 4-like, E3 ubiquitin protein ligase	-2.83	0.0255	Coding
TC09001276.hg.1	RASEF	RAS and EF-hand domain containing	-2.83	0.0129	Coding
TC10000565.hg.1	ZMIZ1	zinc finger, MIZ-type containing 1	-2.85	0.0056	Coding
TC20001292.hg.1			-2.85	0.0692	NonCoding
TC02002612.hg.1	COL5A2	collagen, type V, alpha 2	-2.86	0.0371	Coding
TC05001363.hg.1	PLPP1	phospholipid phosphatase 1	-2.87	0.0389	Coding
TC0X001438.hg.1	LDOC1	leucine zipper, down-regulated in cancer 1	-2.87	0.0744	Coding
TC14000947.hg.1	CDH24	cadherin 24, type 2	-2.87	0.0009	Coding
TC02003777.hg.1			-2.88	0.0497	NonCoding
TC17001803.hg.1	SMURF2	SMAD specific E3 ubiquitin protein ligase 2	-2.88	0.0093	Coding
TC07000735.hg.1	CPED1	cadherin-like and PC-esterase domain containing 1	-2.89	0.0873	Coding
TC03001905.hg.1	GPR87	G protein-coupled receptor 87	-2.9	0.0356	Coding
TC12002424.hg.1	HMGA2	high mobility group AT-hook 2	-2.9	0.0356	NonCoding
TC06001065.hg.1	RAB32	RAB32, member RAS oncogene family	-2.9	0.045	Coding
TC17000654.hg.1	ITGA3	integrin alpha 3	-2.9	0.0921	Coding
TC12002414.hg.1	SRGAP1	SLIT-ROBO Rho GTPase activating protein 1	-2.91	0.0432	NonCoding
TC0X001997.hg.1			-2.91	0.0149	NonCoding
TC01004933.hg.1	LHX9	LIM homeobox 9	-2.93	0.0442	NonCoding
TC04001595.hg.1	RNF150	ring finger protein 150	-2.93	0.0958	Coding
TC03001525.hg.1	PRICKLE2	prickle homolog 2	-2.93	0.0865	Coding
TC12002303.hg.1	LINC00941	long intergenic non-protein coding RNA 941	-2.96	0.0116	NonCoding
TC14000319.hg.1	SAMD4A	sterile alpha motif domain containing 4A	-2.96	0.0108	Coding
TC0Y000352.hg.1	XGY2; SRY	Xg pseudogene, Y-linked 2; sex determining region Y	-2.97	0.0189	Coding
TC22000703.hg.1	MYH9	myosin, heavy chain 9, non-muscle	-2.98	0.0147	Coding
TC03001750.hg.1	MGLL	monoglyceride lipase	-2.98	0.0025	Coding
TC01001753.hg.1	SYT14	synaptotagmin XIV	-2.98	0.0025	Coding
TC15001539.hg.1			-2.99	0.0734	Coding
TC06000737.hg.1	CD109	CD109 molecule	-2.99	0.0724	Coding
TC08002364.hg.1	MYBL1	v-myb avian myeloblastosis viral oncogene homolog-like 1	-3.01	0.0816	NonCoding
TC05000814.hg.1	ADRB2	adrenoceptor beta 2, surface	-3.03	0.0016	Coding
TC19001030.hg.1	LMNB2	lamin B2	-3.04	0.0037	Coding
TC02001746.hg.1	CDC42EP3	CDC42 effector protein (Rho GTPase binding) 3	-3.05	0.0018	Coding
TC06000979.hg.1	TMEM200A	transmembrane protein 200A	-3.05	0.0061	Coding
TC01005864.hg.1			-3.05	0.0033	NonCoding
TC02000230.hg.1	CRIM1	cysteine rich transmembrane BMP regulator 1 (chordin-like)	-3.05	0.0431	Coding
TC14001424.hg.1	EML5	echinoderm microtubule associated protein like 5	-3.06	0.018	Coding
TC15002008.hg.1	PCSK6	proprotein convertase subtilisin/kexin type 6	-3.06	0.0019	Coding
TC07001637.hg.1	TMEM130	transmembrane protein 130	-3.06	0.0188	Coding
TC03003028.hg.1			-3.07	0.0764	NonCoding
TC06001800.hg.1	TRAM2	translocation associated membrane protein 2	-3.08	0.0146	Coding

TC03000173.hg.1	STAC	SH3 and cysteine rich domain	-3.08	0.0028	Coding
TC01001587.hg.1	RGL1	ral guanine nucleotide dissociation stimulator-like 1	-3.09	0.0309	Coding
TC12002360.hg.1	SCN8A	sodium channel, voltage gated, type VIII alpha subunit	-3.09	0.0695	NonCoding
TC04001948.hg.1			-3.1	0.0173	NonCoding
TC11002381.hg.1			-3.11	0.061	Coding
TC19002289.hg.1			-3.12	0.0019	NonCoding
TC03000814.hg.1	TSC22D2	TSC22 domain family, member 2	-3.13	0.0145	Coding
TC15000578.hg.1	TPM1	tropomyosin 1 (alpha)	-3.13	0.038	Coding
TC06002498.hg.1			-3.13	0.042	NonCoding
TC02003538.hg.1	GLI2	GLI family zinc finger 2	-3.14	0.0463	NonCoding
TC02003315.hg.1	ADD2	adducin 2 (beta)	-3.15	0.0124	NonCoding
TC05003057.hg.1	LOC647859	occludin pseudogene	-3.15	0.0104	NonCoding
TC12000283.hg.1	LINC00941	long intergenic non-protein coding RNA 941	-3.16	0.018	Coding
TC08002613.hg.1	LOXL2	lysyl oxidase-like 2	-3.16	0.0145	Coding
TC04001504.hg.1	PDE5A	phosphodiesterase 5A, cGMP-specific	-3.18	0.0117	Coding
TC21000736.hg.1	BACE2	beta-site APP-cleaving enzyme 2	-3.18	0.0155	NonCoding
TC22000615.hg.1			-3.18	0.0519	Coding
TC06003697.hg.1			-3.18	0.016	NonCoding
TC0X002162.hg.1	TMSB15A	thymosin beta 15a	-3.19	0.0758	NonCoding
TC05000083.hg.1	TRIO	trio Rho guanine nucleotide exchange factor	-3.19	0.0009	Coding
TC08002306.hg.1	PLAT	plasminogen activator, tissue	-3.2	0.0075	NonCoding
TC21000113.hg.1	HUNK	hormonally up-regulated Neu-associated kinase	-3.21	0.0307	Coding
TC03001604.hg.1	DCBLD2	discoidin, CUB and LCCL domain containing 2	-3.22	0.0365	Coding
TC05000521.hg.1	CAMK4	calcium/calmodulin-dependent protein kinase IV	-3.24	0.0242	Coding
TC11003389.hg.1			-3.25	0.0559	NonCoding
TC10001134.hg.1	ARMC4	armadillo repeat containing 4	-3.25	0.0349	Coding
TC04001139.hg.1	APBB2	amyloid beta (A4) precursor protein-binding, family B, member 2	-3.26	0.0397	Coding
TC10000199.hg.1	BAMBI	BMP and activin membrane-bound inhibitor	-3.27	0.0832	Coding
TC07000178.hg.1	CREB5	cAMP responsive element binding protein 5	-3.28	0.006	Coding
TC02002808.hg.1	EPHA4	EPH receptor A4	-3.28	0.0259	Coding
TC0X000884.hg.1			-3.28	0.0031	Coding
TC17000965.hg.1	FAM101B	family with sequence similarity 101, member B	-3.28	0.0668	Coding
TC10001439.hg.1	KCNMA1	potassium channel, calcium activated large conductance subfamily M alpha, member 1	-3.3	0.0017	Coding
TC20000019.hg.1	SIRPA	signal-regulatory protein alpha	-3.33	0.042	Coding
TC03003002.hg.1	DCBLD2	discoidin, CUB and LCCL domain containing 2	-3.34	0.0308	NonCoding
TC01001639.hg.1	NEK7	NIMA-related kinase 7	-3.34	0.0095	Coding
TC15000936.hg.1	NR2F2; MIR1469	nuclear receptor subfamily 2, group F, member 2; microRNA 1469	-3.37	0.0119	Coding
TC07000785.hg.1	FLNC	filamin C, gamma	-3.37	0.0018	Coding
TC06003802.hg.1			-3.39	0.0463	NonCoding
TC04001328.hg.1	ANTXR2	anthrax toxin receptor 2	-3.43	0.0056	Coding
TC07003105.hg.1	CCDC71L	coiled-coil domain containing 71-like	-3.43	0.0538	NonCoding
TC05000372.hg.1	F2RL1	coagulation factor II (thrombin) receptor-like 1	-3.43	0.0189	Coding
TC11002439.hg.1	ETS1	v-ets avian erythroblastosis virus E26 oncogene homolog 1	-3.47	0.0094	Coding
TC02001106.hg.1	MIR1245A; MIR1245B	microRNA 1245a; microRNA 1245b	-3.49	0.0139	Coding
TC04000182.hg.1	TBC1D19	TBC1 domain family, member 19	-3.51	0.0017	Coding
TC01001053.hg.1	EMBP1	embigin pseudogene 1	-3.51	0.013	Coding
TC0X000807.hg.1	MXRA5	matrix-remodelling associated 5	-3.53	0.0723	Coding
TC08000140.hg.1			-3.55	0.0625	Coding
TC09000109.hg.1	DMRTA1	DMRT-like family A1	-3.56	0.0111	Coding
TC02002705.hg.1	KLF7	Kruppel-like factor 7 (ubiquitous)	-3.56	0.0707	Coding
TC08001551.hg.1	SAMD12	sterile alpha motif domain containing 12	-3.56	0.0351	Coding
TC15001257.hg.1	EHD4	EH domain containing 4	-3.58	0.0085	Coding

TC16000279.hg.1			-3.59	0.094	Coding
TC11000177.hg.1	SBF2-AS1	SBF2 antisense RNA 1	-3.59	0.0727	Coding
TC14001443.hg.1	FBLN5	fibulin 5	-3.59	0.077	Coding
TC15002503.hg.1	EHD4	EH domain containing 4	-3.59	0.0184	NonCoding
TC10001133.hg.1	MKX	mohawk homeobox	-3.6	0.0307	Coding
TC0X001393.hg.1	MIR503	microRNA 503	-3.61	0.0002	Coding
TC11001115.hg.1	UBASH3B	ubiquitin associated and SH3 domain containing B	-3.61	0.0274	Coding
TC10000190.hg.1			-3.61	0.0371	Coding
TC14001714.hg.1	DAAM1	dishevelled associated activator of morphogenesis 1	-3.62	0.0126	NonCoding
TC10002160.hg.1	ZMIZ1	zinc finger, MIZ-type containing 1	-3.66	0.0019	NonCoding
TC05000569.hg.1	PRR16	proline rich 16	-3.67	0.0321	Coding
TC05001458.hg.1	OCLN	occludin	-3.67	0.0126	Coding
TC06003696.hg.1			-3.67	0.001	NonCoding
TC05001986.hg.1	ADAM19	ADAM metallopeptidase domain 19	-3.68	0.0017	Coding
TC01001348.hg.1	IFI16	interferon, gamma-inducible protein 16	-3.68	0.06	Coding
TC05002283.hg.1	TRIO	trio Rho guanine nucleotide exchange factor	-3.69	0.0011	NonCoding
TC10001744.hg.1	ADAM12	ADAM metallopeptidase domain 12	-3.69	0.0422	Coding
TC09000637.hg.1	LOC100129034	uncharacterized LOC100129034	-3.7	0.044	Coding
TC14000356.hg.1	DAAM1	dishevelled associated activator of morphogenesis 1	-3.72	0.0184	Coding
TC07002321.hg.1	EGFR	epidermal growth factor receptor	-3.72	0.0069	NonCoding
TC01003959.hg.1	C1orf198	chromosome 1 open reading frame 198	-3.74	0.0181	Coding
TC12000747.hg.1	ELK3	ELK3, ETS-domain protein (SRF accessory protein 2)	-3.74	0.0061	Coding
TC06001969.hg.1	SIM1	single-minded family bHLH transcription factor 1	-3.75	0.006	Coding
TC10002885.hg.1			-3.79	0.0558	NonCoding
TC06003777.hg.1			-3.8	0.0093	NonCoding
TC08001985.hg.1	LINC01109	long intergenic non-protein coding RNA 1109	-3.81	0.0526	NonCoding
TC01004781.hg.1	IFI16	interferon, gamma-inducible protein 16	-3.83	0.0393	NonCoding
TC07000159.hg.1	NFE2L3	nuclear factor, erythroid 2-like 3	-3.83	0.0782	Coding
TC10000621.hg.1	PAPSS2	3-phosphoadenosine 5-phosphosulfate synthase 2	-3.84	0.0242	Coding
TC01001213.hg.1	MIR554	microRNA 554	-3.84	0.0101	Coding
TC15001837.hg.1	ANPEP	alanyl (membrane) aminopeptidase	-3.85	0.0737	Coding
TC14002015.hg.1			-3.86	0.0839	NonCoding
TC15000224.hg.1	SCG5	secretogranin V	-3.87	0.0078	Coding
TC01000789.hg.1	NEXN	nexilin (F actin binding protein)	-3.88	0.0107	Coding
TC11000337.hg.1	FJX1	four jointed box 1	-3.88	0.0263	Coding
TC09002248.hg.1	LOC100129034	uncharacterized LOC100129034	-3.89	0.0321	NonCoding
TC15001223.hg.1			-3.92	0.0871	Coding
TC09002563.hg.1			-3.95	0.0485	NonCoding
TC15002592.hg.1	ITGA11	integrin alpha 11	-3.96	0.0836	NonCoding
TC14000130.hg.1	ABHD4	abhydrolase domain containing 4	-3.99	0.0056	Coding
TC01006315.hg.1	SEPN1	selenoprotein N, 1	-4.01	0.0018	Coding
TC07002185.hg.1	ITGB8	integrin beta 8	-4.02	0.0307	NonCoding
TC18000433.hg.1	CDH2	cadherin 2, type 1, N-cadherin (neuronal)	-4.03	0.0353	Coding
TC22001282.hg.1			-4.05	0.0396	NonCoding
TC02001095.hg.1	ZNF804A	zinc finger protein 804A	-4.07	0.0016	Coding
TC03000732.hg.1	PPP2R3A	protein phosphatase 2, regulatory subunit B, alpha	-4.07	0.007	Coding
TC14000943.hg.1	AJUBA	ajuba LIM protein	-4.09	0.058	Coding
TC15001289.hg.1	FRMD5	FERM domain containing 5	-4.09	0.0138	Coding
TC21000737.hg.1	BACE2	beta-site APP-cleaving enzyme 2	-4.09	0.011	NonCoding
TC04000158.hg.1	SLIT2	slit guidance ligand 2	-4.1	0.0171	Coding
TC01001559.hg.1	QSOX1	quiescin Q6 sulfhydryl oxidase 1	-4.1	0.0019	Coding
TC02002210.hg.1			-4.1	0.0104	Coding
TC06000909.hg.1	MARCKS	myristoylated alanine-rich protein kinase C substrate	-4.13	0.0165	Coding
TC12001405.hg.1	PRICKLE1	prickle homolog 1	-4.13	0.0255	Coding
TC15002251.hg.1	SMAD3	SMAD family member 3	-4.14	0.0143	NonCoding

TC09000560.hg.1	UGCG	UDP-glucose ceramide glucosyltransferase	-4.17	0.0171	Coding
TC07001363.hg.1	TNS3	tensin 3	-4.17	0.0213	Coding
TC09000912.hg.1			-4.17	0.06	Coding
TC18000094.hg.1	GATA6	GATA binding protein 6	-4.18	0.0107	Coding
TC01001544.hg.1	RALGPS2	Ral GEF with PH domain and SH3 binding motif 2	-4.18	0.0321	Coding
TC03002281.hg.1	STAC	SH3 and cysteine rich domain	-4.18	0.0019	NonCoding
TC16000378.hg.1	TGFB1I1	transforming growth factor beta 1 induced transcript 1	-4.2	0.0446	Coding
TC19000235.hg.1	NFIX	nuclear factor I/X (CCAAT-binding transcription factor)	-4.21	9.56E-05	Coding
TC11002894.hg.1	TAGLN	transgelin	-4.26	0.0148	NonCoding
TC06000120.hg.1	RNF144B	ring finger protein 144B	-4.28	0.018	Coding
TC17001590.hg.1	C1QL1	complement component 1, q subcomponent-like 1	-4.28	0.0162	Coding
TC14001253.hg.1	ZFP36L1	ZFP36 ring finger protein-like 1	-4.31	0.0056	Coding
TC11001946.hg.1	EFEMP2	EGF containing fibulin-like extracellular matrix protein 2	-4.31	0.0463	Coding
TC10001136.hg.1	MPP7	membrane protein, palmitoylated 7	-4.33	0.0804	Coding
TC22001326.hg.1	MYH9	myosin, heavy chain 9, non-muscle	-4.34	0.0129	NonCoding
TC19000738.hg.1	RCN3	reticulocalbin 3, EF-hand calcium binding domain	-4.34	0.075	Coding
TC06003006.hg.1	MARCKS	myristoylated alanine-rich protein kinase C substrate	-4.34	0.015	NonCoding
TC09002564.hg.1			-4.35	0.0132	NonCoding
TC13000577.hg.1	TRPC4	transient receptor potential cation channel, subfamily C, member 4	-4.36	0.0403	Coding
TC11000394.hg.1	CREB3L1	cAMP responsive element binding protein 3-like 1	-4.37	0.0069	Coding
TC19000055.hg.1	GADD45B	growth arrest and DNA-damage-inducible, beta	-4.4	0.0227	Coding
TC03001489.hg.1	IL17RD	interleukin 17 receptor D	-4.41	0.0555	Coding
TC09000561.hg.1	MIR4668	microRNA 4668	-4.41	0.0333	Coding
TC0Y000140.hg.1	RBMY1A3P	RNA binding motif protein, Y-linked, family 1, member A3 pseudogene	-4.42	0.0949	Coding
TC08000500.hg.1	LINC01111	long intergenic non-protein coding RNA 1111	-4.43	0.0386	Coding
TC08001413.hg.1	RUNX1T1	runt-related transcription factor 1; translocated to, 1 (cyclin D-related)	-4.43	0.0272	Coding
TC13000899.hg.1	GAS6	growth arrest-specific 6	-4.43	0.0327	Coding
TC07003336.hg.1	CDK14	cyclin-dependent kinase 14	-4.45	0.0309	Coding
TC01003671.hg.1	MIR181B1	microRNA 181b-1	-4.49	0.012	Coding
TC04001402.hg.1	TSPAN5	tetraspanin 5	-4.52	0.0019	Coding
TC02002627.hg.1	SDPR	serum deprivation response	-4.53	0.0556	Coding
TC05000929.hg.1	DOCK2	dedicator of cytokinesis 2	-4.54	0.0018	Coding
TC01002708.hg.1	JUN	jun proto-oncogene	-4.6	0.0047	Coding
TC01002166.hg.1	ERRFI1	ERBB receptor feedback inhibitor 1	-4.6	0.0384	Coding
TC01003519.hg.1	MIR199A2; MIR214; DNM3OS	microRNA 199a-2; microRNA 214; DNM3 opposite strand/antisense RNA	-4.61	0.0689	Coding
TC21000738.hg.1	BACE2	beta-site APP-cleaving enzyme 2	-4.61	0.0319	NonCoding
TC05000355.hg.1	ARHGEF28	Rho guanine nucleotide exchange factor 28	-4.62	0.0059	Coding
TC13000585.hg.1	LHFP	lipoma HMGIC fusion partner	-4.62	0.0937	Coding
TC07001559.hg.1	SEMA3C	sema domain, immunoglobulin domain (Ig), short basic domain, secreted, (semaphorin) 3C	-4.66	0.0192	Coding
TC09001164.hg.1	PGM5P2	phosphoglucomutase 5 pseudogene 2	-4.71	0.0028	Coding
TC09000066.hg.1	LURAP1L	leucine rich adaptor protein 1-like	-4.76	0.0373	Coding
TC08000250.hg.1	NRG1	neuregulin 1	-4.8	0.0156	Coding
TC12001837.hg.1	NTN4	netrin 4	-4.84	0.0704	Coding
TC01001966.hg.1	FMN2	formin 2	-4.86	0.0129	Coding
TC03000837.hg.1	RAP2B	RAP2B, member of RAS oncogene family	-4.87	0.0016	Coding
TC13000772.hg.1	MIR4500	microRNA 4500	-4.87	0.0066	Coding
TC03002079.hg.1	IGF2BP2	insulin-like growth factor 2 mRNA binding protein 2	-4.88	0.0018	Coding
TC02004506.hg.1			-4.89	0.0105	NonCoding
TC09002562.hg.1			-4.94	0.0052	NonCoding
TC01005772.hg.1	LOC653513	phosphodiesterase 4D interacting protein-like	-4.95	0.0519	NonCoding

TC12000656.hg.1	NAV3	neuron navigator 3	-4.98	0.0052	Coding
TC01005002.hg.1	SYT14	synaptotagmin XIV	-4.98	0.0033	NonCoding
TC05001909.hg.1	DPYSL3	dihydropyrimidinase-like 3	-5.01	0.0395	Coding
TC11002293.hg.1	IL18	interleukin 18	-5.04	0.0588	Coding
TC0X000574.hg.1	DOCK11	dedicator of cytokinesis 11	-5.07	0.0425	Coding
TC11001948.hg.1	FOSL1	FOS-like antigen 1	-5.11	0.0023	Coding
TC07000811.hg.1			-5.11	0.0348	Coding
TC09001167.hg.1	PGM5P2	phosphoglucomutase 5 pseudogene 2	-5.13	0.009	Coding
TC01005935.hg.1	DNM3OS	DNM3 opposite strand/antisense RNA	-5.15	0.0768	NonCoding
TC01004676.hg.1	EMBP1	embigin pseudogene 1	-5.15	0.006	NonCoding
TC02001965.hg.1	ADD2	adducin 2 (beta)	-5.24	0.0082	Coding
TC19001938.hg.1	GADD45B	growth arrest and DNA-damage-inducible, beta	-5.26	0.0164	NonCoding
TC04000437.hg.1	ANXA3	annexin A3	-5.28	0.061	Coding
TC11000182.hg.1	ADM	adrenomedullin	-5.3	0.0055	Coding
TC05002857.hg.1	SEMA5A	sema domain, seven thrombospondin repeats (type 1 and type 1-like), transmembrane domain (TM) and short cytoplasmic domain, (semaphorin) 5A	-5.37	0.046	NonCoding
TC15002471.hg.1	FMN1	formin 1	-5.41	0.0099	NonCoding
TC15000253.hg.1	C15orf41	chromosome 15 open reading frame 41	-5.41	0.0437	Coding
TC01000411.hg.1	TINAGL1	tubulointerstitial nephritis antigen-like 1	-5.43	0.0121	Coding
TC03000468.hg.1	EPHA3	EPH receptor A3	-5.43	0.0776	Coding
TC05000370.hg.1	F2R	coagulation factor II (thrombin) receptor	-5.47	0.0028	Coding
TC06000945.hg.1	GJA1	gap junction protein alpha 1	-5.47	0.061	Coding
TC02002905.hg.1	COL6A3	collagen, type VI, alpha 3	-5.5	0.0115	Coding
TC10000670.hg.1	PLCE1	phospholipase C, epsilon 1	-5.58	0.0059	Coding
TC09000359.hg.1	TLE4	transducin-like enhancer of split 4	-5.63	0.0033	Coding
TC12001377.hg.1	PKP2	plakophilin 2	-5.67	0.0029	Coding
TC04001673.hg.1	PDGFC	platelet derived growth factor C	-5.7	0.0145	Coding
TC13000314.hg.1	SLITRK5	SLIT and NTRK-like family, member 5	-5.74	0.024	Coding
TC05002282.hg.1			-5.78	0.0386	NonCoding
TC05001752.hg.1	FBN2	fibrillin 2	-5.78	0.038	Coding
TC12000642.hg.1	GLIPR1	GLI pathogenesis-related 1	-5.8	0.0685	Coding
TC01001358.hg.1	LINC01133	long intergenic non-protein coding RNA 1133	-5.8	0.0153	Coding
TC02004330.hg.1			-5.84	0.0298	NonCoding
TC10000081.hg.1	CELF2	CUGBP, Elav-like family member 2	-5.96	0.004	Coding
TC04000706.hg.1	HHIP	hedgehog interacting protein	-5.98	0.0017	Coding
TC11003437.hg.1	FADS3	fatty acid desaturase 3	-6.07	0.0038	Coding
TC0X000046.hg.1	FRMPD4	FERM and PDZ domain containing 4	-6.07	0.0099	Coding
TC05001331.hg.1	EMB	embigin	-6.13	0.0069	Coding
TC0X001291.hg.1	LRCH2	leucine-rich repeats and calponin homology (CH) domain containing 2	-6.19	0.0298	Coding
TC15001211.hg.1	MEIS2	Meis homeobox 2	-6.2	0.0183	Coding
TC05003380.hg.1			-6.26	0.0018	NonCoding
TC20000077.hg.1	LAMP5	lysosomal-associated membrane protein family, member 5	-6.26	0.0607	Coding
TC14001238.hg.1	PLEK2	pleckstrin 2	-6.29	0.0059	Coding
TC11002552.hg.1	SBF2-AS1	SBF2 antisense RNA 1	-6.39	0.036	NonCoding
TC15002722.hg.1	NR2F2-AS1	NR2F2 antisense RNA 1	-6.4	0.0054	NonCoding
TC0X000954.hg.1	SRPX	sushi-repeat containing protein, X-linked	-6.41	0.0079	Coding
TC06001879.hg.1	COL12A1	collagen, type XII, alpha 1	-6.55	0.0111	Coding
TC03001651.hg.1	CCDC80	coiled-coil domain containing 80	-6.56	0.0654	Coding
TC01004560.hg.1			-6.58	0.0029	NonCoding
TC15001825.hg.1	MFGE8	milk fat globule-EGF factor 8 protein	-6.66	0.015	Coding
TC09002617.hg.1	RASEF	RAS and EF-hand domain containing	-6.67	0.0059	NonCoding
TC01002337.hg.1	HTR1D	5-hydroxytryptamine (serotonin) receptor 1D, G protein-coupled	-6.7	0.0152	Coding
TC01001212.hg.1	TUFT1	tuftelin 1	-6.73	0.0056	Coding

TC12000276.hg.1	FAR2	fatty acyl-CoA reductase 2	-6.74	0.0147	Coding
TC06002330.hg.1	THBS2	thrombospondin 2	-6.77	0.0339	Coding
TC0X000015.hg.1	XG; XGY2	Xg blood group; Xg pseudogene, Y-linked 2	-6.77	0.0517	Coding
TC02000729.hg.1			-6.8	0.0258	Coding
TC13001217.hg.1			-6.81	0.026	NonCoding
TC0X002190.hg.1			-6.9	0.0189	NonCoding
TC12001803.hg.1	LUM	lumican	-6.99	0.0698	Coding
TC15001767.hg.1	BNC1	basonuclin 1	-7.03	0.0043	Coding
TC16001498.hg.1			-7.07	0.0729	NonCoding
TC01005143.hg.1	FMN2	formin 2	-7.16	0.0108	NonCoding
TC01002903.hg.1	DPYD	dihydropyrimidine dehydrogenase	-7.16	0.0277	Coding
TC01002338.hg.1	HTR1D	5-hydroxytryptamine (serotonin) receptor 1D, G protein-coupled	-7.33	0.0152	Coding
TC02002480.hg.1	FAP	fibroblast activation protein alpha	-7.35	0.0578	Coding
TC07001256.hg.1	PDE1C	phosphodiesterase 1C, calmodulin-dependent 70kDa	-7.38	0.0229	Coding
TC13001320.hg.1	GAS6-AS2	GAS6 antisense RNA 2 (head to head)	-7.66	0.0148	NonCoding
TC05000682.hg.1	TGFBI	transforming growth factor, beta-induced, 68kDa	-7.72	0.0006	Coding
TC15000971.hg.1	ALDH1A3	aldehyde dehydrogenase 1 family, member A3	-7.75	0.0351	Coding
TC11000272.hg.1	LUZP2	leucine zipper protein 2	-7.87	0.0125	Coding
TC07003339.hg.1	CAV1	caveolin 1	-7.87	0.0032	Coding
TC12000189.hg.1	EMP1	epithelial membrane protein 1	-7.97	0.0216	Coding
TC10001063.hg.1	FAM171A1	family with sequence similarity 171, member A1	-7.98	0.008	Coding
TC01005638.hg.1	ARHGAP29	Rho GTPase activating protein 29	-8.01	0.025	NonCoding
TC0Y000229.hg.1			-8.11	0.0501	NonCoding
TC17001485.hg.1	KRTAP2-3	keratin associated protein 2-3	-8.14	0.0188	Coding
TC04002799.hg.1	PDGFC	platelet derived growth factor C	-8.18	0.0212	NonCoding
TC04001765.hg.1	VEGFC	vascular endothelial growth factor C	-8.2	0.0331	Coding
TC19000576.hg.1	AXL	AXL receptor tyrosine kinase	-8.25	0.0316	Coding
TC03000146.hg.1	RBMS3	RNA binding motif, single stranded interacting protein 3	-8.52	0.0499	Coding
TC11000179.hg.1	SBF2-AS1	SBF2 antisense RNA 1	-8.58	0.0378	Coding
TC12001718.hg.1	PTPRB	protein tyrosine phosphatase, receptor type, B	-8.75	0.0067	Coding
TC05002048.hg.1	FAM196B	family with sequence similarity 196, member B	-9.1	0.0006	Coding
TC14000297.hg.1	FRMD6	FERM domain containing 6	-9.12	0.0017	Coding
TC01000887.hg.1	LOC729987	uncharacterized LOC729987	-9.55	0.0054	Coding
TC13000364.hg.1	ITGBL1	integrin beta like 1	-9.57	0.0351	Coding
TC05000220.hg.1	FST	follistatin	-9.65	0.0215	Coding
TC06002113.hg.1	MOXD1	monooxygenase, DBH-like 1	-9.85	0.0132	Coding
TC05001385.hg.1	PLK2	polo-like kinase 2	-9.93	0.0174	Coding
TC05002988.hg.1	EMB	embigin	-9.98	0.0038	NonCoding
TC01002884.hg.1	ARHGAP29	Rho GTPase activating protein 29	-10.2	0.0477	Coding
TC12001282.hg.1	EPS8	epidermal growth factor receptor pathway substrate 8	-10.22	0.0072	Coding
TC07001566.hg.1	SEMA3E	sema domain, immunoglobulin domain (Ig), short basic domain, secreted, (semaphorin) 3E	-10.37	0.031	Coding
TC05003345.hg.1	FAM196B	family with sequence similarity 196, member B	-10.4	0.0013	NonCoding
TC13001260.hg.1	ITGBL1	integrin beta like 1	-10.45	0.0543	NonCoding
TC15001612.hg.1	UACA	uveal autoantigen with coiled-coil domains and ankyrin repeats	-10.65	0.0061	Coding
TC01004464.hg.1			-10.68	0.0413	NonCoding
TC0X001988.hg.1			-10.71	0.0321	NonCoding
TC13000329.hg.1	GPC6	glypican 6	-10.79	0.0621	Coding
TC08001248.hg.1	TOX	thymocyte selection-associated high mobility group box	-10.88	0.0111	Coding
TC18000230.hg.1	SERPINB7	serpin peptidase inhibitor, clade B (ovalbumin), member 7	-11.13	0.0321	Coding
TC03002264.hg.1			-11.29	0.0629	NonCoding
TC01002886.hg.1	F3	coagulation factor III (thromboplastin, tissue factor)	-11.32	0.0184	Coding

TC17001682.hg.1	COL1A1	collagen, type I, alpha 1	-11.79	0.0998	Coding
TC10001166.hg.1	NRP1	neuropilin 1	-11.91	0.0033	Coding
TC0X001579.hg.1			-12.21	0.0696	NonCoding
TC03001145.hg.1	OXTR	oxytocin receptor	-12.22	0.0146	Coding
TC07000668.hg.1	LRRC17	leucine rich repeat containing 17	-12.79	0.0063	Coding
TC01003491.hg.1	DPT	dermatopontin	-12.8	0.0496	Coding
TC11003210.hg.1	EFEMP2	EGF containing fibulin-like extracellular matrix protein 2	-12.89	0.0413	NonCoding
TC14001147.hg.1			-13.13	0.0699	Coding
TC09002032.hg.1			-13.26	0.0017	NonCoding
TC14001148.hg.1	BMP4	bone morphogenetic protein 4	-13.34	0.018	Coding
TC10001061.hg.1	NMT2	N-myristoyltransferase 2	-14.13	0.0042	Coding
TC02001083.hg.1	ITGA4	integrin alpha 4	-14.66	0.0115	Coding
TC13000431.hg.1	GAS6-AS2	GAS6 antisense RNA 2 (head to head)	-14.7	0.0143	Coding
TC06001271.hg.1	ELOVL2	ELOVL fatty acid elongase 2	-14.75	0.0143	Coding
TC08000598.hg.1	MATN2	matrilin 2	-14.8	0.0171	Coding
TC01002654.hg.1	RAB3B	RAB3B, member RAS oncogene family	-15.08	0.0031	Coding
TC07000559.hg.1	COL1A2	collagen, type I, alpha 2	-16.71	0.0744	Coding
TC08002421.hg.1			-17.28	0.0121	NonCoding
TC12001907.hg.1			-18.7	0.0017	Coding
TC06000779.hg.1	NT5E	5-nucleotidase, ecto (CD73)	-19.1	0.059	Coding
TC02002747.hg.1	FN1	fibronectin 1	-19.3	0.0163	Coding
TC07002222.hg.1	CREB5	cAMP responsive element binding protein 5	-19.34	0.01	NonCoding
TC03002131.hg.1	LRRC15	leucine rich repeat containing 15	-19.36	0.0628	Coding
TC04000387.hg.1	AMTN	amelotin	-19.49	0.0925	Coding
TC0X000865.hg.1			-19.88	0.0409	Coding
TC07002463.hg.1	COL1A2	collagen, type I, alpha 2	-20.08	0.0896	NonCoding
TC04001494.hg.1	PRSS12	protease, serine, 12 (neurotrypsin, motopsin)	-20.79	0.0144	Coding
TC03000534.hg.1	ALCAM	activated leukocyte cell adhesion molecule	-21.05	0.0132	Coding
TC07003161.hg.1			-21.4	0.0059	NonCoding
TC05002939.hg.1			-21.9	0.0006	NonCoding
TC07002874.hg.1	PDE1C	phosphodiesterase 1C, calmodulin-dependent 70kDa	-22.06	0.0247	NonCoding
TC04001565.hg.1	PCDH18	protocadherin 18	-24.9	0.0675	Coding
TC15000226.hg.1	GREM1	gremlin 1, DAN family BMP antagonist	-25.43	0.0773	Coding
TC07000810.hg.1	CPA4	carboxypeptidase A4	-25.45	0.0645	Coding
TC18000538.hg.1	ATP8B1	ATPase, aminophospholipid transporter, class I, type 8B, member 1	-26.01	0.003	Coding
TC16000647.hg.1	CDH13	cadherin 13	-26.22	0.0061	Coding
TC12002841.hg.1	PRICKLE1	prickle homolog 1	-26.54	0.0207	NonCoding
TC01000752.hg.1	LRRC7	leucine rich repeat containing 7	-30.78	0.028	Coding
TC12001429.hg.1	SLC38A4	solute carrier family 38, member 4	-31.11	0.0149	Coding
TC12001804.hg.1	DCN	decorin	-33.38	0.0495	Coding
TC02004331.hg.1	ADD2	adducin 2 (beta)	-38.48	0.0219	NonCoding
TC07000643.hg.1	SERPINE1	serpin peptidase inhibitor, clade E (nexin, plasminogen activator inhibitor type 1), member 1	-40.29	0.0189	Coding
TC15000670.hg.1	LOXL1	lysyl oxidase-like 1	-41.9	0.014	Coding
TC07001570.hg.1	SEMA3D	sema domain, immunoglobulin domain (Ig), short basic domain, secreted, (semaphorin) 3D	-43.3	0.0108	Coding
TC07001154.hg.1	DGKB	diacylglycerol kinase, beta 90kDa	-48.29	0.0036	Coding
TC07002499.hg.1	SERPINE1	serpin peptidase inhibitor, clade E (nexin, plasminogen activator inhibitor type 1), member 1	-49.65	0.0241	NonCoding
TC10001678.hg.1	GFRA1	GDNF family receptor alpha 1	-57.6	0.0155	Coding
TC05000159.hg.1	IL7R	interleukin 7 receptor	-62.95	0.0307	Coding
TC10002843.hg.1	GFRA1	GDNF family receptor alpha 1	-105.37	0.0129	NonCoding
TC13000576.hg.1	POSTN	periostin, osteoblast specific factor	-715.72	0.0332	Coding

Appendix D: Transcriptome microarray validation by RT-qPCR analysis

Validation of whole-transcriptomic microarray data via RT-qPCR analysis using 54 representative genes. Genes were randomly selected to include top up and down-regulated DEGs as well as moderate DEGs. Fold change and associated p-value generated via microarray and RT-qPCR is listed for each gene. Comparison of fold changes between RT-qPCR and microarray were generally similar and in the same order of magnitude.

Gene	qPCR		HTA 2.0	
	FC	p-value	FC	p-value
ADD2	-38.82	2.94E-06	-4.42	8.25E-03
ALDH1A3	-4.06	1.23E-01	-5.47	3.51E-02
ATP6AP1	2.26	7.95E-04	2.30	1.24E-03
BMP2	12.57	2.75E-04	9.78	7.49E-03
BMP4	-10.96	3.89E-02	-9.79	1.80E-02
CACNB2	2.55	1.97E-01	6.46	2.15E-02
CAV1	-18.75	1.10E-04	-7.15	3.20E-03
CHD13	-2.35	3.35E-03	-23.61	6.08E-02
COL12A1	-4.53	1.07E-03	-5.43	1.11E-02
COL4A5	3.58	1.74E-04	2.41	4.56E-04
EGFR	-1.35	2.54E-02	-2.63	8.03E-03
EPHA4	-2.10	7.92E-03	-2.51	2.59E-02
F2R	-110.57	3.02E-06	-4.81	2.83E-03
F3	-8.50	8.46E-04	-8.59	1.84E-02
FN1	-8.74	2.62E-03	-15.10	1.63E-02
FZD2	-4.54	2.26E-05	-2.08	7.65E-03
FZD3	4.66	3.35E-04	5.00	3.17E-02
GFRA1	-5.45	1.48E-03	-33.86	1.55E-02
HPD	29.34	2.49E-05	63.91	4.56E-04
ID2	29.99	1.62E-04	7.00	5.22E-02
IL7R	-14.34	1.90E-03	-33.82	3.07E-02
ITGA4	-16.91	1.51E-03	-10.73	1.15E-02
ITGB8	-3.13	1.24E-02	-3.64	2.33E-02
ITPR1	10.47	1.77E-04	18.56	1.49E-03
KYNU	6466.37	2.67E-05	67.06	1.81E-02
LAMA1	14.43	2.00E-05	8.90	4.37E-02
LINC00473	1745.15	6.51E-07	850.11	1.58E-08
LOXL1	-24.52	1.16E-05	-28.00	1.40E-02

LRRC7	-97.87	5.64E-05	-16.61	2.80E-02
MAP7	7.60	5.32E-05	41.46	5.61E-03
MAPK4	138.88	1.83E-08	81.14	1.45E-02
PC	5.54	1.59E-05	4.15	1.10E-02
PDE10A	154.19	2.99E-07	96.11	1.91E-05
PDE1C	-44.27	3.26E-04	-6.23	2.29E-02
PDE3A	299.23	1.83E-08	1645.07	2.32E-09
PDE3B	2.27	3.84E-03	3.40	1.00E-02
PDE8B	6.12	2.81E-04	13.17	2.47E-03
PDK4	82.26	4.84E-05	38.30	1.24E-02
PI15	3593.04	9.67E-07	404.96	2.95E-04
POSTN	-658.57	2.19E-07	-383.42	3.32E-02
PPP1R3C	3.55	4.79E-04	5.26	1.38E-02
PRICKLE1	-20.80	4.45E-04	-3.79	2.55E-02
PTP4A1	9.69	6.27E-07	6.72	6.76E-05
PTPRB	-123.09	2.23E-05	-7.49	6.70E-03
RHOB	11.60	6.99E-07	10.00	2.81E-03
RHOV	25.37	1.24E-06	6.55	1.17E-02
SEMA3D	-25.21	6.87E-05	-34.93	1.08E-02
SEMA6D	2.60	1.71E-03	16.43	1.87E-03
SERPINE1	-24.87	3.33E-06	-31.15	1.89E-02
SMAD2	1.44	9.63E-02	3.65	3.68E-04
SMAD3	-2.17	1.75E-03	-3.06	1.00E-02
SMOC1	1556.97	2.18E-04	410.91	8.84E-09
TGFβI	-11.83	2.12E-06	-7.46	5.94E-04
TLR4	1.31	1.64E-02	8.84	9.47E-04

Appendix E: Upstream regulators predicted by IPA in GIM vs CON analysis

Full list of predicted upstream regulators identified using IPA regulator analysis and ranked by Z-score. IPA upstream regulator analysis was performed using the DEG list for GIM versus CON. Upstream regulators with overlap p-value <0.01 and activation Z-score of <-2 or >2 are presented. Upstream regulators with negative z-score refer to master regulators that are predicted to be down-regulated in GIM relative to CON, and vice versa.

Upstream Regulator	Molecule Type	Z-score	p-value of overlap
TGFβ1	growth factor	-5.165	1.35E-30
SMAD3	transcription regulator	-3.412	1.57E-10
TP53	transcription regulator	-3.358	3.26E-13
CTGF	growth factor	-3.092	6.42E-04
EDN1	cytokine	-3.023	3.16E-08
NUPR1	transcription regulator	-2.987	2.62E-08
TWIST2	transcription regulator	-2.965	4.44E-07
WNT3A	cytokine	-2.878	9.25E-06
SMARCA4	transcription regulator	-2.801	2.11E-12
F2	peptidase	-2.631	7.80E-16
BRD4	kinase	-2.61	9.97E-07
RAC1	enzyme	-2.596	5.84E-04
IGF2BP1	translation regulator	-2.449	7.11E-05
HOXD3	transcription regulator	-2.449	7.11E-05
AGT	growth factor	-2.433	8.09E-20
PAX6	transcription regulator	-2.353	2.25E-01
NONO	other	-2.333	1.76E-08
CTNNB1	transcription regulator	-2.31	2.16E-09
MKL2	transcription regulator	-2.236	9.28E-03
VGLL3	other	-2.236	2.94E-05
PCDH11Y	other	-2.236	9.44E-04
ASAH1	enzyme	-2.216	2.61E-03
NKX2-3	transcription regulator	-2.208	2.35E-03
FOSB	transcription regulator	-2.191	6.63E-03
Smad2/3-Smad4	complex	-2.19	3.26E-04
TGFβR1	kinase	-2.173	1.46E-04
EIF4E	translation regulator	-2.156	6.37E-02
C5	cytokine	-2.149	5.04E-02
IGFBP2	other	-2.145	1.23E-05
TET2	enzyme	-2.121	1.12E-02
CD44	other	-2.118	3.99E-03
GT	transcription regulator	-2.027	2.77E-06
KLF5	transcription regulator	2.021	2.34E-03

ENG	transmembrane receptor	2.09	1.57E-03
EOMES	transcription regulator	2.111	6.75E-04
ZNF217	transcription regulator	2.138	5.76E-03
TAF4	transcription regulator	2.157	1.34E-08
PAX3	transcription regulator	2.166	1.82E-05
XDH	enzyme	2.168	7.57E-03
mir-1	microrna	2.178	2.10E-03
mir-34	microrna	2.187	3.45E-02
HNF1B	transcription regulator	2.228	2.42E-07
EFNA4	kinase	2.236	2.06E-02
EFNA3	kinase	2.236	2.26E-02
DICER1	enzyme	2.244	1.56E-08
EFNA1	other	2.345	5.79E-04
IKZF1	transcription regulator	2.354	4.87E-04
WISP2	growth factor	2.359	3.25E-07
EFNA5	kinase	2.433	1.23E-03
estrogen receptor	group	2.552	9.63E-11
INHA	growth factor	2.557	1.89E-05
AHR	ligand-dependent nuclear receptor	2.688	2.63E-11
ANGPT2	growth factor	2.715	5.54E-05
EFNA2	kinase	2.828	2.69E-04
miR-1-3-p	mature microrna	3.23	1.25E-03
MYCN	transcription regulator	3.242	3.72E-03
SMAD7	transcription regulator	3.587	2.65E-11

Appendix F: Technical primer information for genes analyzed by RT-qPCR in GIM-FRA1 vs GIM-pcDNA3 analysis

Gene	Sequence (5'to 3')	T_A (°C)	Accession ID
ALPI	TACACGTCCATCCTGTACGG TACACGTCCATCCTGTACGG	57	NM_001631.4
BAX	CCTTTTCTACTTTGCCAGCAAAC GAGGCCGTCCCAACCAC	60	NM_001291428.1
CREB5	TGAAGGCTGCATTGACTCAC ATCATGTGTCCCATGGTGTTCA	62	NM_182898.3
cFOS	AAAAGGAGAATCCGAAGGGAAA GTCTGTCTCCGCTTGGAGTGTAT	60	NM_005252.3
FRA1	CATGTTCCGAGACTTCGGGG ACCAGGTGGAACTTCTGCTG	60	NM_005438.4
GAPDH	AAGGTGAAGGTCGGAGTCAA AATGAAGGGGTCATTGATGG	60	NM_002046.5
HSPC3	CCAAAAAGCACCTGGAGATCA TGTCGGCCTCAGCCTTCT	60	NM_001271969.1
IL7R	TCCAACCGGCAGCAATGTAT AGGATCCATCTCCCCTGAGC	60	NM_002185.3
cJUN	TCGACATGGAGTCCCAGGA GGCGATTCTCTCCAGCTTCC	60	NM_002228.3
LAMA1	TCAGAAAGGCCTAAGCTGGC CACTGTTCTGGAAAAGCCCG	60	NM_001198608.1
p53	TCAACAAGATGTTTTGCCAACTG ATGTGCTGTGACTGCTTGTAGATG	60	NM_000546.5
PDE10A	CTTCGGCTCCGACATGGAAG ATGTGCTGTGACTGCTTGTAGATG	60	NM_001130690.2
PDE3B	GGCTATCGAGACATTCCTTATCACA GAACTGGCCGTGTTGTCAGA	60	NM_000922.3
PI15	TGCTACCACATAGCAAAGAACC AGAGTTAGGGTCTCTGCACAA	60	NM_001324403.1
RHOB	GTGTGTCTGTTCGACTCCCC AAGGGATATCAAGCTCCCGC	60	NM_004040.3
RHOV	TCAGCTACACCTGCAATGGG AAAATCCTCCTGTCCCGCTG	60	NM_133639.3
RPS18	ATTAAGGGTGTGGGCCGAAG GGTGATCACACGTTCCACCT	60	NM_022551.2

Appendix G: Differentially expressed genes in GIM-FRA1 vs GIM-pcDNA3 analysis

ID	Gene Symbol	P-val	Fold Change	Description	Group
TC11001948.hg.1	FOSL1	4.46E-07	2.23	FOS-like antigen 1	Coding
TC6_cox_hap2000102.hg.1	SLC39A7	4.65E-06	-2.53	solute carrier family 39 (zinc transporter), member 7	Coding
TC6_dbb_hap3000094.hg.1	SLC39A7	4.65E-06	-2.53	solute carrier family 39 (zinc transporter), member 7	Coding
TC6_mann_hap4000086.hg.1	SLC39A7	4.65E-06	-2.53	solute carrier family 39 (zinc transporter), member 7	Coding
TC6_mcf_hap5000087.hg.1	SLC39A7	4.65E-06	-2.53	solute carrier family 39 (zinc transporter), member 7	Coding
TC6_qbl_hap6000093.hg.1	SLC39A7	4.65E-06	-2.53	solute carrier family 39 (zinc transporter), member 7	Coding
TC06000412.hg.1	SLC39A7	9.03E-06	-2.58	solute carrier family 39 (zinc transporter), member 7	Coding
TC12000234.hg.1	SPX	1.79E-05	2.04	spexin hormone	Coding
TC0X001666.hg.1		4.03E-05	33.88		NonCoding
TC14001832.hg.1	BDKRB1	5.90E-05	13.95	bradykinin receptor B1	NonCoding
TC0X000205.hg.1	LOC101927501	6.81E-05	26.71	uncharacterized LOC101927501	Coding
TC03003184.hg.1	KPNA4	7.13E-05	2.01	karyopherin alpha 4 (importin alpha 3)	NonCoding
TC08000256.hg.1	LOC105379362	0.0001	4.55	uncharacterized LOC105379362	Coding
TC14002311.hg.1	BDKRB1	0.0001	5.92	bradykinin receptor B1	Coding
TC08000497.hg.1	PI15	0.0001	-70.73	peptidase inhibitor 15	Coding
TC01005864.hg.1		0.0002	2.65		NonCoding
TC12000182.hg.1	GPRC5A; MIR614	0.0003	4.17	G protein-coupled receptor, class C, group 5, member A; microRNA 614	Coding
TC12001513.hg.1	KRT80	0.0003	9.21	keratin 80, type II	Coding
TC07000536.hg.1	STEAP1	0.0003	2.88	six transmembrane epithelial antigen of the prostate 1	Coding
TC05000262.hg.1	ZSWIM6	0.0003	2.26	zinc finger, SWIM-type containing 6	Coding
TC19002707.hg.1	PSG8	0.0004	2.48	pregnancy specific beta-1-glycoprotein 8	Coding
TC03000565.hg.1		0.0004	4.3		Coding
TC03000768.hg.1	PLS1	0.0005	2.18	plastin 1	Coding
TC02004735.hg.1	PDE1A	0.0006	-10.68	phosphodiesterase 1A, calmodulin-dependent	NonCoding
TC19001581.hg.1	PSG2; PSG5; PSG3	0.0006	2.42	pregnancy specific beta-1-glycoprotein 2; pregnancy specific beta-1-glycoprotein 5; pregnancy specific beta-1-glycoprotein 3	Coding
TC07002499.hg.1	SERPINE1	0.0006	3.17	serpin peptidase inhibitor, clade E (nexin, plasminogen activator inhibitor type 1), member 1	NonCoding
TC05000159.hg.1	IL7R	0.0008	20.72	interleukin 7 receptor	Coding
TC0X001995.hg.1	PIR-FIGF	0.0009	-2.57	PIR-FIGF readthrough	NonCoding
TC01002823.hg.1	LPAR3	0.001	7.72	lysophosphatidic acid receptor 3	Coding
TC12002256.hg.1		0.001	5.61		NonCoding

TC19001579.hg.1	PSG7	0.0011	2.02	pregnancy specific beta-1-glycoprotein 7 (gene/pseudogene)	Coding
TC10000350.hg.1	DKK1	0.0011	29.79	dickkopf WNT signaling pathway inhibitor 1	Coding
TC11000944.hg.1	ARHGAP42	0.0012	2.71	Rho GTPase activating protein 42	Coding
TC01003745.hg.1	NUAK2	0.0012	2.95	NUAK family, SNF1-like kinase, 2	Coding
TC08001875.hg.1		0.0012	2.41		NonCoding
TC01002708.hg.1	JUN	0.0013	3.11	jun proto-oncogene	Coding
TC17001647.hg.1	HOXB9	0.0013	5.25	homeobox B9	Coding
TC12000399.hg.1	METTL7A	0.0014	-2.5	methyltransferase like 7A	Coding
TC06001426.hg.1	HIST1H1B	0.0014	-2.4	histone cluster 1, H1b	Coding
TC19002351.hg.1	ADGRL1	0.0015	2.39	adhesion G protein-coupled receptor L1	NonCoding
TC12000418.hg.1	KRT7	0.0015	2.31	keratin 7, type II	Coding
TC19002457.hg.1	DMKN	0.0018	9.35	dermokine	NonCoding
TC03001274.hg.1	SUSD5	0.0019	2.64	sushi domain containing 5	Coding
TC11000182.hg.1	ADM	0.0019	2.39	adrenomedullin	Coding
TC11001638.hg.1		0.0019	2.27		Coding
TC10002237.hg.1		0.002	-2.17		NonCoding
TC01004027.hg.1	CHML	0.002	2.2	choroideremia-like (Rab escort protein 2)	Coding
TC05000338.hg.1	PTCD2	0.002	2.17	pentatricopeptide repeat domain 2	Coding
TC03003001.hg.1		0.0022	2.38		NonCoding
TC03000878.hg.1	ARL14	0.0022	2.08	ADP-ribosylation factor like GTPase 14	Coding
TC05000280.hg.1	ERBB2IP	0.0022	2.3	erbb2 interacting protein	Coding
TC19000689.hg.1	SNAR-A3; SNAR-A4; SNAR-A5; SNAR-A7; SNAR-A11; SNAR-A9; SNAR-A6; SNAR-A8; SNAR-A10; SNAR-A14	0.0024	2.96	small ILF3/NF90-associated RNA A3; small ILF3/NF90-associated RNA A4; small ILF3/NF90-associated RNA A5; small ILF3/NF90-associated RNA A7; small ILF3/NF90-associated RNA A11; small ILF3/NF90-associated RNA A9; small ILF3/NF90-associated RNA A6; small ILF3/NF90-associated RNA A8; small ILF3/NF90-associated RNA A10; small ILF3/NF90-associated RNA A14	Coding
TC19001731.hg.1	SNAR-A14; SNAR-A3; SNAR-A4	0.0024	2.96	small ILF3/NF90-associated RNA A14; small ILF3/NF90-associated RNA A3; small ILF3/NF90-associated RNA A4	Coding
TC19001732.hg.1	SNAR-A14; SNAR-A3; SNAR-A4	0.0024	2.96	small ILF3/NF90-associated RNA A14; small ILF3/NF90-associated RNA A3; small ILF3/NF90-associated RNA A4	Coding
TC19001733.hg.1	SNAR-A14; SNAR-A3; SNAR-A4	0.0024	2.96	small ILF3/NF90-associated RNA A14; small ILF3/NF90-associated RNA A3; small ILF3/NF90-associated RNA A4	Coding
TC19001734.hg.1	SNAR-A14; SNAR-A3; SNAR-A4	0.0024	2.96	small ILF3/NF90-associated RNA A14; small ILF3/NF90-associated RNA A3; small ILF3/NF90-associated RNA A4	Coding
TC19001735.hg.1	SNAR-A14; SNAR-A3; SNAR-A4	0.0024	2.96	small ILF3/NF90-associated RNA A14; small ILF3/NF90-associated RNA A3; small ILF3/NF90-associated RNA A4	Coding
TC19001736.hg.1	SNAR-A14; SNAR-A3; SNAR-A4	0.0024	2.96	small ILF3/NF90-associated RNA A14; small ILF3/NF90-associated RNA A3; small ILF3/NF90-associated RNA A4	Coding
TC19001737.hg.1	SNAR-A14; SNAR-A3; SNAR-A4	0.0024	2.96	small ILF3/NF90-associated RNA A14; small ILF3/NF90-associated RNA A3; small ILF3/NF90-associated RNA A4	Coding
TC19001738.hg.1	SNAR-A14; SNAR-A3; SNAR-A4	0.0024	2.96	small ILF3/NF90-associated RNA A14; small ILF3/NF90-associated RNA A3; small ILF3/NF90-associated RNA A4	Coding

TC19001739.hg.1	SNAR-A14; SNAR-A3; SNAR-A4	0.0024	2.96	small ILF3/NF90-associated RNA A14; small ILF3/NF90-associated RNA A3; small ILF3/NF90-associated RNA A4	Coding
TC04000158.hg.1	SLIT2	0.0025	4.36	slit guidance ligand 2	Coding
TC19000688.hg.1	SNAR-A1; SNAR-A2	0.0026	2.95	small ILF3/NF90-associated RNA A1; small ILF3/NF90-associated RNA A2	Coding
TC19000691.hg.1	SNAR-A2; SNAR-A1	0.0026	2.95	small ILF3/NF90-associated RNA A2; small ILF3/NF90-associated RNA A1	Coding
TC19001582.hg.1	PSG5; PSG3	0.0026	8.76	pregnancy specific beta-1-glycoprotein 5; pregnancy specific beta-1-glycoprotein 3	Coding
TC12000283.hg.1	LINC00941	0.0027	2.53	long intergenic non-protein coding RNA 941	Coding
TC14002198.hg.1	SNAPC1	0.0029	2.97	small nuclear RNA activating complex polypeptide 1	Coding
TC19001233.hg.1	ADGRL1	0.0029	2.82	adhesion G protein-coupled receptor L1	Coding
TC0X002327.hg.1	PIR	0.003	-2.34	pirin	Coding
TC05001395.hg.1	SMIM15	0.0031	2.43	small integral membrane protein 15	Coding
TC05003057.hg.1	LOC647859	0.0032	4.34	occludin pseudogene	NonCoding
TC03000585.hg.1	ZDHHC23	0.0032	2.15	zinc finger, DHHC-type containing 23	Coding
TC06001077.hg.1	UST	0.0032	2.47	uronyl-2-sulfotransferase	Coding
TC19001445.hg.1	DMKN	0.0033	4.49	dermokine	Coding
TC05000218.hg.1	ITGA2	0.0034	10.68	integrin, alpha 2 (CD49B, alpha 2 subunit of VLA-2 receptor)	Coding
TC07000643.hg.1	SERPINE1	0.0036	3	serpin peptidase inhibitor, clade E (nexin, plasminogen activator inhibitor type 1), member 1	Coding
TC01000619.hg.1	CDKN2C	0.0037	-2.51	cyclin-dependent kinase inhibitor 2C (p18, inhibits CDK4)	Coding
TC06003607.hg.1		0.0038	-2.15		NonCoding
TC15002462.hg.1		0.0038	-2.07		NonCoding
TC19001584.hg.1	PSG9	0.004	3.32	pregnancy specific beta-1-glycoprotein 9	Coding
TC12000564.hg.1	SRGAP1	0.0041	2.67	SLIT-ROBO Rho GTPase activating protein 1	Coding
TC19000624.hg.1	PVR	0.0041	2.04	poliovirus receptor	Coding
TC12002414.hg.1	SRGAP1	0.0043	3.38	SLIT-ROBO Rho GTPase activating protein 1	NonCoding
TC19001622.hg.1		0.0045	2.84		Coding
TC03001956.hg.1	KPNA4	0.0047	2.19	karyopherin alpha 4 (importin alpha 3)	Coding
TC10000702.hg.1	MARVELD1	0.0048	-2.14	MARVEL domain containing 1	Coding
TC17001416.hg.1		0.0049	-2.3		Coding
TC17000751.hg.1		0.0049	-2.3		Coding
TC17000733.hg.1		0.0049	-2.3		Coding
TC17000455.hg.1		0.0049	-2.3		Coding
TC17000432.hg.1		0.0049	-2.3		Coding
TC05002282.hg.1		0.0049	3.26		NonCoding
TC02000158.hg.1	TMEM214	0.0049	-2.11	transmembrane protein 214	Coding
TC05000304.hg.1	OCLN	0.0051	3.49	occludin	Coding
TC06000184.hg.1	BTN3A2	0.0051	-2.78	butyrophilin, subfamily 3, member A2	Coding
TC02001030.hg.1	ITGA6	0.0052	3.04	integrin alpha 6	Coding
TC05001458.hg.1	OCLN	0.0052	4.07	occludin	Coding
TC0X000323.hg.1	MAGED2	0.0053	-3.1	MAGE family member D2	Coding

TC19000686.hg.1	SNAR-A12; SNAR-A13	0.0053	2.38	small ILF3/NF90-associated RNA A12; small ILF3/NF90-associated RNA A13	Coding
TC19000693.hg.1	SNAR-A13; SNAR-A12	0.0053	2.38	small ILF3/NF90-associated RNA A13; small ILF3/NF90-associated RNA A12	Coding
TC07003081.hg.1	GATS	0.0054	-2.49	GATS, stromal antigen 3 opposite strand	NonCoding
TC11002249.hg.1	CASP1P2	0.0057	2.33	caspase 1 pseudogene 2	Coding
TC19002497.hg.1		0.0058	2.63		NonCoding
TC17000419.hg.1		0.0059	-2.32		Coding
TC17000426.hg.1		0.0059	-2.32		Coding
TC17000412.hg.1		0.0059	-2.32		Coding
TC06001655.hg.1		0.006	-2.56		Coding
TC19001580.hg.1	PSG11	0.0061	2.14	pregnancy specific beta-1-glycoprotein 11	Coding
TC22000288.hg.1	H1F0	0.0062	6.55	H1 histone family, member 0	Coding
TC0X001720.hg.1	MAGED2	0.0064	-2.97	MAGE family member D2	NonCoding
TC06003578.hg.1		0.0065	-2.77		NonCoding
TC05000083.hg.1	TRIO	0.0066	2.1	trio Rho guanine nucleotide exchange factor	Coding
TC18000692.hg.1	SETBP1	0.0068	2.57	SET binding protein 1	NonCoding
TC05002283.hg.1	TRIO	0.007	2.52	trio Rho guanine nucleotide exchange factor	NonCoding
TC03002118.hg.1	MB21D2	0.0072	8.67	Mab-21 domain containing 2	Coding
TC02001400.hg.1	ALPI	0.0073	-26.42	alkaline phosphatase, intestinal	Coding
TC02002419.hg.1	RND3	0.0073	2.67	Rho family GTPase 3	Coding
TC16000378.hg.1	TGFB1I1	0.0076	-2.17	transforming growth factor beta 1 induced transcript 1	Coding
TC05000209.hg.1	PARP8	0.0078	2.81	poly(ADP-ribose) polymerase family member 8	Coding
TC05000301.hg.1	CDK7	0.0078	2.13	cyclin-dependent kinase 7	Coding
TC06000186.hg.1	BTN3A1	0.0079	-2.46	butyrophilin, subfamily 3, member A1	Coding
TC07000159.hg.1	NFE2L3	0.008	5.82	nuclear factor, erythroid 2-like 3	Coding
TC0X000721.hg.1	MAMLD1	0.0084	-2.65	mastermind-like domain containing 1	Coding
TC07000521.hg.1	CROT	0.0084	2.62	carnitine O-octanoyltransferase	Coding
TC11000718.hg.1	CCND1	0.0085	2.07	cyclin D1	Coding
TC09001568.hg.1		0.0088	-2.04		Coding
TC12002303.hg.1	LINC00941	0.0091	2.58	long intergenic non-protein coding RNA 941	NonCoding
TC01003977.hg.1	PCNXL2	0.0092	2.29	pecanex-like 2 (Drosophila)	Coding
TC03000548.hg.1	DZIP3	0.0093	2.13	DAZ interacting zinc finger protein 3	Coding
TC05001524.hg.1	MTX3	0.0093	2.63	metaxin 3	Coding
TC19002708.hg.1	PSG1	0.0097	2.42	pregnancy specific beta-1-glycoprotein 1	Coding
TC15000143.hg.1		0.0098	-2.05		Coding
TC06000188.hg.1	BTN3A3	0.0101	-3.34	butyrophilin, subfamily 3, member A3	Coding
TC14001432.hg.1	TTC7B	0.0102	2.88	tetratricopeptide repeat domain 7B	Coding
TC10001573.hg.1	CRTAC1	0.0103	-2.41	cartilage acidic protein 1	Coding
TC08001097.hg.1	KIF13B	0.0103	2.63	kinesin family member 13B	Coding
TC12001992.hg.1	LINC01234	0.0104	5.47	long intergenic non-protein coding RNA 1234	Coding
TC11001048.hg.1	SIDT2	0.0104	-2.38	SID1 transmembrane family, member 2	Coding

TC06002724.hg.1	RNF5P1	0.0104	-2.09	ring finger protein 5, E3 ubiquitin protein ligase pseudogene 1	NonCoding
TC03000814.hg.1	TSC22D2	0.0108	2.14	TSC22 domain family, member 2	Coding
TC02001916.hg.1	SERTAD2	0.0109	2.72	SERTA domain containing 2	Coding
TC20000878.hg.1	SDC4	0.0109	3.67	syndecan 4	Coding
TC03002133.hg.1	ATP13A3	0.011	3.8	ATPase type 13A3	Coding
TC11003000.hg.1	H19	0.0111	-8.52	H19, imprinted maternally expressed transcript (non-protein coding)	NonCoding
TC06000178.hg.1	HIST1H2BI	0.0112	-3.06	histone cluster 1, H2bi	Coding
TC05001366.hg.1	IL6ST	0.0113	2.91	interleukin 6 signal transducer	Coding
TC15000368.hg.1	SEMA6D	0.0113	-3.68	sema domain, transmembrane domain (TM), and cytoplasmic domain, (semaphorin) 6D	Coding
TC05000764.hg.1	PCDHGB5	0.0116	-2.75	protocadherin gamma subfamily B, 5	Coding
TC05003005.hg.1		0.0119	3.58		NonCoding
TC12001798.hg.1	ATP2B1	0.0119	2.68	ATPase, Ca++ transporting, plasma membrane 1	Coding
TC04002187.hg.1	FGF2	0.012	3.06	fibroblast growth factor 2 (basic)	NonCoding
TC07001377.hg.1	COBL	0.0122	-2.68	cordon-bleu WH2 repeat protein	Coding
TC12003093.hg.1	LINC01234	0.0124	3.87	long intergenic non-protein coding RNA 1234	NonCoding
TC02000894.hg.1	SPOPL	0.0127	2.11	speckle-type POZ protein-like	Coding
TC11001273.hg.1	H19; MIR675	0.0128	-6.2	H19, imprinted maternally expressed transcript (non-protein coding); microRNA 675	Coding
TC19000356.hg.1	GDF15	0.0131	24.91	growth differentiation factor 15	Coding
TC01002375.hg.1		0.0135	2.01		Coding
TC07000463.hg.1	GATSL2	0.0136	-3.25	GATS protein-like 2	Coding
TC04001496.hg.1	SEC24D	0.0137	-2.41	SEC24 homolog D, COPII coat complex component	Coding
TC05003028.hg.1	SGTB	0.0138	2.49	small glutamine-rich tetratricopeptide repeat (TPR)-containing, beta	NonCoding
TC07002410.hg.1		0.0139	-3.4		NonCoding
TC04002756.hg.1		0.0141	2.22		NonCoding
TC06001684.hg.1	CCDC167	0.0142	-2.13	coiled-coil domain containing 167	Coding
TC06001654.hg.1		0.0144	-2.17		Coding
TC11000976.hg.1	RAB39A	0.0148	2.91	RAB39A, member RAS oncogene family	Coding
TC02000535.hg.1	LINC00152; MIR4435-2HG	0.0148	2.56	long intergenic non-protein coding RNA 152; MIR4435-2 host gene	Coding
TC16000401.hg.1		0.0148	-2.62		Coding
TC05000355.hg.1	ARHGEF28	0.0149	3.76	Rho guanine nucleotide exchange factor 28	Coding
TC06001427.hg.1	HIST1H3I	0.015	-3.03	histone cluster 1, H3i	Coding
TC01005631.hg.1	TGFBR3	0.0154	-3	transforming growth factor beta receptor III	NonCoding
TC14001238.hg.1	PLEK2	0.0154	3	pleckstrin 2	Coding
TC07000137.hg.1	IL6	0.0154	20.04	interleukin 6	Coding
TC05003313.hg.1	SPARC	0.0158	-2.01	secreted protein, acidic, cysteine-rich (osteonectin)	NonCoding
TC05001110.hg.1	LPCAT1	0.0161	-2.01	lysophosphatidylcholine acyltransferase 1	Coding
TC02003382.hg.1	MIR4435-2HG; LINC00152	0.0162	2.52	MIR4435-2 host gene; long intergenic non-protein coding RNA 152	NonCoding
TC07001868.hg.1	LINC-PINT	0.0163	2.13	long intergenic non-protein coding RNA, p53 induced transcript	Coding

TC03002079.hg.1	IGF2BP2	0.0163	2.29	insulin-like growth factor 2 mRNA binding protein 2	Coding
TC06000328.hg.1	HLA-A	0.0163	-2.15	major histocompatibility complex, class I, A	Coding
TC14000896.hg.1		0.0164	2.32		Coding
TC12001377.hg.1	PKP2	0.0167	3.44	plakophilin 2	Coding
TC07001189.hg.1	LOC541472	0.0167	17.92	uncharacterized LOC541472	Coding
TC02001399.hg.1	ALPPL2	0.0169	-5.33	alkaline phosphatase, placental like 2	Coding
TC06001844.hg.1	LGSN	0.0169	-4.66	lengsin, lens protein with glutamine synthetase domain	Coding
TC07000794.hg.1		0.0169	-2.23		Coding
TC20000816.hg.1	NDRG3	0.017	-2.13	NDRG family member 3	Coding
TC10002935.hg.1	BMI1	0.0174	2.49	BMI1 proto-oncogene, polycomb ring finger	Coding
TC0X001776.hg.1		0.0175	2.34		NonCoding
TC07003360.hg.1	GATSL2	0.0176	-3.13	GATS protein-like 2	Coding
TC07000385.hg.1	ZNF107	0.0177	2.07	zinc finger protein 107	Coding
TC06002217.hg.1	LRP11	0.0177	-2.45	LDL receptor related protein 11	Coding
TC6_dbb_hap3000070.hg.1	HSPA1B; HSPA1A	0.0177	-2.41	heat shock 70kDa protein 1B; heat shock 70kDa protein 1A	Coding
TC12000749.hg.1	NEDD1	0.0177	2.22	neural precursor cell expressed, developmentally down-regulated 1	Coding
TC6_cox_hap2000079.hg.1	HSPA1B; HSPA1A	0.0179	-2.41	heat shock 70kDa protein 1B; heat shock 70kDa protein 1A	Coding
TC02002207.hg.1	MIR4435-2HG	0.0182	2.29	MIR4435-2 host gene	Coding
TC03002108.hg.1	CLDN1	0.0182	8.17	claudin 1	Coding
TC05001947.hg.1	ANXA6	0.0184	-2.68	annexin A6	Coding
TC14000319.hg.1	SAMD4A	0.0185	2.14	sterile alpha motif domain containing 4A	Coding
TC03001699.hg.1	IQCB1	0.0186	2.76	IQ motif containing B1	Coding
TC6_apd_hap1000040.hg.1	HSPA1B; HSPA1A	0.0187	-2.39	heat shock 70kDa protein 1B; heat shock 70kDa protein 1A	Coding
TC02002194.hg.1	MALL	0.0187	2.07	mal, T-cell differentiation protein-like	Coding
TC10000128.hg.1		0.0193	-2.31		Coding
TC12002919.hg.1		0.0194	-2.09		NonCoding
TC04000434.hg.1	FRAS1	0.0195	2.74	Fraser extracellular matrix complex subunit 1	Coding
TC13000599.hg.1	KBTBD6	0.0195	-2.02	kelch repeat and BTB (POZ) domain containing 6	Coding
TC6_qbl_hap6000070.hg.1	HSPA1B; HSPA1A	0.0197	-2.46	heat shock 70kDa protein 1B; heat shock 70kDa protein 1A	Coding
TC03001919.hg.1	DHX36	0.0198	2.09	DEAH (Asp-Glu-Ala-His) box polypeptide 36	Coding
TC01004964.hg.1	MDM4	0.02	2.61	MDM4, p53 regulator	NonCoding
TC20000621.hg.1	JAG1	0.02	3.17	jagged 1	Coding
TC07001615.hg.1		0.0202	-3.94		Coding
TC01000931.hg.1	FAM102B	0.0205	-5.01	family with sequence similarity 102, member B	Coding
TC06000115.hg.1	FAM8A1	0.0206	-2.2	family with sequence similarity 8, member A1	Coding
TC11002371.hg.1	THY1	0.0207	-2.6	Thy-1 cell surface antigen	Coding
TC10000670.hg.1	PLCE1	0.021	3.02	phospholipase C, epsilon 1	Coding
TC17001984.hg.1	WDR45B	0.0212	2.06	WD repeat domain 45B	Coding
TC11003505.hg.1	CASP1	0.0217	2.02	caspase 1	Coding

TC11003054.hg.1		0.0218	2.04		NonCoding
TC20001565.hg.1	NDRG3	0.0224	-2.12	NDRG family member 3	NonCoding
TC09000535.hg.1	SLC44A1	0.0224	3.53	solute carrier family 44 (choline transporter), member 1	Coding
TC07002222.hg.1	CREB5	0.0224	6.83	cAMP responsive element binding protein 5	NonCoding
TC01000398.hg.1	PTPRU	0.0225	-3.39	protein tyrosine phosphatase, receptor type, U	Coding
TC07003171.hg.1		0.0231	2.31		NonCoding
TC16001498.hg.1		0.0231	-3.3		NonCoding
TC03002566.hg.1		0.0232	2.58		NonCoding
TC06003069.hg.1	MYB	0.0232	2.13	v-myb avian myeloblastosis viral oncogene homolog	NonCoding
TC05000302.hg.1	RAD17	0.0234	2.45	RAD17 checkpoint clamp loader component	Coding
TC03003091.hg.1		0.0236	2.33		NonCoding
TC12000264.hg.1	ARNTL2	0.0239	5.35	aryl hydrocarbon receptor nuclear translocator-like 2	Coding
TC04001132.hg.1	SMIM14	0.024	-2.95	small integral membrane protein 14	Coding
TC15001650.hg.1	SCAMP2	0.0243	-2.17	secretory carrier membrane protein 2	Coding
TC05000220.hg.1	FST	0.0244	11.1	follistatin	Coding
TC01005286.hg.1		0.0247	4.48		NonCoding
TC19001741.hg.1	SNAR-B1; SNAR-B2	0.0248	2.94	small ILF3/NF90-associated RNA B1; small ILF3/NF90-associated RNA B2	Coding
TC19001740.hg.1	SNAR-B2; SNAR-B1	0.0248	2.94	small ILF3/NF90-associated RNA B2; small ILF3/NF90-associated RNA B1	Coding
TC04002519.hg.1		0.0251	-3.68		NonCoding
TC16000948.hg.1	CDR2	0.0254	-2.05	cerebellar degeneration related protein 2	Coding
TC17000396.hg.1	SLFN5	0.0256	3.48	schlafen family member 5	Coding
TC03003362.hg.1	PHLDB2	0.0258	8.19	pleckstrin homology-like domain, family B, member 2	Coding
TC06000385.hg.1	HSPA1B; HSPA1A	0.0258	-2.21	heat shock 70kDa protein 1B; heat shock 70kDa protein 1A	Coding
TC01001212.hg.1	TUFT1	0.026	3.35	tuftelin 1	Coding
TC09000038.hg.1	PDCD1LG2	0.0261	3.22	programmed cell death 1 ligand 2	Coding
TC16001909.hg.1	KIFC3	0.0263	2.17	kinesin family member C3	NonCoding
TC12000150.hg.1		0.0264	2.24		Coding
TC01006075.hg.1	PLXNA2	0.0265	2.19	plexin A2	NonCoding
TC11002293.hg.1	IL18	0.0269	6.68	interleukin 18	Coding
TC06002355.hg.1	OR2J2	0.0272	-3.57	olfactory receptor, family 2, subfamily J, member 2	NonCoding
TC06002301.hg.1	SDIM1	0.0273	-2.51	stress responsive DNAJB4 interacting membrane protein 1	Coding
TC06001659.hg.1	C6orf106	0.0275	-2.43	chromosome 6 open reading frame 106	Coding
TC14000205.hg.1	ARHGAP5	0.0277	2.34	Rho GTPase activating protein 5	Coding
TC04001765.hg.1	VEGFC	0.0277	6.12	vascular endothelial growth factor C	Coding
TC05000144.hg.1	NPR3	0.0277	7.86	natriuretic peptide receptor 3	Coding
TC01000745.hg.1	GADD45A	0.0278	2.13	growth arrest and DNA-damage-inducible, alpha	Coding
TC15001173.hg.1		0.0282	-3.69		Coding
TC15001139.hg.1		0.0282	-3.69		Coding
TC15000960.hg.1		0.0282	-3.69		Coding

TC15000185.hg.1		0.0282	-3.69		Coding
TC15000159.hg.1		0.0282	-3.69		Coding
TC09001167.hg.1	PGM5P2	0.0282	3.06	phosphoglucomutase 5 pseudogene 2	Coding
TC6_mann_hap4000021.hg.1		0.0282	-2.01		Coding
TC02004035.hg.1	MBOAT2	0.0283	4.63	membrane bound O-acyltransferase domain containing 2	NonCoding
TC01003266.hg.1	S100A4	0.0284	-2.56	S100 calcium binding protein A4	Coding
TC01004535.hg.1		0.0285	2.09		NonCoding
TC03000881.hg.1	NMD3	0.0287	2.37	NMD3 ribosome export adaptor	Coding
TC06002221.hg.1	RAET1K	0.029	2.23	retinoic acid early transcript 1K pseudogene	Coding
TC05001522.hg.1	HOMER1	0.029	2.49	homer scaffolding protein 1	Coding
TC01001753.hg.1	SYT14	0.0291	2.95	synaptotagmin XIV	Coding
TC11000542.hg.1	FADS2	0.0296	-2.03	fatty acid desaturase 2	Coding
TC17001370.hg.1	SLFN12	0.0297	2.46	schlafen family member 12	Coding
TC01002338.hg.1	HTR1D	0.0298	2.92	5-hydroxytryptamine (serotonin) receptor 1D, G protein-coupled	Coding
TC01005002.hg.1	SYT14	0.0299	3.85	synaptotagmin XIV	NonCoding
TC02001556.hg.1	MBOAT2	0.0301	4.37	membrane bound O-acyltransferase domain containing 2	Coding
TC03001641.hg.1	LOC151760	0.0305	2.07	putative uncharacterized protein LOC151760	Coding
TC01001201.hg.1	MLLT11	0.0307	-3.2	myeloid/lymphoid or mixed-lineage leukemia; translocated to, 11	Coding
TC03000880.hg.1	PPM1L	0.0308	2.79	protein phosphatase, Mg2+/Mn2+ dependent, 1L	Coding
TC09002564.hg.1		0.031	2.3		NonCoding
TC12003251.hg.1	RAB3IP	0.0311	2.74	RAB3A interacting protein	Coding
TC12002339.hg.1		0.0311	2.93		NonCoding
TC05001059.hg.1		0.0313	2.32		Coding
TC07000468.hg.1		0.0315	-2.06		Coding
TC02004505.hg.1		0.0318	2.26		NonCoding
TC12002426.hg.1		0.0318	-2.13		NonCoding
TC12001751.hg.1	PHLDA1	0.0319	2.35	pleckstrin homology-like domain, family A, member 1	Coding
TC18000496.hg.1	SMAD2	0.0322	2.01	SMAD family member 2	Coding
TC15001482.hg.1	ALDH1A2	0.0323	-2.86	aldehyde dehydrogenase 1 family, member A2	Coding
TC08001815.hg.1		0.0326	2.09		NonCoding
TC07001874.hg.1	PODXL	0.0327	2.26	podocalyxin-like	Coding
TC04000254.hg.1	LIMCH1	0.0327	2.43	LIM and calponin homology domains 1	Coding
TC10001565.hg.1		0.0327	-2.22		Coding
TC07001275.hg.1	DPY19L2P1	0.0331	5.49	DPY19L2 pseudogene 1	Coding
TC08001983.hg.1		0.0332	2.72		NonCoding
TC12000955.hg.1	P2RX7	0.0334	-2.15	purinergic receptor P2X, ligand gated ion channel, 7	Coding
TC02002569.hg.1	TTC30A	0.0336	-2.17	tetratricopeptide repeat domain 30A	Coding
TC07000112.hg.1	AHR	0.0337	2.13	aryl hydrocarbon receptor	Coding
TC07002602.hg.1		0.0337	-2.86		NonCoding
TC02002590.hg.1	PDE1A	0.0338	-3.22	phosphodiesterase 1A, calmodulin-dependent	Coding

TC09000593.hg.1	PAPPA	0.034	5.19	pregnancy-associated plasma protein A, pappalysin 1	Coding
TC01001675.hg.1	PPP1R12B	0.0342	-2.01	protein phosphatase 1, regulatory subunit 12B	Coding
TC15002553.hg.1		0.0346	-2.07		NonCoding
TC05000336.hg.1	MAP1B	0.0347	5.89	microtubule associated protein 1B	Coding
TC0X000370.hg.1	IGBP1	0.0349	-2.33	immunoglobulin (CD79A) binding protein 1	Coding
TC10000715.hg.1	ABCC2	0.0351	-2.56	ATP binding cassette subfamily C member 2	Coding
TC03003341.hg.1	ACAD11; NPHP3-ACAD11	0.0352	2.31	acyl-CoA dehydrogenase family, member 11; NPHP3-ACAD11 readthrough (NMD candidate)	Coding
TC18000105.hg.1		0.0354	-2.06		Coding
TC21000922.hg.1		0.0356	2.37		NonCoding
TC10000089.hg.1	DHTKD1	0.0359	-2.01	dehydrogenase E1 and transketolase domain containing 1	Coding
TC15001330.hg.1	MYEF2	0.036	3.19	myelin expression factor 2	Coding
TC07002911.hg.1		0.036	2		NonCoding
TC05001314.hg.1		0.036	-2.53		Coding
TC0X001252.hg.1	LOC286437	0.0362	-2.24	uncharacterized LOC286437	Coding
TC03000774.hg.1	U2SURP	0.0364	2.13	U2 snRNP-associated SURP domain containing	Coding
TC02001398.hg.1	ALPP	0.0367	-3.32	alkaline phosphatase, placental	Coding
TC02001750.hg.1	CYP1B1	0.0383	-2.61	cytochrome P450, family 1, subfamily B, polypeptide 1	Coding
TC12002445.hg.1	LOC100507330	0.0385	2.17	uncharacterized LOC100507330	NonCoding
TC0X000353.hg.1	MSN	0.0385	-2.16	moesin	Coding
TC10000163.hg.1	MSRB2	0.0386	2.1	methionine sulfoxide reductase B2	Coding
TC11003367.hg.1	BACE1	0.0386	-2.08	beta-site APP-cleaving enzyme 1	NonCoding
TC10001182.hg.1		0.0387	2.25		Coding
TC09000912.hg.1		0.0388	3.26		Coding
TC17001795.hg.1		0.0388	2.54		Coding
TC03001720.hg.1	HEG1	0.0389	2.34	heart development protein with EGF-like domains 1	Coding
TC06002591.hg.1		0.039	-2.73		NonCoding
TC0X000237.hg.1	ARAF	0.0394	-2.13	A-Raf proto-oncogene, serine/threonine kinase	Coding
TC0X001042.hg.1	NUDT11	0.04	2.32	nudix hydrolase 11	Coding
TC06003598.hg.1	LOC100507547	0.0401	-2.98	uncharacterized LOC100507547	NonCoding
TC14001636.hg.1	ARHGAP5	0.0403	2.71	Rho GTPase activating protein 5	NonCoding
TC16000804.hg.1	ZNF213-AS1	0.0404	-2.03	ZNF213 antisense RNA 1 (head to head)	Coding
TC12002552.hg.1		0.0406	5.91		NonCoding
TC10001533.hg.1		0.0406	-2.07		Coding
TC6_mann_hap4000208.hg.1	PRRT1	0.0408	-2.18	proline-rich transmembrane protein 1	Coding
TC12001282.hg.1	EPS8	0.0408	6.04	epidermal growth factor receptor pathway substrate 8	Coding
TC17000807.hg.1	MAP2K6	0.041	-3.69	mitogen-activated protein kinase kinase 6	Coding
TC10001617.hg.1	LDB1	0.041	-2.05	LIM domain binding 1	Coding
TC05002434.hg.1	MAP1B	0.0411	16.35	microtubule associated protein 1B	NonCoding
TC06000223.hg.1	HIST1H2AG	0.0412	-2.02	histone cluster 1, H2ag	Coding

TC19001593.hg.1	PLAUR	0.0415	2.86	plasminogen activator, urokinase receptor	Coding
TC11001593.hg.1		0.0416	2.3		Coding
TC15001683.hg.1	NRG4	0.0416	-2.53	neuregulin 4	Coding
TC06001089.hg.1	ULBP1	0.0418	4.01	UL16 binding protein 1	Coding
TC16001083.hg.1	SHCBP1	0.0422	-2.23	SHC SH2-domain binding protein 1	Coding
TC08000209.hg.1	SCARA3	0.0423	-4.3	scavenger receptor class A, member 3	Coding
TC06001313.hg.1	MBOAT1	0.0425	-2.37	membrane bound O-acyltransferase domain containing 1	Coding
TC03003320.hg.1	NFKBIZ	0.0437	2.79	nuclear factor of kappa light polypeptide gene enhancer in B-cells inhibitor, zeta	Coding
TC03002732.hg.1	HES1	0.0444	12.25	hes family bHLH transcription factor 1	NonCoding
TC05000277.hg.1	PPWD1	0.0445	2.04	peptidylprolyl isomerase domain and WD repeat containing 1	Coding
TC03000917.hg.1	SKIL	0.0446	2.23	SKI-like proto-oncogene	Coding
TC01004676.hg.1	EMBP1	0.0446	3.5	embigin pseudogene 1	NonCoding
TC17002746.hg.1		0.0446	2.23		NonCoding
TC09000323.hg.1	MAMDC2	0.0446	-4.49	MAM domain containing 2	Coding
TC14001994.hg.1		0.045	11.09		NonCoding
TC11001458.hg.1	USH1C	0.0451	-3.01	Usher syndrome 1C	Coding
TC18000202.hg.1	NEDD4L	0.0453	2.17	neural precursor cell expressed, developmentally down-regulated 4-like, E3 ubiquitin protein ligase	Coding
TC01003267.hg.1	S100A3	0.0456	-3.11	S100 calcium binding protein A3	Coding
TC03002656.hg.1	SKIL	0.0458	2.15	SKI-like proto-oncogene	NonCoding
TC01001053.hg.1	EMBP1	0.0466	3.28	embigin pseudogene 1	Coding
TC09000592.hg.1		0.047	7.72		Coding
TC07001994.hg.1	RNY1	0.0476	-2.78	RNA, Ro-associated Y1	Coding
TC05002424.hg.1	SMN2	0.0477	2.49	survival of motor neuron 2, centromeric	NonCoding
TC12001170.hg.1	SLC2A3	0.048	-2.71	solute carrier family 2 (facilitated glucose transporter), member 3	Coding
TC01004845.hg.1	PAPPA2	0.0483	4.23	pappalysin 2	NonCoding
TC16001483.hg.1		0.0484	-2.46		NonCoding
TC04000087.hg.1	HTRA3	0.0491	-6.97	HtrA serine peptidase 3	Coding
TC04000960.hg.1	RNF212	0.0496	-2.1	ring finger protein 212	Coding
TC15001245.hg.1	RHOV	0.0496	-2.34	ras homolog family member V	Coding
TC18000761.hg.1	SOCS6	0.0497	2.63	suppressor of cytokine signaling 6	NonCoding
TC19002613.hg.1	PSG4	0.0497	4.67	pregnancy specific beta-1-glycoprotein 4	Coding
TC15001680.hg.1		0.0499	-5.43		Coding

Appendix H: Hierarchy of all cell lines utilized in previous gene expression studies with the CGL1 cell system